# A STUDY OF IN-SERVICE ULTRASONIC INSPECTION PRACTICE FOR BWR PIPING WELDS

EPRI NP-436-SR
(Technical Planning Study 75-609)

Special Report

August 1977

Prepared by

Eugene R. Reinhart
Systems and Materials Department
Nuclear Power Division

Electric Power Research Institute
3412 Hillview Avenue
Palo Alto, California 94304

---

## FOREWORD

This summary report, prepared by the Department of Systems and Materials, Nuclear Division of the Electric Power Research Institute (EPRI), summarizes the work performed under EPRI Technical Planning Study TPS-75-609. Technical planning studies are conducted by EPRI to support research and development planning for the engineering, environmental, and economic feasibility of proposed technological development and/or hardware options. Such studies permit identification of the most promising options and the major technological issues which must be resolved before the initiation of a comprehensive research program.

EPRI-funded inspection groups that participated in the test program were:

CONAM Inspection Division, Nuclear Energy Services, Inc.
Nuclear Energy Division, General Electric Company
Nuclear Services Corp.
Peabody Testing, Division of Magnaflux Corp.
Southwest Research Institute

Consulting services, including planning and laboratory monitoring of the test program and sectioning of specimens, were obtained from Battelle, Columbus Laboratories through an EPRI Technical Services Agreement (TSA). Consulting and laboratory facilities were provided by General Electric Company through a joint EPRI/GE cost-sharing program. General Electric also provided the test samples used in the project. Failure Analysis Associates provided input for planning the test program under funding from an existing EPRI Research Project (RP217-1).

ACKNOWLEDGMENTS

The author acknowledges the significant input of EPRI staff members Dr. G. J. Dau, Dr. K. S. Stahlkopf, and Dr. E. L. Zebroski in providing valuable ideas regarding program planning and review of this report.

This study would not have been possible without the excellent support given by Messrs. R. Witek and J. Clark and the staff of the Nondestructive Testing Unit, Development Engineering Section, General Electric Company. General Electric also provided laboratory space for conducting the study at its Vallecitos Nuclear Center. Dr. Matthew Golis of Battelle, Columbus Laboratories, Mr. Al Sather of Argonne National Laboratory, and Mr. Howard Sager of Col-X provided invaluable input for the planning and coordination of the study.

The author also appreciates the effort of Ms. Gail Horiuchi and Dr. Robert Railey in their rapid analysis of the considerable data generated during this study.

# PREFACE

Periodic maintenance inspection of the primary and secondary pressure boundary of the commercial light water moderated nuclear reactor system is a requirement of the Nuclear Regulatory Commission (NRC) in order to operate a nuclear reactor in the United States. The detailed requirements for these in-service inspections are set forth in the ASME Boiler and Pressure Vessel Code, Section XI, "Rules for In-Service Inspection of Nuclear Power Plant Components," and in various supplemental directives issued by the NRC. One of the major nondestructive evaluation (NDE) inspection methods used to satisfy the requirements of the Code is ultrasonic inspection. This technique has the ability to interrogate large volumes of the pressure-containing structure for service-induced flaws without the need for access to the inside surface.

In-service ultrasonic inspection is important because this technique, along with the many redundant on-line monitoring techniques and backup coolant supply and containment systems, constitutes the method used to ensure the operational safety and availability of the nuclear reactor system. Since in-service inspection can play such an important role in plant safety and availability, continued technological improvement has been carried forward by the utilities, the government, and the various inspection groups. NDE technology development is certainly important, but it is equally important to assess the actual performance of NDE when used to detect and analyze natural flaws under real working conditions of access and environment.

To address this need, EPRI recently conducted a technical planning study to determine current in-service inspection practice for stainless steel piping. This study was conducted specifically to quantify the ability of code-required ultrasonic inspection methods to detect the presence of the intergranular stress corrosion cracks in stainless steel piping as used in the bypass and core spray lines of boiling water reactors (BWRs). During the past several years, flaws of this nature were discovered in a number of BWR bypass and core spray lines. This study represents the first nuclear in-service NDE performance evaluation program conducted in the United States. The details and results of the program are discussed in this report.

Eugene R. Reinhart
EPRI Project Manager

ABSTRACT

The occasional occurrence of intergranular stress corrosion cracks (IGSCCs) in bypass lines and core spray lines on boiling water reactors (BWRs) has made it desirable to quantify the response of Code-required ultrasonic inspection methods to flaws of this nature. To quantify the ability of the ultrasonic method to detect IGSCC flaws, EPRI conducted a technical round robin evaluation of actual piping removed from operating plants, including both cracked and uncracked pipe samples (Technical Planning Study TPS-75-609). Five industry teams performed the examinations. In addition to evaluation of the flaw detection and analysis capability of each inspection group, the variables of code interpretation, procedures, techniques, standards, equipment, and training were studied. The overall results of the program indicate that ultrasonic examination is a viable in-service volumetric inspection method for the detection of IGSCCs. The majority of the ultrasonic inspections found indications in essentially all of the flawed pipes (as determined by destructive examinations of specimens), but interpretation varied as to whether further confirmation was needed to establish the importance of the indications. Comparing the geometric location of the source of suspect signals with the previously established probable location of IGSCCs appears to be one of the most useful methods of analyzing data.

At the present time, training of personnel specifically for the detection and analysis of IGSCCs appears to be the single most important factor in obtaining a high probability of correct inspection results. Techniques, equipment, and standards all influence the inspection process, but to a lesser degree. The program results have been used by EPRI to initiate programs intended to further improve the decision-making process of the inspector (EPRI research project RP892). The program results also indicate that the necessary guidelines have now been established for conducting future inspection quantification programs in the utility industry.

The details of planning and conducting the study and analysis of the inspection results are covered in the report. In addition, appendices to the report contain

a detailed description of the test samples used in the study, examination procedures and data forms, a statistical analysis of test results, and a metallurgical characterization of the test samples.

CONTENTS

FIGURES

FIGURES (Cont'd.)

TABLES

## SUMMARY

EPRI has conducted a round robin study to quantify the ability of Code-required* ultrasonic inspection methods to detect the presence of intergranular stress corrosion cracks (IGSCCs) in stainless steel piping as used in the bypass and core spray lines of boiling water reactors (BWRs). During the past several years, flaws of this nature were discovered in a number of BWR bypass and core spray lines.

Detailed knowledge of ultrasonic in-service inspection performance is important because this technique, along with the many redundant on-line monitoring techniques (drywell leak detection, radiation monitors, sump water monitors, etc.) and backup coolant supply and contaminant systems (coolant charging system, emergency core cooling system, containment building, etc.), constitutes the method used to ensure the operational safety and availability of the nuclear reactor system. The principle of in-depth safety protection through several redundant and supplemental systems is based on the experience that even though one or more of these lines of safety defense may occasionally break down, simultaneous failure of all lines of defense has a sufficiently low probability of occurrence to make its consequences an acceptable risk.

This program addressed only the technique of ultrasonic nondestructive examination (NDE). It was not intended as an evaluation of the total in-service inspection and analysis process, because ultimate decisions regarding the nature and consequences of defects are usually reached only after use of additional supplementary inspection techniques (dye penetrant, radiography, etc.), followed by an extensive analysis of the stress, material performance, and operating environment at the suspect area.

---

*Code refers to the American Society of Mechanical Engineers (ASME) Boiler and Pressure Vessel Code, Section XI, "Rules for In-Service Inspection of Nuclear Power Plant Components," 1974.

The program had two objectives:

- To lay the necessary groundwork for any future NDE quantification effort by the utility industry.
- To determine industry inspection performance and to discover ways of improving any deficiencies found in that performance.

From the overall results of the program, the following points were found to be important in conducting a successful round robin test of this type:

- An on-site EPRI representative provided a valuable link between the test groups and the project manager. By observing the detailed performance of each test group, the representative obtained valuable insight into the inspection process.
- Pretest briefings and posttest debriefings were valuable in ensuring that the objectives of the test program were met, and in providing additional insight into inspection details and philosophy.
- Permanent reference marks on the test samples, a standard summary sheet for results, and uniform, fixed allotted time periods for inspection and analysis were all key factors in the program.
- Before the simulated inspections were conducted, a third-party inspection team performed a dry run to check test details.

Since the results of the program show considerable reproducibility of data, and since the group-to-group analysis of cracked as well as uncracked pipe is similar, the objective of providing a valid, realistic test program appears to have been met. The experience gained in this program will be valuable in conducting future inspection quantification programs in the utility industry.

The inspection quantification portion of the program involved performance by five industry teams of simulated in-service examinations of both cracked and uncracked pipe samples obtained from an operating BWR. The inspections were conducted in two phases. In the first phase the groups used their own inspection procedures, equipment, and standards. The second phase repeated the ultrasonic inspection using a reference procedure and standards defined and supplied by EPRI. Both sets of procedures were within the same range of Code-acceptable inspection sensitivity. After the tests were completed, the test samples were sectioned and the actual nature, depth, and orientation of the flaws determined. Although the data base of actual cracked and uncracked pipe samples was less than ideal from a statistical point of view, several significant results and trends can be derived from the results. These are listed below.

1. The destructive examinations categorized the 16 test samples analyzed in the program into the following groups:

   - Five test samples that had stress corrosion cracks;
   - Two test samples that had lack of weld fusion and lap defects and were considered defective;
   - Nine test samples that were considered free from service-induced or major fabrication defects.

   In all five of the pipes containing stress corrosion cracks (SCCs), the majority of inspection teams found indications of stress corrosion cracks and successfully identified the pipes as cracked. For each of the five test specimens with SCCs, two inspections were performed by the five test groups, for a total of 50 separate inspections. The groups successfully detected and recorded flaws in 43 of these 50 pipe inspections (successfully detected is defined as an indication plotted in the proper location on the pipe with accompanying ultrasonic amplitude data). Of the 43 detections, 28 were successfully analyzed as service-induced cracks. (Successful analysis is defined as calling a plotted indication a crack. Terms such as linear indication or defect indication were not acceptable in this analysis, although this information would be useful to the plant operator in conducting further examinations.)

   For the two specimens containing lack of fusion or lap flaws, the majority of inspection teams detected and defined these specimens as flawed, although the differentiation between SCC and lack of fusion was not usually made. For these two specimens, 18 separate inspections were performed by the five groups (one group did not inspect one of the specimens). All of the 18 inspections appeared to detect the flaws successfully. In many cases a group's original data were reviewed to determine the possibility that a flaw was detected but the detection was not reported on the final EPRI data form. Consequently, it was found that some groups did apparently detect flaws in these two specimens but did not report them. Of the 18 inspections, 10 were successfully analyzed as lack of fusion or a crack (either definition was accepted).

   For each of the nine nondefective pipe samples, two inspections were performed by each of the five groups for a total of 90 inspections. Of these, 23 were called cracked. One pipe sample containing an internal fabrication reflector was involved in seven of the unsuccessful inspection calls. One

sample containing severe geometric changes on the inside surface contributed to four of the miscalls. The remainder of the miscalls were randomly distributed; they were attributed to other weld fabrication anomalies such as root drop-through, overlap, and irregular weld preparation geometries. The inspection teams pointed out that many of these miscalls might have been eliminated if detailed fabrication inspection data had been made available or if supplemental inspection techniques (such as radiography) had been used.

The correct analysis of cracked pipe segments tends significantly to outweigh the several cases in which uncracked pipe was identified as defective. The tendency toward such overcalls indicates a conservative inspection philosophy which could result in the unnecessary repair of unflawed pipe during a reactor outage. However, this conservative approach would also allow fewer flaws with the potential of growing to leak conditions to remain in the piping system. The repair of a leaking flaw that causes reactor shutdown is an order of magnitude more costly (in terms of plant availability) than the same repair completed during normal periods of reactor shutdown.

2. Since some of the specimens contained several flaws of various depths and orientations, the individual flaws were analyzed to determine what effect flaw size, shape, and orientation had on defect detection and analysis. As expected, the orientation of a flaw rather than its depth appears to be a significant controlling factor. The shape of flaws is also important: a high depth-to-surface-length ratio contributes to lack of detection. Skewed cracks (those not parallel or perpendicular to the weld) were extremely difficult to detect in the simulated inspections using the normal field inspection procedures of scanning parallel and perpendicular to the weld. They were detected in the laboratory by rotating the transducer. From observations of previous field-cracked pipe, skewed cracks in which no portion of the crack surface has an orientation parallel or perpendicular to the weld centerline appear to be very rare.

3. Considering the overall results and relative performance of the groups, a conventional transducer size greater than 0.375-in. diameter (with conventional wedge) may reduce the number of stress corrosion cracks detected in some 10-in. pipe because of the physical interference between the front edge of the search unit and a raised weld crown. This observation was verified by laboratory study.

4. The principal difference between these inspections and inspections for other types of flaws was the way in which the data were analyzed. The groups that were most successful in correctly identifying flaws plotted ultrasonic test (UT) data carefully on cross-section drawings of the weld configuration and then used the location of a suspect signal to decide upon its identity (geometry, stress corrosion crack, etc.). These groups used the criterion that a stress corrosion crack usually occurs between the fusion zone of the weld and the inside diameter counterbore (if any exists).

The overall results of this program indicate that pulse-echo shear wave ultrasonics is a viable in-service volumetric inspection method for the detection of IGSCC defects in welded 300 series core spray lines of BWR reactors (the number of bypass line samples included in the program was insufficient to draw conclusions). If the mechanism of IGSCC has started in the primary system of a BWR, and if the past historical pattern of crack growth is present (cracks at various depths and orientations and in more than one location), then there is a high probability that the presence of the IGSCCs will be detected by a well-trained inspection team using present in-service inspection methods. However, the detection and analysis of a limited number of small IGSCC flaws at one or a few locations in the entire piping system could be missed or incorrectly analyzed by this technique; this possibility is higher than desirable and needs improvement.

The sensitivity of the technique is not limited, as very small flaws can be detected; rather, the fundamental problem in using the technique is correctly recognizing the detected signals as signals from a flaw and not from other sources. The results also tend to show that the final result of the inspection process is dependent most of all upon the decision-making process of the individual inspector, and any improvement in this area would have the greatest effect on the total inspection process. Equipment, techniques, codes, and procedures influence the inspection process to a lesser degree, but there appears to be room for considerable short-term improvement in one or all of these areas, since past development effort for inspecting IGSCCs appears minimal. Access, working conditions, and limited inspection time also influence the inspection process, but their contribution is difficult to assess and correct on a short-term basis.

The major drawback in using the ultrasonic technique is the time-consuming analysis required to distinguish flaws from other signals. This creates a tendency to miscall fabrication anomalies as service-induced cracks. (Small fabrication

anomalies have not been observed to grow with time in the manner of stress corrosion cracks.) This situation is aggravated by the rather low ratio of flaw signal to noise, and the considerable difficulty in detecting small IGSCCs skewed to the major axis of the pipe. Previous inspection data and supplemental inspection techniques such as radiography could probably aid in the analysis and decision-making process, but their exact contribution to improving the inspection process was not studied in this program.

To improve the overall inspection process, the following steps can be taken:

- For short-term improvements, inspection equipment (primarily the transducer) should be evaluated to determine what parameters enhance the detection and analysis of IGSCCs. From this analysis, specialized systems should be derived and evaluated, using actual flawed hardware. Since very little past effort has been directed toward improving the conventional inspection system for IGSCCs, overall performance improvement could be considerable, particularly in the enhancement of crack-signal-to-noise ratio.

- Training of inspection personnel using defective pipe and improvement of inspection analysis procedures are also short-term methods of improving the overall inspection process.

- The results of this study also indicate that some attention should be given to improving methods of detecting off-axis flaws, either by improved techniques or scanning procedures.

- Long-term changes could include changes in field welding procedures and weld configurations to improve in-service inspection (counterbore moved from weld fusion zone, less taper on counterbore, etc.).

- Other long-term improvements might be achieved by specialized methods of processing the ultrasonic data or by developing and using supplemental inspection techniques (such as portable radiography) to aid in flaw analysis.

Since a major development effort in this area was initiated several months ago by EPRI (including training of inspectors, specialized transducer designs, improved inspection analysis procedures, etc.), improvement in the overall inspection process is expected shortly. And since many inspection groups are already applying these improvements to actual field inspection, overall inspection performance may already have been enhanced. However, continued development effort in this area is recommended until similar round robin industry evaluations show performance improvement to acceptable levels in all aspects: improved detection, better discrimination, and reduced radiation exposure for inspectors.

## BACKGROUND

The safety of the nuclear power plant has received considerable attention by the commercial utility industry ever since the introduction of the first experimental reactors at various utility sites more than 15 years ago. The excellent safety record of the nuclear industry is attributable in large part to the use of methods that ensure the delivered quality and operational integrity of plant components. These methods include quality assurance, preoperational testing, on-line surveillance, backup coolant supply systems, and in-service inspection. The principle of in-depth safety protection through several redundant and supplemental systems is based on the assumption that even though one or more of these lines of safety defense may break down, simultaneous failure of all lines of defense has an extremely low probability of occurrence.

The first step in the safety defense is to ensure the quality of the fabricated hardware through an extensive quality assurance program.* The term quality assurance (QA) generally refers to all activities monitoring the total fabrication process, including necessary inspections, to ensure that all steps of the process are followed exactly. This quality assurance program is continued through the final construction at the plant site. After installation, preoperational tests are performed to ensure the functional performance of the components. For the primary system, hydrostatic pressure and leak tests are the most important, since past experience has shown that once a pressurized system has successfully passed these tests, the possibility of an in-service failure is extremely small (1). During this time, plant inspections are also conducted to establish a baseline for all future in-service examinations.

Once the plant is operational, on-line surveillance systems such as containment sump water level monitors, drywell humidity monitors, drywell radioactivity monitors, and containment pressure monitors are used to detect any abnormal leaks in the reactor system. In addition to these systems, surveillance capsules containing representative samples of primary system structural materials are used to determine the long-term effect of the plant environment (primarily temperature and radiation)

---

*The ASME definition of quality assurance is discussed in Article NA-4000, "Quality Assurance," of ASME Boiler and Pressure Vessel Code, Section III, Division 1, "Rules for Construction of Nuclear Power Plant Components," 1974.

upon material performance. These various surveillance systems are important because the structures used in the pressure retaining system are designed to leak before any flaw can develop to a size of concern to the structural integrity of the system. This "leak before break" design criterion has been verified several times in operation: the timely detection of leaks has allowed for repair before any major component failure occurred.

To accommodate any possible leak situation, several backup and redundant coolant supply systems (coolant charging and emergency core cooling system) are also used in the nuclear system. Both the emergency core cooling system and the containment system are designed to accommodate a pipe rupture. Also, early indication of a leak is given by the leak detection systems which permit shutdown and depressurization before a leak could grow to a size requiring use of emergency cooling systems. However, early detection of cracks is advantageous to avoid unscheduled shutdown and repairs in response to in-service leaks.

An added help in ensuring the reliability and safety of the plant is periodic in-service inspection. The in-service inspection of nuclear reactor coolant systems as presently required by the Nuclear Regulatory Commission (NRC) essentially follows the ASME Boiler and Pressure Vessel Code Section XI, "Rules for In-Service Inspection of Nuclear Power Plant Components" (2). This document states that specific areas of the coolant system, such as welds, vessel cladding, vessel penetrations, etc., will be inspected completely using nondestructive evaluation (NDE) methods several times during the projected 40-year life of the plant. Practically speaking, this means that some of the total inspection will be conducted during the periodic plant shutdown for refueling, which usually occurs on a yearly basis. These inspections provide a statistical sample of the condition of all critical areas of the primary system. If defects are detected during an inspection, if defects are detected in another plant of similar design and thought to be generic, or if there is an indication of possible material degradations (leaks, excessive vibration, etc.), the sampling inspection process is changed to a complete inspection of all similar areas of all similar components of a system. As a recent example, a leaking crack was discovered in one of the welds in one loop of the emergency core cooling system (ECCS) of a boiling water reactor (BWR). The sampling inspection process was immediately changed to inspection of all welds of both loops of the ECCS. In addition, other, similar BWR reactor systems were notified and required to increase their inspection coverage of the ECCS (3,4).

In this case, the requirements of ASME Code Section XI were augmented by directives (usually called Nuclear Regulatory Guides) from the NRC. This practice, common in the industry, has led to timely updates of the inspection process whenever generic problems have been disclosed.

The total in-service inspection process uses complementary volumetric and surface inspection techniques to detect, locate, and analyze service-induced flaws. Ultimate decisions regarding the nature and consequences of defects are usually reached only after the suspect area has been thoroughly analyzed by supplementary inspection techniques and after the impact of the flaw on the system has been determined by analysis of the stress, material performance, and operating environment at the suspect area. The overall inspection and analysis process is shown in Figure S-1. The first series of steps involves the development and/or selection of appropriate inspection techniques to satisfy all regulatory requirements as well as any supplemental requirements of a particular utility. It is at this point that in-service inspection can be of double value to the utility operator. First, the safety requirements are met by complying with the regulatory requirements. Second, specific additional requirements based on operational plant experience can be added to the inspection process to increase plant availability significantly. An example of this would be the early detection of any condition that could lead to premature plant shutdown. Although such a shutdown might in no way affect plant safety, unscheduled plant shutdowns have a significant effect on plant availability and ultimately on the cost of delivered power.

Since in-service inspection can play such an important role in plant safety and availability, continued technological improvement has been carried forward by the utilities, the government, and the various inspection groups (5,6,7). NDE technology development is certainly important, but it is equally important to assess the actual performance of NDE when used to detect and analyze natural flaws under real working conditions of access and environment. To date, NDE evaluation programs in the utility industry have primarily addressed methods used in shop fabrication of nuclear system components (8). EPRI recently conducted a program to determine current in-service inspection practice for stainless steel piping. This represents the first nuclear in-service NDE evaluation program conducted in the U.S. The overall program is discussed in the following sections.

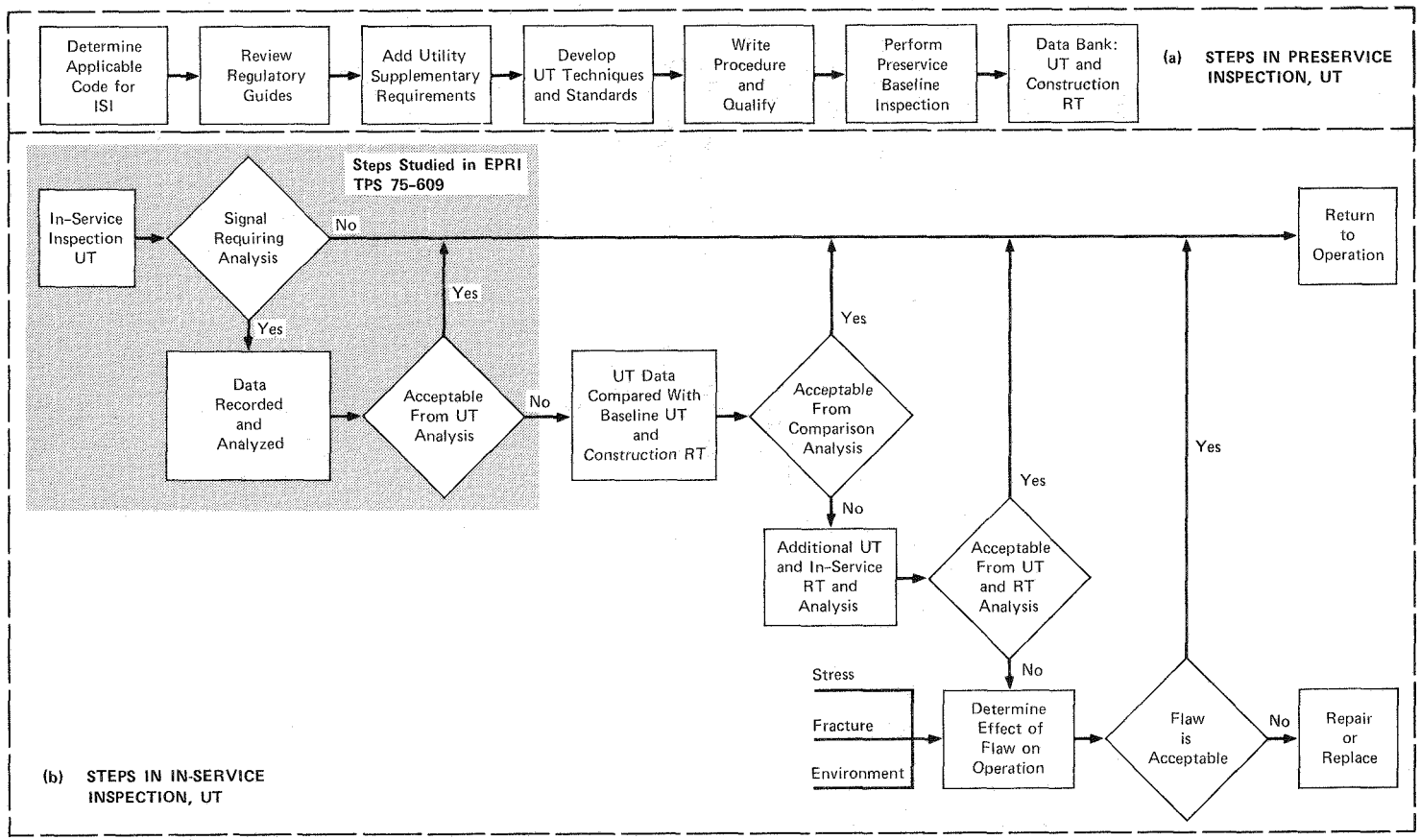


Figure S-1 Steps in the In-Service Inspection Process

# Section 1

# INTRODUCTION

Beginning in late 1974, intergranular cracks were detected in the stainless steel recirculation bypass piping and core spray piping of a number of operating BWR nuclear plants (9) by either the drywell leakage monitoring system or by a combination of in-service nondestructive evaluation (NDE) techniques such as visual inspection, ultrasonic testing (UT), dye penetrant testing (DPT), or radiographic testing (RT) (10). Metallurgical examination of cracked pipes removed from these plants indicated that the cracking appeared to be caused by a mechanism of intergranular stress corrosion. Such a mechanism is reported to result from a complex interaction among stress (including fabrication and duty-related stress), sensitization, and an oxygenated high-purity aqueous environment (11).

In late 1974 and early 1975, in order to determine the nature and extent of the problem, the Nuclear Regulatory Commission (NRC) called for special inspections of all BWRs in operation (12). The primary volumetric nondestructive examination technique for these inspections was pulse-echo ultrasonics.

Although the special inspections revealed few additional cracks, the industry was still interested in upgrading present in-service inspection techniques for detection of the specific type of intergranular stress corrosion-initiated cracking encountered in BWR piping (13). This concern first arose in 1974, when cracks in piping were discovered by means other than ultrasonics after the pipe had been inspected according to the nuclear Code requirements applicable at that time (14).

Metallurgical examinations have shown that many of these intergranular stress corrosion cracks (IGSCCs) are found near the heat-affected zone on the inside surface of the pipe (Figure 1-1). In some cases, the inside surface contains significant changes in geometry--pipe counterbore, grinding works, and weld anomalies such as drop-through and mismatch--that are near the location of the

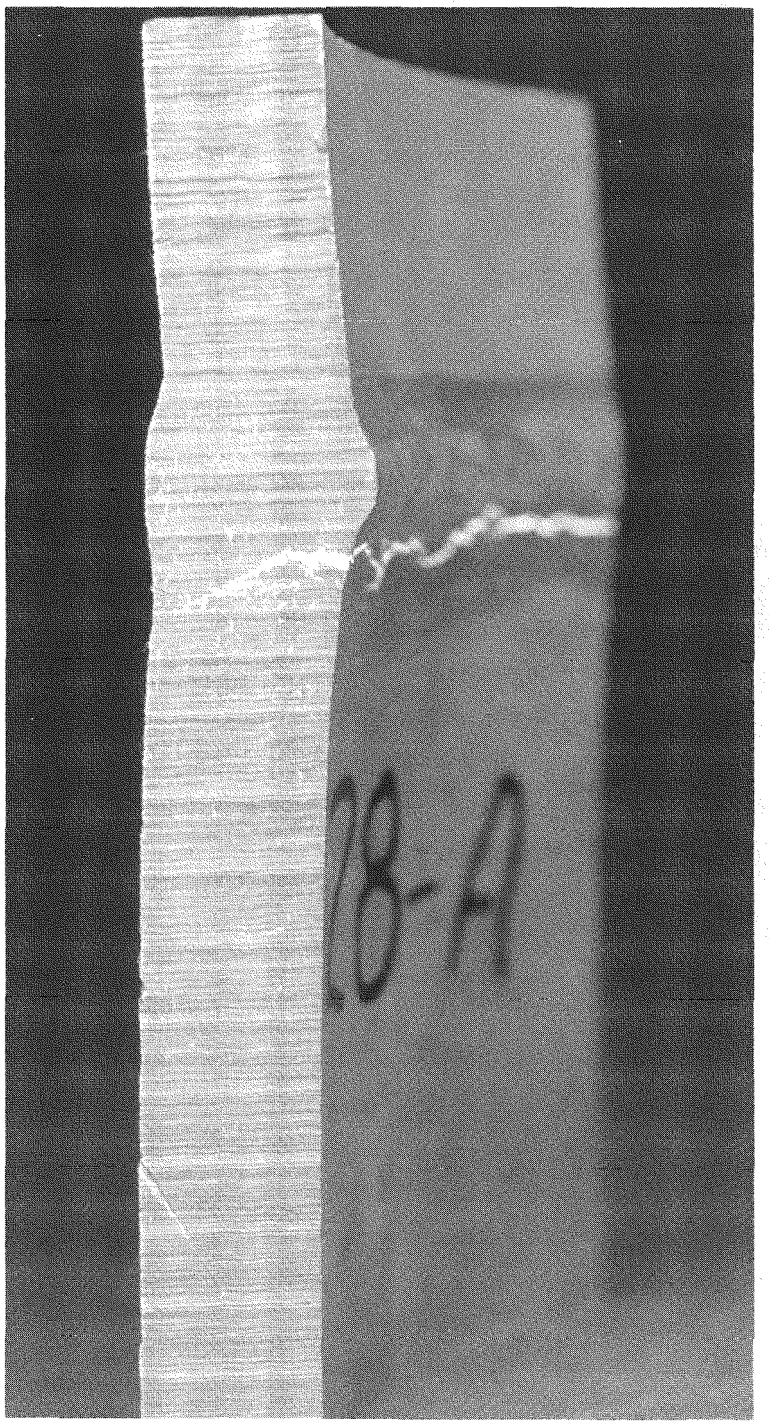


Figure 1-1 Fluorescent Dye Penetrant Indication of Intergranular Stress Corrosion Cracks in 10-in. Diameter Pipe Sample

stress corrosion cracks (10). The shapes of these geometrical changes provide ideal reflectors for ultrasonic energy.

These geometric reflectors tend to mask the reflection of ultrasonic energy from the crack to the extent that, in some cases, careful analysis must be used to distinguish the crack signals from the geometric signals. Instead of presenting the essentially straight and highly reflective surface of classic fatigue cracking (on which many NDE techniques are based), IGSCCs present a very diffuse face which follows the grain boundaries in the material and tends to provide rather poor ultrasonic response relative to typical machined calibration reflectors (Figure 1-2). This reflective characteristic of IGSCCs compounds the inspection problem because it results in lower probability of detection at equivalent fatigue crack sensitivity levels. Thus there is less margin for error in calibration sensitivity, inspection procedure, and visual interpretation of the ultrasonic signals received from an IGSCC.

Present in-service inspection practice, as required by ASME Code Section XI, uses pulse-echo ultrasonics to detect and define the nature of flaws in primary system piping (14). This technique is the most appropriate volumetric inspection method presently available. However, time has not permitted a full evaluation of detection probability for the specific type of intergranular stress corrosion cracking observed in BWR piping.

To achieve the best possible inspection, it is imperative to know how efficiently in-service inspection can detect the presence and degree of through-wall penetration of IGSCCs. The through-wall penetration of these flaws during operation is not a critical safety issue because of the design of the plant: structurally safe, leak-before-break performance has been designed into these piping systems and verified by several years of reactor operation. Nevertheless, such penetration represents a considerable loss in availability when repair and cleanup operations require plant shutdown. Thus the present ultrasonic inspection practice used for stainless steel piping should be evaluated extensively to define limitations and effect improvements.

In order to define the ability of present ultrasonic and radiographic methods to detect IGSCCs, EPRI recently completed a project that included a round robin evaluation of cracked and uncracked pipe samples by five groups who are currently providing in-service inspection services to the commercial nuclear power industry.

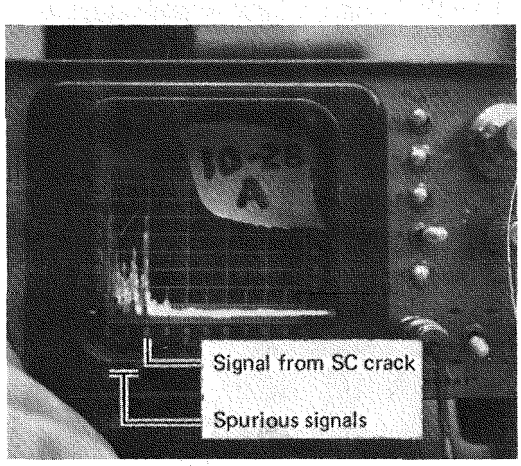


Figure 1-2 Ultrasonic Signal From Stress Corrosion Crack, Sample 1028A (IGSCC at 2 on 0 - 10 scale)

In addition to evaluation of the flaw detection and analysis capability of each inspection group, the variables studied included Code interpretation, procedures, techniques, standards, equipment, and training. The details and preliminary results of this program are presented in this report.

The initial phase of this study evaluated the inspection technique of ultrasonics; the results of this phase are summarized in this report. Since the complete in-service inspection process uses other inspection techniques to verify the results of ultrasonic inspection, a later phase of the study evaluated the performance of in-service radiography as a complement to ultrasonics. Those results will be reported separately.

The practical realism of the study was enhanced by using actual cracked bypass and core spray lines obtained from two BWRs. The flawed pipe sections were radioactive and therefore had to be examined under simulated field conditions in accordance with radiation safety work procedures.

Section 2

# PLANNING THE PROGRAM

The EPRI study was designed to evaluate current practice for in-service inspection of BWR pipe welds using ultrasonics; to gain insight into the factors affecting the performance of in-service inspection practice; to determine flaw detection probability; and to establish a baseline on which to build future research.

The inspection team's training and experience, the Code requirements, procedures, techniques, standards, equipment, and field conditions were determined to be the performance-controlling variables of an in-service inspection. To achieve a realistic simulation of an in-service inspection, each of the variables was addressed.

## INSPECTION TEAM TRAINING AND EXPERIENCE

To achieve a valid representation of industry practice, participants in the program were selected according to the following criteria:

- They must have been offering in-service inspection to the utility industry as a major activity of their organization.
- They must have been involved in the inspection of stainless steel piping in BWRs.
- They must have been involved in the special in-service inspection required by NRC in late 1974 and early 1975 (3,4).

Of eight inspection groups that satisfied the above criteria, five were selected on the basis of their more extensive involvement in BWR pipe inspections. These were:

CONAM Inspection Division, Nuclear Energy Services, Inc.
Nuclear Energy Division, General Electric Company
Nuclear Services Corp.
Peabody Testing, Division of Magnaflux Corp.
Southwest Research Institute

Since this study was designed to evaluate representative industry inspection teams and was not to be used as a training exercise or as an evaluation of inexperienced NDE personnel, certain qualifications were established for membership on each of the three-member teams.

Two members were to be Level II inspectors in ultrasonic examination, as currently defined by the American Society of Nondestructive Testing (ASNT) (15). These inspectors must have participated in actual in-service inspection of BWR piping during the calendar years of 1974 or 1975. Furthermore, at least one of these two members must have participated in the reinspection of BWR piping required by the AEC Office of Inspection and Enforcement (AEC IE) Bulletin 75-01 (3). Both must have been certified as Level II inspectors before January 30, 1975.

The third team member was to be a Level III inspector in ultrasonic examination as defined by ASNT, who had participated in actual in-service inspections of BWR piping or in the analysis of inspection data. This member must also have participated in the reinspection of BWR piping or in the analysis of reinspection data as required by AEC IE Bulletin 75-01, and must have been certified as a Level III inspector before January 30, 1975.

## INSPECTION PROCEDURES, TECHNIQUES, AND STANDARDS

To evaluate the variables associated with the application of in-service inspection, each team was requested to conduct a simulated in-service inspection using its own procedures, techniques, standards, and equipment. These inspection procedures followed the existing ASME Code Section XI requirements as of May 1, 1975.

The proposed Appendix III addition to Section XI (16) was not to be incorporated into these procedures. The volume of material inspected was to be in accordance with AEC IE Bulletin 75-01 (3). Choosing the specific methods of inspecting this volume of material was left to the individual inspection team.

Each group was asked to perform these inspections using the same personnel, procedures, techniques, standards, and equipment that would be used to perform an actual in-service inspection of a nuclear reactor for the utility industry if contracted to do so at the time of the study.

## SIMULATED FIELD CONDITIONS

The following procedures were followed in order to simulate actual field conditions:

- BWR pipe samples containing actual IGSCCs were selected for inspection. To permit access to the outside surface only, the samples were either closed at both ends or mounted on wooden pallets (figures 2-1 to 2-4). A number of nonflawed samples were also included for inspection.
- Although decontaminated, the pipe samples retained some degree of residual radioactivity. For this reason the inspectors wore full anti-contamination clothing, including cloth overalls, cap, shoe covers, and gloves (Figure 2-5).
- To further simulate field conditions, a time limit was placed on the evaluation of each set of samples.

All tests were conducted in a radioactivity control area at the Vallecitos Nuclear Center of the General Electric Company, Pleasanton, California (see Figure 2-6).

## TEST SAMPLES

The test samples used in this program are described in detail in Appendix A. They contained circumferential pipe welds in the following pipe sizes:

- 10-inch, schedule 80, Type 304 stainless steel (SS) seamless piping (nominal wall thickness 0.594 in.). These samples were cut from the core spray line of the primary system of an operational BWR (figures 2-7 and 2-8).
- 4-inch, schedule 80, Type 304 SS seamless piping (nominal thickness 0.337 in.). These pipe samples were cut from the bypass line of the primary system of an operational BWR (Figure 2-9).

## LABORATORY EXAMINATIONS

Before the study began, each sample was examined by pulse-echo ultrasonics using longitudinal wave and various angles of shear wave inspection techniques. Dye

Figure 2-1 Typical 360° Section Test Sample, 10-in. Diameter

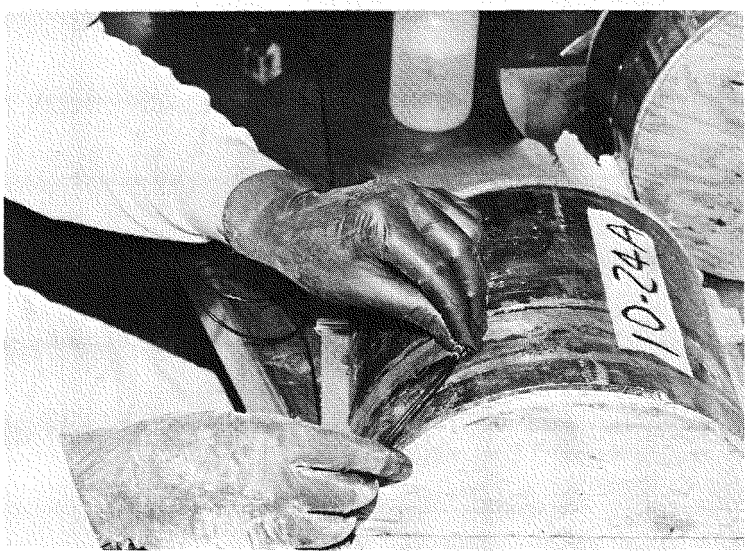


Figure 2-2 Typical 180° Section Test Sample, 10-in. Diameter


Figure 2-3 Typical 36° Section Test Samples, 10-in. Diameter

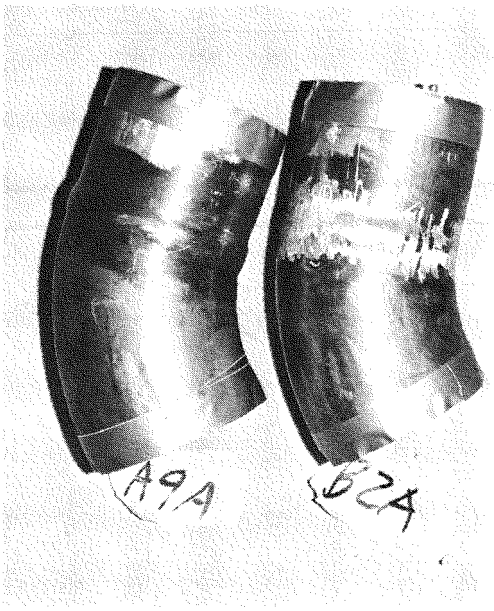


Figure 2-4 Test Samples, 4-in. Diameter

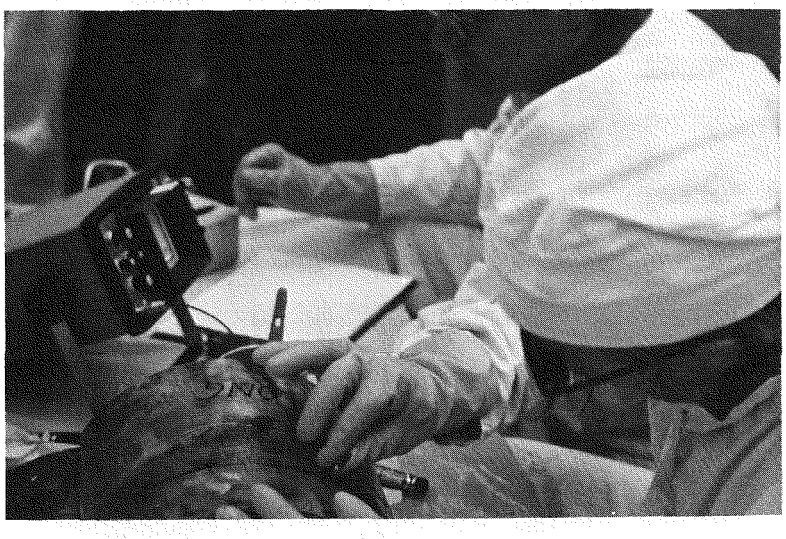

Figure 2-5 Test Conditions During Simulated Inspections

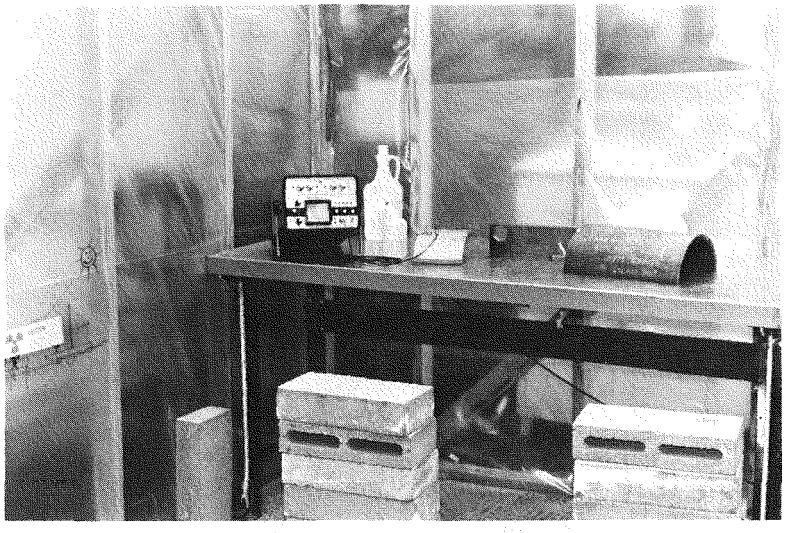

Figure 2-6 Pipe Inspection Work Area, GE Vallecitos Nuclear Center

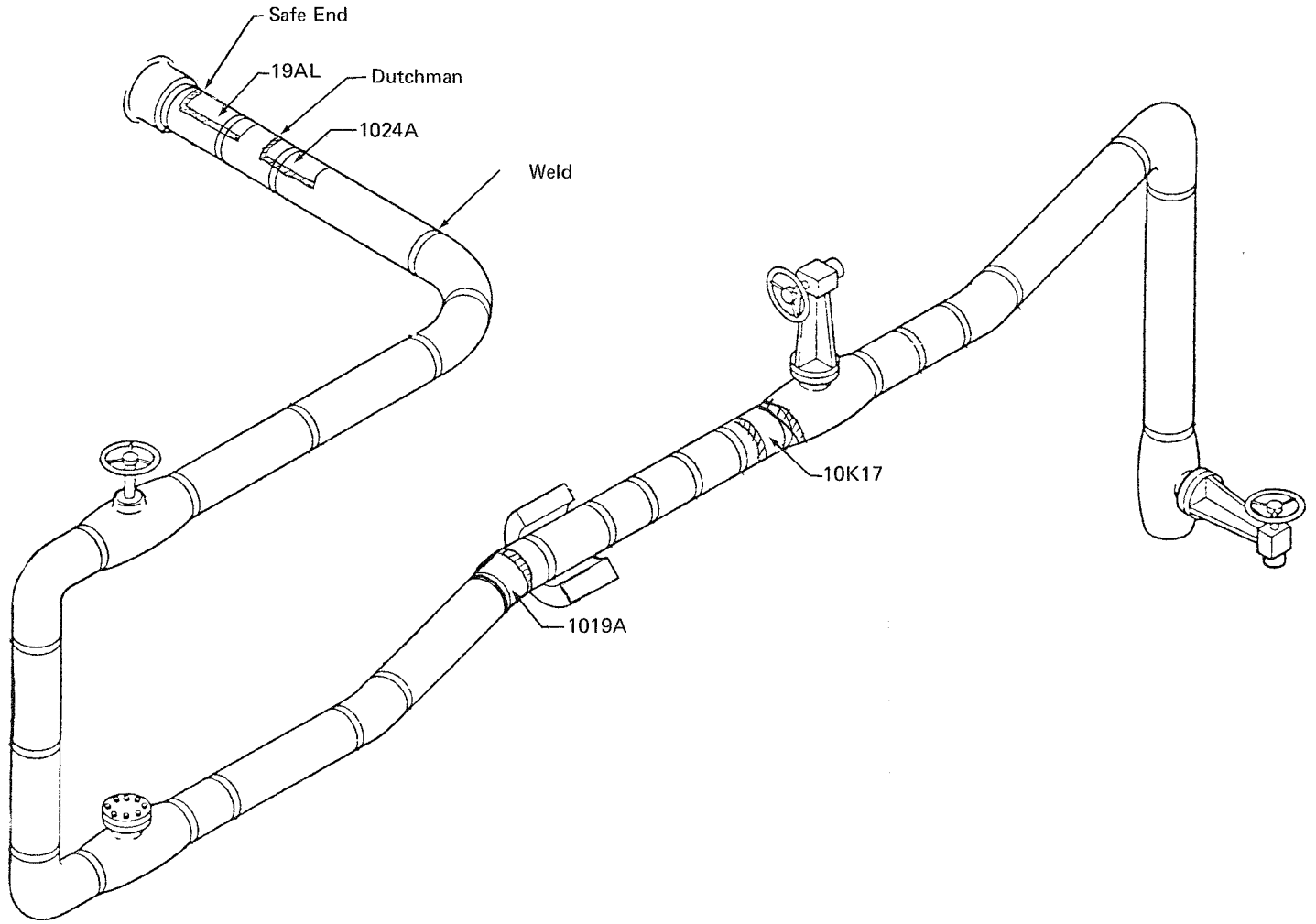


Figure 2-7 Origin of Test Samples From Core Spray Line, Loop A

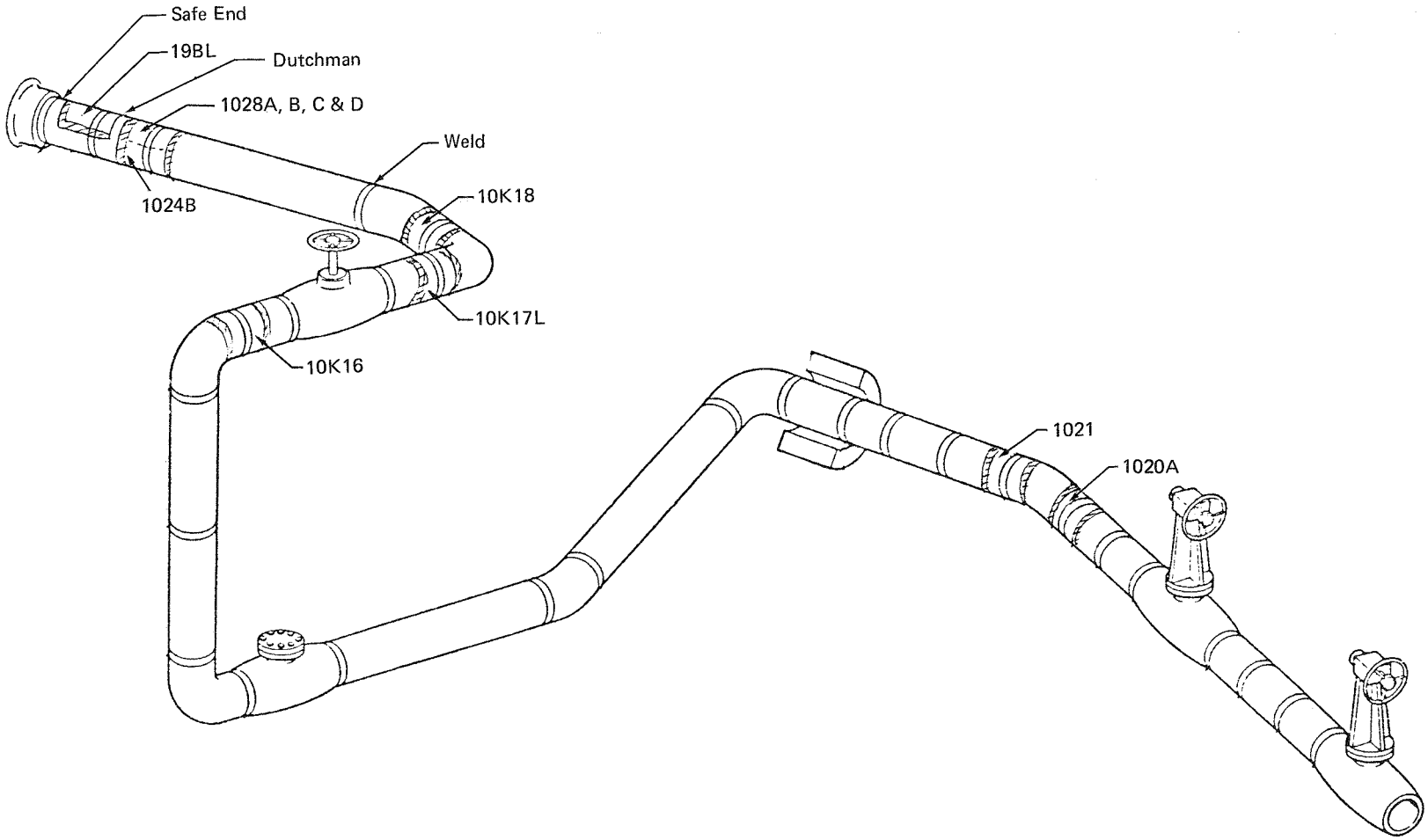


Figure 2-8 Origin of Test Samples From Core Spray Line, Loop B

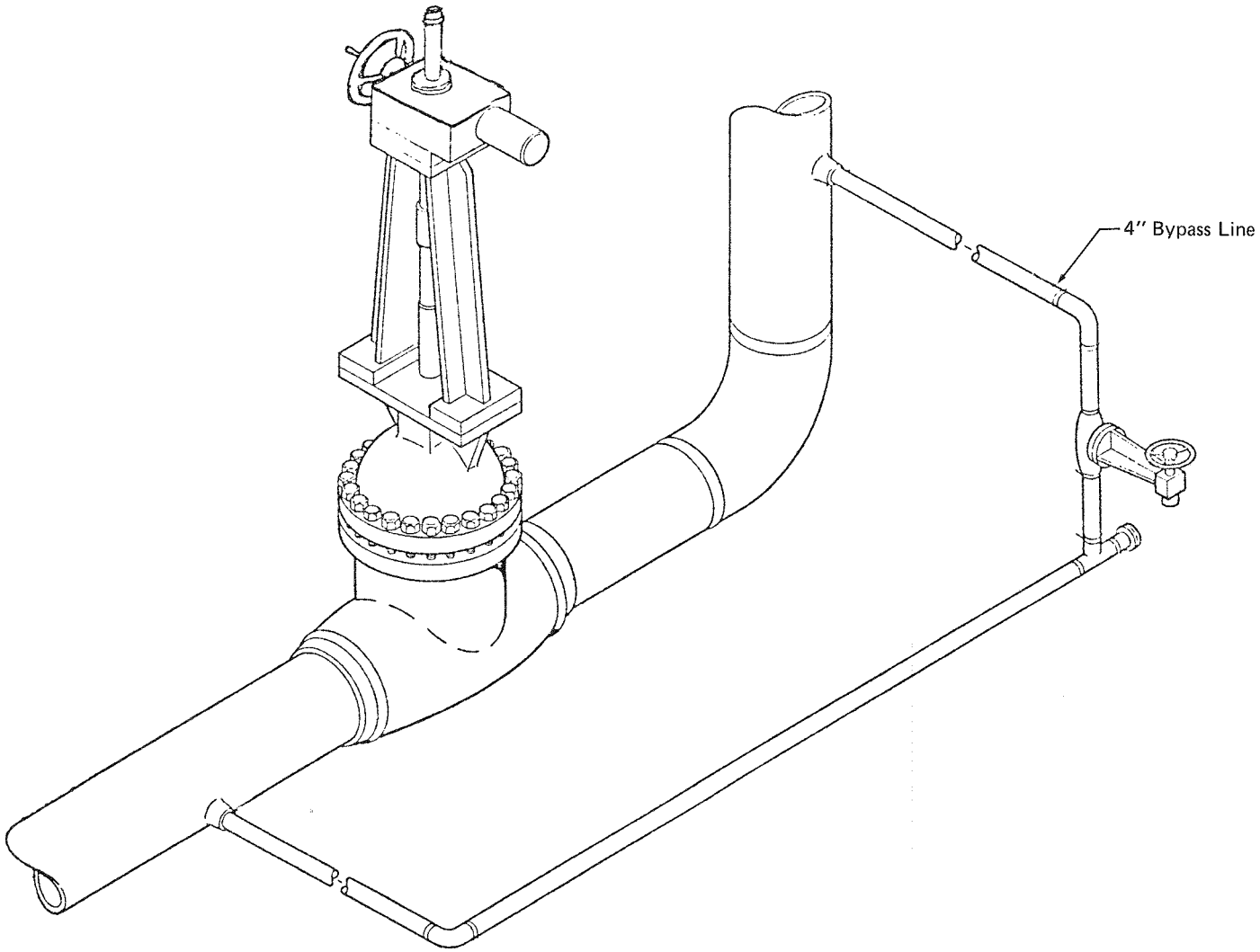


Figure 2-9 Origin of Test Samples From Recirculation Bypass Lines, Loops A and B

penetrant inspection was performed on the inside surface of each sample. The approximate depth of flaws was determined using an electric resistance gauge (ERG). Wherever possible, supplemental volumetric NDE was performed with radiography ($Ir_{192}$ and X-ray). Limited metallurgical examinations were also carried out on material cut from a number of samples to confirm the presence of IGSCCs. To aid in evaluating the flaw-locating accuracy of each group, a reference mark was stamped on the centerline of each weld. The groups were instructed to make all measurements from this reference mark for plotting data on specially prepared data forms.

A summary of the configuration and results of laboratory nondestructive evaluation is shown in Table 2-1. Samples 1021 and 10K18 contained flaws that could not be differentiated from lack of fusion without destructive examination. Sample 10K17L also contained two pinpoint indications (by dye penetrant) that would require metallurgical examination before positive flaw identification could be made. Sample 1024A contained a number of cracks skewed at approximately 45° to the centerline of the weld. These cracks were extremely difficult to detect by the normal field inspection procedures of scanning parallel and perpendicular to the weld. A final analysis of the above flaws is given in Section 5, "Destructive Examination," and in Appendix D.

The cracks in samples 1028A, 1028B, and 1024A were all assumed to be caused by intergranular stress corrosion, since metallurgical examinations of flaws in sections of pipe cut from the end of each of these samples proved them to be stress-corrosion type flaws. The tight, irregular nature of the through-wall crack in sample 19AL also appeared to be caused by intergranular stress corrosion. Although this was a through-wall crack, it was difficult to find by normal inspection procedures because its location was approximately 1.00 in. from the weld centerline and its orientation was perpendicular to the weld centerline.

Unfortunately, several additional samples containing IGSCCs were dropped from the test program because the pipe weld had been cut through the weld centerline for removal from the primary system. This cut area reflected sonic energy and tended to mask the signals from the IGSCC cracks. Most of the samples containing these cuts were of the 4-in. diameter size. The round robin evaluation was primarily, then, an evaluation of 10-in. diameter pipe.

Table 2-1
Laboratory Nondestructive Evaluation of Test Samples[a]

| *SAMPLE IDENTIFICATION AND NOMINAL PIPE DIAMETER, IN.* | *DESCRIPTION* | *DYE PENETRANT (PT)* | *SHEAR WAVE ULTRASONIC ANALYSIS (UT)* | *RADIOGRAPHIC CONFIRMATION (RT)* |
|---|---|---|---|---|
| 19AL, 10 | Dutchman to safe end, welds ground flush ID and OD | Through-wall axial[b] crack 1.25 in. on ID by 0.60 in. on OD, SCC | Signals from two sources, one confirmed, one unconfirmed, high amplitude signals | Through-wall flaw agrees with UT and PT , easy to read, possible second crack |
| 1028A, 10 | Dutchman to pipe weld, considerable drop-through, is partially ground | Radial[c] crack completely across sample, confirmed as SCC, depth of 0.12-0.5 in. by electric resistance gauge (ERG) measurement[d] | High amplitude signals from flaw, several spurious signals | Good agreement with PT, easy to read |
| 1028B, 10 | As above | Three short radial cracks 1 in. long continuation of the cracks in 1028A; confirmed as SCCs, depth of 0.10 in. by ERG | High amplitude signal from flaw, spurious signals from weld root | Good agreement with PT, easy to read |
| 1024A,10 | Dutchman to pipe weld, partially ground crown | Eight cracks detected, one axial, one radial, the rest skewed at 45°. Very tight cracks. All are considered SCCs. Depths by ERG are 0.10 to 0.12 in. | Extremely difficult to find and characterize all cracks. Transducer must be oscillated ±45° into weld to detect skewed cracks | Majority of flaws confirmed but very difficult to read |
| B2A, 4 | Pipe to elbow, welds ground smooth, sharp counterbore on ID | Two small indications analyzed as possible SCCs[f] | Low amplitude signals from flaw, many signals from geometry | Not performed |
| 10K18,10 | Pipe to 90° elbow, partially ground crown | Intermittent radial indications, one crack confirmed UT indications, 0.03 to 0.06 in. depth by ERG[e] | Many geometric indications, two evaluated as possible radial cracks, difficult to UT | Sharp reentry, lack of fusion |
| 1021, 10 | Elbow to pipe weld, crown is partially ground | Straight radial indication, ~7.87 in. long, possible lack of fusion[e] | Series of high UT signals correspond to PT indications, several unconfirmed signals | Long cracklike indication confirms PT |
| 10K17L, 10 | Pipe to 90° elbow, partially ground crown | Two small spots with possible radial interconnecting crack 1.50 in. long; internally ground area | Many geometric signals, UT signals agree with PT indications, very difficult to UT | Sharp undercut |
| 10K17, 10 | Pipe to pipe | No indications | Geometric signals completely around weld | Undercut and sharp reentry |
| 1020A, 10 | Pipe to elbow | No indications | Limited number of geometric signals[g] | Not performed |
| 1024B, 10 | Dutchman to pipe | No indications | As above | Not performed |
| 1028C, 10 | Dutchman to pipe weld, considerable drop-through, is partially ground | No indications | Spurious signals from weld root | Sharp reentry or root crack |
| 1028D, 10 | As above | No indications | As above | As above |
| 1019A,10 | Pipe to elbow, unground crown, extreme suck-up on ID | No indications | Few indications | Porosity, linear indications, suck-up |
| 19BL,10 | Dutchman to safe end, welds ground flush, ID and OD | No indications | Many geometric indications, time consuming to record, plot, and evaluate[h] | Appears clean |

[a] See Table 6-2 and Appendix D for final analysis of specimens

[b] Axial crack is perpendicular to weld centerline

[c] Radial crack is parallel to weld centerline

[d] Confirmed IGSCC by destructive test (DT)

[e] Lack of fusion confirmed by DT

[f] Single porosity confirmed by DT

[g] Root overlap of weld confirmed by DT

[h] Fabrication defect interpreted from DT

After the teams completed the study, the samples were descaled, decontaminated, and reexamined by dye penetrant, ultrasonics, and radiography. They were then selectively sectioned and examined by metallographic techniques. The results of this effort are discussed in a later section (see Table 6-2 and Appendix D).

## Section 3

## STEPS IN THE STUDY

In order to evaluate the many aspects of in-service inspection, the study was divided into three phases.

### PHASE A

In this phase, the inspection teams were asked to supply their own procedures and equipment to perform the simulated in-service inspection. The main objective of this phase was to determine the present inspection practice and performance of representative industrial inspection groups. The inspection groups were permitted to use their own data forms for recording information but were requested to plot their final results on an inspection summary form supplied by EPRI (see Appendix B). The teams were also asked to make a decision on whether or not each sample was cracked and to state this decision on the EPRI form. The teams were to perform the simulated inspection just as they would for a contracting utility.

### PHASE B

All pipe samples were reinspected by the teams, using uniform procedures, techniques, standards, and equipment determined and supplied by EPRI. The objective of this phase was to determine inspection team performance by eliminating the variables of different procedures, equipment, and standards.

The inspection procedure (shown in Appendix B) was written as a two-part process: detection and analysis. The detection phase consisted of a rapid scan of the pipe samples to locate areas for further investigation. The analysis phase consisted of an in-depth reinspection of each area suspected of containing a flaw.

The technique used for the detection phase was contact pulse-echo 45° shear wave ultrasonics. The transducer was unfocused, 0.25-in. diameter, 2.25 MHz. Plexiglass wedges were used to mode convert and transmit the sound into the steel. Glycerin was the couplant.

For the analysis phase, a focused transducer was used. The size of the transducer and wedge as well as the couplant and frequency remained the same. During this phase the groups were also allowed to record wall thickness measurements with a longitudinal wave transducer.

The standards used for this evaluation were supplied by EPRI. The primary calibration reflector was a notch machined on the inside surface of the standard to a depth of 3% of the pipe wall thickness (T). An additional 3% T notch was placed on the outside surface. To allow calibration for both directions of scan (into the weld and around the weld), notches were machined in both axial and radial directions. To correlate this calibration sensitivity to existing Code requirements, side-drilled holes were also machined in the standard. Their response with respect to the notches was recorded prior to each inspection. The standard for the 10-in. pipe is shown in Figure 3-1.

The procedure, standards, and techniques used in Phase B reflected input from laboratory studies conducted by the Nondestructive Testing Unit of the Development Engineering Section, General Electric Company, and by two consultants to EPRI (Battelle, Columbus Laboratories and Argonne National Laboratory). Portions of the new proposed Appendix III addition to Section XI (16) were also incorporated into the procedure and design of the standard. A notable exception was the use of 3% T calibration notches in the EPRI standard rather than the 10% T notches shown in the Appendix III addition to ASME Code Section XI (Table III-3430). This was done to ensure that the inspection would be sensitive enough to detect all the flaws examined in the laboratory studies. One drawback of this increased sensitivity is the subsequent increase in the number of spurious signals requiring analysis. This might tend to cause an inspector to call an unflawed pipe cracked.

Before beginning the study, EPRI consultants conducted a one-week trial evaluation at the test site to determine logistics and to test the performance of the Phase B procedure.

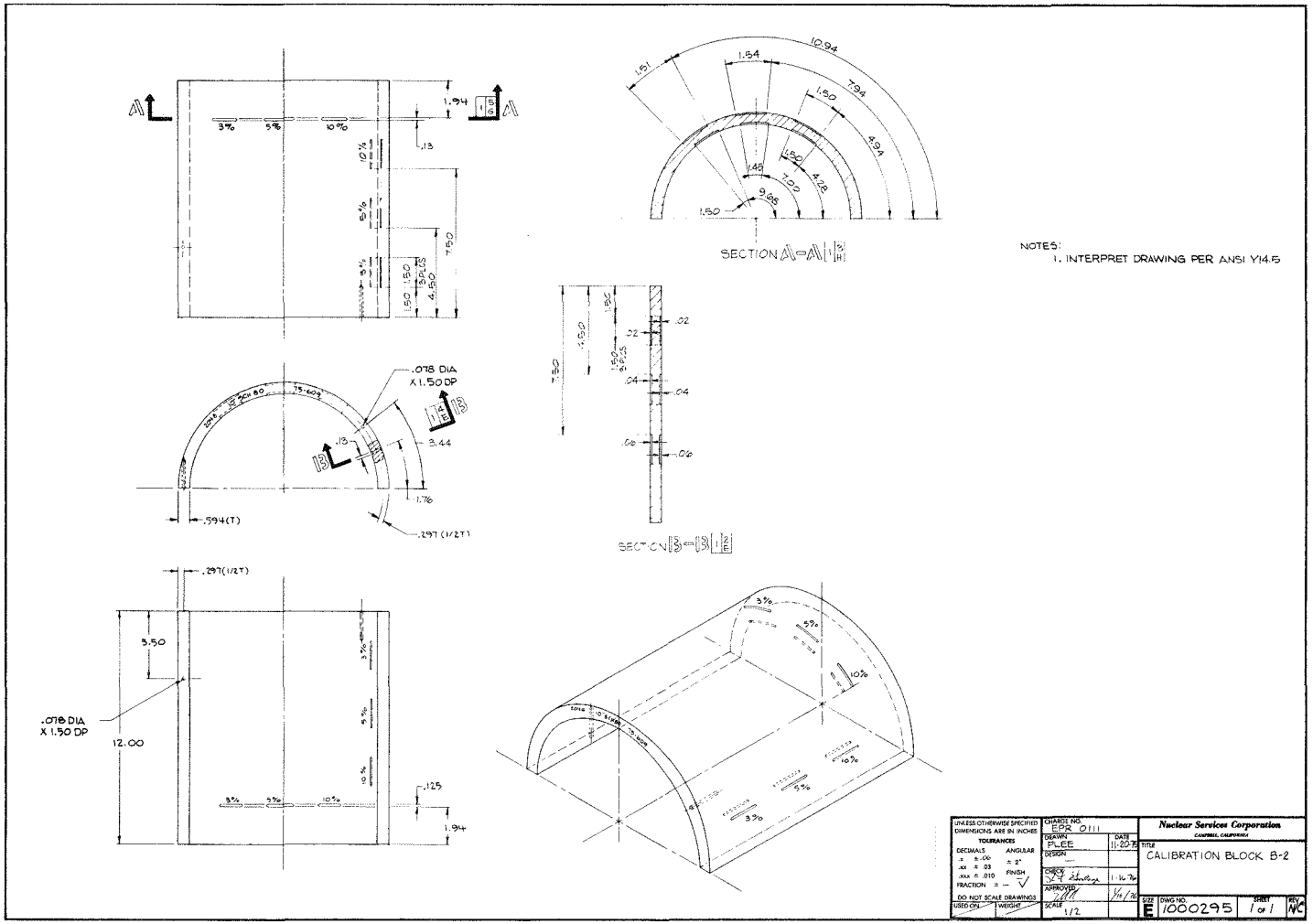


Figure 3-1 EPRI 10-in. Standard

It should be emphasized that the Phase B procedure was used primarily to reduce the variable of procedure difference among the teams; it was not intended as a recommended procedure for field use.

The use of 0.25-in. diameter transducers in Phase B reflects an attempt to standardize the inspection techniques of each team for the purposes of the study; these should not be considered as recommended transducers for all field use. This philosophy has one notable exception, however. Because of the raised weld crown in many of the samples, the small size of the 0.25-in. diameter search unit (transducer and shoe) allowed the ultrasonic sound beam to be directed at the location of suspected corrosion cracks in all samples. Detection of all the suspected flaws using a larger transducer, such as 0.50-in. diameter, was difficult because of physical interference of the raised weld crown with the front edge of the shoe. The smaller shoe may be more difficult to use in actual field inspection because of smaller area coverage and difficulty in handling during manual inspections. However, the smaller shoe did ensure that each team in Phase B had a chance to detect all the suspected flaws and was not restricted by shoe geometry.

An important aspect of the procedure used in Phase B was the requirement that the inspectors oscillate or skew the transducers approximately 45° to either side of a line perpendicular to the weld for scans into the weld. A similar rotation was required on scans parallel to either side of the weld. This method of scanning is described in Appendix B.

The scan method described above was required in order to test the effectiveness of extreme transducer rotation for detecting IGSCC flaws oriented at 45° to the weld centerline. During the laboratory studies, UT detection of these flaws was effective only when the transducer was positioned normal to the flaw orientation (that is, at 45° to the weld).

Prior to testing the specimens in Phase B, each team was given time to become familiar with the instrument, the calibration standard, and the test procedure.

PHASE C

This phase of the study examined the variability in response from various field calibration standards. Since this phase is significantly different from the simulated field inspections, and since the results have been only partially analyzed, this phase will not be discussed further in this report.

Section 4

# CONDUCTING THE STUDY

All simulated inspections were conducted during August and September 1975. The general schedule is shown in Table 4-1. Throughout the simulated inspections, a test monitor remained at the site to coordinate the inspections, collect data and field reports, and observe the performance of the various inspection teams.

The test teams were each given a specified number of samples and allowed a definite time period to evaluate them. The samples were then removed and replaced by a new set. Between phases A and B, the samples were disguised and given new identification, and the composition of each set was changed. The teams were not told that they were in fact conducting two evaluations of the same set of test samples. Although some samples were undoubtedly recognized during the second phase of the study, the subtle differences in data and results obtained by the teams indicate that each sample was actually evaluated using two separate procedures. The observations of the test monitor also tend to confirm this opinion.

At the end of each inspection day, all data were collected by the test monitor. At the end of each phase, all data were transferred by the teams to summary data sheets (supplied by EPRI) and given to the test monitor. A brief discussion of the results was then conducted with each team prior to initiating the next phase. Besides providing a preliminary evaluation of each group's performance, these debriefings yielded valuable insights into the current inspection philosophy in the nuclear industry.

Table 4-1

TEST SCHEDULE

| | Phase | Day | Event |
|---|---|---|---|
| A. | Participants' Procedure | 1 | Briefing, setup, calibration, and initial limited inspection |
| | | 2-4 | Simulated inspections |
| | | 5 | Analysis and preparation of a field report and discussion of results |
| B. | EPRI Procedure | 6 | Briefing, setup, calibration, and initial inspection |
| | | 7 | Break |
| | | 8 | Simulated inspections |
| | | 9 | Field report and discussion of results |
| C. | Evaluation of Calibration Standards | 10 | Comparative testing of field calibration standards; decontamination and removal of test equipment |
| | Debriefing on All Phases | 11 | Final discussion of the study, conducted at EPRI |

Section 5

# DESTRUCTIVE EXAMINATION

To determine the actual depth, orientation, shape, and nature of the flaws in the test specimens accurately, a destructive examination of the test specimens was conducted at Battelle, Columbus Laboratories (BCL). Since the test specimens have considerable value, both for future use in technique and procedure improvement and as training samples, the sectioning was performed in a manner that allowed portions of flawed specimens to remain for later studies. For example, the long radial flaw in specimen 1024A was sectioned in such a way that two pieces remained that were still amenable to ultrasonic shear wave scan. The destructive examination was conducted primarily on those specimens initially defined as flawed by the laboratory tests at the GE Vallecitos facility (shown in Table 2-1). Complete details and results of the destructive examination are included in Appendix D.

In addition, specimens thought to be defective by more than one of the five inspection groups were extensively reinspected and then sectioned. To confirm the initial laboratory studies further, all specimens, identified as cracked or not, were descaled and extensively reinspected.

The destructive examination process followed three steps:

1. Decontamination and descaling. The components were decontaminated and descaled in an alkaline permanganate-ammonium citrate descaling solution to reduce the level of radioactivity below 50 mr gamma and 200 mr beta at surface. The following procedure was used:

    a. Soak 1 hour in a solution containing 100 g/liter NaOH and 30 g/liter $KMnO_4$ at a temperature just below boiling.

    b. Rinse in water.

c. Soak 1 hour in a solution containing 100 g/liter $(NH_4)_2HC_6H_5O_7$ (ammonium citrate) at a temperature just below boiling.

d. Scrub and rinse.

e. Repeat procedure if necessary.

2. Nondestructive characterization. Before the samples were cut and/or broken, the following nondestructive examinations were performed:

a. Radiography (RT). The samples were radiographed by optimized X-ray procedures to assure the maximum contrast and detailed resolution in the vicinity of the detected cracks. In particular, single-wall techniques were used, with film in the ID and the source outside the pipe. A large source-to-film distance was used to assure a minimum of geometric unsharpness. Hand processing and high resolution films were used in all cases. With these procedures, a sensitivity of 0.7% was achieved.

b. Electric Resistance Gaging (ERG). The depth of cracks was assessed with electrical resistance measurement techniques. Where possible, at least four sets of readings were made at each crack location, one set orthogonal to the other three. Thus, the effective resistivity in the immediate vicinity of the crack was measured, and then the deviation from this reading caused by the interruption of the current flow by the transverse orientation of the crack was determined (Figure 5-1).

As specimens were sectioned and actual crack depths determined, a relationship between ERG readings and actual crack depth developed. This correction factor was used to estimate crack depth for all unsectioned flaws (see Appendix D).

c. Liquid Penetrant Examination. The surface contour of the cracks was recorded by photographing the liquid penetrant indications present after the descaling operations. This was done because previous experience with detection of IGSCCs by the penetrant method has indicated a strong possibility that flaws may be masked by scale on the pipe. This indication proved accurate in the case of specimen 1024A, in which additional flaws were found after the descaling operation (figures 5-2 to 5-6).

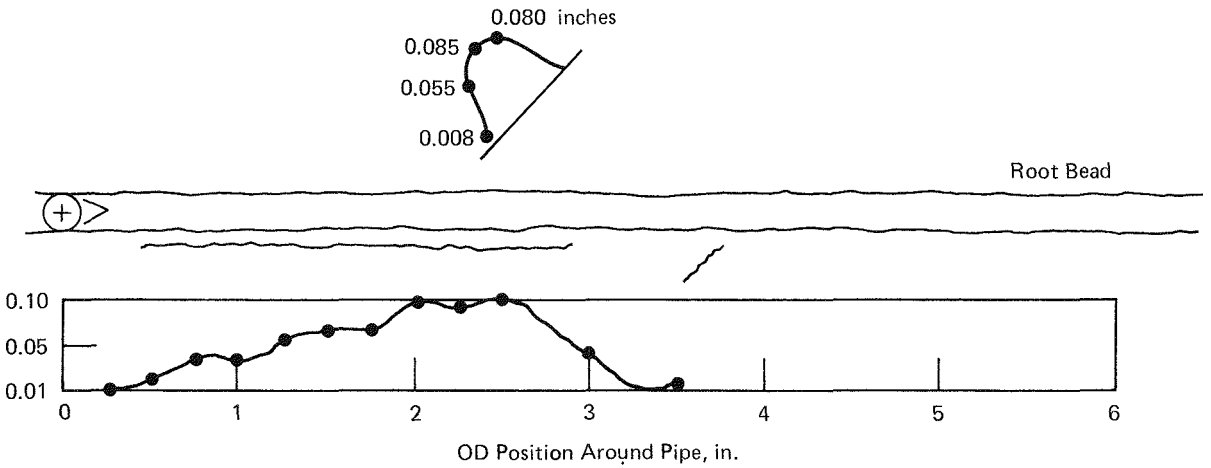


Figure 5-1 Electric Resistance Gauge (ERG) Data Plots for Specimen 1024A

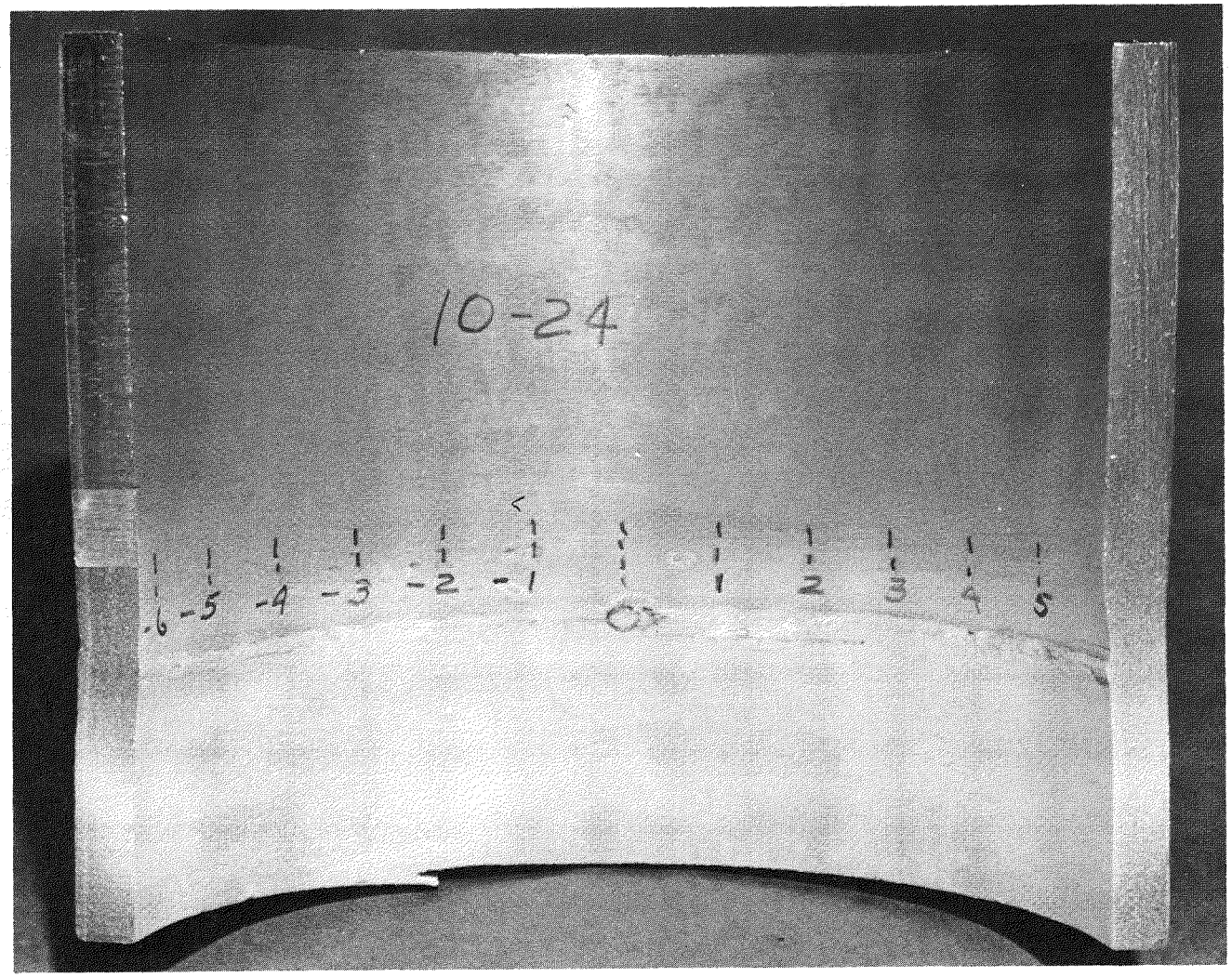


Figure 5-2 Inside Surface of Test Specimen 1024A

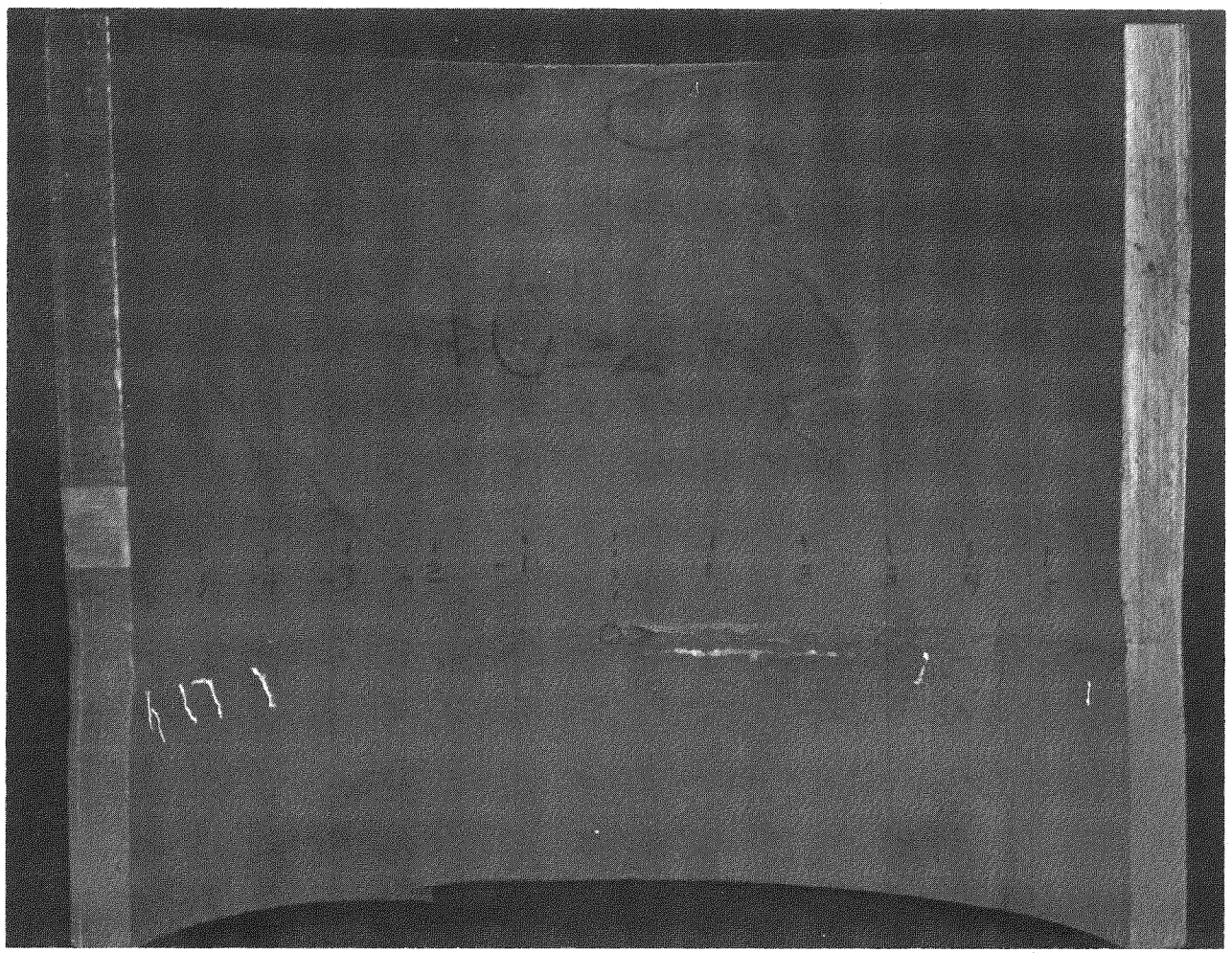

Figure 5-3 Fluorescent Dye Penetrant Indications, Specimen 1024A

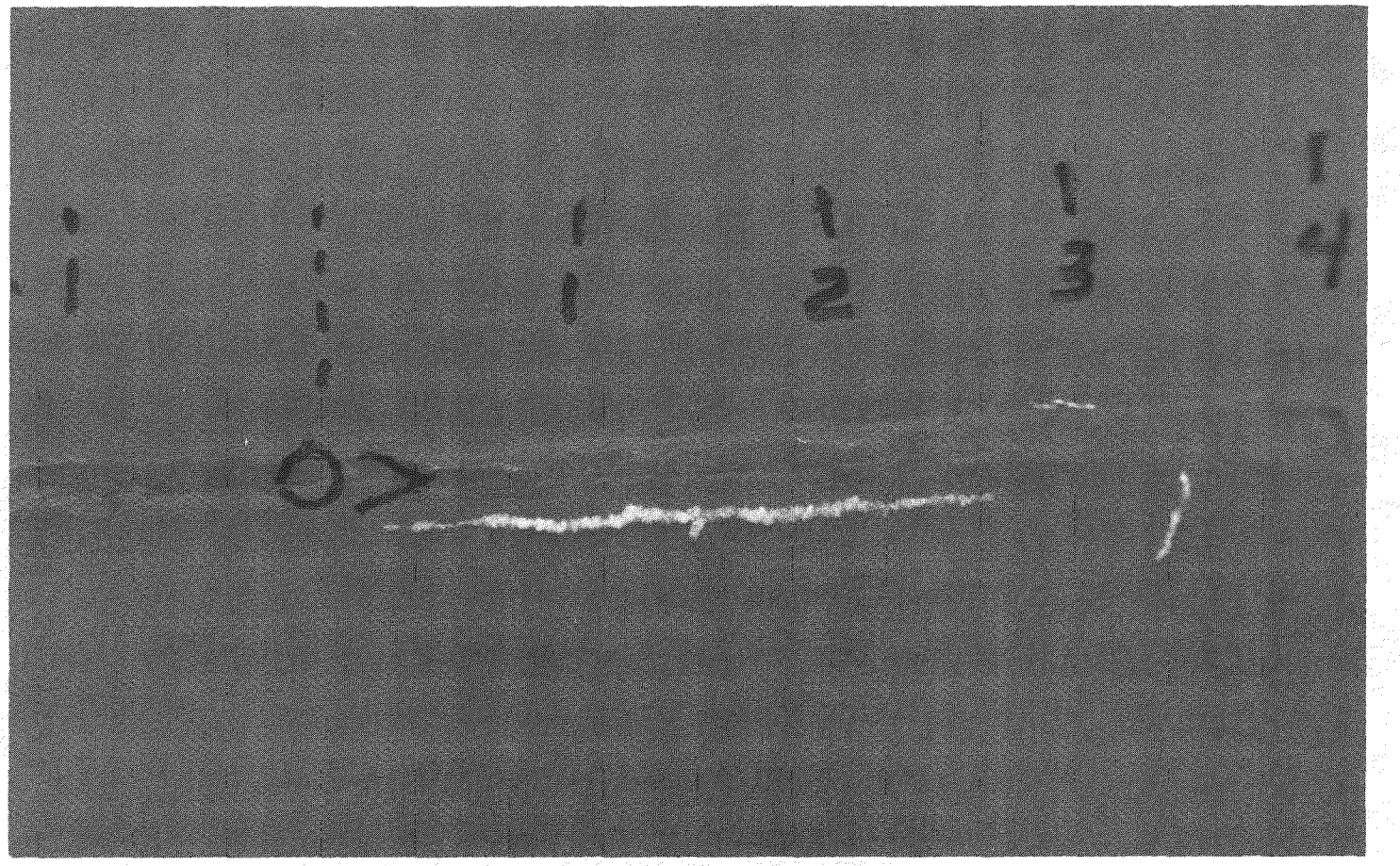

Figure 5-4 Fluorescent Dye Penetrant Indications of Two Radial Cracks and One Axial Crack (Slightly Skewed), Specimen 1024A, 0 to +4 in.

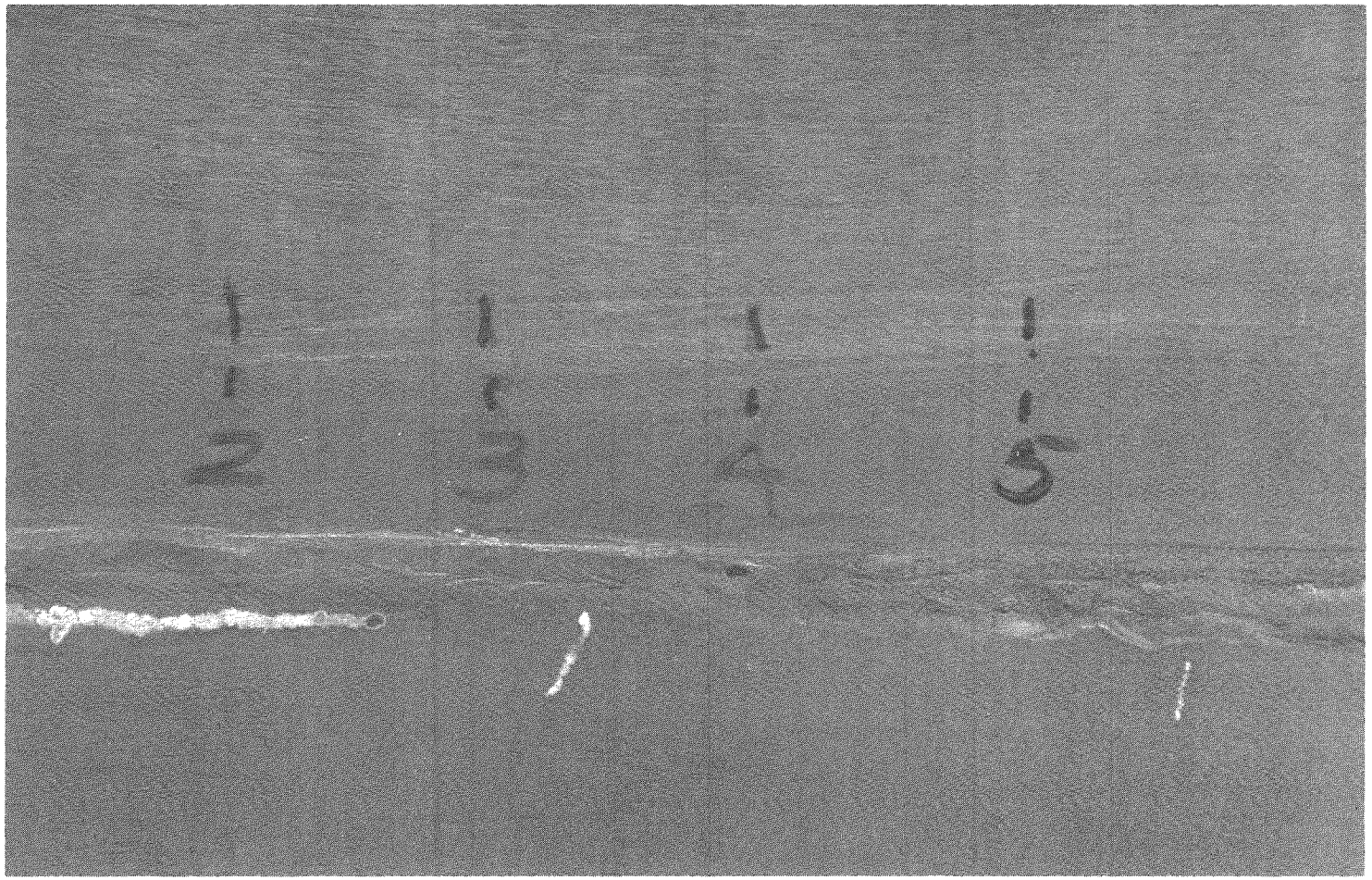

Figure 5-5 Fluorescent Dye Penetrant Indications of Radial and Axial Cracks in Specimen 1024A, +1 to +6 in.

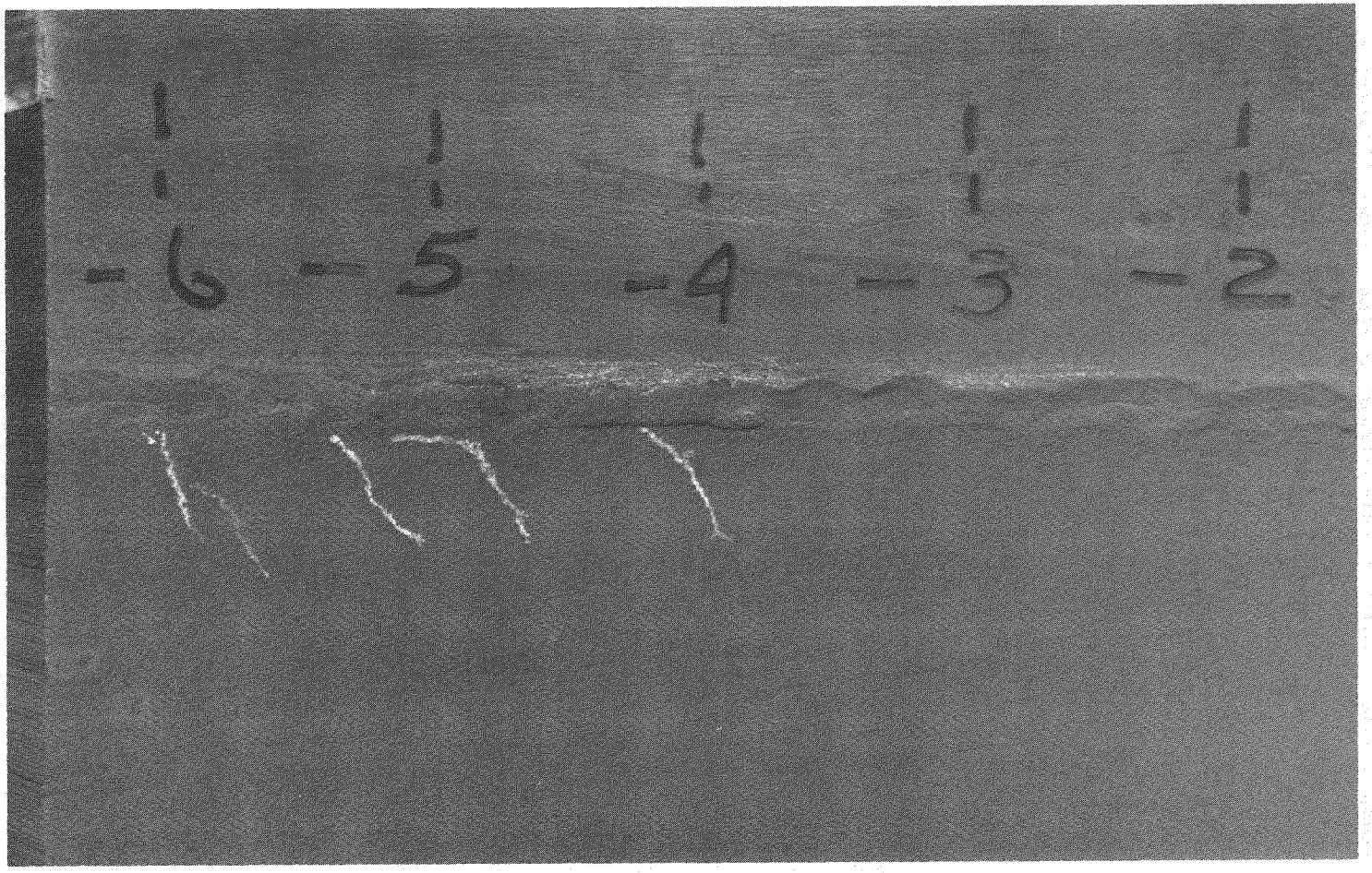


Figure 5-6 Fluorescent Dye Penetrant Indications of Five Skewed Cracks in Specimen 1024A, -1 to -6 in.

d. Ultrasonic Characterization. The patterns of ultrasonic signals received from the cracks within the pipes were recorded as follows:

(1) The transducers used for the characterization were profiled by plotting on a continuous basis the signal amplitude received from the side-drilled hole (SDH) in the EPRI calibration block. The transverse beam profile was taken similarly, using a through-wall hole of the same dimension.

(2) The characterizations were made using a 0.25-in. diameter, 2.25 MHz, 45° shear wave transducer. Additional data were acquired using 45° shear wave transducers with diameters of 0.375 in. and 0.5 in.

(3) System sensitivity was set according to the requirements of ASME Code Section XI and relatable to a standard International Institute of Welding (IIW) block containing SDH.

(4) All recordings were expressed in terms of percents of DAC (distance-amplitude-correction). Cathode ray tube displays were video recorded in selected intervals to show both transducer position and CRT display. Figures 5-7 to 5-10 show typical scan patterns and experimental results.

(5) All readings and measurements were made with hand-held techniques to assure maximum contact and optimum angulation for maximization of echo amplitude.

(6) Plots were made of the measured signal responses in such a manner that crack location with respect to weld location was shown, as well as variation in signal height along with the length of the crack (see Appendix D).

3. Metallographic characterization. After the nondestructive characterization had accurately located the flaw, a metallographic examination was conducted according to the following steps:

a. ID surface was examined at 15X and 20X.

b. Crack areas were sawed out and photographed at 8X to 100X (Figure 5-11).

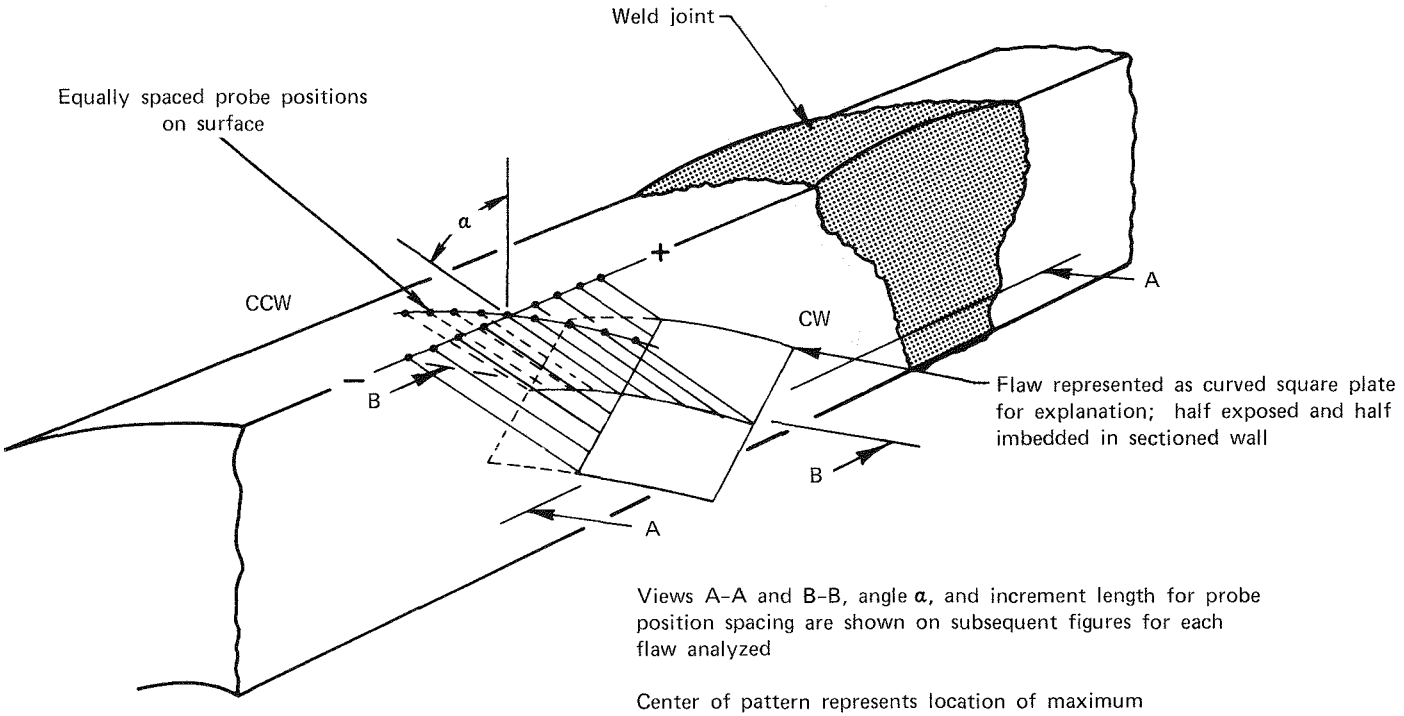


Views A–A and B–B, angle α, and increment length for probe position spacing are shown on subsequent figures for each flaw analyzed

Center of pattern represents location of maximum ultrasonic indication

+ and – indicate longitudinal direction, + = toward weld

CW and CCW indicate clockwise and counterclockwise circumferential direction

Figure 5-7 Ultrasonic Scan Method

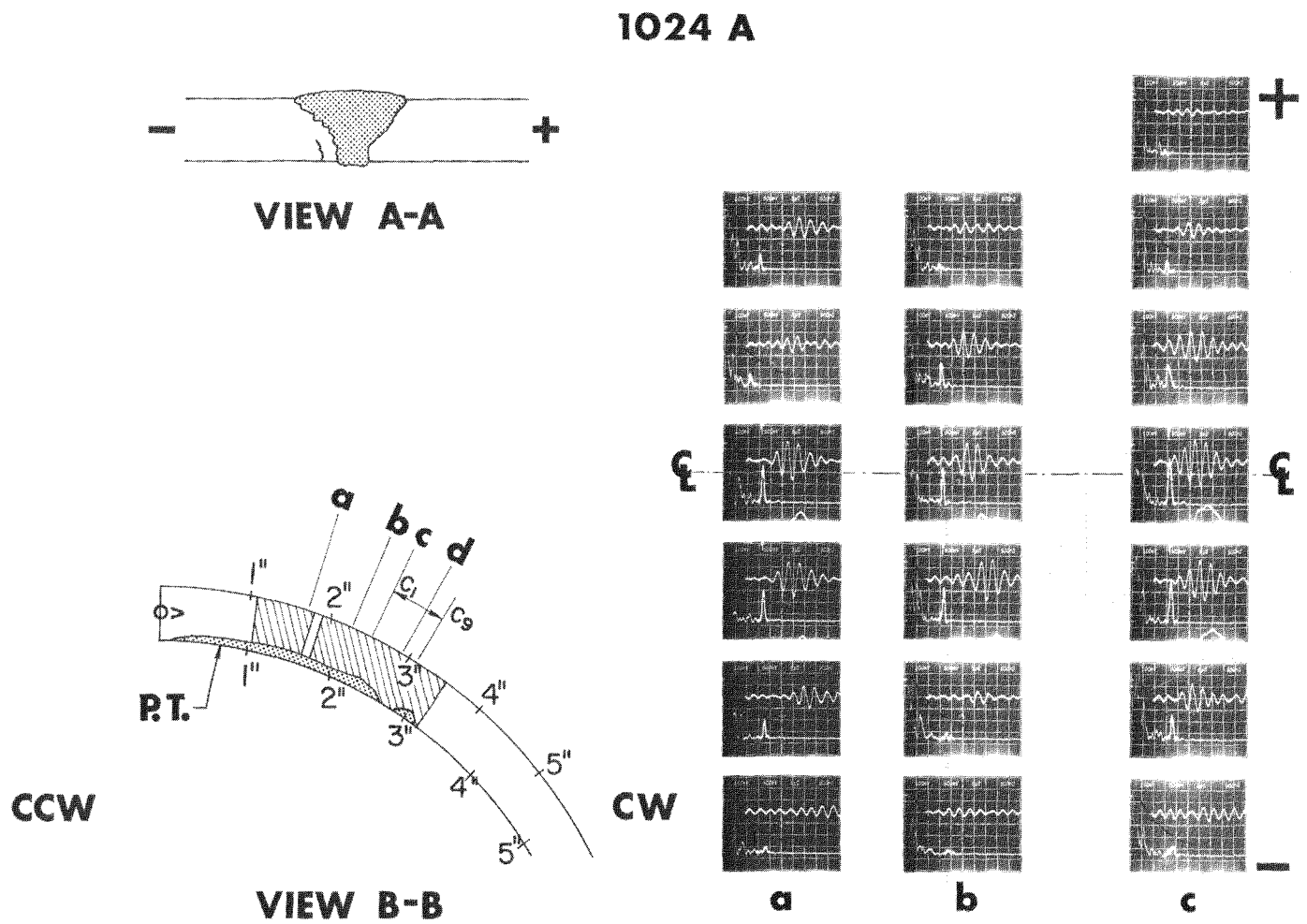


Figure 5-8 Ultrasonic Data From Scans a-c of Radial IGSCC in Specimen 1024A

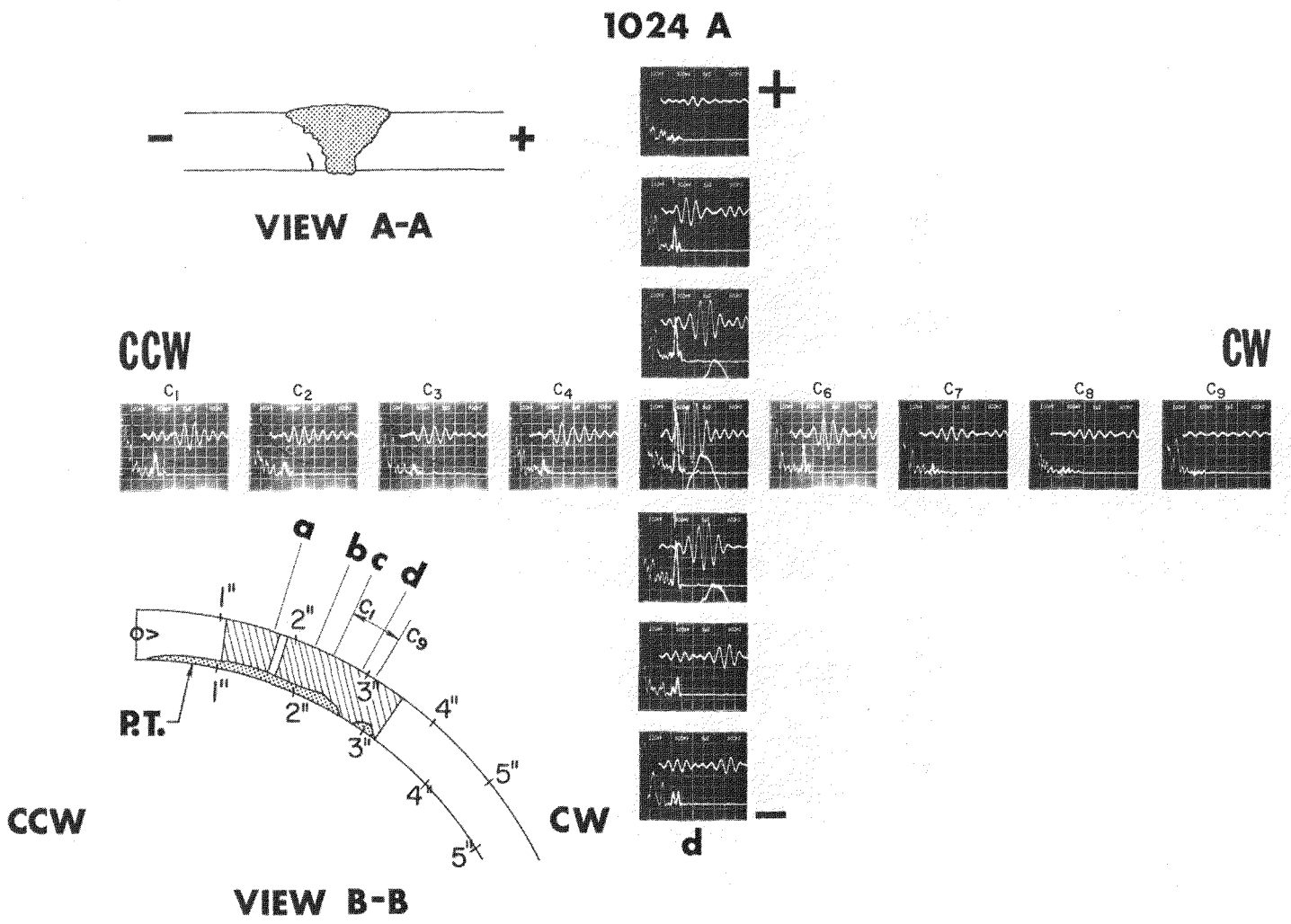


Figure 5-9 Ultrasonic Data From Scan d of Radial IGSCC in Specimen 1024A

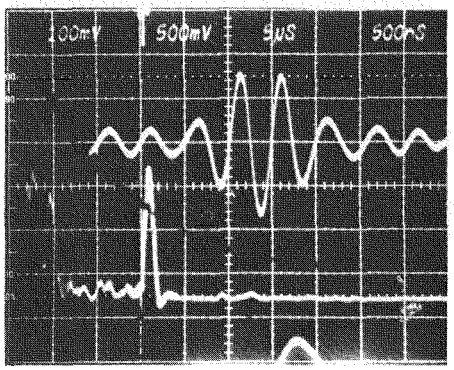


Figure 5-10 Photograph of CRT Screen Showing Processed and RF Signal From IGSCC in Specimen 1024A

c. Surface length of each crack was measured.

d. Metallographic examination of the crack cross section was then performed by various etching techniques. These examinations were conducted to determine whether the mode of cracking was similar to that of cracks found in components in previous examinations: that is, degree of cold working, sensitization of structure, intergranular cracking, grain size, hardness, and location in or out of heat-affected zone. Photomicrographs and photomacrographs showing crack morphology and structure were then taken.

e. The remainder of the crack was then broken open and the profile and depth of the crack were measured and sketched.

f. Finally, scanning electron microscope (SEM) examinations were performed on the fracture surface to confirm metallographic findings. Representative SEM photographs were also taken.

Selected areas of samples 19BL, 1024A, 10K17L, 10K18, 1020A, and 1021 were all destructively examined using portions of the above procedure. In addition, specimens 10K17, 1028C, 1028D, and 1019A were descaled and reexamined using either dye penetrant, ultrasonic, and/or radiographic techniques. Specimens 1028A and 1028B and portions of 1024A had previously been sectioned and analyzed by General Electric at its Vallecitos facility and had been confirmed as containing IGSCCs. Flaw depth and orientation for these specimens was again confirmed by BCL, and two additional flawed areas in specimen 1024A were sectioned. Details of the specific tests performed on each specimen can be found in Table D-1 of Appendix D.

(a) 8x MAGNIFICATION

(b) 100x MAGNIFICATION OF LOWER LEFT HAND AREA OF FIGURE 5-11a

Figure 5-11 Photomicrographs of Radial IGSCC in Specimen 1024A

TYPICAL DESTRUCTIVE EXAMINATION

The destructive examination of specimen 1024A may be described as typical. Fluorescent penetrant indications are shown in figures 5-2 through 5-6. Note that the dimensions shown on the part are ID measurements and do not conform to the outside diameter measurements usually discussed in ultrasonic results. A 2.5-in. indication can be seen from +0.25 in. to +2.8 in. (figures 5-4 and 5-5). Several other indications can be seen in Figure 5-6 in the area of -4 in. to -6 in. These cracks are angled with respect to the "normal" anticipated orientation of stress-induced cracks. The small indications shown in Figure 5-5 at +3 in. and +5.5 in. had not been reported by any previous investigators. The descaling operations probably made these flaws visible.

Figure 5-1 shows the electric resistance gauge (ERG) readings for specimen 1024A. These readings are not corrected for differences between ERG and visual metallographic measurements.

Figure 5-11 shows two photomicrographs of an area cut from specimen 1024A at +1.7 in. (refer to figures 5-2 and 5-3). About two-thirds of the defective area is identifiable as a given crack. The last one-third is more like a region of general stress corrosion attack. Using the best radiographic practices (0.7%), the film did show this area, but the indications were not so distinct as those typical of a more clearly defined crack such as a fatigue crack.

In order to show both video and RF presentations of UT signals, the ultrasonic test sensitivity was set to display the 2/8 Vee path side-drilled hole (SDH) in the EPRI calibration block at 75% of full scale on the CRT. A Matek pulser/receiver was combined with a Tektronix 7000 series scope for display of signals.

Figure 5-7 describes the method of scanning the specimen. Figures 5-8 to 5-10 indicate the extensive ultrasonic recording of data. Ultrasonic data were taken by scanning toward the weld to obtain a peak signal and then past this position until the signal disappeared. Data were also taken at various points around the specimen, in both clockwise (CW) and counterclockwise (CCW) directions from the area that was eventually sectioned. In addition to photographs taken of the CRT screen, video tape recordings of the screen were obtained for all scans. With this data, a complete three-dimensional reconstruction of ultrasonic response from the flawed area can be made.

Figure 5-10 is a detailed presentation of the CRT originally seen in Figure 5-8. The signal trace presented at the bottom of the screen is the "normal" video signal seen by an ultrasonic inspector. The signal from the flaw is shown at three divisions from the left-hand edge of the screen grid. The amplitude from the flaw is approximately 150% of inspection sensitivity specified in ASME Code Section XI.

The upper trace and time-scale divisions on the screen correspond to the unprocessed RF signal from the flaw. The data can be used for either spectral or signature analysis purposes.

## RESULTS OF DESTRUCTIVE EXAMINATION

From the destructive examination, the following results were obtained:

- Specimens 19AL, 1024A, 1028A, and 1028B all contain intergranular stress corrosion cracks. Specimen 19AL contains one axial crack (direction approximately 10° relative to the longitudinal axis of the pipe), 1.25 in. long on the inside by 0.4 in. long on the outside. This crack is located approximately 1 in. from the weld centerline. Specimen 1024A contains nine separate cracks in and near the weld heat-affected zone, with orientations in the axial, radial, and skewed directions (approximately 45° relative to the longitudinal axis of the pipe). Specimen 1028A contains two radial cracks in the heat-affected zone. Specimen 1028B contains three short cracks at one edge of the specimen. These cracks are axial and slightly skewed. Unfortunately, the total number of IGSCCs is far less than anticipated, considering the total number of pipe specimens processed for this study.

- Specimens 1021, 10K17L, and 10K18, originally thought to contain IGSCCs, were found instead to contain flaws of a different nature. Specimen 1021 contains a base material defect (a lap). This was confirmed by visual and penetrant examination of cut sections. The depth of the lap defect from the inside surface ranges from 0.002 in. to 0.022 in. The flaw in specimen 10K18 is lack of fusion at the weld root. The depth ranges from 0.015 in. to 0.040 in. with an average of 0.020 in. Specimen 10K17L contains two tiny indications: one appears to be a gas pore, and the other is a localized hard particle (weld spatter?). These indications are in an area of the pipe that had been partially ground out; this could have led to the false laboratory ultrasonic readings.

- Specimen 1020A, originally thought to be unflawed, revealed DPT indications after descaling. This specimen was then sectioned and found to contain small areas of weld overlap.

- Specimen 19BL was classified as free from flaws by the original laboratory study. Since most of the inspection teams indicated that this specimen contained flaws, in similar locations, a destructive test was performed. The results of this examination show a barely discernible

indication of an internal lack of fusion between weld passes. This defect was probably missed by radiography because of its orientation, size, and location; however, it could have given an ultrasonic signal during the simulated inspection. Flaws of this nature have caused many problems in relating ultrasonic inspection to radiography. They have also resulted in costly repairs when a flaw could not be identified as an internal fabrication flaw rather than a service-induced flaw.

- All remaining specimens were determined to be free from service-induced flaws or major fabrication flaws.

## Section 6

## RESULTS OF THE SIMULATED INSPECTION

The tables of this section summarize the ultrasonic inspection results of the five test teams on the 16 welded pipe samples described in Appendix A and Table 2-1. Although the data base is small, the round robin results may be useful in detecting specific faults in the inspection process, and to some degree they quantify an in-service inspection. A number of approaches can be taken to analysis of the data. The simplest approach is to consider each pipe sample as a single set of data. The pipe sample was either flawed or not, and the pipe was called flawed or unflawed, without consideration of flaw depth. According to this analysis, the pipe is judged as either defective or nondefective for further operation. In some respects, this reflects current industry practice, since pipes analyzed as cracked are replaced, no matter what the flaw length or depth is determined to be.

This approach has obvious drawbacks. A team could score high by simply guessing the correct result (true-false analogy). In addition, this approach evaluates only the ultimate decision-making process of calling a pipe defective or not. It sheds no light on the detection process, since credit is not given for a flaw successfully detected and plotted, but then analyzed as geometry. Because of these considerations, the initial approach taken in interpreting the data was that shown in Table 6-1. This table compares all results obtained by the test teams in Phase A (own procedures) to the descaling, nondestructive testing, and metallurgical results obtained by BCL. The laboratory results are shown in the table by a black square if the pipe is interpreted as cracked, and by a white square if uncracked. The significant lack of fusion discovered in sample 10K18 and the lap defect in sample 1021, originally classified as IGSCCs, are also considered as defects. Classification of these pipe samples as defective could be debated, since the flaws are not service-induced. Consideration of these samples as defective pipe can be defended in that they represent sharp linear imperfections that have some depth and are similar to fatigue cracks or well-developed IGSCCs. If

Table 6-1

Summary of Test Results, Phase A, Complete Samples

| SAMPLE IDENTI-FICATION | PIPE DIAMETER (in.) | PIPE SECTION (deg) | FLAW DESCRIPTION (UT[a] confirmed by DPT[b]) | BASIS FOR EVAL.[f] | TEST TEAM RESULTS[g] A | B | C | D | E | EVALUATION CRITERIA |
|---|---|---|---|---|---|---|---|---|---|---|
| 19AL | 10 | 180 | SCC[c], axial, through wall | ■ | ■ | ■ | ■ | ■ | ▨ | Pipe must be called "cracked" on EPRI form. |
| 1028A | | 36 | SCC, radial, across sample[d] | ■ | ■ | ■ | | ■ | ▨ | |
| 1028B | | | SCC, skewed angle, edge crack[d] | ■ | ■ | ■ | | ▨ | ■ | |
| 1024A | | 180 | SCC, radial, axial, and skewed, spotty[d] | ■ | ■ | ■ | ■ | ▨ | ▨ | |
| B2A | 4 | 360 | SCC,small spots[c] | ■ | ▨ | ▨ | | ■ | ▨ | |
| 10K18 | 10 | 360 | Lack of fusion[e] | ■ | ■ | ▨ | ▨ | ▨ | ▨ | Pipe must by called "cracked" or "lack of fusion." |
| 1021 | | | Lap, radial, 1 in. long[e] | ■ | ■ | ■ | ■ | no test | ▨ | |
| 10K17L | | | Porosity[e] | | ■ | | | | | Indications must not be called cracks. |
| 10K17 | | | None by penetrant | | ■ | | | ■ | | |
| 1020A | | | Weld overlap[e] | | | | | | | |
| 1024B | | 180 | None by penetrant | | | | | | | |
| 1028C | | 36 | None by penetrant | | | | | ■ | | |
| 1028D | | | None by penetrant | | | | | | | |
| 1019A | | 360 | None by penetrant | | ■ | | | ■ | | |
| 19BL | | 180 | Internal reflector from weld[e] | | ■ | | ■ | | | |
| A9A | 4 | 360 | None by penetrant | | | ■ | | ■ | | |

[a]Ultrasonic

[b]Dye penetrant test

[c]Flaw interpreted as stress corrosion crack

[d]SCC confirmed by metallurgy

[e]Confirmed by metallurgy

[f] □ Unflawed ■ Flawed

[g]Results as shown:

■ Crack called

▨ Crack signal detected, crack not called

□ No crack detected

preservice or radiographic information had been available to the test teams, these samples could have been analyzed differently; but under the given conditions, they represent significant reportable indications. To compensate for the possible differences in analysis of the defects in these two samples, credit was given in Table 6-1 to the teams calling them either cracked or lack of fusion.

In Table 6-1, results obtained by inspection teams A through E for each sample are shown to the right of the laboratory destructive and/or NDE results. The results are tabulated in three categories:

- A pipe was identified as cracked (shown as a black square).
- A crack appeared to be detected on a cracked pipe, but it was not called a crack (shown as a cross-hatched square).
- A crack was not called or detected (shown as a white square).

As an example, team D detected a flaw in sample 19AL and properly called it a crack (square is black). For the same specimen, a second result is shown on the table for team E. The result presented for team E--a crack detected but not called a crack (cross-hatched)--was determined according to the criterion that an indication must be plotted in the proper location, have proper orientation, and be similar in length to the penetrant results. In many instances, determining this required analysis of the inspection team's original data, since in most cases only data considered as a crack were plotted on the EPRI data form as final results. Review of the original data was also a check on relative inspection sensitivity, since an absence of indications detected or plotted could indicate a significantly reduced level of data recording sensitivity.

For a perfect correlation between the simulated field inspections and the laboratory results, the top portion of the table (samples 19AL through 1021) would have been solid black and the bottom portion completely white. Most inspection teams did not achieve this perfect correlation, though teams A and B did come close. In addition, several teams detected flaws but would not call them cracks from the results of this inspection alone. The through-wall crack in sample 19AL appeared to be detectable by all teams. Although this crack extends right through the wall, its tight nature renders it undetectable with the unaided eye. The long, partial through-wall cracks in samples 1028A and 1024A and the small cracks in 1028B were also detected by most teams.

Table 6-2 presents the results of both Phase A (teams' own procedure) and Phase B (EPRI procedure). In Table 6-2, results obtained by inspection teams A through E for each sample are shown to the right of the laboratory results. The portion of each square above the slanted line represents results obtained by the test team using its own procedures, standards, and equipment (Phase A). The bottom portion of each square represents the results obtained using the procedure supplied by EPRI (Phase B). The results are tabulated in three categories:

- A pipe was identified as cracked (shown as black).
- A crack appeared to be detected on a cracked pipe, but it was not called a crack (shown cross-hatched).
- A crack was not called or detected (shown as white).

As an example, team D, using its own procedure, detected a flaw in sample 19AL and properly called it a crack (top half of the square is black). However, when this team used the EPRI procedure, it did not call any indications a crack in this same sample.

In general, the results of the two phases are similar. The cracks in specimens 19AL, 1028A, 1028B, and 1024A were again detected by the majority of teams, although in some cases a flaw detected in Phase A was not detected again by the same team in Phase B. With reference to incorrect calls, sample 19BL appeared to cause all the teams a great deal of difficulty in both phases. As discussed previously, this specimen, when sectioned, revealed what appeared to be a tiny internal fabrication reflector.

Tables 6-1 and 6-2 present the results of the simulated inspections on the basis of a "crack" or "no crack" decision for the entire set of samples, with no consideration of proper flaw location. As previously mentioned, this type of analysis would not disclose any tendency on the part of the inspection teams to guess. To eliminate or at least reduce this chance, the results can also be judged using proper location as an additional criterion for correct judgment of a cracked or uncracked pipe. Table 6-3 represents this approach.

For this analysis, the pipe sections are divided into four equal quadrants, or 90° sectors, around the pipe. A flaw located in a sector and properly called in that sector is considered a correct inspection. The selection of a quadrant analysis is based on discussions with one of the inspection teams using strip chart data

Table 6-2

Summary of Test Results, Phases A and B, Complete Samples

| *SAMPLE IDENTI-FICATION* | *FLAW DESCRIPTION (UT[a] confirmed by DPT[b])* | *BASIS FOR EVAL.*[f] | *TEST TEAM RESULTS*[g] | | | | | *EVALUATION CRITERIA* |
|---|---|---|---|---|---|---|---|---|
| | | | *A* | *B* | *C* | *D* | *E* | |
| 19AL | SCC[c], axial, through wall | ■ | ◥◢ | ◥◢ | ◥◢ | ◥◢ | ◥◢ | Pipe must be called "cracked" on EPRI form. |
| 1028A | SCC, radial, across sample[d] | ■ | ◥◢ | ◥◢ | ◥◢ | ◥◢ | ◥◢ | |
| 1028B | SCC, skewed angle, edge crack[d] | ■ | ◥◢ | ◥◢ | ◥◢ | ◥◢ | ◥◢ | |
| 1024A | SCC, radial, axial, and skewed, spotty[d] | ■ | ◥◢ | ◥◢ | ◥◢ | ◥◢ | ◥◢ | |
| B2A | SCC, small spots | ■ | ◥◢ | ◥◢ | ◥◢ | ◥◢ | ◥◢ | |
| 10K18 | Lack of fusion[e] | ■ | ◥◢ | ◥◢ | ◥◢ | ◥◢ | ◥◢ | Pipe must be called "cracked" or "lack of fusion." |
| 1021 | Lap[e] | ■ | ◥◢ | ◥◢ | ◥◢ | no test | ◥◢ | |
| 10K17L | Porosity | | ◥◢ | ◥◢ | ◥◢ | ◥◢ | ◥◢ | Indications must not be called cracks. |
| 10K17 | None by penetrant | | ◥◢ | ◥◢ | ◥◢ | ◥◢ | ◥◢ | |
| 1020A | Weld overlap[e] | | ◥◢ | ◥◢ | ◥◢ | ◥◢ | ◥◢ | |
| 1024B | None by penetrant | | ◥◢ | ◥◢ | ◥◢ | ◥◢ | ◥◢ | |
| 1028C | None by penetrant | | ◥◢ | ◥◢ | ◥◢ | ◥◢ | ◥◢ | |
| 1028D | None by penetrant | | ◥◢ | ◥◢ | ◥◢ | ◥◢ | ◥◢ | |
| 1019A | None by penetrant | | ◥◢ | ◥◢ | ◥◢ | ◥◢ | ◥◢ | |
| 19BL | Internal reflector from weld[e] | | ◥◢ | ◥◢ | ◥◢ | ◥◢ | ◥◢ | |
| A9A | None by penetrant | | ◥◢ | ◥◢ | ◥◢ | ◥◢ | ◥◢ | |

[a] Ultrasonic test

[b] Dye penetrant test

[c] Flaw interpreted as stress corrosion crack

[d] SCC confirmed by metallurgy

[e] Confirmed by metallurgy

[f] □ Unflawed ■ Flawed

[g] Test procedure, Phase A (inspection group) → ◥◢ ← Phase B (EPRI)
Results as shown:
◥◢ Crack called ◥◢ No crack detected ◥◢ Crack signal detected, crack not called

Table 6-3

Summary of Test Results by Quadrant

| SAMPLE IDENTIFICATION | PIPE DIAMETER (in) | PIPE SECTION (deg) | BASIS FOR EVALUATION[a] (QUADRANTS) | | | | TEST TEAM RESULTS[b,c] | | | | | | | | | | | | | | | | | | | |
|---|---|---|---|---|---|---|---|---|---|---|---|---|---|---|---|---|---|---|---|---|---|---|---|---|---|---|
| | | | | | | | A | | | | B | | | | C | | | | D | | | | E | | | |
| | | | 1 | 2 | 3 | 4 | 1 | 2 | 3 | 4 | 1 | 2 | 3 | 4 | 1 | 2 | 3 | 4 | 1 | 2 | 3 | 4 | 1 | 2 | 3 | 4 |
| 19AL | 10 | 180 | ■ | | | | ◪ | | | ◪ | ◪ | | | ◪ | ◪ | | | | ◪ | | | ◹ | ◪ | | | ◹ |
| 1028A | | 36 | ■ | | | | ◪ | | | | ◪ | | | | ◪ | | | | ◪ | | | | ◪ | | | |
| 1028B | | | ■ | | | | ◪ | | | | ◪ | | | | ◪ | | | | ◪ | | | | ◪ | | | |
| 1024A | | 180 | ■ | | | ■ | ◪ | | | ◹ | ◪ | | | ◹ | ◪ | | | ◹ | ◪ | | | ◪ | ◪ | | | ◹ |
| B2A | 4 | 360 | | ■ | | | ◹ | ◪ | ◹ | ◹ | ◪ | ◪ | ◹ | ◹ | ◪ | ◪ | ◪ | ◹ | ◪ | ◪ | ◹ | ◪ | ◹ | ◪ | ◹ | ◹ |
| 10K18 | 10 | 360 | ■ | ■ | ■ | | ◪ | ◪ | ◪ | ◪ | ◪ | ◪ | ◹ | ◹ | ◹ | ◹ | ◹ | ◹ | ◪ | ◪ | ◪ | ◪ | ◪ | ◪ | ◪ | ◹ |
| 1021 | | | | ■ | ■ | | ◹ | ◪ | ◪ | ◹ | ◹ | ◪ | ◹ | ◹ | ◹ | ◹ | ◪ | ◹ | not measured | | | | ◹ | ◪ | ◪ | ◹ |
| 10K17L | | | | | | | ◪ | ◪ | ◪ | ◹ | ◹ | ◹ | ◹ | ◹ | ◹ | ◹ | ◹ | ◹ | ◹ | ◹ | ◹ | ◹ | ◹ | ◹ | ◹ | ◹ |
| 10K17 | | | | | | | ◪ | ◹ | ◪ | ◹ | ◹ | ◹ | ◹ | ◹ | ◹ | ◹ | ◹ | ◹ | ◪ | ◹ | ◹ | ◪ | ◹ | ◹ | ◹ | ◹ |
| 1020 A | | | | | | | ◹ | ◹ | ◹ | ◹ | ◹ | ◹ | ◹ | ◹ | ◹ | ◹ | ◹ | ◹ | ◪ | ◹ | ◪ | ◪ | ◹ | ◹ | ◹ | ◹ |
| 1024B | | 180 | | | | | ◹ | ◹ | ◹ | ◪ | ◹ | ◹ | ◹ | ◪ | ◹ | ◹ | ◹ | ◪ | ◹ | ◹ | ◹ | ◪ | ◹ | ◹ | ◹ | ◪ |
| 1028C | | 36 | | | | | ◹ | ◹ | ◹ | ◹ | ◹ | ◹ | ◹ | ◹ | ◪ | ◹ | ◹ | ◹ | ◪ | ◹ | ◹ | ◹ | ◹ | ◹ | ◹ | ◹ |
| 1028D | | | | | | | ◹ | ◹ | ◹ | ◹ | ◹ | ◹ | ◹ | ◹ | ◪ | ◹ | ◹ | ◹ | ◹ | ◹ | ◹ | ◹ | ◹ | ◹ | ◹ | ◹ |
| 1019A | | 360 | | | | | ◹ | ◪ | ◹ | ◹ | ◹ | ◹ | ◹ | ◹ | ◹ | ◹ | ◹ | ◹ | ◹ | ◹ | ◪ | ◹ | ◹ | ◹ | ◹ | ◹ |
| 19BL | | 180 | | | | | ◪ | ◹ | ◹ | ◪ | ◪ | ◹ | ◹ | ◪ | ◪ | ◹ | ◹ | ◹ | ◪ | ◹ | ◪ | ◪ | ◹ | ◹ | ◹ | ◪ |
| A9A | 4 | 360 | | | | | ◹ | ◹ | ◪ | ◪ | ◹ | ◹ | ◪ | ◹ | ◹ | ◹ | ◹ | ◹ | ◹ | ◹ | ◪ | ◹ | ◹ | ◹ | ◹ | ◹ |

[a]Location determined by dye penetrant test: ☐ Unflawed quadrant ■ Flawed quadrant

[b]Test procedure, Phase A (inspection group) → ◪ ← Phase B (EPRI)

[c]Results as shown: ◤ Crack called ◪ Crack signal plotted, not called crack ◹ No crack detected

recording techniques. Members of this group indicated they normally locate a flaw around the pipe within one quadrant. If location accuracy more precise than this is used, the data of the team using the chart recording method in Phase A may have to be discarded.

Table 6-3 is similar to Table 6-2 in the method of indicating test team results: crack, no crack, or crack detected but not called. The 36° samples are counted as a full inspection quadrant. Because of the reference marks on the specimen, a 36° sample is in the first quadrant (0° to 90°). Such specimens are 1028A, 1028B, 1028C, and 1028D. Pipe specimens cut in half (180°) have inspection quadrants in the first (0° to 90°) and last (270° to 360°). Specimens in this category are 1024A, 1024B, 19AL, and 19BL. Full pipe specimens have the normal four inspection quadrants. These are specimens 1021, 10K17L, 10K18, 10K17, 1020A, 1019A, QC1-B2A, and A9A. In Table 6-3, the two specimens 10K18 and 1021 are again considered flawed.

A comparison of the results shown in tables 6-2 and 6-3 indicates that the teams did in fact derive their conclusions from actual inspection data rather than guessing, since successful determination of the presence of a crack in a pipe usually corresponded to successful location of the crack in the proper quadrant. As a further check on this premise, data on specimen 19AL from all the teams and from the laboratory study were plotted together. In most cases, the flaw was located within ruler measurement accuracy. In general, the relative performance (total pipe vs. quadrant analysis) of the teams is also similar but indicates a definite problem in calling uncracked quadrants cracked.

Reviewing the inspection data by quadrant also revealed that the radial and axial flaws in the first quadrant of specimen 1024A were generally detectable, whereas the short flaws skewed at approximately 45° to weld centerline in the last quadrant were not. This sample may indicate the flaw and pipe condition at the lower level of inspection sensitivity. Sensitivity, in this case, refers to the inspection system's overall ability to detect and define a flaw; it is not necessarily a function of the amount of ultrasonic energy transmitted or received during the inspection process. Because of the apparent low ultrasonic reflectivity of the IGSCC flaws, analysis techniques other than relative signal amplitude seem to be required in order to distinguish flaw signals from spurious signals such as geometry and material anomalies.

The results obtained from this sample also indicate that some attention should be given to improving methods of detecting off-axis flaws, either by technique or scanning procedure.

The number of flaws correctly detected and plotted but not called cracks and the large number of conservative calls (noncracked quadrants called cracked) suggest that the decision-making process of the inspectors should be improved. It remains to be investigated whether improvement can be achieved through increased training, improved techniques, or the application of supplemental inspection techniques such as radiography.

To keep the results of these simulated inspections in proper perspective, the true degree of simulation represented by the study should be discussed. These inspections were conducted in a laboratory and not at an inspection site; thus the problems of limited access, tight inspection schedules, logistics, and long, fatiguing working hours were not truly simulated. Although the exact influence of such field conditions on overall inspection performance is not known, the performance of an actual field inspection might be somewhat below the results obtained in this study, if the results are judged on data obtained during a single inspection.

On the other hand, the inspection teams involved in this study did not have preservice or previous in-service inspection information (RT or UT) with which to compare their results. Since some of the teams felt that a comparison of results from one inspection to another can indicate the initiation and growth of a flaw or identify geometry, the lack of this information in the study could have handicapped the decision-making process of the inspectors.

To judge the real performance of this inspection process, the relationship of the simulated inspections to a real plant inspection for IGSCC flaws must be considered. Past history has shown that once IGSCCs have been initiated, they usually occur in the heat-affected zone of the pipe at various depths, orientations, and lengths, and in more than one weld of a piping loop. Since the test samples in this program were obtained from a real system, and since the cracks did occur at several locations and were at various depths, orientations, etc., the complete testing of all the samples by an inspection team does essentially simulate an actual in-service inspection of one loop of a real system. If detection for the presence of

IGSCCs is the main objective of the inspection process (analogous to detecting a disease), then all the teams that participated in the program appear to be capable of performing this function, since they all detected and correctly analyzed the presence of IGSCCs in the simulated piping loop (as represented by all the samples).

Section 7

# ANALYSIS OF DATA

One of the principal goals of a study of this type is quantification of the inspection process. Since the data base of cracked pipe turned out to be smaller than initially anticipated, and since the distribution of flaw sizes, shapes, and orientations was random, it may be difficult to generate such desirable results as characterization of detection probability as a function of flaw depth and/or size. Since this program also involved the testing of human inspectors, an inherent problem involves unknown variables influencing the inspectors' performance. Past researchers in this field have used statistical analysis approaches to overcome some of these problems and to derive useful information from seemingly small amounts of data.

As a start, the data in Table 6-2 were analyzed using statistical approaches to determine if there was any real difference between using the groups' own procedures and the single procedure supplied by EPRI. This initial analysis also addressed the probability that the results given in Table 6-2 were real indications of inspection performance and not simply a random guessing situation. The details of this analysis are discussed in Appendix C.

This analysis indicates that the overall results obtained in Phases A and B were essentially the same. The change in procedure appeared to have little effect on the combined results obtained by the teams or on their relative performance. Statistical analysis of the results given in Table 6-2 also shows that the results were obtained from actual data rather than from simply guessing, which was also the conclusion reached by the quadrant analysis of the data. The correct analysis of cracked pipe tends to outweigh significantly the calling of uncracked pipe as defective.

By performing a very detailed analysis of selected cracks in the pipe samples and the inspection data corresponding to them, additional insight into the inspection

process may be obtained. Seven individual cracks in seven separate pipe quadrants were analyzed for this purpose; the results are shown in Table 7-1. For this table, the number of groups detecting and analyzing a flaw was determined from the quadrant results shown in Table 6-3. Since this is still an analysis by quadrant, direct correlation of an individual crack to inspection performance may not be completely correct. The dimensions for computing depths and areas were obtained from ERG readings and/or destructive metallography. Since the shape of the flaw was assumed in the majority of cases, the areas must be considered approximate. Only one of the skewed cracks of a quadrant in specimen 1024A is listed, since this was the only crack of this type sectioned.

The flaws were characterized by the parameters shown in Table 7-1 for the following reasons:

1. Flaw Area. The flaw area is usually estimated from ultrasonic inspection data, since the amount of ultrasonic energy reflected from a flaw should be some function of the area normal to the sound beam. Flaw area is also a valid parameter in which to judge flaw severity, since the flaw area normal to the maximum stress in the piping system determines the degree of loss in structural integrity. Normally, the probability of flaw detection should decrease with smaller flaw area; this appears to be the general case observed in the simulated inspections, except for the skewed IGSCC flaw in specimen 1024A. Although this flaw was similar in apparent area to the IGSCC in 1028B and the fabrication flaws in 10K18 and 1021, most teams did not appear to detect this flaw or the other five skewed flaws in the same quadrant of the pipe. IGSCC flaws are apparently much less reflective than fabrication type flaws with the same area, and this difference seems to be significant. This is discussed in Appendix D. Small cross-sectional area, skewed orientation, and intergranular flaw characteristics appear to be the factors which caused the majority of groups to miss the skewed flaws in sample 1024A.

   To keep this evaluation in proper perspective, one must remember that all the flaw areas shown in Table 7-1 were significantly smaller than the minimum size that would cause concern for the integrity of the piping system even under the most severe of loading and environmental conditions (17).

2. Flaw Depth (Percent Through Wall). This parameter represents the maximum depth of the flaw relative to the wall thickness; it is used as an estimate

Table 7-1

PHYSICAL CHARACTERIZATION OF FLAWS IN 10-IN. PIPE

| Test Sample | Defect Type | Number of Groups: Detecting Crack Signal | | Number of Groups: Calling Signal as Crack | | Flaw Area, $in^2$ | Flaw Depth, % Through Wall[b] | Flaw Depth/Flaw Length[c,d] | Flaw Orientation, ° From Weld Centerline[f] |
|---|---|---|---|---|---|---|---|---|---|
| | | Phase A | Phase B | Phase A | Phase B | | | | |
| 19AL | Axial IGSCC | 5 | 4 | 4 | 4 | 0.50 | 100 | 0.5 | 80 |
| 1028B | Axial IGSCC | 4 | 5 | 3 | 4 | 0.17 | 30 | 0.2[e] | 25 |
| 1028A | Radial IGSCC | 4 | 5 | 3 | 2 | 1.32 | 77 | 0.2 | 0 |
| 1024A | Radial IGSCC | 5 | 5 | 3 | 2 | 0.65 | 72 | 0.2 | 0 |
| 1024A | Skewed IGSCC | 0 | 1 | 0 | 0 | 0.14 | 75 | 0.8 | 45 |
| 10K18 | Radial LOF | 5 | 5 | 1 | 3 | 0.22 | 3 | 0.002 | 0 |
| 1021 | Radial lap | 4[a] | 4 | 3 | 3 | 0.11 | 3 | 0.004 | 0 |

[a] Evaluated by four groups only

[b] Flaw depth/pipe wall x 100%

[c] By metallographic sectioning except as noted

[d] Length as measured on inside surface

[e] ERG measurement only

[f] Flaws parallel to weld are at 0°, perpendicular to weld at 90°

of flaw severity in many structures. For the piping systems, this parameter is less a measure of structural integrity than of flaw growth from initiation and the possibility of leak.

3. Flaw Depth/Flaw Length. This characteristic can influence flaw detection in piping systems, since a small depth-to-length ratio, even when the flaw is small, can reflect considerable ultrasonic energy from the "pocketing effect" of the intersection of the flaw with the inside surface. This may explain the high detection rate of the flaws in specimens 10K18 and 1021. Conversely, the high depth-to-length ratio of the skewed flaw in specimen 1024A may be a significant factor in its low detectability. The IGSCC flaws discussed in Table 7-1 all exhibit a definite "leak before break" characteristic, since their ratio of flaw depth to inside surface length is large and their cross-sectional area is small. This characteristic indicates that the flaws tend to penetrate the wall long before they grow large enough to affect the integrity of the pipe.

4. Flaw Orientation (Degrees From Weld Centerline). From the results of the simulated inspections and the laboratory studies, this factor appears to have a significant effect on flaw detection probability, although the effect does not appear to become pronounced until the orientation becomes greater than 25° to the centerline of the weld.

Using the data from Table 7-1, the number of teams successfully detecting a flaw is plotted as a function of flaw depth in Figure 7-1. In a similar manner, the number of teams successfully analyzing a detected flaw is plotted against flaw depth in Figure 7-2. As would be expected, the successful analysis of a crack tended to fall with decreasing wall penetration, with the significant exception of the skewed crack in sample 1024A. In all cases, the teams had considerable difficulty in detecting and analyzing skewed cracks. To further emphasize the effect of flaw orientation, the analysis performance of the inspection teams is plotted as a function of flaw orientation in Figure 7-3.

As these figures show, the orientation of an IGSCC flaw rather than its depth appears to be the controlling factor in successful detection. The shape of the flaw (high depth-to-length ratio) may also contribute to its difficulty of detection. As previously discussed, the skewed cracks were extremely difficult to detect in the laboratory evaluations using the normal field inspection procedures

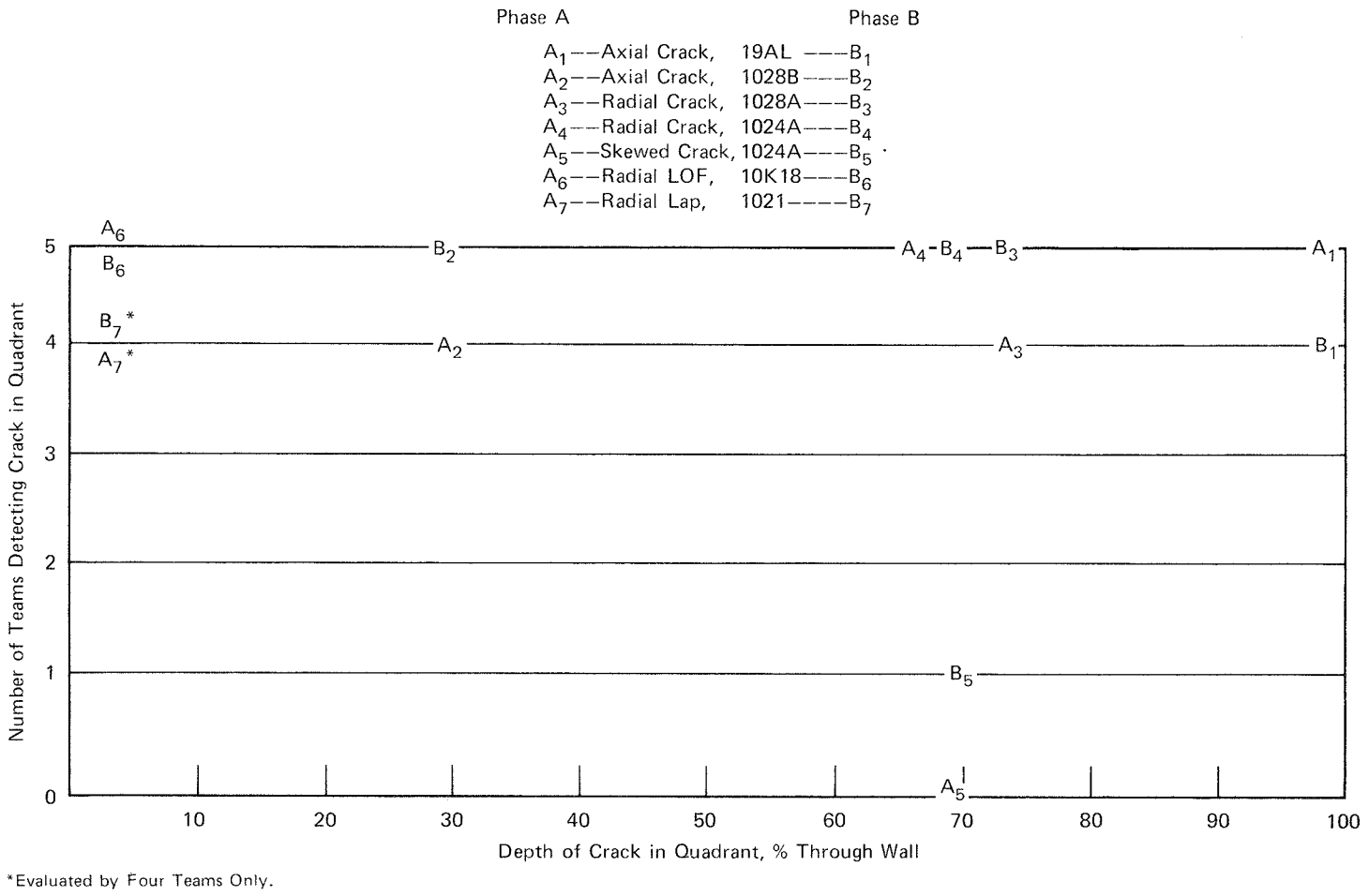


*Evaluated by Four Teams Only.

Figure 7-1 Detection of Flaws by Inspection Team vs. Flaw Depth

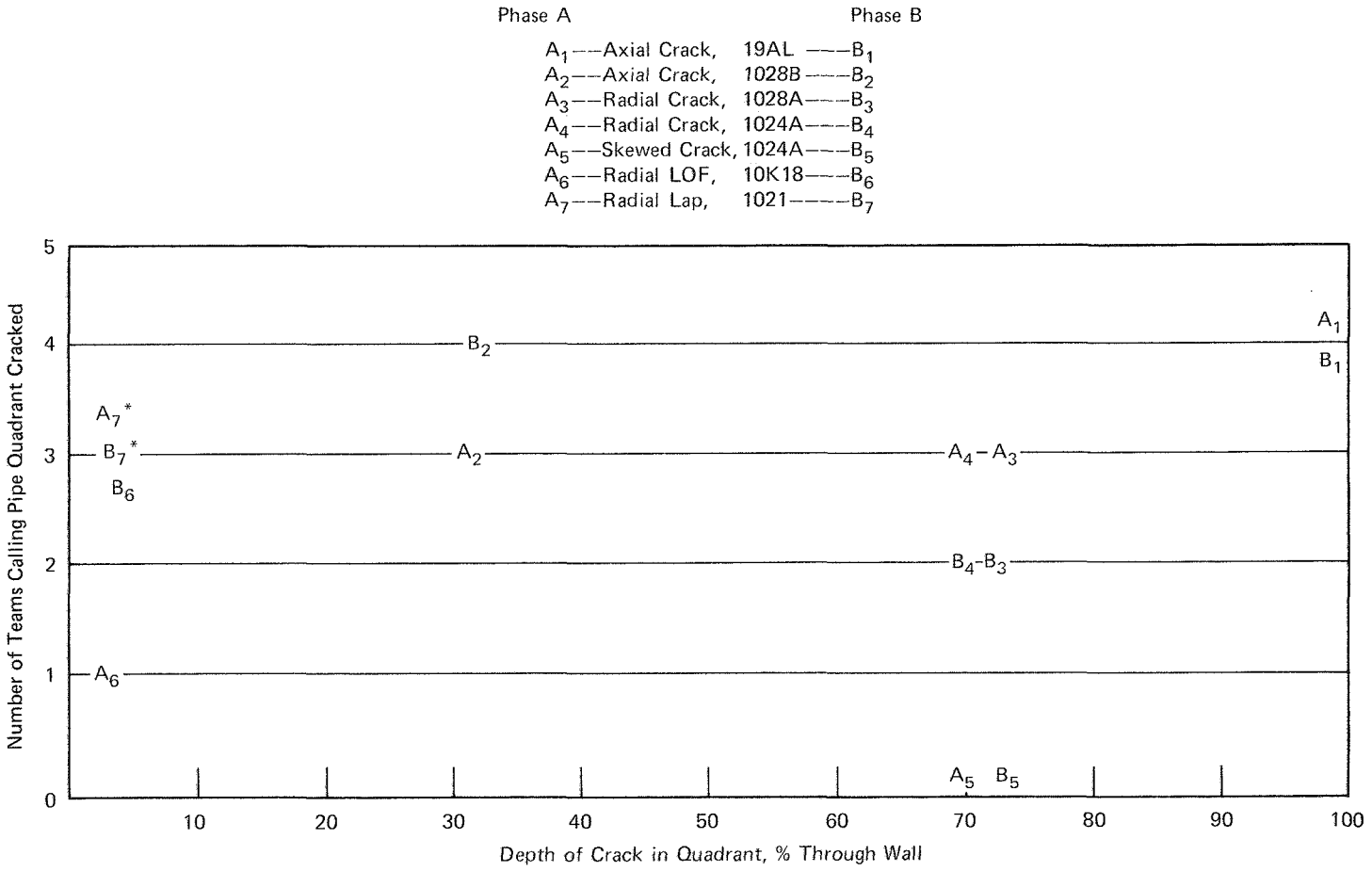


*Evaluated by Four Teams Only.

Figure 7-2 Analysis of Flaws by Inspection Team vs. Flaw Depth

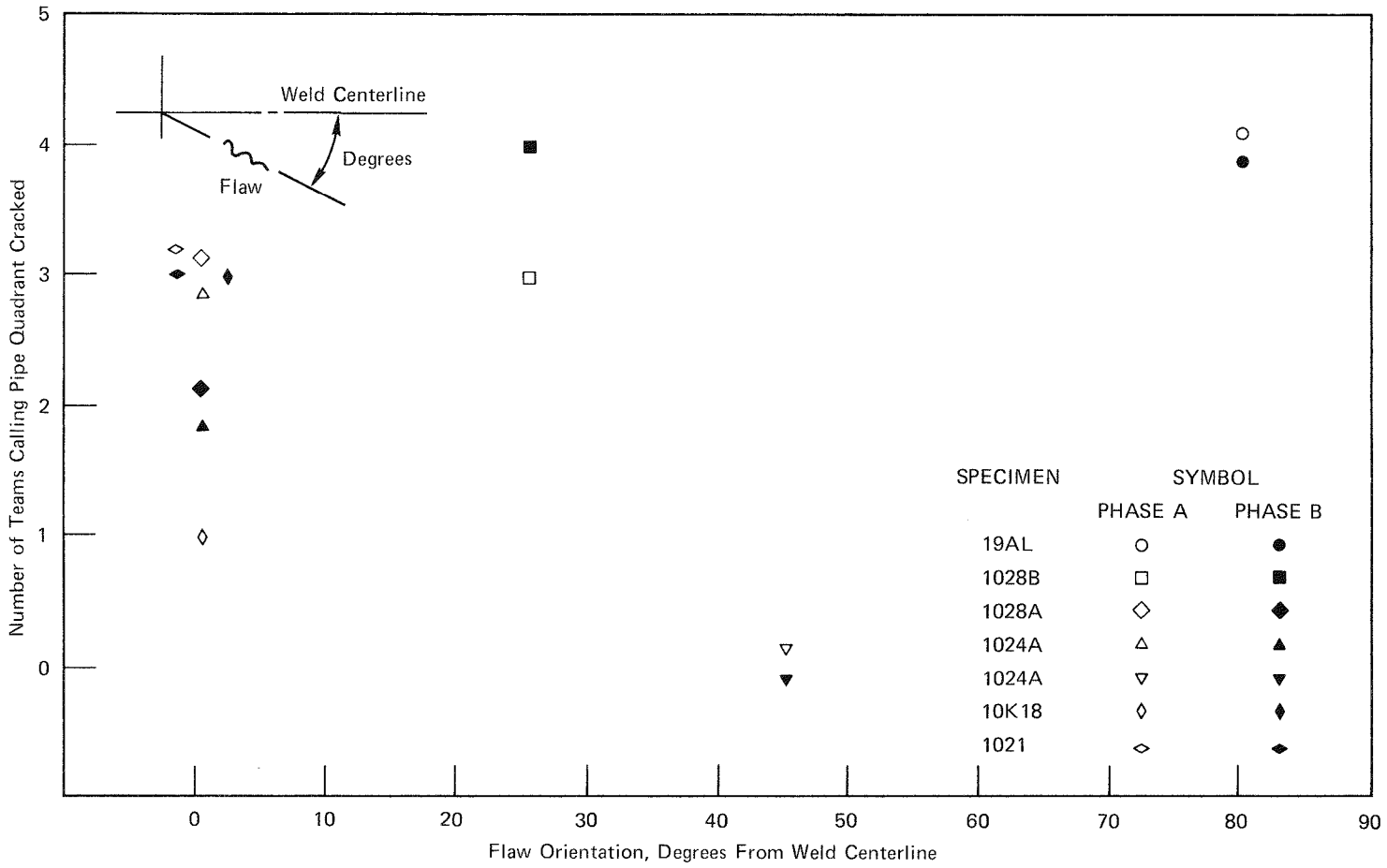


Figure 7-3 Analysis of Flaws by Inspection Team vs. Flaw Orientation

of scanning parallel and perpendicular to the weld. From observations of previous field-cracked pipe, skewed cracks in which no portion of the crack surface has an orientation parallel or perpendicular to the weld centerline appear to be very rare. Consequently, any pipe containing flaws that have grown to a size of concern may be assumed to contain one or more flaws with some portion of their orientation favorable to present inspection scan directions. On the other hand, a simple change in scan procedure or technique could improve the detection of skewed cracks, no matter how small or limited in occurrence they may be. What changes would be appropriate, and how practical these changes would be, remains to be determined.

Section 8

# CONCLUDING STATEMENTS

## REVIEW OF PROGRAM DETAILS

This study has provided valuable guidelines for conducting future programs of this nature. The factors that appeared to have the most influence on the success of the program were:

- Preliminary Dry Run. Before conducting any phase of this study, preliminary tests were performed to ensure that inspection times, procedures, and logistics were as planned. Several important modifications to the program resulted from these tests.

- Permanent Reference Marks. The reference marks provided an easy method of comparing the flaw location accuracy of each team with laboratory results.

- Standard Summary Sheet for Results. Use of a standard summary sheet to record the final results of each team reduced the data analysis time significantly. This summary sheet also provided a quick assessment of results before the teams left the site and permitted the correction of any reporting errors before a team continued to the next phase of the program.

- Test Monitor. The on-site EPRI representative provided a valuable link between the test teams and the project manager. By observing the detailed performance of each test group, the test monitor could detect and assess deviations from written procedures.

In conducting future programs similar to this one, the following items should be considered:

- To handle and analyze the incoming data rapidly, methods for inputting the data easily to a computer should be developed and checked out completely before the test phase begins.

- To optimize the data base for later statistical analysis, the number of test samples, their exact configuration, and the number and nature of flaws in the samples should be determined before the tests are conducted.

- For simulation of field conditions, the test samples should be fixed in position in a surrounding environment that duplicates the working conditions present during actual in-service inspection of a nuclear reactor.

- As an aid in investigating the various parameters that can influence the results of an in-service inspection, and to quantify an inspection process, it would be desirable to develop methods that can create simulated IGSCC flaws in pipe specimens to controlled depths, shapes, and orientations. Methods of determining the exact configuration of these flaws without sectioning would also be desirable.

## CURRENT INSPECTION PRACTICE

Observations of the test teams' performance, review of their procedures, and discussions during the briefings have led to the following general comments regarding current inspection practice:

- The inspection equipment, including the ultrasonic testing instrument and transducer, appeared to be standard "off-the-shelf" items. No unique equipment specially developed for detection and analysis of IGSCCs in BWR piping was used.

- The techniques and written procedures used by the teams were essentially the same as those used to detect fatigue type flaws in carbon steel pipe. Any specific analysis procedure for IGSCCs was reflected in the training of the inspection teams rather than in their written procedures. The major difference between these inspections and inspections for other types of flaws was the way in which the data were analyzed. The teams that were most successful in correctly identifying flaws were those who carefully plotted UT data on cross-section drawings of the weld configuration and then used the location of a suspect signal to decide upon its identity (geometry, stress corrosion crack, etc.). These teams used the criterion that a stress corrosion crack usually occurs between the fusion zone of the weld and the inside diameter of a counterbore, if one exists.

- In general, the relative inspection performance, based upon correct identification of flaws, did not appear to be affected by type of ultrasonic test instrument, type of couplant, use of data recording equipment, or years of experience, training, or formal education (recall that the program required qualified level II and III inspectors).

- The nominal size of transducers ranged from 0.25 in. diameter to 0.75 in. diameter. A 0.25-in. diameter transducer was usually used on the 4-in. pipe and a 0.50-in. diameter transducer was generally used on the 10-in. pipe. The test frequency ranged from 1.0 MHz to 5.0 MHz; the majority of inspections were conducted at 2.25 MHz. Considering the overall results and relative performance of the groups, it appears that a conventional transducer diameter greater than 0.375 in. (with conventional wedge) may reduce the number of IGSCCs detected in some 10-in. pipe welds because of the previously mentioned interference between the front edge of the search unit and the weld crown. This observation was verified by laboratory study.

- All of the inspection procedures used by the various teams appeared to satisfy minimum ASME Code Section XI requirements.

- The teams all felt that their own procedures were superior to the EPRI-supplied procedure used in Phase B; however, the results tend to indicate that the procedure had little effect on the groups' ability to detect or analyze IGSCCs. The results from phases A and B were generally similar, both by team and for all teams combined. It is also interesting to note that the hoped-for improvement in detection of skewed cracks, using the rotating transducer motion required by the Phase B procedure, did not materialize. The extremely unnatural motion may have caused fatigue during the extended inspections, and the operator may have consciously or unconsciously reduced the angle of the rotation. Observations by the test monitor tend to confirm this premise. If future techniques require such a scanning motion, then inspectors should realize the intent and need for the scanning motion and plan a procedure that reduces fatigue. The inspectors in the simulated inspections were not briefed on the reason behind the scanning motion or any other aspect of the procedure used in Phase B. The above results emphasize one of the most difficult objectives to achieve in in-service inspection: the transfer of improvements developed in the laboratory to field practice.

## FUTURE EFFORT

The major project objectives of this planning study have been met; however, the study has provided EPRI with a considerable data base for future studies of specific aspects of the inspection process. Evaluation of the raw data may make it possible to investigate some of the following aspects of the in-service inspection:

- What UT signal amplitude or characteristic caused the inspector to stop the scanning procedure and begin analysis; that is, what triggered the inspector's attention?

- What was the relative scanning sensitivity of the teams?

- What effect did the various standards have on results?

Since the above effort is beyond the scope of this planning study, any additional analysis will be reported separately.

## RELATED EFFORTS

Since the results of this study show a definite need for improved inspection analysis capability for flaws near geometric reflectors and other problems, related efforts are under way to define more fully the extent and nature of this situation

and to effect solutions. The following ongoing programs are being conducted under the sponsorship of EPRI:

1. EPRI In-House Study TPS-75-609: "Correlation of Ultrasonic and Radiographic In-Service Inspection Results." This study is being conducted to determine the value of in-service radiography as a supplement to ultrasonic inspection in the analysis of stress corrosion cracks in stainless steel piping.

2. EPRI Technical Planning Study TPS-75-620: "A Study to Define Areas of NDT Research for Inspection of Stainless Steel." A number of laboratories, including the groups involved in the initial EPRI study, have indicated areas in which research in NDT might improve the overall process of detection and analysis. EPRI is therefore making available the samples used in the initial round robin study to laboratories requiring information from actual flawed samples to define more fully their technical approach to the problem of inspecting stress corrosion cracking in stainless steels.

3. EPRI Research Program RP449-1: "Ultrasonic Nondestructive Testing." Argonne National Laboratory is studying basic parameters that can influence UT inspection: size of transducer, frequency, etc.

4. NDE Experts Meeting on Austenitic Pipe Inspection. This meeting, held on September 30, 1975, was cosponsored by EPRI, Energy Research and Development Agency (ERDA), Nuclear Regulatory Commission (NRC), and the Pressure Vessel Research Committee (PVRC). The purpose of the meeting was to determine what possible improvements in ultrasonics and in fabrication procedures could lead to improved flaw detectability in austenitic stainless steels. Although the agenda was directed primarily toward nuclear components, the overall scope of the meeting was much broader. The results of this meeting were reported in an EPRI technical report, EPRI SR-30, February 1976.

5. EPRI Research Program: "Adaptive Learning Networks." This program will investigate the feasibility of utilizing advanced computer "learning techniques" to analyze ultrasonic inspection data, with the objective of distinguishing the flaw signal from masking signals such as geometry and material anomalies.

6. EPRI Research Program RP892: "Ultrasonic System Optimization Study." The objective of this three-year project is to increase substantially the ability to find and characterize flaws in pressure vessels and piping by improved discrimination, calibration, and reproducibility of ASME Code-approved in-service ultrasonic inspection techniques and procedures. Improvement in repeatability by standardization of preferred techniques is needed in order to assure continued licensability and reliability of the nuclear pressure boundary system. In addition, improved surveillance methods are needed to detect flaws and track their growth during reactor operations, thus avoiding the need for a shutdown to search for suspected problems.

## REFERENCES


1. A. G. Pickett and E. R. Reinhart. "Review of Recent Utility Experience With Power Reactor Coolant Pressure Boundary Inspection Regarding Service Condition, Defect Detection Capabilities, Defect Size, and Defect Orientation." Project I SwRI Project 17-2440, EEI Project RP79, Final Biannual Progress Report No. 8, In-Service Inspection Program for Nuclear Reactor Vessels, May 21, 1973. NTIS PB No. 222 701.

2. ASME Boiler and Pressure Vessel Code, Section XI, "Rules for In-Service Inspection of Nuclear Power Plant Components," July 1, 1971, with applicable semiannual addenda.

3. U.S. Atomic Energy Commission, Office of Inspection and Enforcement. "Through-Wall Cracks in Core Spray Piping of Dresden 2." Bulletin IE-75-01, January 30, 1975.

4. U.S. Atomic Energy Commission, Office of Inspection and Enforcement. "Additional Clarification of IE Bulletin 75-01," (Issue date of January 1975 assumed).

5. R. D. Wylie. "A General Review of the Status of the EEI-TVA Research Program on In-Service Inspection." Paper No. 31, Fourth Annual Information Meeting of the Heavy Section Steel Technology (HSST) Program, Oak Ridge National Laboratory, March 31-April 1, 1970.

6. E. V. Waite and D. L. Parry. "Field Evaluation of Heavy-Walled Pressure Vessels Using Acoustic Emission Analysis." Materials Evaluation, June 1971, pp. 117-124.

7. E. R. Reinhart. "State of the Art of Inservice Inspection of Components at Nuclear Stations." Symposium on Materials Performance in Operating Nuclear Systems, Ames Laboratory USAEC, Iowa State University, Ames, Iowa, August 1973.

8. R. A. Buchanan and T. F. Talbot. "Analysis of the Nondestructive Examination of PVRC Plate-Weld Specimen 251J." A report for the PVRC Subcommittee on Nondestructive Examination of Materials for Pressure Components, Pressure Vessel Research Committee, Welding Research Council, May 21, 1973.

9. "Extra: The BWR Pipe-Crack Situation." Nucleonics Week, Special Issue, January 31, 1975.

10. H. H. Klepfer et al. Investigation of Cause of Cracking in Austenitic Stainless Steel Piping, Volume 2. Report NEDO-21000-1, 75NED35, Class 1, General Electric Co., July 1975.

11. H. H. Klepfer et al. Investigation of Cause of Cracking in Austenitic Stainless Steel Piping, Volume 1. Report NEDO-21000-1, 75NED35, Class 1, General Electric Co., July 1975.

12. "A Congressional Hearing on the 10-in. Pipe Cracks Problem." Nucleonics Week, February 6, 1975, p. 2.

13. "All but One BWR 10-in. Pipe Inspection Complete, and No New Cracks." Nucleonics Week, February 27, 1975, p. 3.

14. ASME Boiler and Pressure Vessel Code, Section XI, "Rules for In-Service Inspection of Nuclear Power Plant Components." 1974 edition, with applicable semiannual addenda.

15. American Society of Nondestructive Testing. "Recommended Practice for Nondestructive Testing Personnel Qualification and Certification." Document SNT-TC-1A, 1968 edition and supplements.

16. "Appendix III: Ultrasonic Examination Method for Class 1 and 2 Piping Systems Made From Ferritic Steels." Proposed addition to ASME Boiler and Pressure Vessel Code, Section XI. Draft date: March 28, 1975.

17. Mechanical Fracture Predictions for Sensitized Stainless Steel Piping with Circumferential Cracks. Prepared by Battelle, Columbus Laboratories, September 1976. EPRI NP-192.

APPENDIX A

# PIPING TEST SAMPLES USED IN EPRI TECHNICAL PLANNING STUDY TPS-75-609

E. R. Reinhart, Electric Power Research Institute

and

R. F. Gostage, Nuclear Services Corp.*

*Funded Under EPRI Technical Services Agreement, TSA 75-38-2.

Appendix A

PIPING TEST SAMPLES USED IN EPRI

TECHNICAL PLANNING STUDY

TPS-75-609

This appendix consists of drawings detailing the configuration of the pipe samples used in conducting EPRI Technical Planning Study TPS-75-609, "A Program to Evaluate Current Ultrasonic Inspection Practice for BWR Piping Welds." Each drawing also gives the origin (reactor, piping system, etc.) of the pipe sample, a description of the pipe-to-weld-to-pipe configuration (such as 316 dutchman to 304 pipe), and a summary of laboratory nondestructive evaluation of the piping sample as received from the reactor site, uncleaned and unsectioned.

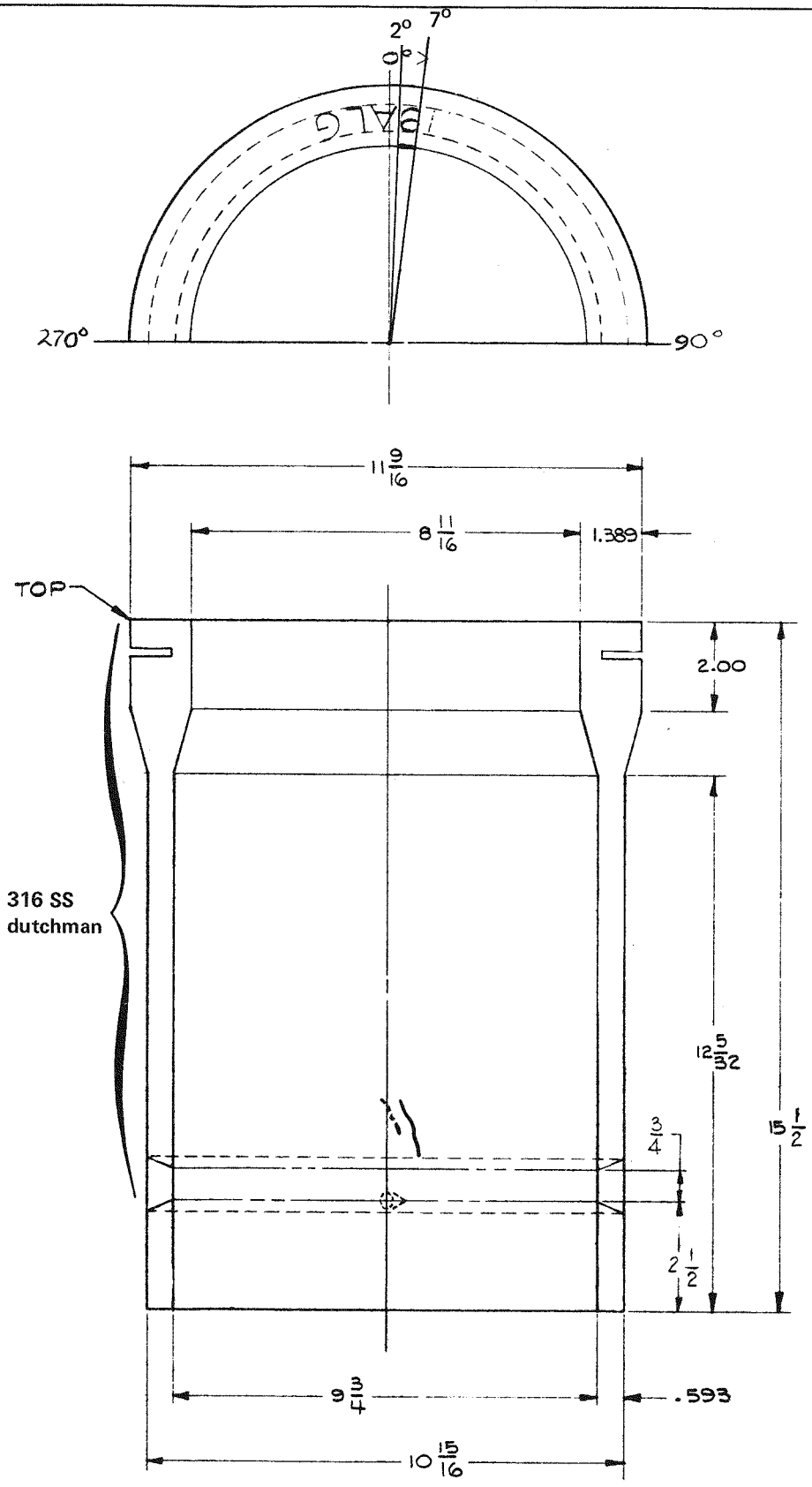
2°
7°
0°
270°
90°
11 9/16
8 11/16
1.389
TOP
2.00
316 SS
dutchman
12 5/32
15 1/2
3/4
2 1/2
9 3/4
.593
10 15/16

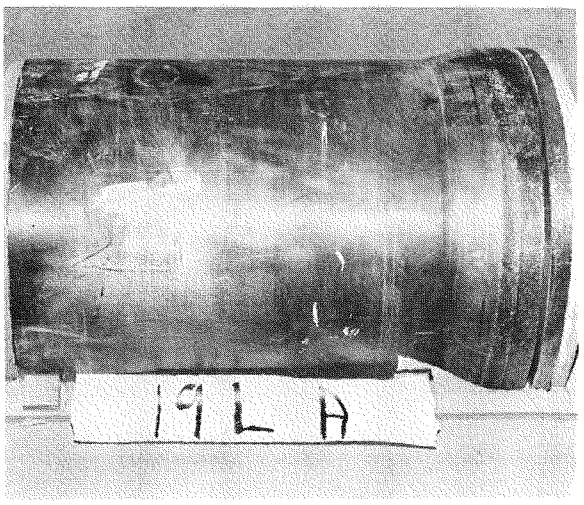


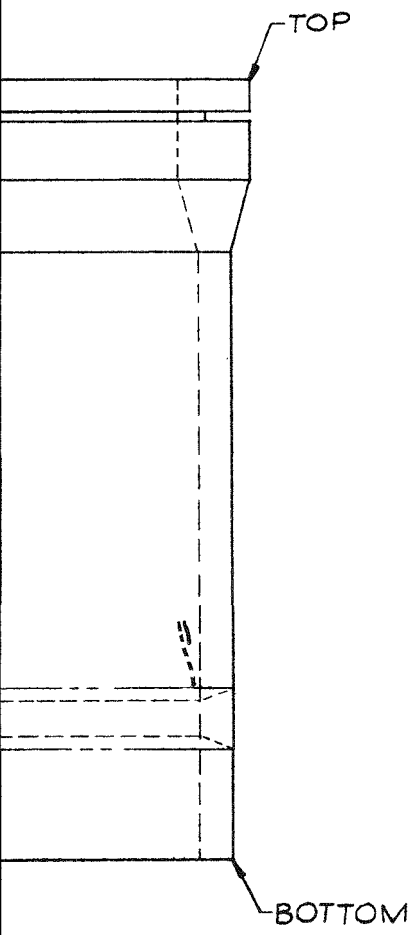


## SAMPLE IDENTIFICATION: 19AL

*ORIGIN:*

Dresden II Nuclear Reactor, 10 in.
A-loop core spray line.

*DESCRIPTION:*

Type of Weld—Pipe to Dutchman
Material—304 SS Pipe to 316 dutchman

*LABORATORY NDE:*

Nozzle section with a weld that is difficult to find since both inside and outside surfaces are flush. Two distinct series of UT indications, both high amplitudes and very similar. Only one DPT indication, through wall axial crack approximately 0.6 in. (1.52 cm) on outside diameter. In summary, one confirmed crack and one possible crack, moderately difficult to detect.

Figure A-1 Sample 19AL

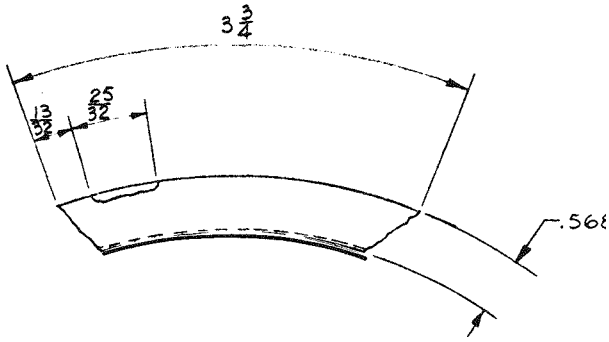
3 3/4
13/32
25/32
.568

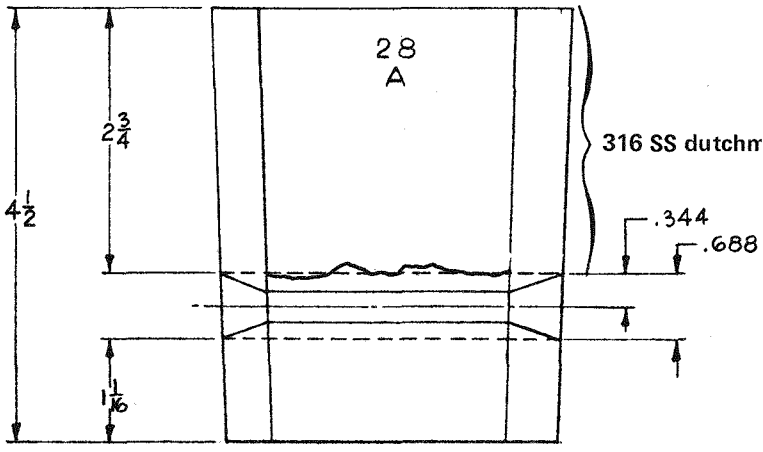
28
A
4 1/2
2 3/4
1 1/16
316 SS dutchm
.344
.688

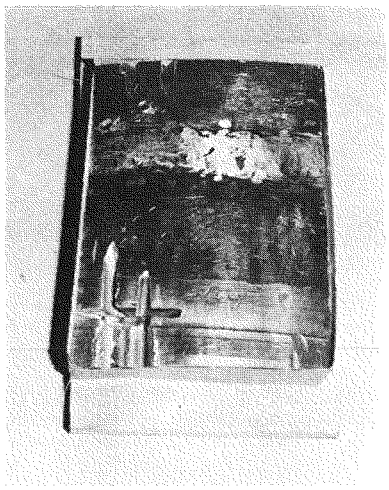

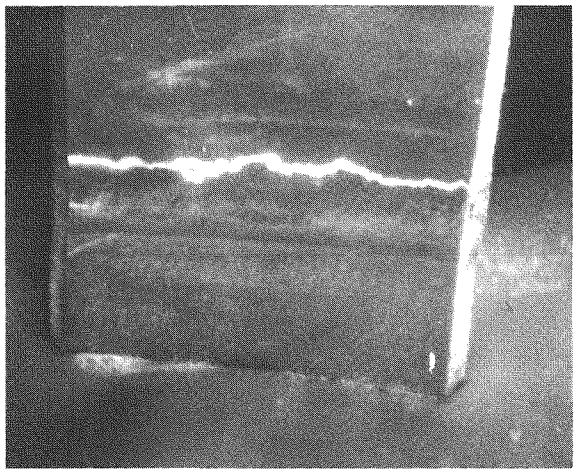

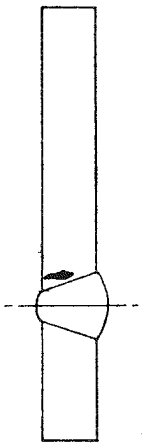

## SAMPLE IDENTIFICATION: 1028A

*ORIGIN:*

Dresden II Nuclear Reactor, 10 in.
B-Loop core spray line.

*DESCRIPTION:*

Type of Weld—Dutchman to pipe
Material—316 SS dutchman to 304 SS pipe

*LABORATORY NDE:*

Continuous high amplitude UT signals across sample. Confirmed full width crack by DPT. Depth of crack ranges from 0.12 in. to 0.5 in. (1.52-3.18 cm) by ERG measurements. Moderately easy to detect.

Figure A-2 Sample 1028A

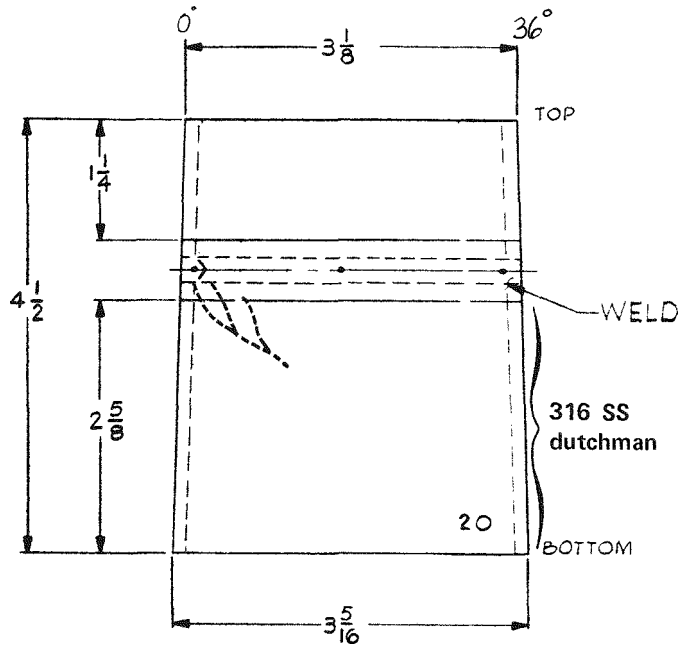
0°
36°
3 1/8
TOP
1 1/4
4 1/2
WELD
316 SS
dutchman
2 5/8
20
BOTTOM
3 5/16

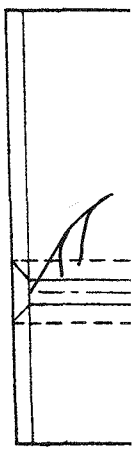

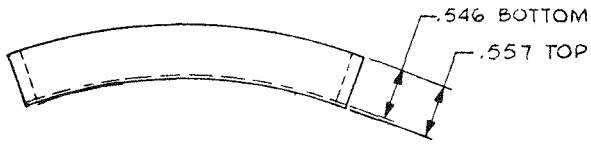
.546 BOTTOM
.557 TOP

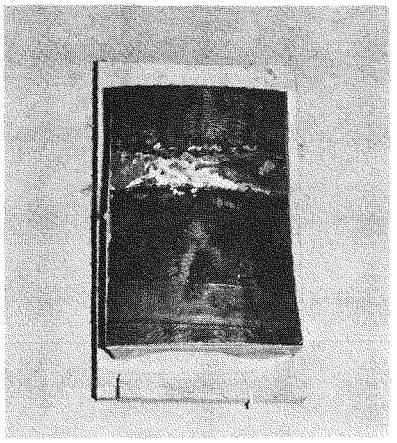

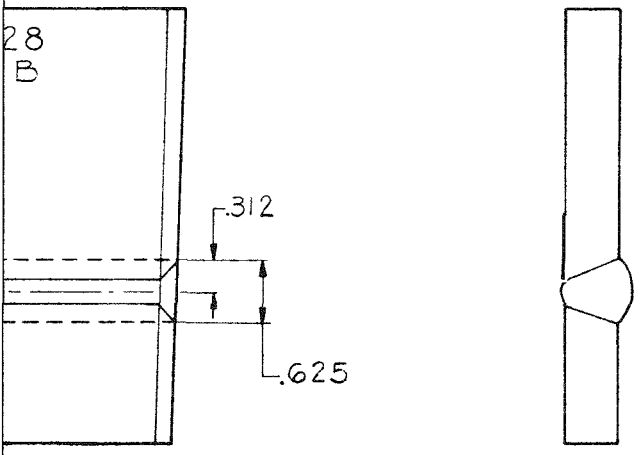


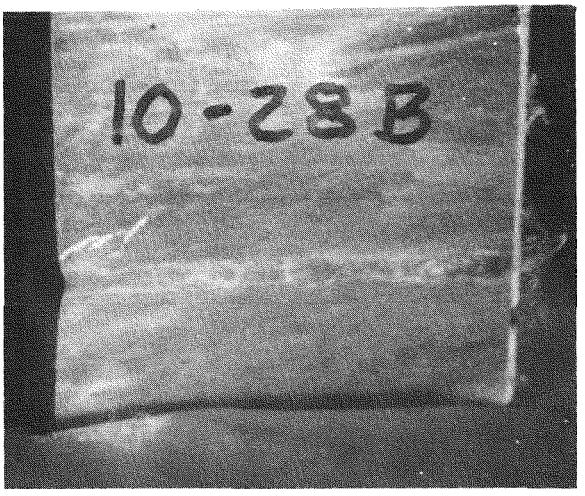


## SAMPLE IDENTIFICATION: 1028B

*ORIGIN:*

Dresden II Nuclear Reactor, 10 in.
B-Loop core spray line.

*DESCRIPTION:*

Type of Weld—Dutchman to pipe
Material—316 SS dutchman to 304 SS pipe

*LABORATORY NDE:*

Fairly continuous geometry signal on UT. One confirmed by DPT, a triple intersecting crack approximately 1 in. (2.54 cm) long (continuation of crack in sample 1028A). Depth of 0.12 in. to 0.5 in (0.3-1.27 cm) by ERG. Crack signal is relatively easy to find but difficult to determine characteristics. Overall, the specimen is difficult to inspect.

Figure A-3 Sample 1028B

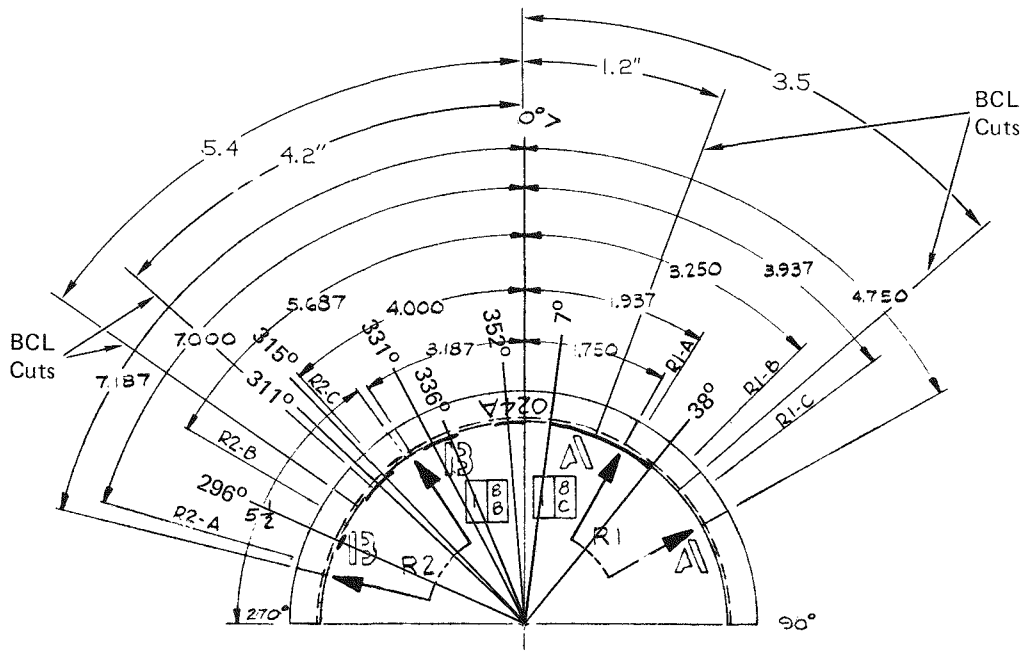


| | A | B | C |
|---|---|---|---|
| 0° | $8\frac{13}{16}$ | $5\frac{13}{16}$ | $2\frac{3}{8}$ |
| 90° | $8\frac{13}{16}$ | $5\frac{11}{16}$ | $2\frac{7}{16}$ |
| 180° | N/A | N/A | N/A |
| 270° | $8\frac{11}{16}$ | $5\frac{3}{4}$ | $2\frac{1}{4}$ |

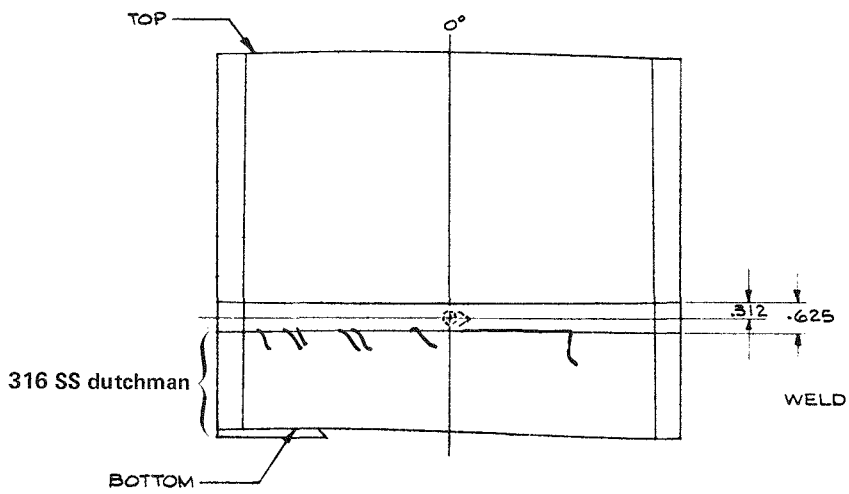


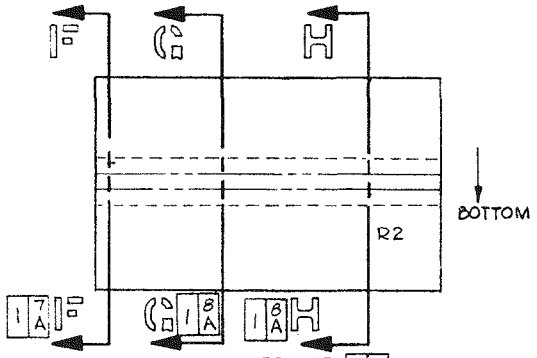


VIEW B-B 1/2C

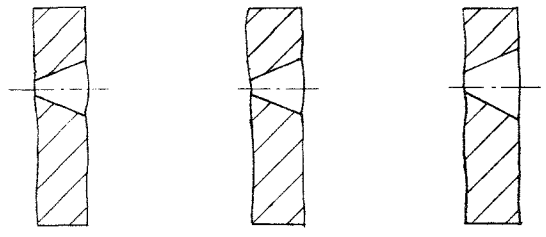


SECTION C-C 1/7C SECTION D-D 1/7C SECTION E-E 1/7C

| WALL THICKNESS BOTTOM | | STAMPED NO. TOP O.D. DIM. | STAMPED NO. TOP I.D. DIM. | BOTTOM O.D. DIM. | BOTTOM I.D. DIM. |
|---|---|---|---|---|---|
| .600 | 0°-180° | N/A | N/A | N/A | N/A |
| .592 | 90°-270° | $10\frac{9}{16}$ | $9\frac{3}{8}$ | $10\frac{3}{4}$ | $9\frac{7}{16}$ |
| N/A | | | | | |
| .604 | | | | | |


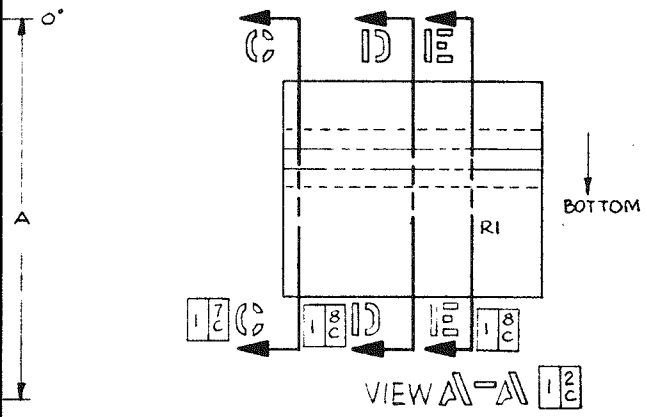


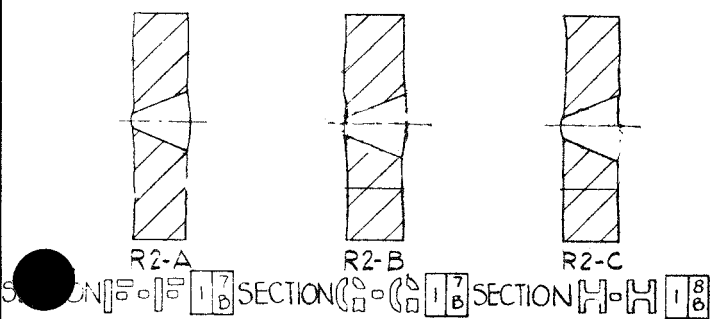


## SAMPLE IDENTIFICATION; 1024A

*ORIGIN:*

Dresden II Nuclear Reactor, 10 in. A-Loop core spray line.

*DESCRIPTION:*

Type of Weld—Dutchman to pipe
Material—316 SS dutchman to 304 SS pipe

*LABORATORY NDE:*

Eight cracks on dutchman (short) side of weld, all SCC confirmed by DPT. One crack axial, one radial, and six skewed at 45°. Depth by ERG are 0.1 in. to 0.12 in. (0.25-0.48 cm) Skewed cracks are extremely difficult to find and characterize. Transducer must be oscillated ±45° into weld to detect. Radial crack is relatively easy to find.

Figure A-4 Sample 1024A

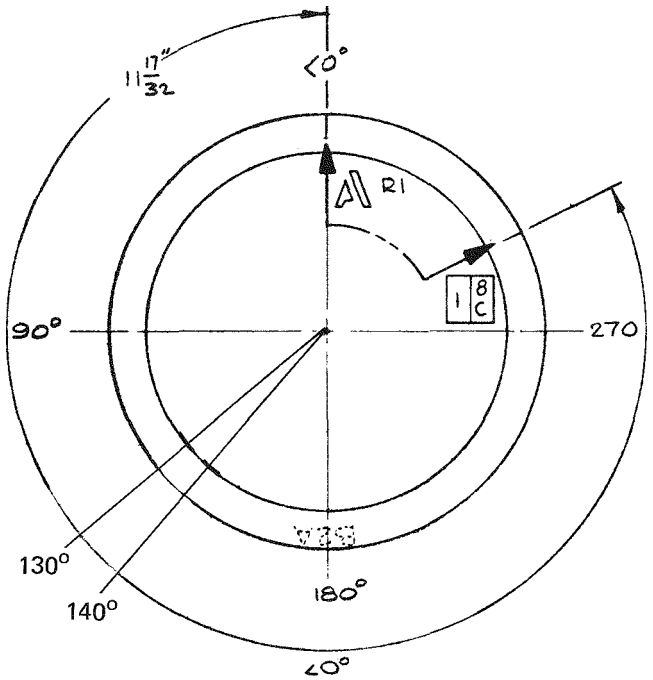


| | A | B | C | WALL THICKNESS TOP |
|---|---|---|---|---|
| 0° | 9.0 | 2 3/4 | 5 5/8 | .371 |
| 90° | | | | .368 |
| 180° | 5 5/8 | 2 11/16 | 2 1/4 | .367 |
| 270° | | | | .366 |

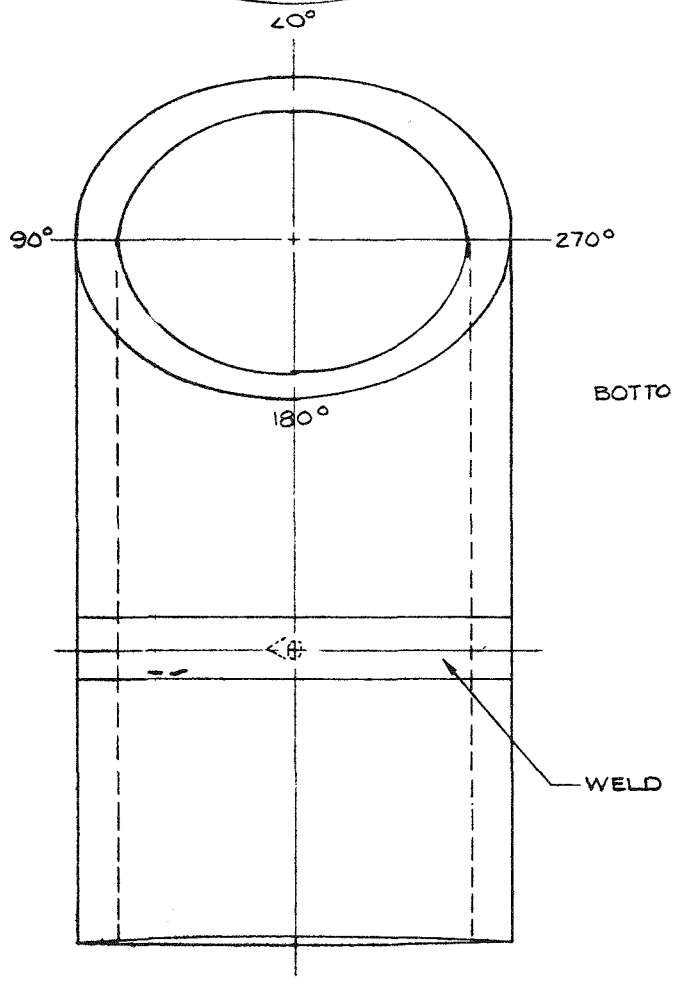


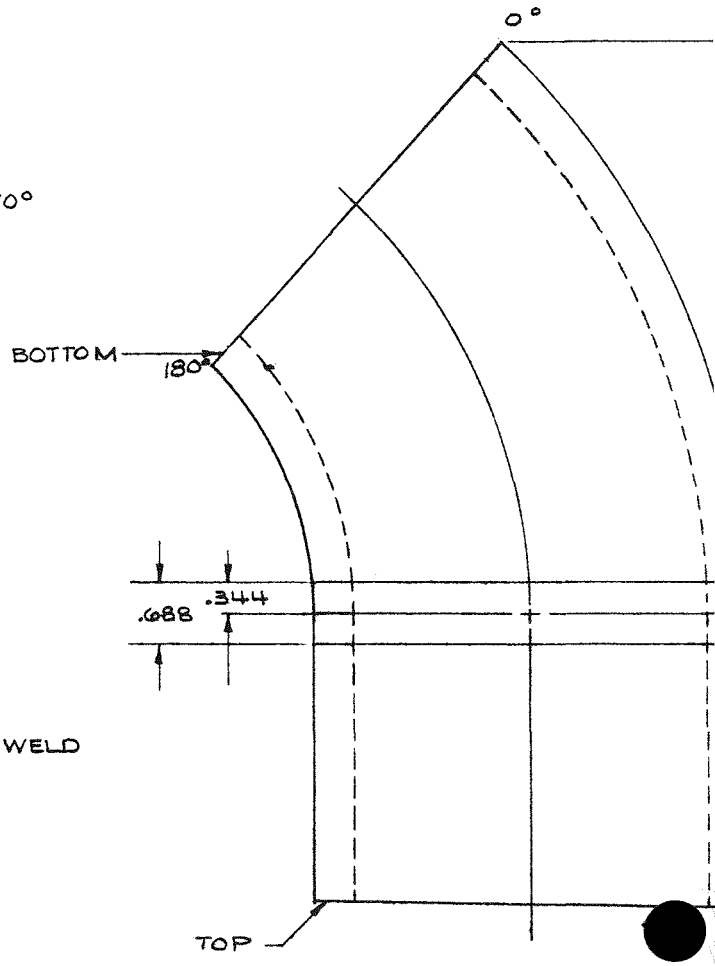

| | | TOP | | BOTOM | |
|---|---|---|---|---|---|
| | | O.D. DIM | I.D. DIM | O.D. DIM | I.D. DIM |
| B | 0°-180° | $4\frac{1}{2}$ | $3\frac{27}{32}$ | $4\frac{9}{16}$ | $3\frac{11}{16}$ |
| D | 90°-270° | $4\frac{1}{2}$ | $3\frac{27}{32}$ | $4\frac{1}{2}$ | $3\frac{11}{16}$ |
| | | | | | |
| | | | | | |

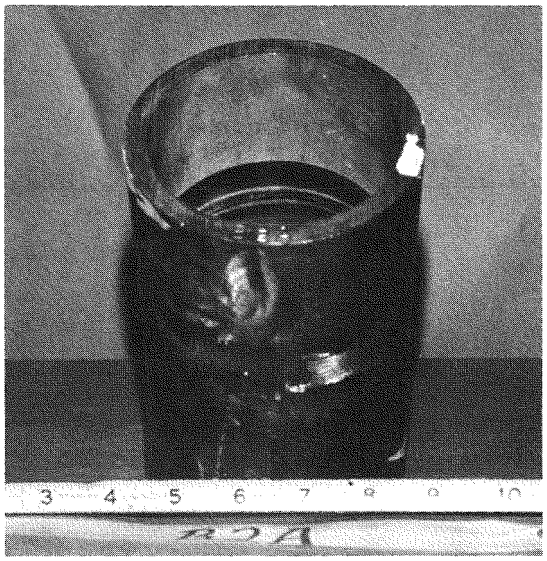

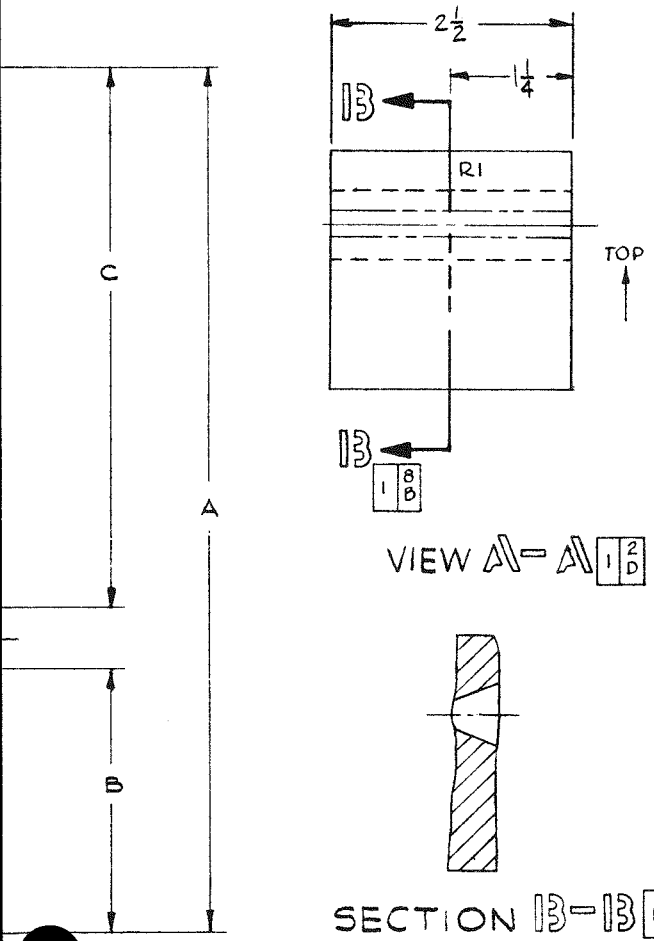


VIEW A-A 1 2 D



SECTION B-B 1 7 C

## SAMPLE IDENTIFICATION: B2A

*ORIGIN:*
Quad Cities I Nuclear Reactor, 4 in.
A and B loops, recirculation bypass lines

*DESCRIPTION:*
Type of Weld—Pipe to Elbow
Material—Both 304 SS

*LABORATORY NDE:*
Many UT geometry signals and low amplitude signals from flaws. Low amplitude signals confirmed as possible SCC by DPT.

Figure A-5 Sample B2A

| | A | B | C | WALL THICKNE | |
|---|---|---|---|---|---|
| | | | | TOP | BO |
| 0° | $5\frac{3}{16}$ | $2\frac{7}{8}$ | $1\frac{7}{16}$ | .628 | . |
| 270° | $4\frac{25}{32}$ | $2\frac{25}{32}$ | 1 | .663 | . |
| 180° | $4\frac{17}{32}$ | $2\frac{25}{32}$ | $\frac{7}{8}$ | .776 | . |
| 90° | $4\frac{7}{8}$ | $2\frac{13}{64}$ | $1\frac{1}{4}$ | .661 | . |

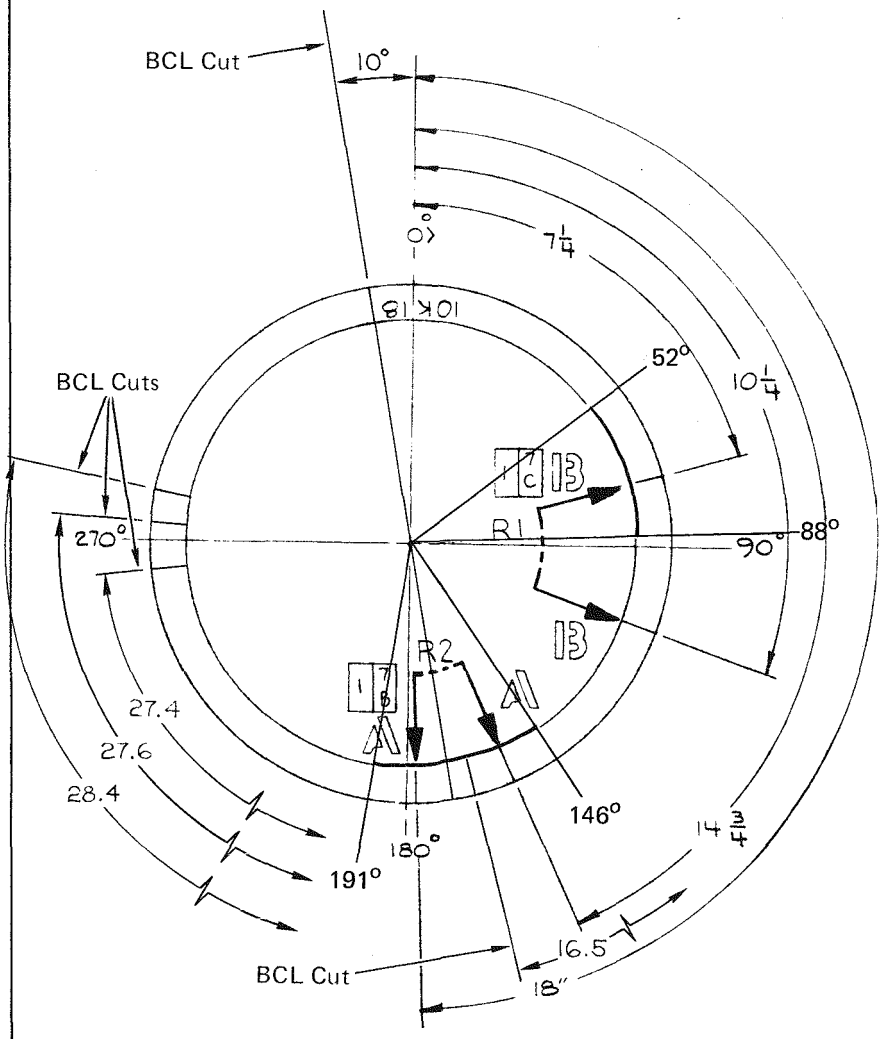


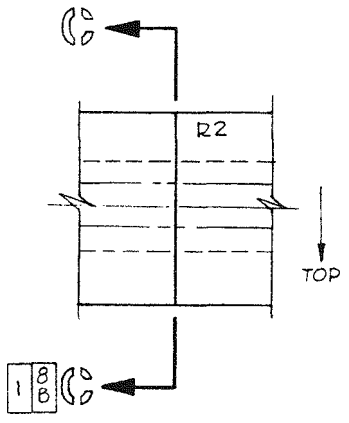


VIEW A-A

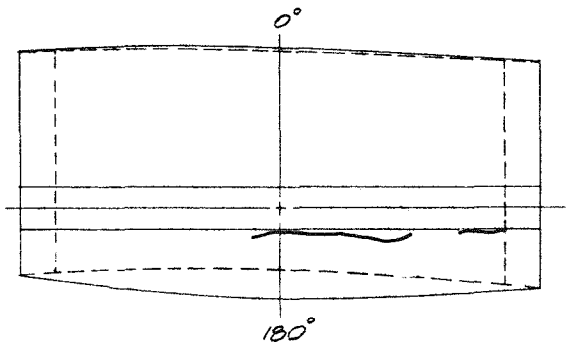


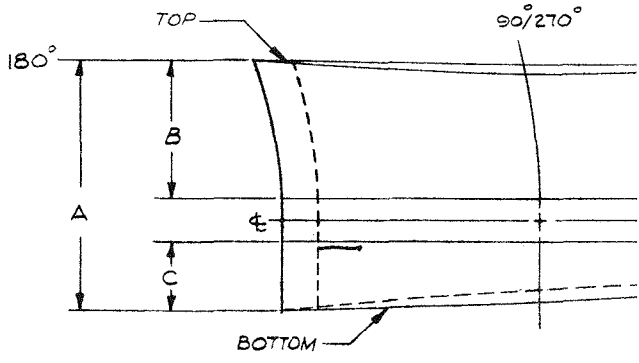

| | TOP | | BOTTOM | |
|---|---|---|---|---|
| | O.D. DIM. | I.D. DIM. | O.D. DIM. | I.D. DIM. |
| 0°-180° | $11\frac{1}{32}$ | $9\frac{11}{16}$ | $10\frac{23}{32}$ | $9\frac{7}{16}$ |
| 90°-270° | $10\frac{13}{16}$ | $9\frac{1}{2}$ | $10\frac{3}{4}$ | $9\frac{7}{16}$ |
| | | | | |
| | | | | |

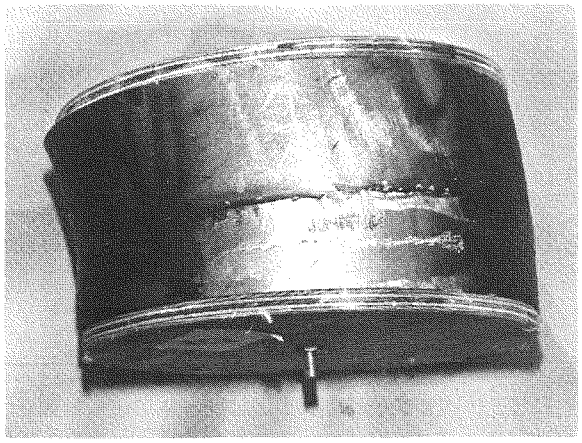

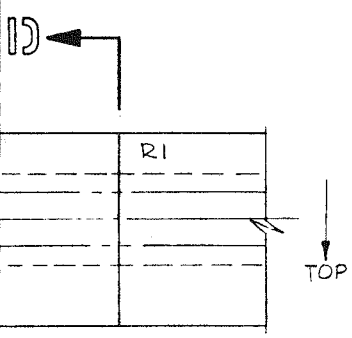


VIEW B-B 1 2C

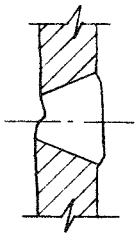

SECTION C-C 1 7E

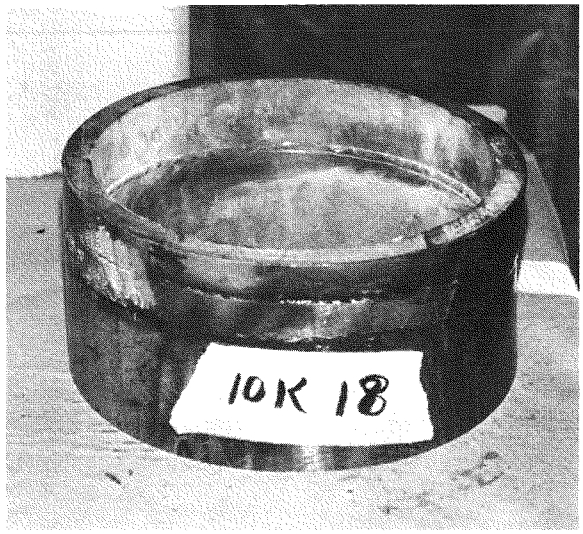


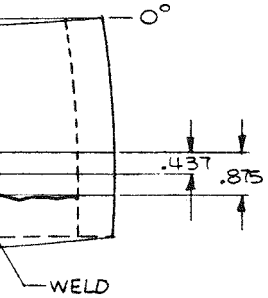


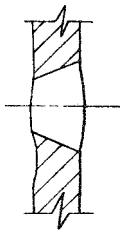

SECTION D-D 1 7C

## SAMPLE IDENTIFICATION: 10K18

*ORIGIN:*

Dresden II Nulcear Reactor, 10 in. B-Loop core spray line.

*DESCRIPTION:*

Type of Weld—Pipe to 90° Elbow
Material—Both 304 SS

*LABORATORY NDE:*

Six intermittent UT signals spread over total 360° sample. Two evaluated as possible radial cracks, one approximately 5.0 in. long at approximately 180° and the other 0.375 in. (0.95 cm) long at 90°. DPT confirmed longer crack at 180° with ERG measurements of 0.03 in. to 0.06 in. (0.08 to 0.15 cm) depth over 1.75 in. (4.445 cm). Difficult to evaluate.

Figure A-6 Sample 10K18

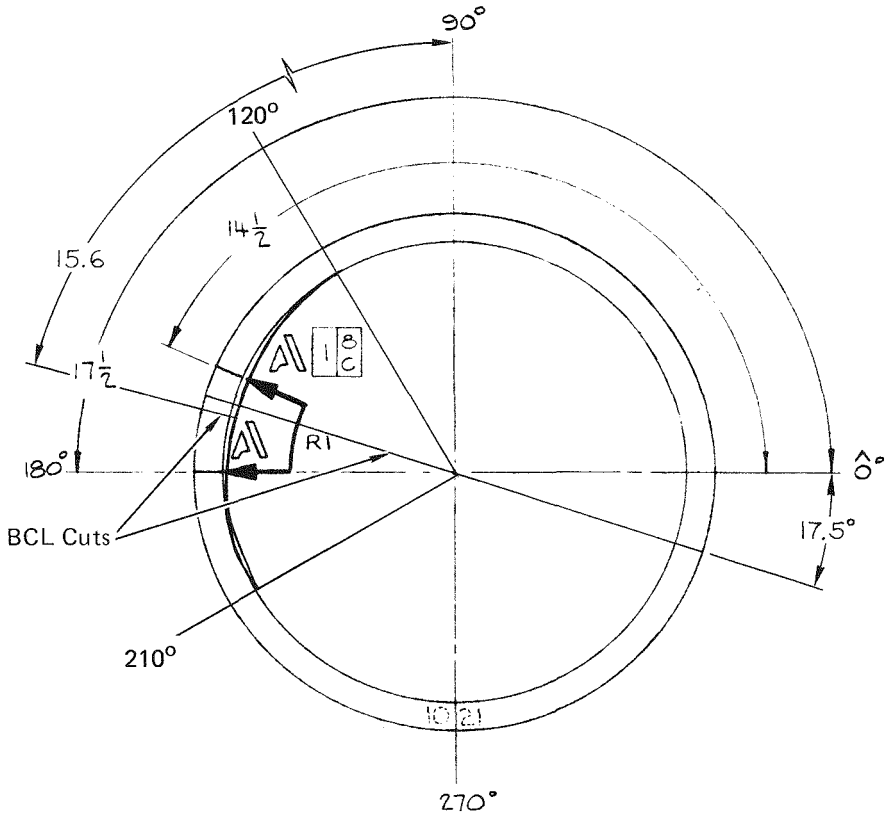


| | A | B | C | WA THICK BOTTO |
|---|---|---|---|---|
| 0° | $6\frac{3}{16}$ | 2 | 3 | .910 |
| 270° | $4\frac{7}{8}$ | $\frac{15}{16}$ | $3\frac{1}{8}$ | .960 |
| 180° | $7\frac{1}{4}$ | $2\frac{7}{8}$ | $3\frac{5}{16}$ | .882 |
| 90° | $8\frac{3}{16}$ | $3\frac{13}{16}$ | $3\frac{1}{4}$ | .785 |

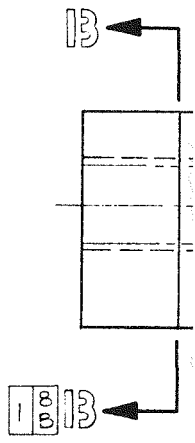


VIEW

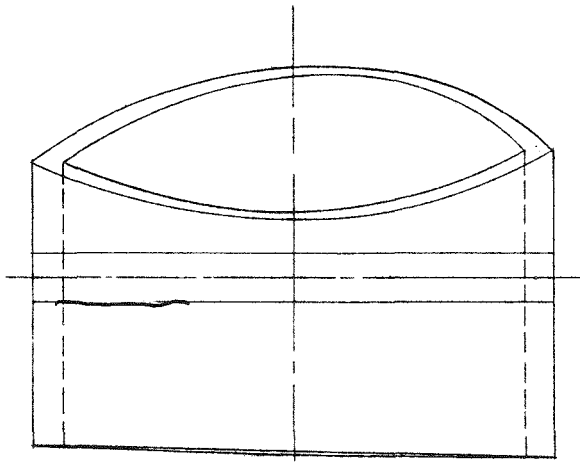

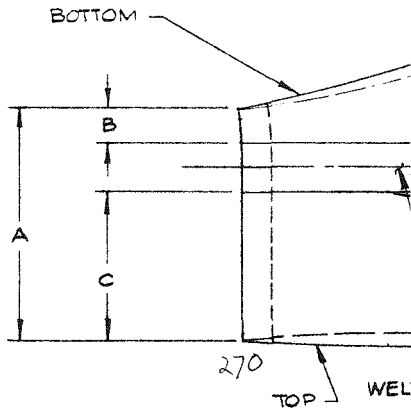

| SS / OP | | BOTTOM | | TOP | |
|---|---|---|---|---|---|
| | | O.D. DIM. | I.D. DIM. | O.D. DIM. | I.D. DIM. |
| 644 | 0°-180° | $10\frac{15}{16}$ | $9\frac{3}{16}$ | $10\frac{3}{4}$ | $9\frac{7}{16}$ |
| 655 | 90°-270° | $10\frac{7}{8}$ | $9\frac{1}{8}$ | $10\frac{3}{4}$ | $9\frac{7}{16}$ |
| 649 | | | | | |
| 650 | | | | | |

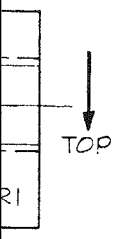


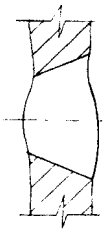


-A 1 2 C

SECTION B-B 1 7 C

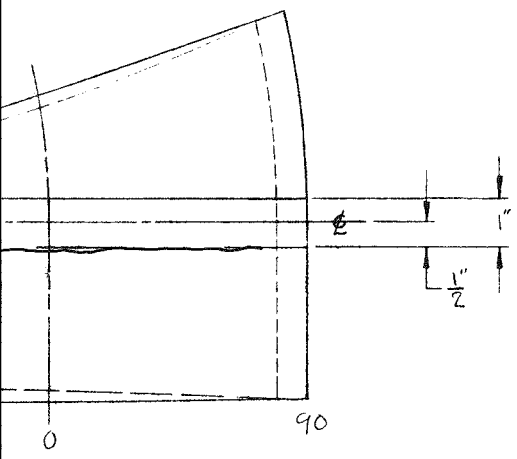


## SAMPLE IDENTIFICATION: 1021

*ORIGIN:*
Dresden II Nuclear Reactor, 10 in.
B-Loop core spray line.

*DESCRIPTION:*
Type of Weld—Pipe to elbow
Material—Both 304 SS

*LABORATORY NDE:*
Six UT signals in two areas, one area confirmed by DPT 180° from reference, approximately 7.87 in. (20.0 cm) long, very straight and uniform indication defined as crack or lack of fusion. In summary, one confirmed crack or lack of fusion and one possible crack or lack of fusion. Moderately difficult to detect.

Figure A-7 Sample 1021

| | A | B | C | WALL THICKNESS TOP | WALL THICKNESS BOTTOM | | BOTTOM O.D. DIM. | BOTTOM I.D. DIM. | BOTTOM O.D. DIM. | BOTTOM I.D. DIM. |
|---|---|---|---|---|---|---|---|---|---|---|
| 0° | $4\frac{27}{32}$ | $2\frac{7}{16}$ | $1\frac{5}{8}$ | .672 | .555 | 0°-180° | $11\frac{1}{32}$ | $9\frac{5}{8}$ | $10\frac{3}{4}$ | $9\frac{11}{16}$ |
| 90° | $4\frac{3}{4}$ | $2\frac{1}{2}$ | $1\frac{1}{2}$ | .657 | .561 | 90°-270° | $10\frac{23}{32}$ | $9\frac{15}{32}$ | $10\frac{3}{4}$ | $9\frac{11}{16}$ |
| 180° | $4\frac{13}{16}$ | $2\frac{1}{2}$ | $1\frac{1}{2}$ | .654 | .537 | | | | | |
| 270° | $4\frac{7}{8}$ | $2\frac{3}{8}$ | $1\frac{9}{16}$ | .748 | .564 | | | | | |

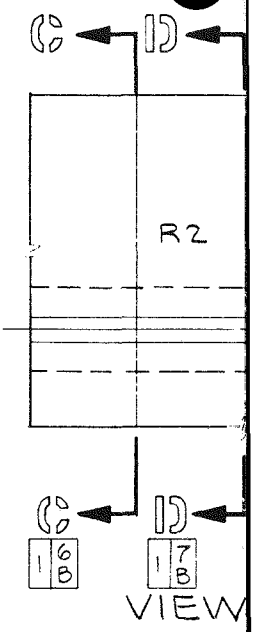


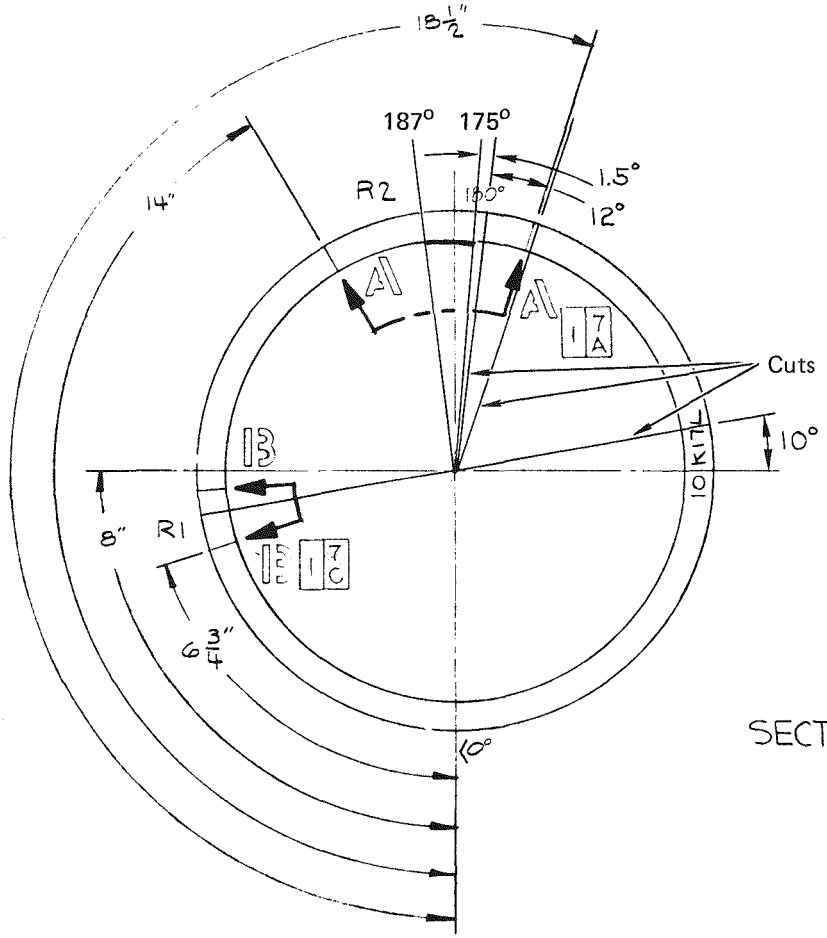


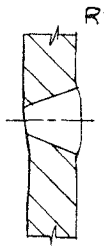


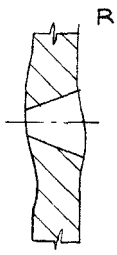


SECTION C-C

SECTION D-D

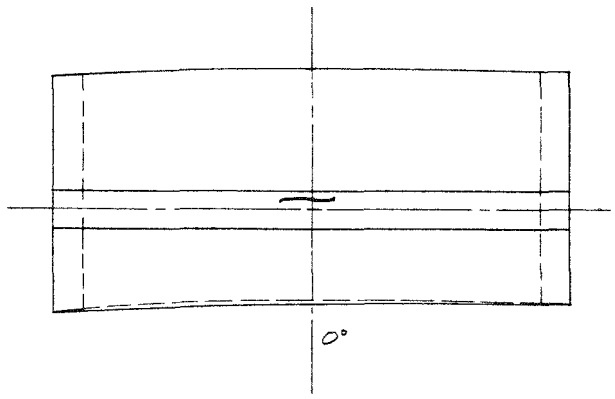


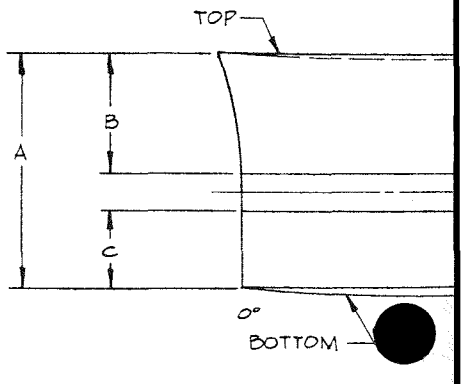

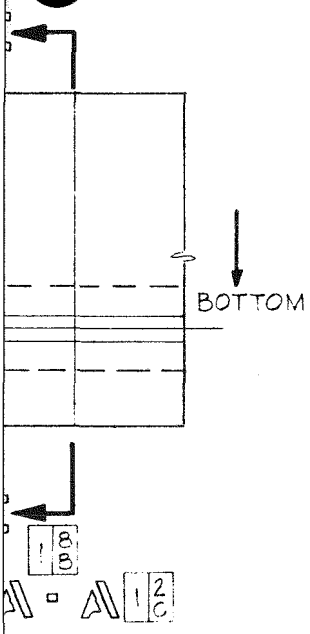


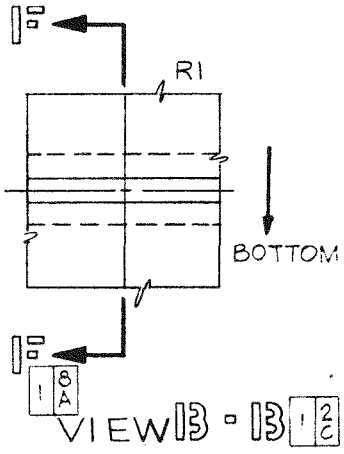


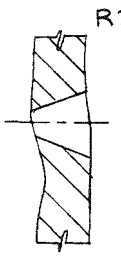


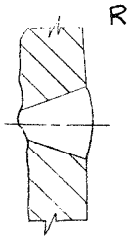


SECTION A-A SECTION C-C

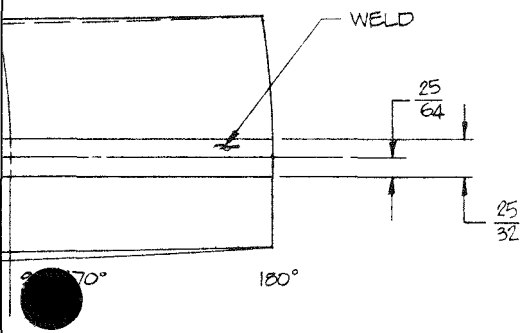




**SAMPLE IDENTIFICATION: 10K17L**

*ORIGIN:*

Dresden II Nuclear Reactor, 10 in.
B-Loop core spray line.

*DESCRIPTION:*

Type of Weld—90° elbow to pipe
Material—304 SS elbow to 304 SS pipe

*LABORATORY NDE:*

Nine geometric signals including one series approximately 1.5 in. (3.8 cm) long and 15 in. (38.1 cm) from B-B reference (stamp mark on sample) in an internally ground area approximately 180° from B-B reference. DPT indicates two spots with possible interconnecting crack in the ground area (Photo). In summary, one possible crack approximately 1.5 in. (3.8 cm) long and difficult to detect by UT.

Figure A-8 Sample 10K17L

| | A | B | C | WALL THICKNESS | |
|---|---|---|---|---|---|
| | | | | TOP | BOTTOM |
| 0° | $4\frac{3}{4}$ | $2\frac{7}{8}$ | $1\frac{3}{16}$ | .550 | .669 |
| 90° | $3\frac{21}{32}$ | $2\frac{3}{4}$ | N/A | .553 | .671 |
| 180° | $2\frac{13}{16}$ | $2\frac{11}{16}$ | N/A | .547 | .631 |
| 270° | $3\frac{1}{2}$ | $2\frac{3}{4}$ | N/A | .551 | .683 |

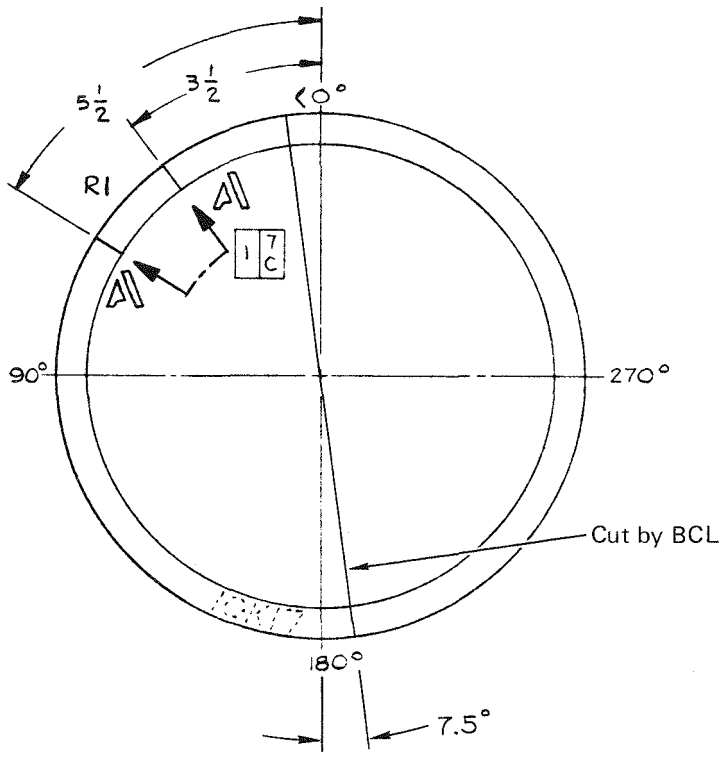


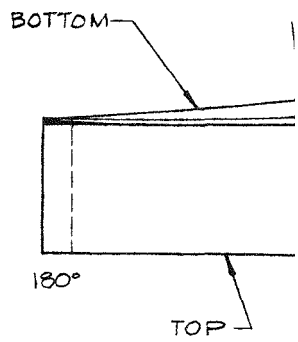


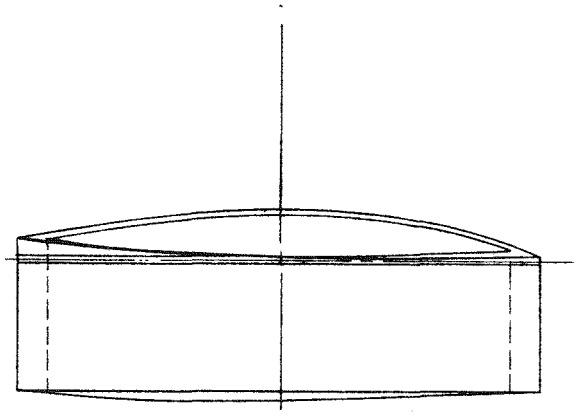

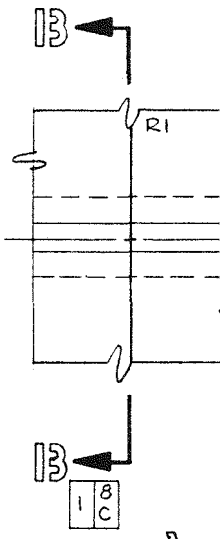


VIEW A

| | TOP | | BOTTOM | |
|---|---|---|---|---|
| | O.D. DIM. | I.D. DIM. | O.D. DIM. | I.D. DIM. |
| 0°-180° | $10\frac{13}{16}$ | $9\frac{23}{32}$ | $10\frac{27}{32}$ | $9\frac{9}{16}$ |
| 90°-270° | $10\frac{13}{16}$ | $9\frac{23}{32}$ | $10\frac{21}{32}$ | $9\frac{3}{8}$ |
| | | | | |
| | | | | |

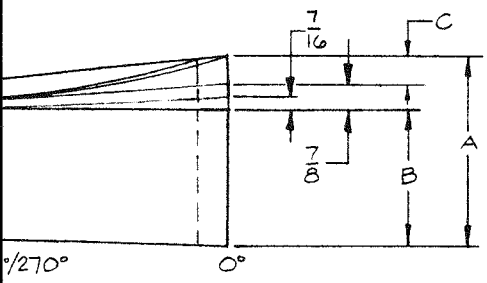



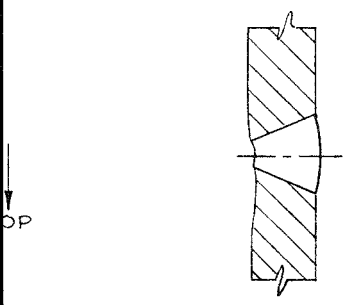

SECTION 13 - 13 1 7C

1 2C

## SAMPLE IDENTIFICATION: 10K17

*ORIGIN:*

Dresden II Nuclear Reactor, 10 in. A-Loop core spray line.

*DESCRIPTION:*

Type of Weld—Pipe-to-valve assembly
Material—304 SS pipe to 304 SS valve

*LABORATORY NDE:*

No DPT indications. UT shows geometry signals completely around weld. No confirmed cracks.

Figure A-9 Sample 10K17

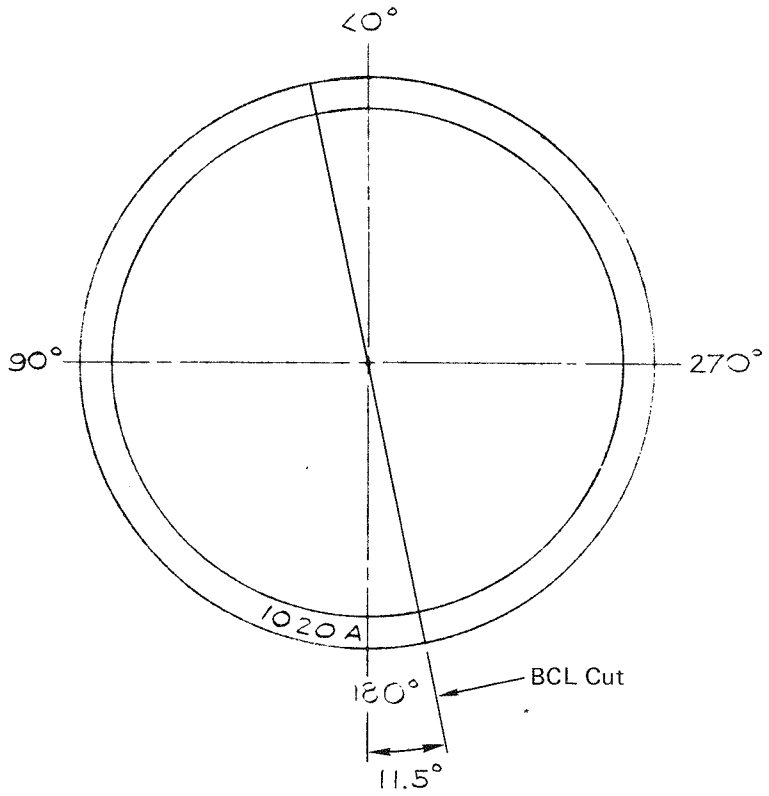


| | A | B | C | WA THICK TOP |
|---|---|---|---|---|
| 0° | $6\frac{15}{16}$ | $3\frac{5}{16}$ | $2\frac{7}{8}$ | .800 |
| 90° | $5\frac{1}{2}$ | $1\frac{1}{2}$ | $2\frac{15}{16}$ | .918 |
| 180° | $4\frac{1}{8}$ | $\frac{1}{2}$ | $2\frac{5}{8}$ | .907 |
| 270° | $5\frac{1}{2}$ | $1\frac{7}{8}$ | $2\frac{5}{8}$ | .887 |

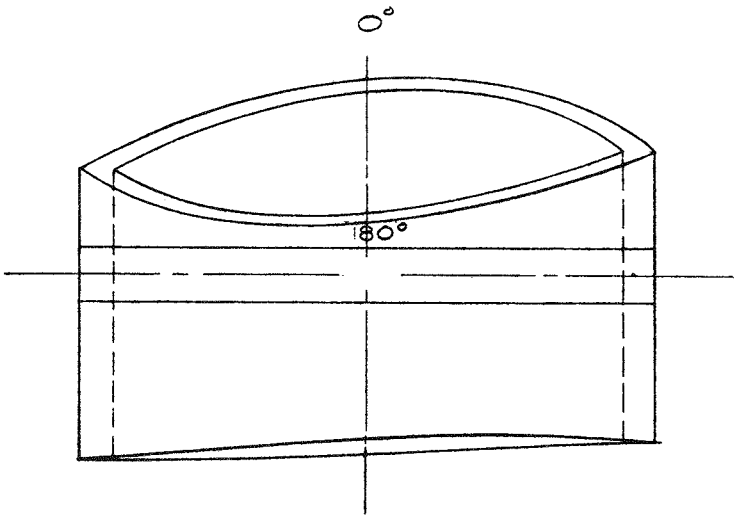


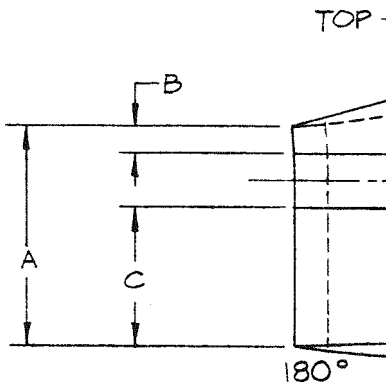


BOTT

| SS TTOM | | TOP | | BOTTOM | |
|---|---|---|---|---|---|
| | | O.D. DIM. | I.D. DIM. | O.D. DIM. | I.D. DIM. |
| 662 | 0°-180° | $10\frac{29}{32}$ | $9\frac{7}{32}$ | $10\frac{13}{16}$ | $9\frac{1}{2}$ |
| 657 | 90°-270° | 11 | $9\frac{7}{32}$ | $10\frac{13}{16}$ | $9\frac{9}{16}$ |
| 663 | | | | | |
| 654 | | | | | |

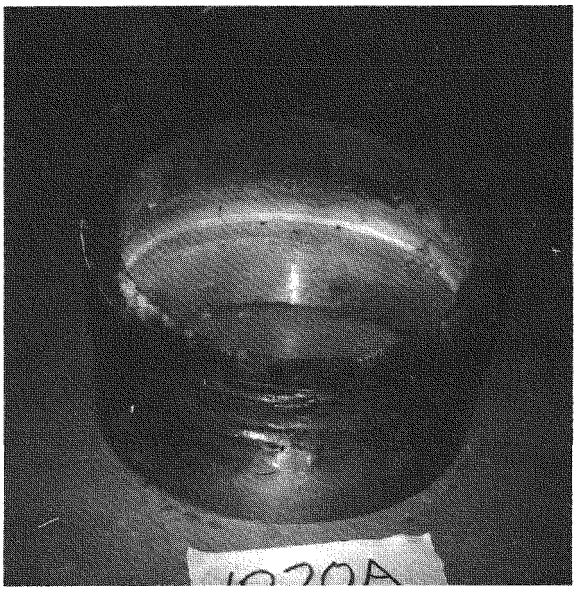


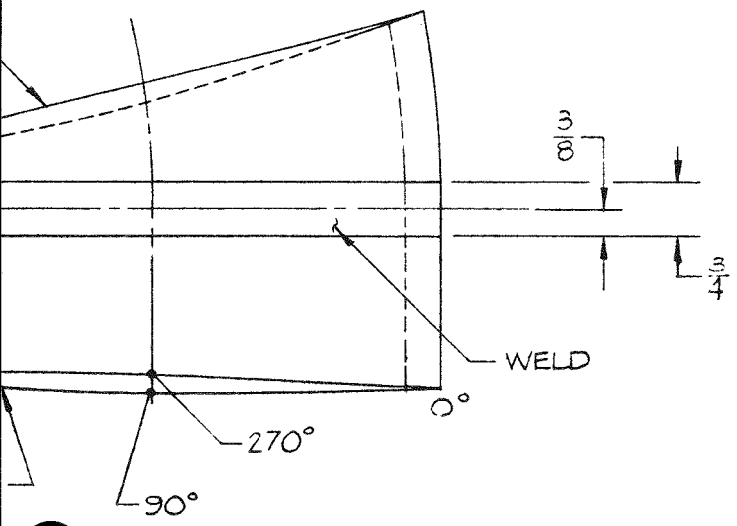


## SAMPLE IDENTIFICATION: 1020A

*ORIGIN:*
Dresden II Nuclear Reactor, 10 in.
B-Loop core spray line.

*DESCRIPTION:*
Type of Weld—Elbow to pipe
Material—Both 304 SS

*LABORATORY NDE:*
No DPT indications and limited number of geometric signals. No cracks.

Figure A-10 Sample 1020A

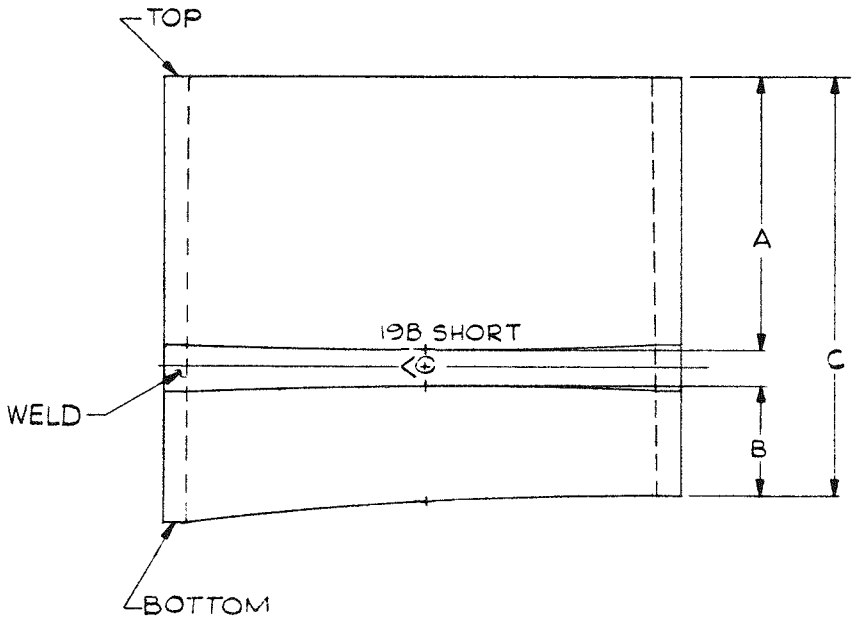


| | A | B | C |
|---|---|---|---|
| 0° | $5\frac{5}{8}$ | $2\frac{3}{8}$ | $8\frac{13}{16}$ |
| 90° | $5\frac{3}{4}$ | $2\frac{1}{4}$ | $8\frac{11}{16}$ |
| 270° | $5\frac{11}{16}$ | $2\frac{3}{4}$ | $9\frac{5}{32}$ |

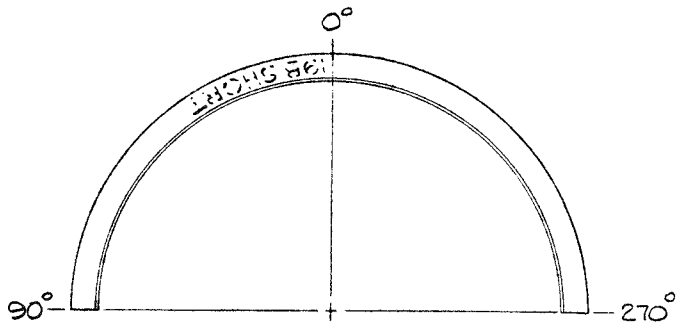


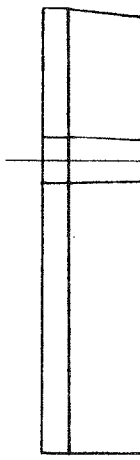

| WALL THICKNESS | | | TOP | | BOTTOM | |
|---|---|---|---|---|---|---|
| OP | BOTTOM | | O.D. DIM. | I.D. DIM. | O.D. DIM. | I.D. DIM. |
| 549 | .558 | 0° | | | | |
| 551 | .556 | 90°-270° | $10\frac{13}{16}$ | $9\frac{13}{16}$ | $10\frac{13}{16}$ | $9\frac{3}{4}$ |
| 552 | .559 | | | | | |

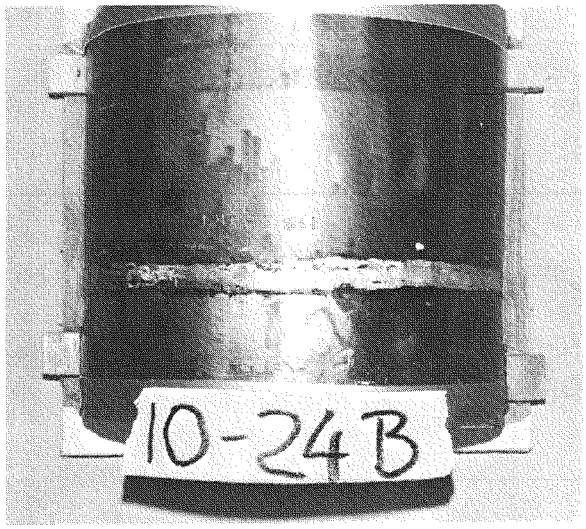


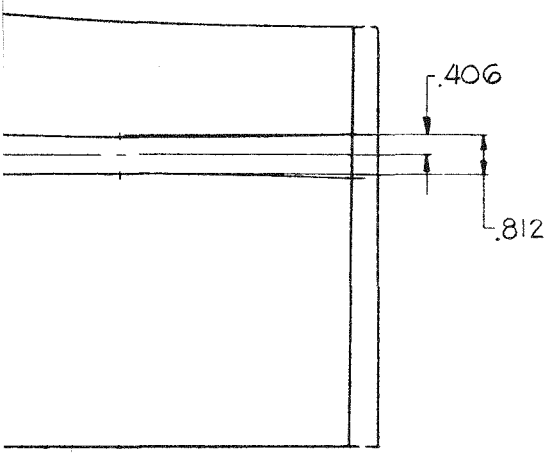


## SAMPLE IDENTIFICATION: 1024B

*ORIGIN:*

Dresden II Nuclear Reactor, 10 in.
B-Loop core spray line.

*DESCRIPTION:*

Type of Weld—Dutchman to pipe
Material—316 SS dutchman to 304 SS pipe

*LABORATORY NDE:*

No DPT indications and few UT geometry signals. Easy to inspect, no cracks.

Figure A-11 Sample 1024B

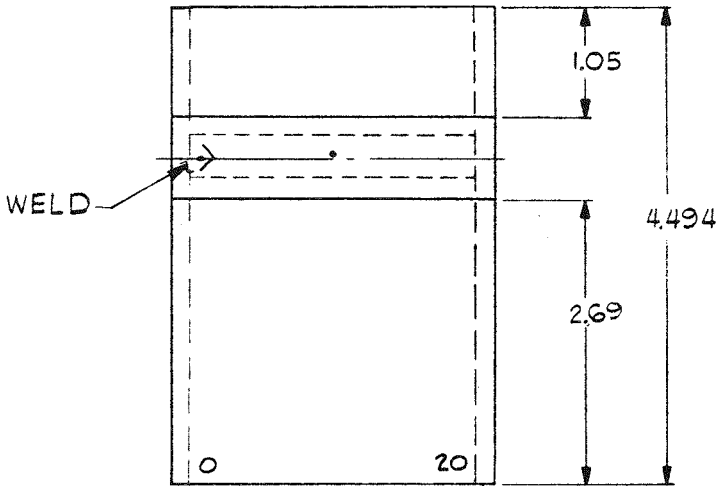


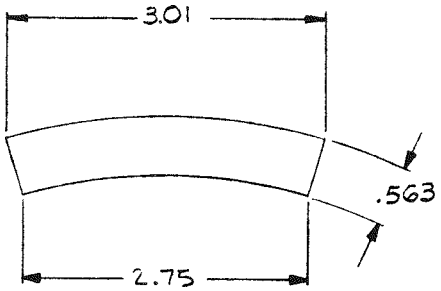


316 SS
dutchman

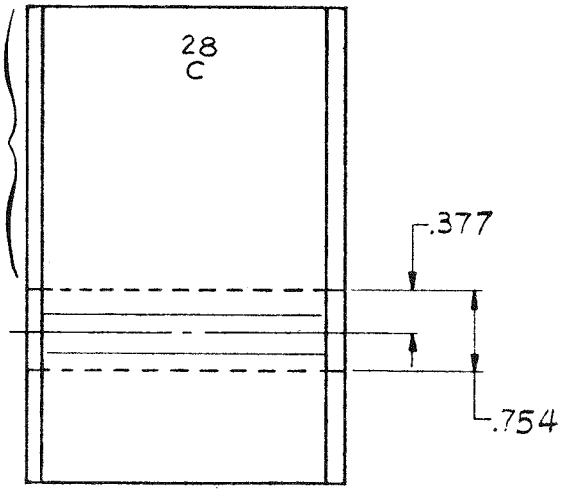

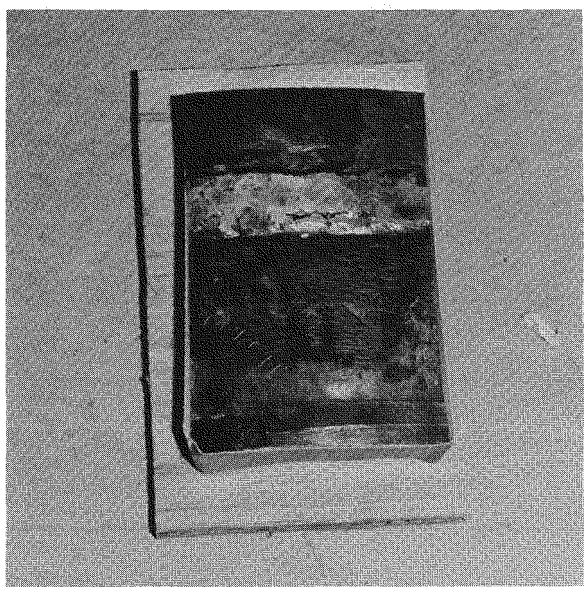

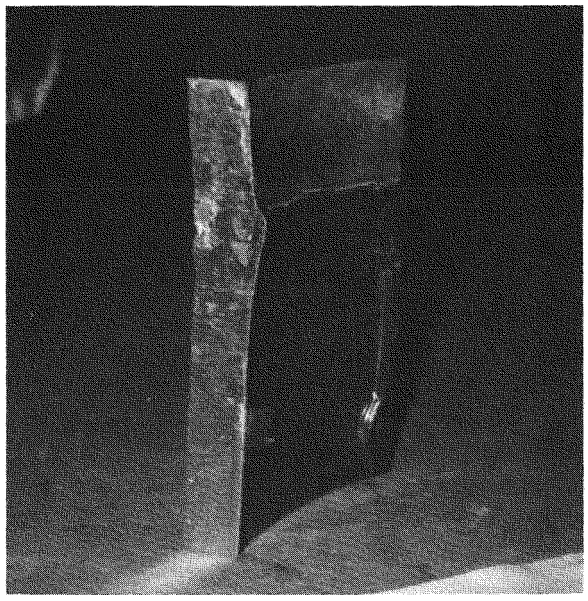

**SAMPLE IDENTIFICATION: 1028C**

*ORIGIN:*
Dresden II Nuclear Reactor, 10 in.
B-Loop core spray line.

*DESCRIPTION:*
Type of Weld—Dutchman to pipe
Material—316 SS dutchman to 304 SS pipe

*LABORATORY NDE:*
No DPT indications and spurious UT signals from weld root. No cracks.

Figure A-12 Sample 1028C

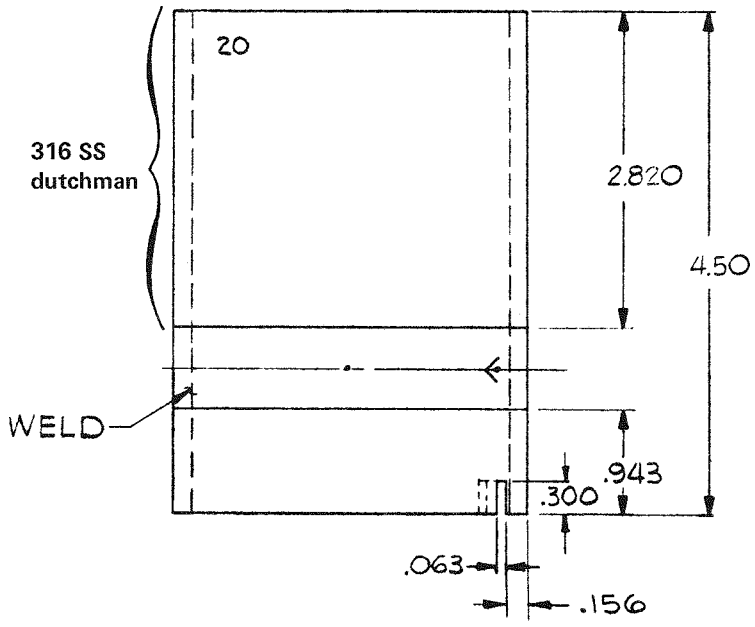
20
316 SS
dutchman
2.820
4.50
WELD
.943
.300
.063
.156

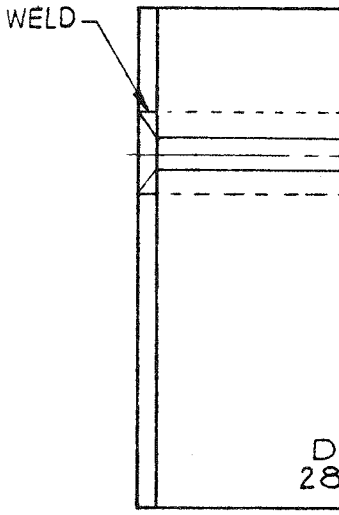
WELD

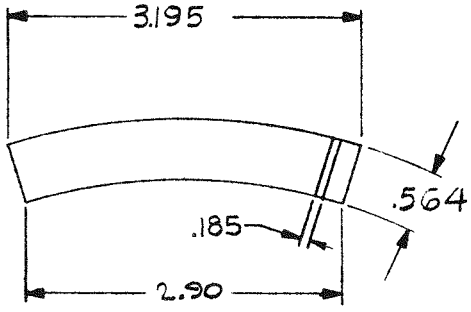
3.195
.564
.185
2.90

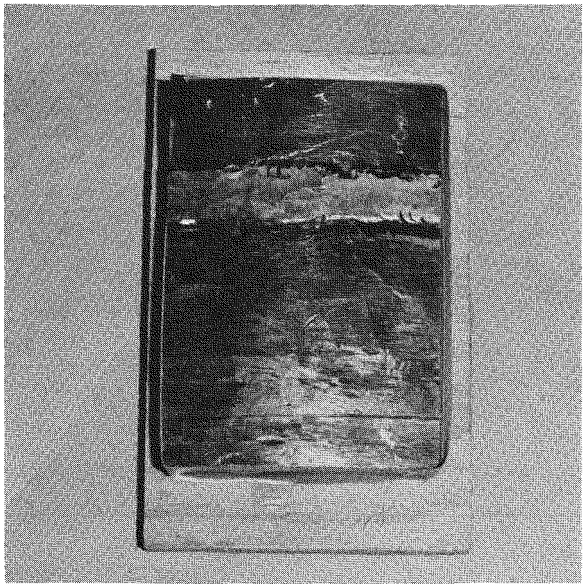

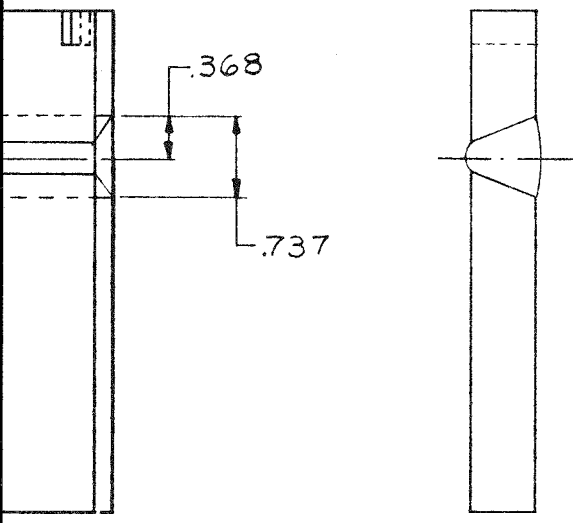


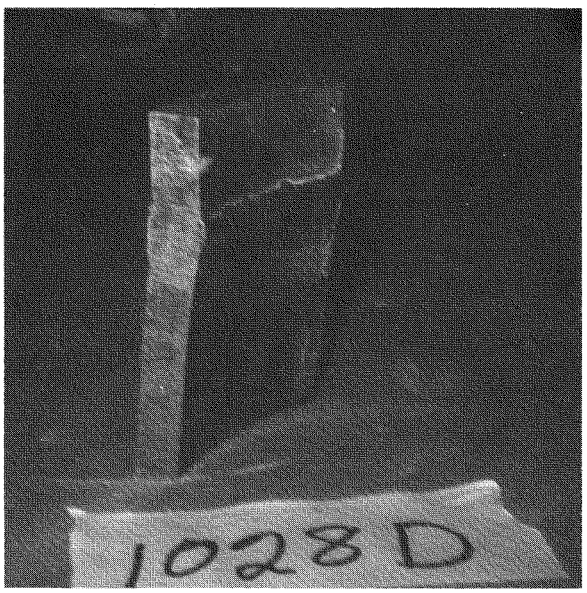


## SAMPLE IDENTIFICATION: 1028D

*ORIGIN:*

Dresden II Nuclear Reactor, 10 in.
B-Loop core spray line.

*DESCRIPTION:*

Type of Weld–Dutchman to pipe
Material–316 SS Dutchman to 304 SS pipe

*LABORATORY NDE:*

No DPT indications and spurious UT signals from weld root.

Figure A-13 Sample 1028D

| | A | B | C | WALL THICKNESS | | | STAMPED NO. TOP | | BOTTOM | |
|---|---|---|---|---|---|---|---|---|---|---|
| | | | | TOP | BOTTOM | | O.D. DIM. | I.D. DIM. | O.D. DIM. | I.D. DIM. |
| 0° | $5\frac{11}{16}$ | $5\frac{1}{16}$ | N/A | .773 | N/A | 0°-180° | $11\frac{1}{32}$ | $9\frac{11}{32}$ | $10\frac{13}{16}$ | $9\frac{3}{8}$ |
| 90° | $5\frac{1}{8}$ | $3\frac{21}{32}$ | N/A | .908 | N/A | 90°-270° | $10\frac{15}{16}$ | $9\frac{1}{8}$ | $10\frac{13}{16}$ | $9\frac{7}{16}$ |
| 180° | $4\frac{9}{32}$ | $3\frac{1}{8}$ | N/A | .961 | N/A | | | | | |
| 270° | 5 | $4\frac{3}{8}$ | N/A | .898 | N/A | | | | | |

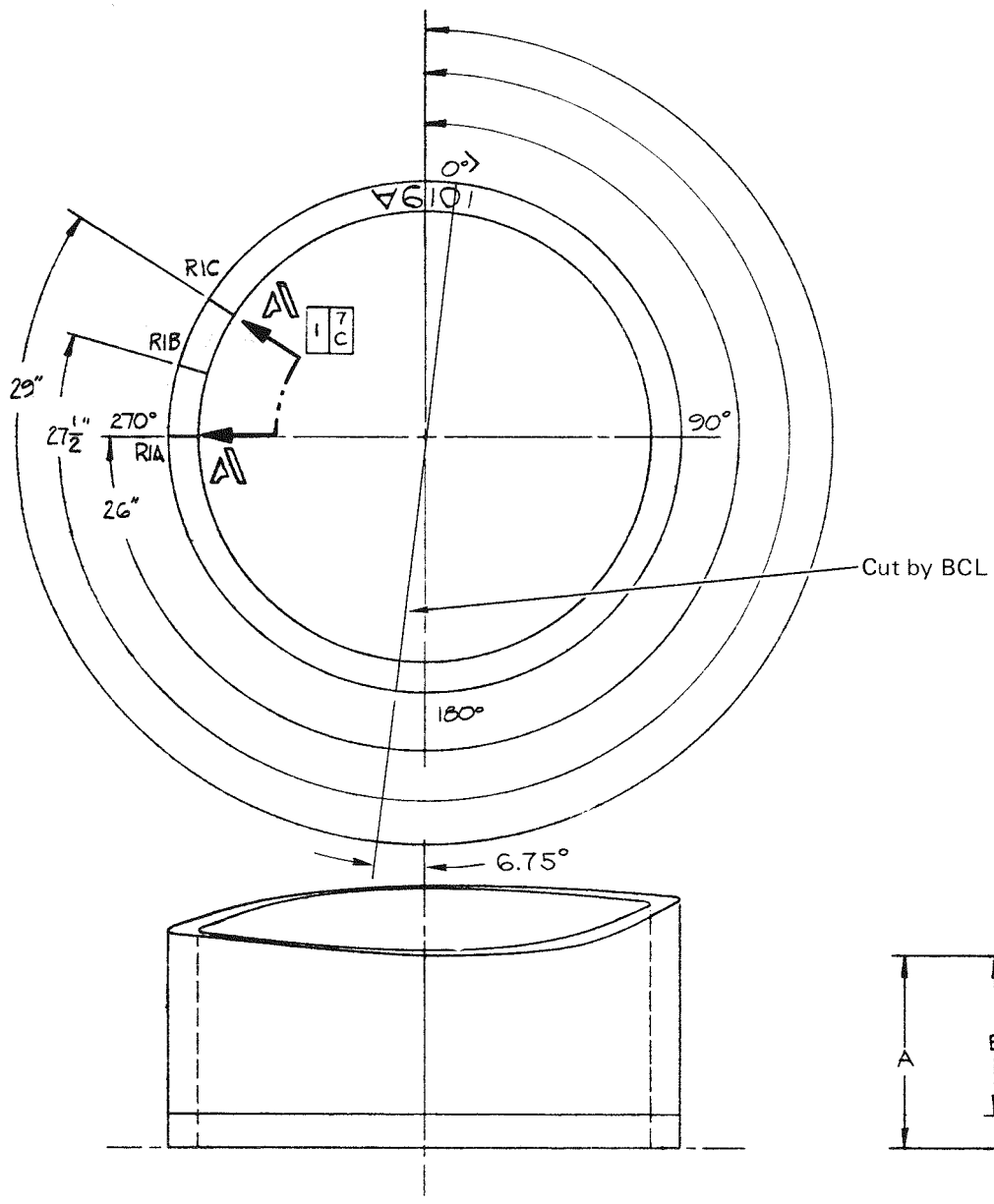


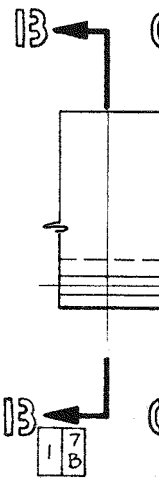


V

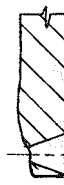

SECTION

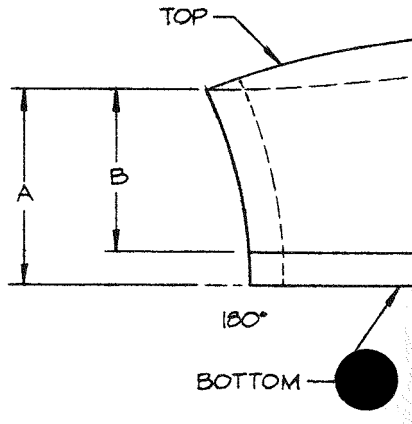

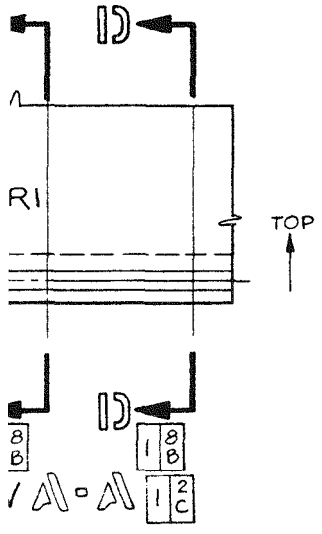


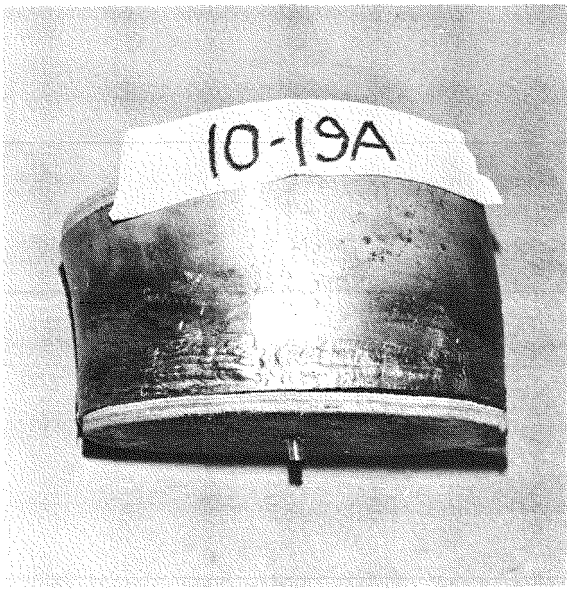


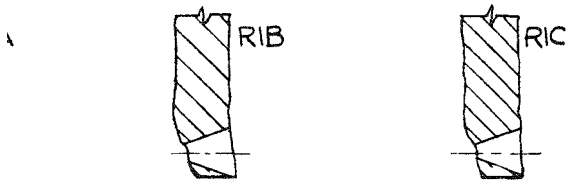


B - B 1 6 C SECTION C - C 1 7 C SECTION D - D 1 7 C

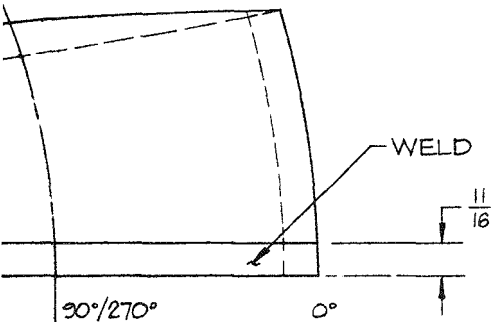


## SAMPLE IDENTIFICATION: 1019A

*ORIGIN:*
Dresden II Nuclear Reactor, 10 in.
A-Loop core spray line.

*DESCRIPTION:*
Type of Weld—Pipe to elbow
Material—Both 304 SS

*LABORATORY NDE:*
Numerous geometric UT indications due to unground weld crowns and extreme suck-up on the inside of the pipe. No DPT indications. Difficult to inspect and time-consuming to record, plot, and evaluate. No cracks.

Figure A-14 Sample 1019A

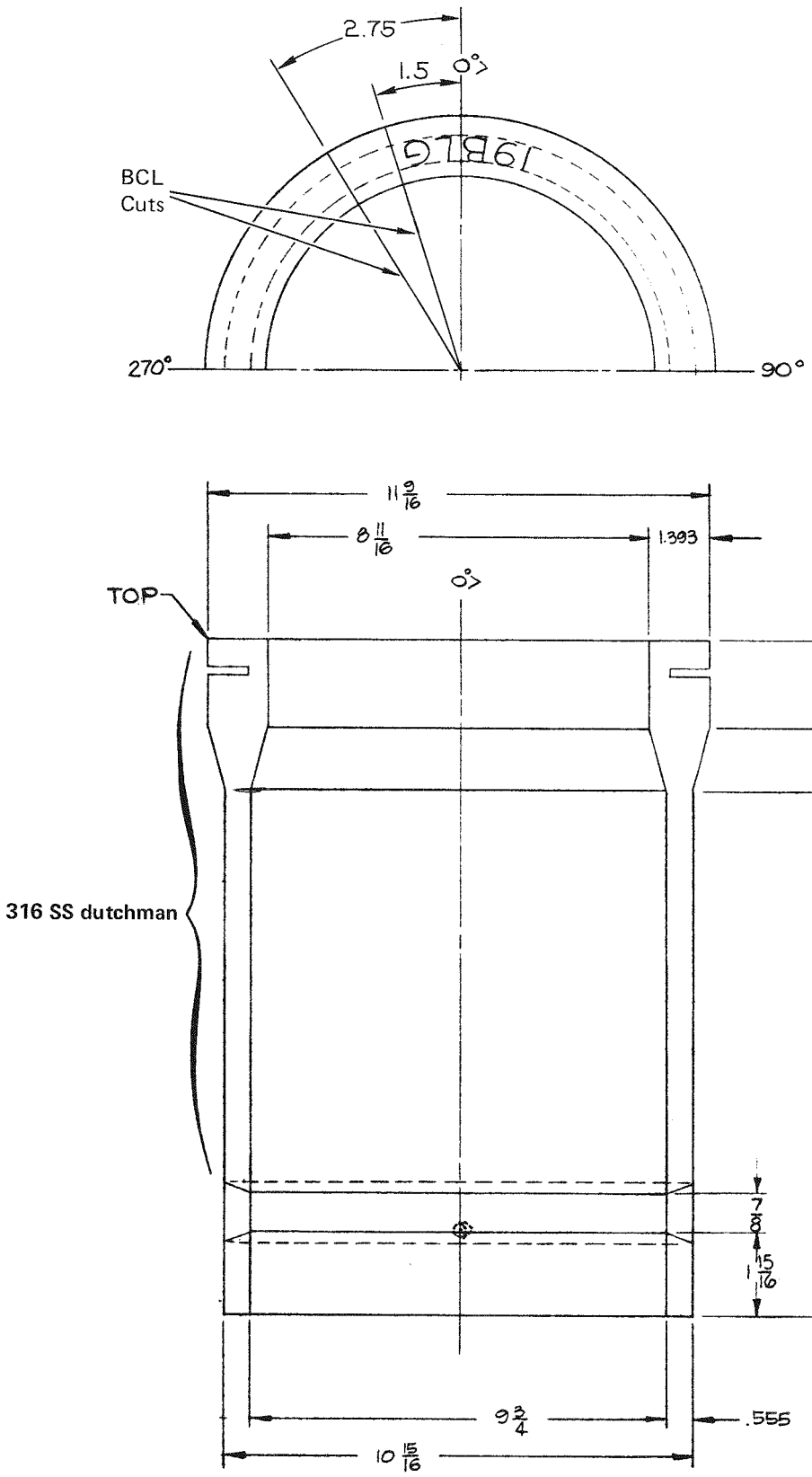
2.75
1.5
0°
19BLG
BCL
Cuts
270°
90°
11 9/16
8 11/16
1.393
0°
TOP
316 SS dutchman
2 3/32
11 15/16
15 1/2
7/8
1 15/16
9 3/4
.555
10 15/16

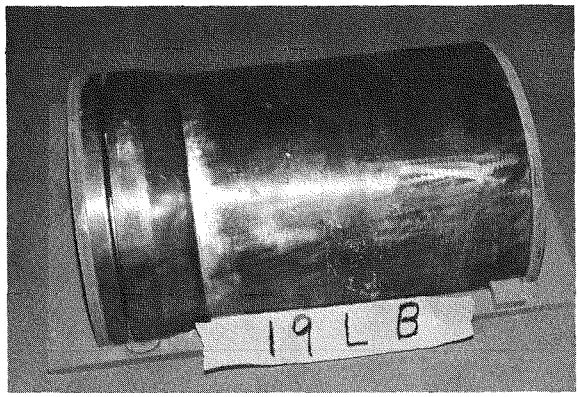


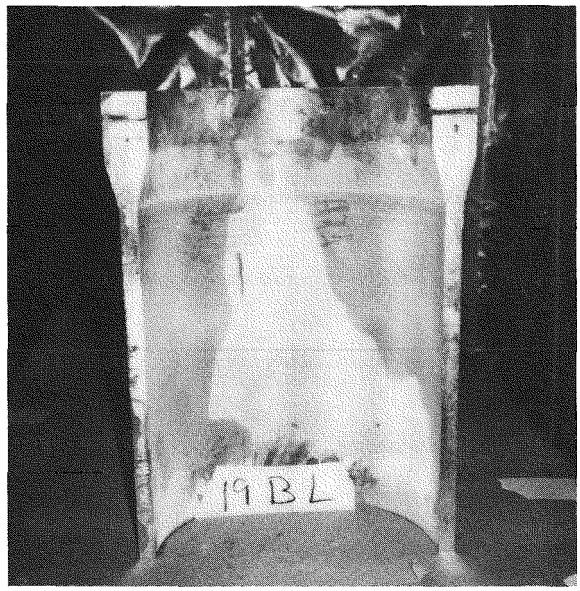


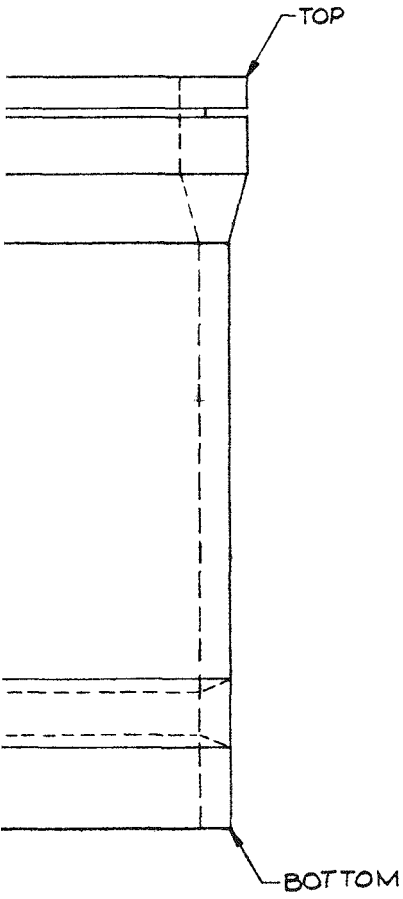


## SAMPLE IDENTIFICATION: 19BL

*ORIGIN:*
Dresden II Nuclear Reactor, 10 in. B-Loop core spray line.

*DESCRIPTION:*
Type of Weld—Pipe to Dutchman
Material—304 SS pipe to 316 SS dutchman

*LABORATORY NDE:*
Relatively clean UT signals and no indications with DPT. No cracks, easy to inspect. (This sample is the other half of samples 1028A, 1028B, 1028C, and 1028D).

Figure A-15 Sample 19BL

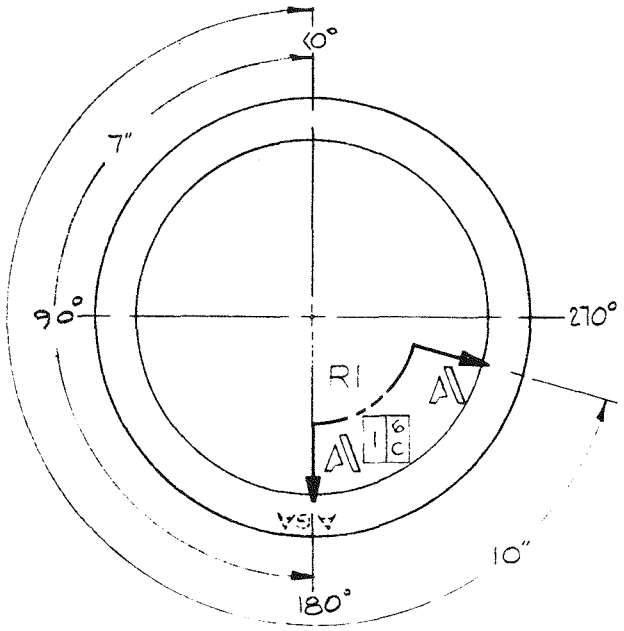


| | A | B | C | WALL THICKNESS TOP | WALL THICKNESS BOTTOM | |
|---|---|---|---|---|---|---|
| 0° | $9\frac{9}{16}$ | $2\frac{1}{2}$ | $6\frac{3}{8}$ | .358 | .403 | 0°-180° |
| 270° | | | | .355 | .424 | 90°-270° |
| 180° | $5\frac{11}{16}$ | $2\frac{7}{16}$ | $2\frac{13}{32}$ | .371 | .499 | |
| 90° | | | | .375 | .445 | |

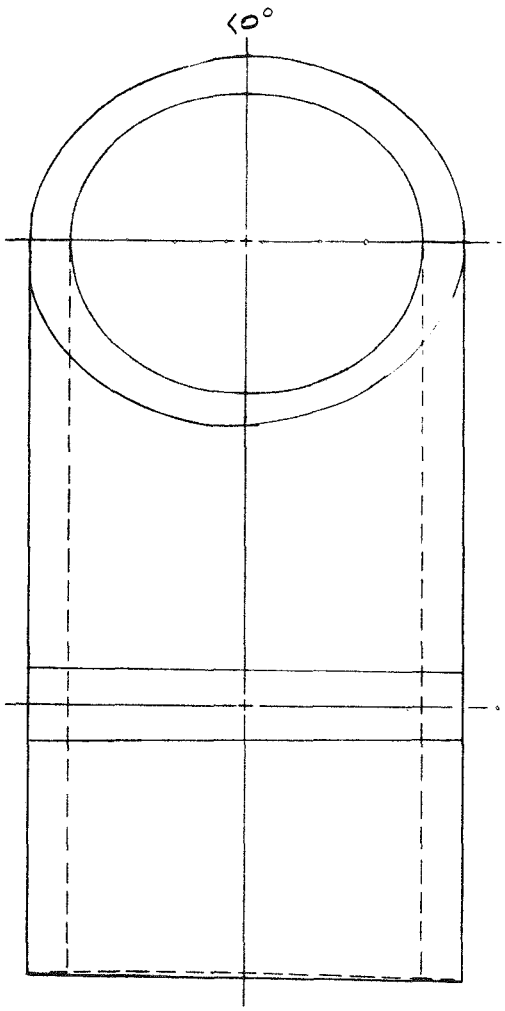


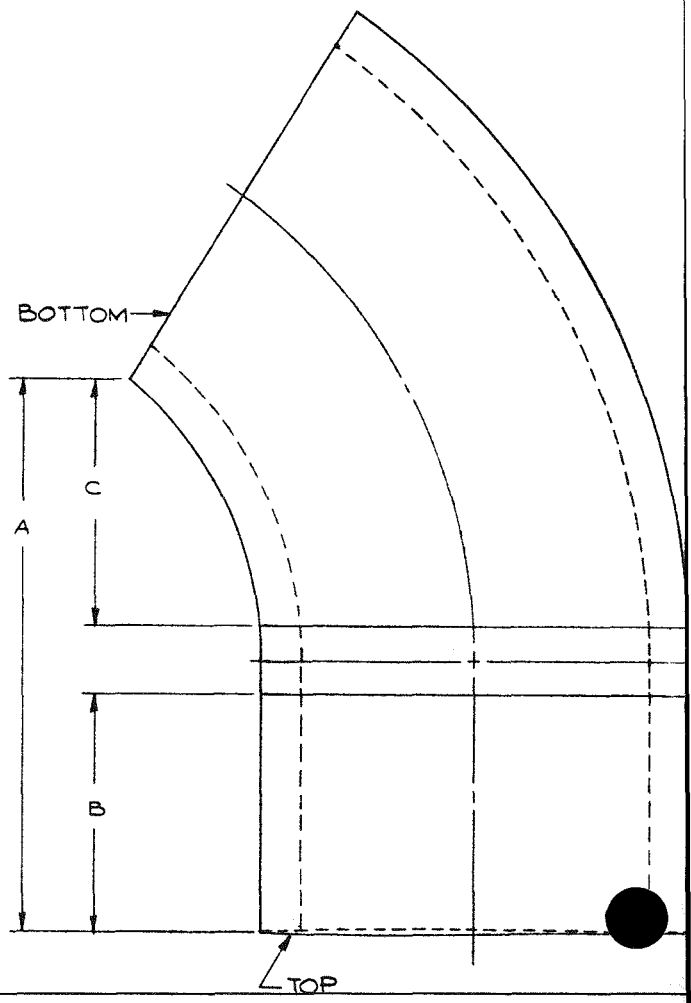

| TOP | | BOTTOM | |
|---|---|---|---|
| O.D. DIM | I.D. DIM | O.D. DIM | I.D. DIM |
| 4.500 | 3.794 | 4.573 | 3.691 |
| 4.500 | 3.794 | 4.500 | 3.626 |
| | | | |
| | | | |

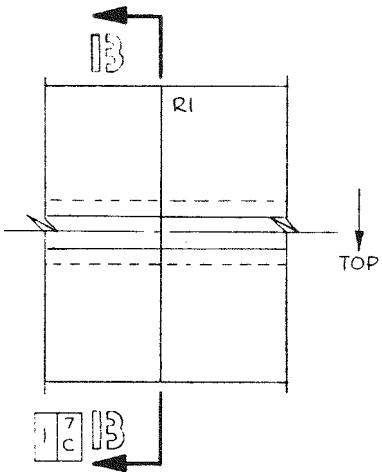


VIEW A-A 1 2 D

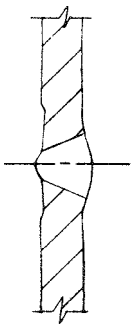

SECTION B - B 1 6 C

## SAMPLE IDENTIFICATION: A9A

*ORIGIN:*

Quad Cities I Nuclear Reactor, 4 in. (10.16 cm) A and B Loops, recirculation bypass lines.

*DESCRIPTION:*

Type of Weld—Pipe to elbow
Material—Both 304 SS

*LABORATORY NDE:*

Many geometry UT signals, no DPT indications.

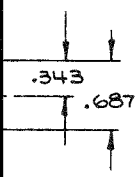


Figure A-16 Sample A9A

APPENDIX B

# EPRI ULTRASONIC EXAMINATION PROCEDURES AND DATA FORMS USED IN TECHNICAL PLANNING STUDY TPS-75-609

M. J. Golis, Battelle, Columbus Laboratories*

and

E. R. Reinhart, Electric Power Research Institute

*Funded under EPRI Technical Services Agreement TSA 75-32.

Appendix B

EPRI ULTRASONIC EXAMINATION PROCEDURES

AND DATA FORMS USED IN TECHNICAL PLANNING

STUDY TPS-75-609

This appendix compiles the various procedures and data forms used in conducting EPRI Technical Planning Study TPS-75-609, "A Program to Evaluate Current Ultrasonic Inspection Practice for BWR Piping Welds." The procedures and data forms were used in the program as follows:

1. The data forms listed as "Analysis of Ultrasonic Examination," 75-609-C-1 and 75-609-C-4, shown on pages B-2 and B-3, were used to submit the final results of the first series of simulated inspections to the EPRI on-site program monitor. This series of tests was called Phase A; in this phase, the inspection teams used their own procedures, standards, and equipment.

2. The procedure and data forms listed as "Ultrasonic Examination Procedure Outline" were used in the second or B phase of the program by all inspection teams. In this phase the procedures, search units, ultrasonic test instrument, couplant, data forms, and calibration standard were all supplied by EPRI and were the same for each test group. The procedure consists of two parts, EPRI-1 and EPRI-2. EPRI-1 is an inspection-detection phase and EPRI-2 is an analysis phase. The data forms shown on pages B-2 and B-3 were again used to submit the final results to the EPRI on-site monitor.

3. The third and final phase of the program (Phase C) was an evaluation of relative inspection sensitivity as a function of different calibration standards. The procedure and data forms are shown as "EPRI-3, Analysis of Calibration Blocks."

EPRI-1: ULTRASONIC EXAMINATION PROCEDURE OUTLINE

Purpose: To describe and control the examination requirements to be used during the round robin "Program to Evaluate Ultrasonic Inspection Practice for BWR Piping Welds."

Responsibility: The on-site Level III examiner shall be held responsible for assuring that this procedure is followed during Phase B of the program.

General Requirements: Personnel, equipment, and calibration standards shall be in accordance with TPS-75-609.

## ANALYSIS OF ULTRASONIC EXAMINATION

Organization _____ Program Step _____ Date _____ Operator _____

Recorder _____ Observer _____ Procedure _____ Equipment _____

Transducer I.D. _____ Weld Identification _____ Start Time _____ End Time _____

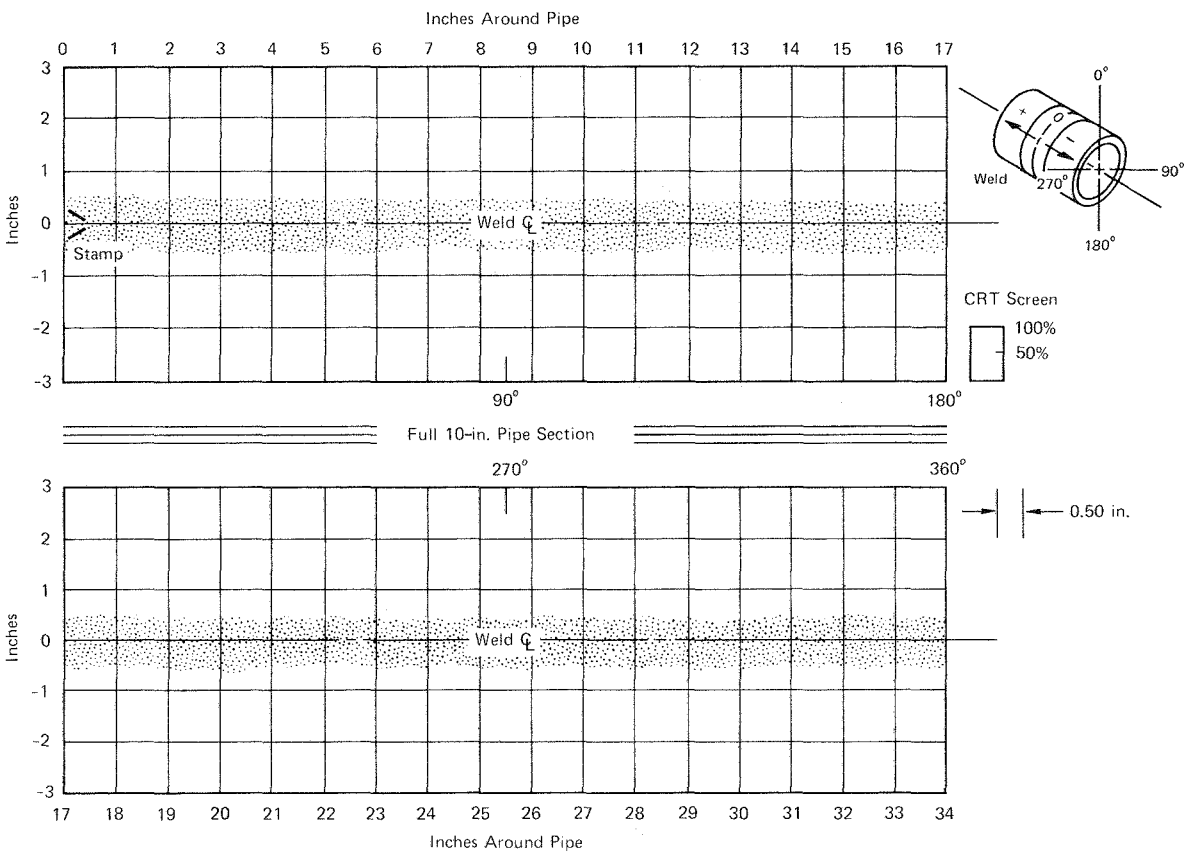


Form TPS-75-609-C-1

## ANALYSIS OF ULTRASONIC EXAMINATION

Organization _____ Program Step _____ Date _____ Operator _____

Recorder _____ Observer _____ Procedure _____ Equipment _____

Transducer I.D. _____ Weld Identification _____ Start Time _____ End Time _____

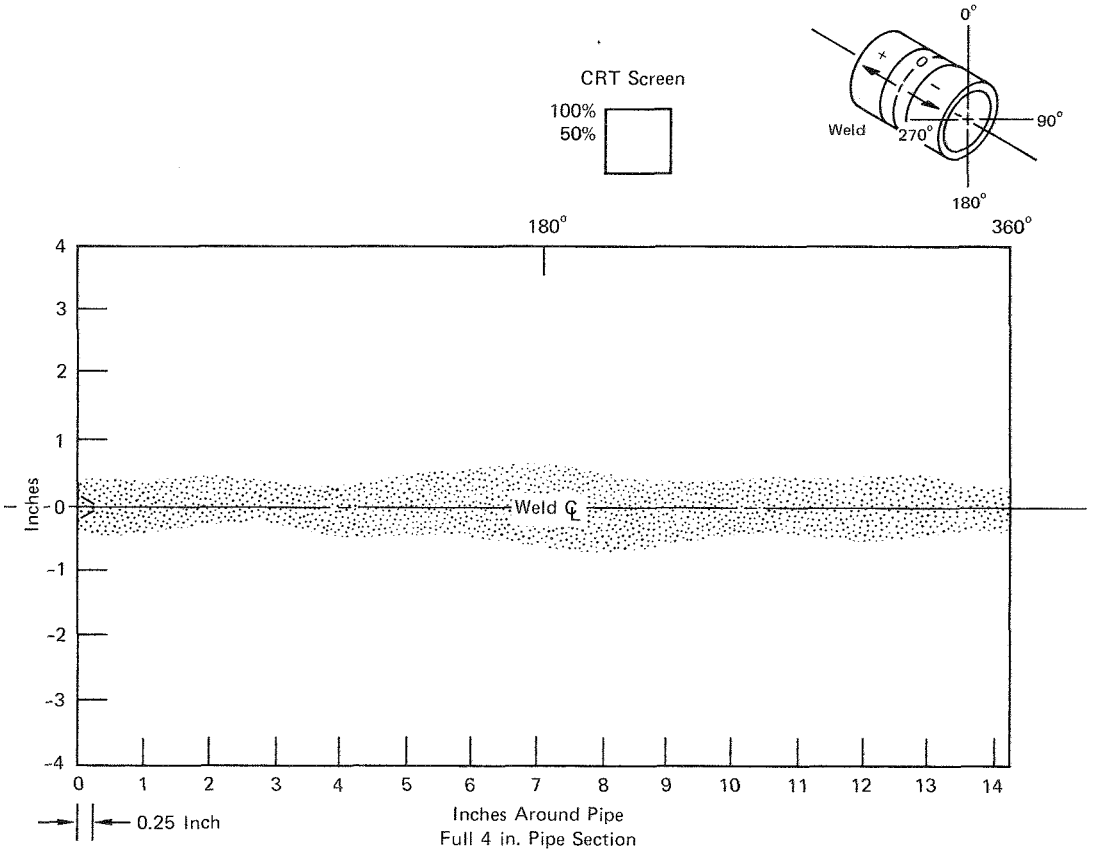


Form 75-609-C-4

Test Samples: Examinations are to be conducted on the samples of the complete piping and fragments to be supplied during the program. These contain natural flaws which have been found in service. The flaws can be located in and near the pipe welds. They may be oriented in any random manner. All examinations shall be conducted from the "outside" of the pipe. All surfaces are to remain in the as-is condition and only cleaning solvents may be applied upon completion of the examination. At no time is information concerning the internal surface geometrical conditions to be gathered through visual examination (no peeking).

Basic Calibration Block: All final calibration of ultrasonic systems shall be on the calibration block supplied by the program monitor. This block contains a 3%T square-bottom notch on both the ID and OD as well as a 3/32-in. side-drilled hole in both the longitudinal and circumferential directions.

Equipment: The commercial pulse-echo type equipment (Krautkramer-Branson 303B) supplied by the monitor shall be used along with the transducer, wedge, cable, and couplant (glycerin) as per his instructions. Familiarity with and linearity checks of the equipment should be completed prior to examination of any test pipe. Linearity should be checked using the two SDHs according to supplement 4 of Appendix III, "Ultrasonic Examination Method for Classes 1 and 2 Piping Systems Made From Ferritic Steels."* The transducers are nominally 0.25-in., 2.25 MHz, 45° shear in steel. Verify the instrument's vertical linearity by setting a test reflector's signal height at the reference settings listed in the amplitude control linearity table in the "Record of Ultrasonic Calibration." Then change the instrument's sensitivity by $\pm$ 6 and $\pm$ 12 db in accordance with the table and record the pulse height in the appropriate column. The preexamination readings are to be placed to the left of the slash mark, the postexam data to the right.

Examination Calibration: System calibration includes both horizontal and vertical instrument assignments.

- Time Sweep Calibration: Set horizontal display so that 3, 6, and 9 on the horizontal scale correspond to the 1/2, 1, and 3/2 Vee path distances looking in the circumferential direction.

- Sensitivity Calibration (DAC): The initial sensitivity level measured on the 1/2 Vee path, 3%T notch, is set at 80% of full screen height. The instrument sensitivity is increased 6 db (2X) and then the DAC curve is completed for the 1 and 1 1/2 Vee path positions. These points, when connected, constitute the primary reference level. Note that the 1/2 Vee path signal at the primary reference level is off scale at this sensitivity.

- Correlation to SDH: After the calibration on the notch is complete, record the response from the side-drilled hole of the calibration block on the calibration sheet at 2/8, 6/8, and 10/8 nodes (if possible). 6/8 and 10/8 should be recorded as a minimum requirement. You may have to put in or take out gain to do this; if so, record what you did on the calibration sheet. Also record the response from the 1/8-in. SDH of the IIW block for the shortest sound path. This step is to be performed at the initial calibration only, for examination of 4-in. and 10-in. pipe. Do not repeat for each recalibration.

*Proposed addition to ASME Boiler and Pressure Vessel Code, Section XI. Draft date: March 28, 1975.

## RECORD OF ULTRASONIC CALIBRATION

Organization _____ Program Step _____ Date _____

Operator _____ Recorder _____ Observer _____

Procedure _____ Pipe Size _____ Scan Direction: Circum _____

Start Time _____ Completion Time _____

Equipment _____

Flaw Detection Unit S/N _____ Transducer I.D. _____

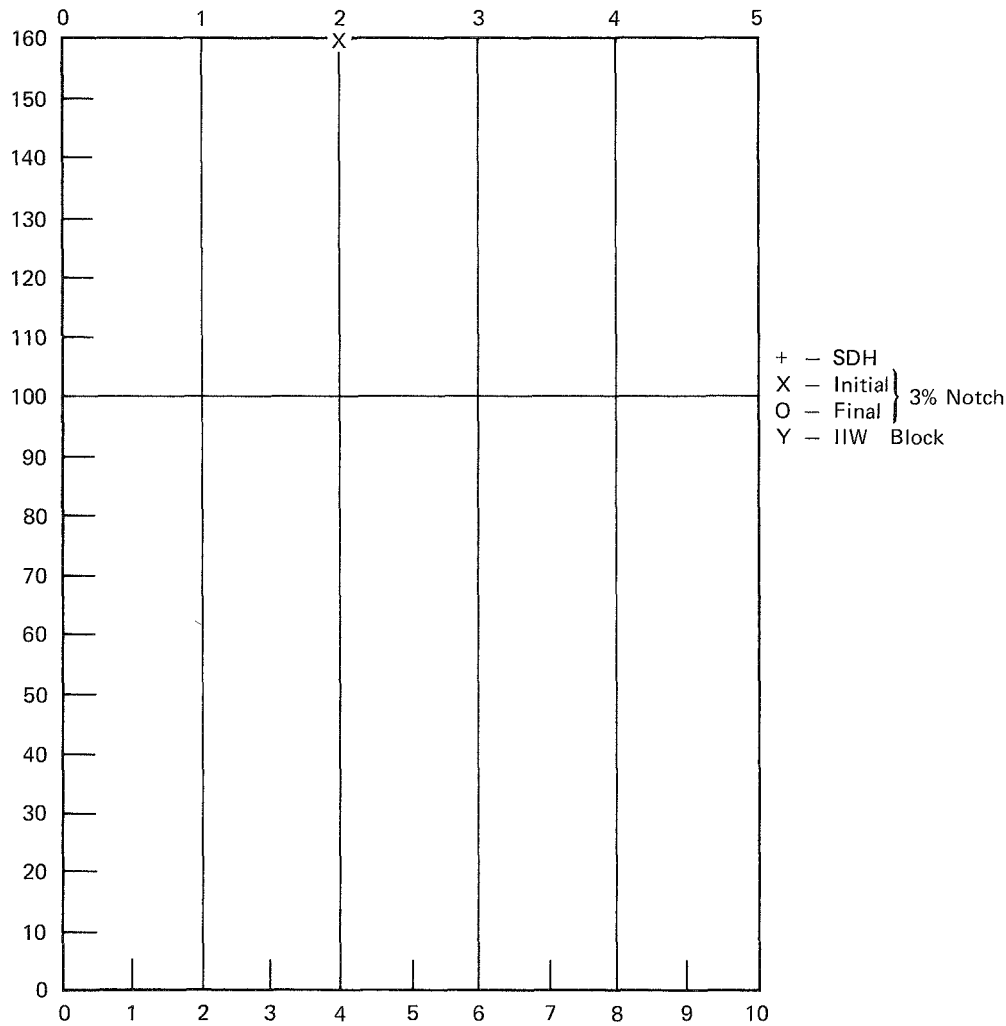


Comments: _____

_____

_____

Form EPRI-TPS-75-609-A

Instrument Settings

Matl Cal _____

Range _____

Delay _____

Reject _____

Gain _____

Damping _____

Frequency _____

Rep Rate _____

Filter _____

| Screen Height Linearity | | | |
|---|---|---|---|
| A | Upper Limit | B | Lower Limit |
| 100 | 55 | / | 45 |
| 90 | 50 | / | 40 |
| 80 | | 40 | |
| 70 | 40 | / | 30 |
| 60 | 35 | / | 25 |
| 50 | 30 | / | 20 |
| 40 | 25 | / | 15 |
| 30 | 20 | / | 10 |
| 20 | 15 | / | 5 |

Photo of OD Notch Presentation and DAC From CRT Screen

| Amplitude Control Linearity | | | | | |
|---|---|---|---|---|---|
| Ref. Set, % | db Charge | Reading | | | |
| 80 | -6 | 32 | — | / | -48 |
| 80 | -12 | 16 | — | / | -24 |
| 40 | +6 | 64 | — | / | -96 |
| 20 | +12 | 64 | — | / | -96 |

- Reject Control: Off (minimum).

- Time of Calibration: Prior to and following each examination of a set of test pipes. No single period of examination shall exceed four hours. Calibrations should be run when operators change. Amplitude calibration upon completion of each examination or series of examinations shall be within ± 20% (± 2 db) of the original DAC. Sweep calibration shall be within ± 5% of full scale. Loss of calibration voids the previous examination(s) since last successful calibration, and all affected data must be retaken.

- Calibration Documentation: Each initial calibration shall be recorded on Form EPRI-TPS-75-609-A. This includes all initial and final DAC data points and instrument settings.

Inspection

- The total inspection will be conducted in two steps: examination and evaluation. The examination is a rapid scan to locate areas that may contain flaws (EPRI-1). The evaluation is an in-depth examination of the areas found in the examination (EPRI-2). These steps are described in the next section.

Examination

- Location and Position: Location of any indication around the circumference of the weld is to be identified by its distance from the reference zero and its + or - direction. Position of any indication is to be measured from the (usually weld centerline) zero position punch mark for distance and +, -. Direction (Arrow Punch Mark) is to be taken as the direction that a right-hand screw would advance when rotated from the 0-360° markings on the pipe samples. Locations are to be recorded in inches (see the sketch on the data sheet).

- Area: Scan 2 in. (minimum) from the edge of the weld and on both sides of weld if possible. Scanning across the weld is optional, but let us know if you did by noting this on your data sheet.

- Straight Beam: N/A.

- The Search Unit will consist of a 0.25-in. x 0.25-in., Flat Transducer 2.25 MHz, and a damped 45° Plexiglas wedge.

- Angle Beam Reflector Parallel to Weld:

  -- The coverage should be 360° if possible.

  -- Scan in an approximately perpendicular direction to the weld with transducer rotation to be ± 45° (see Figure B-1).

  -- Overlap is to be at least 10% of the effective transducer area.

  -- Maximum scan rate is 6 in./sec.

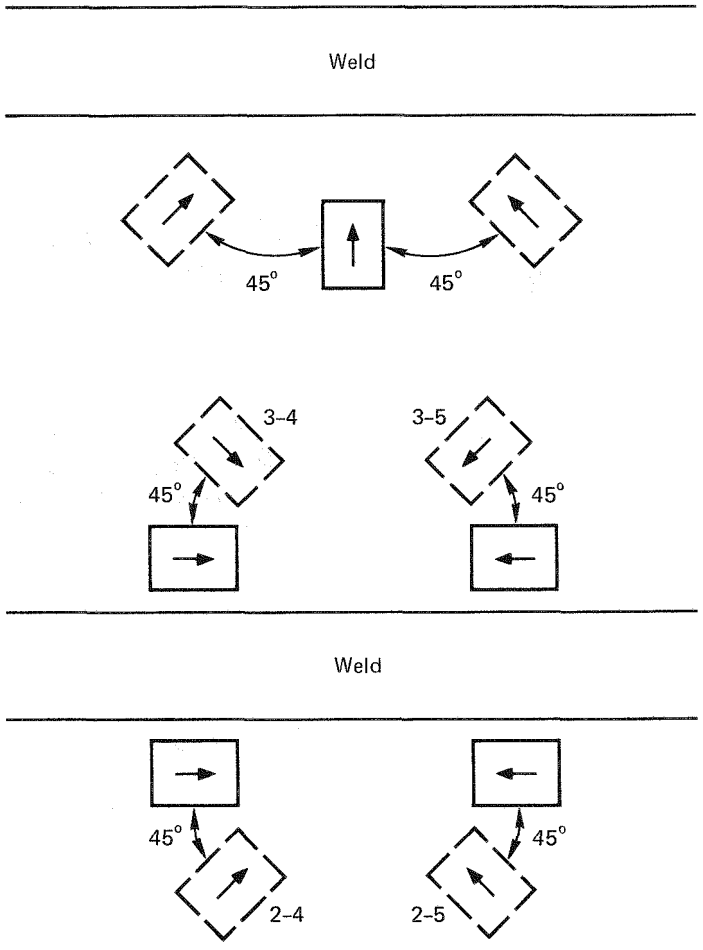


Figure B-1 Rotation of Transducer During Scan
(The Arrow Is the Direction of Scan.)

- Angle Beam Reflector Perpendicular to Weld:

  -- Scan 360° if possible. Scan both CW/CCW, generally parallel to weld with both sides of the weld ± 45° rotation (see Figure B-1).

  -- Scan at 2X (6 db) gain over reference, if possible.

- Postexamination Cleaning: Remove couplant from the specimens.

Preliminary Evaluation Criteria: If reflectors are above 30% of DAC curve and/or are considered suspect, briefly record on the attached form EPRI-75-609-B. Record the signal amplitude you initially saw, not what you observed after peaking. Record the location on the form and/or on the pipe (optional) for later evaluation.

Acceptance Criteria: None.

Records: See attached form EPRI-TPS-75-609-B.

- Plot exam results which are adjudged as reflectors other than geometry.

- List general observations and observed technique limitations.

Evaluation: Evaluation of reflectors detected in the initial inspection will utilize Evaluation Procedure, EPRI-2.

EPRI-2: ULTRASONIC ANALYSIS PROCEDURE OUTLINE

Purpose: To describe and control the analysis requirements to be used during the round robin "Program to Evaluate Ultrasonic Inspection Practice for BWR Piping Welds," Phase B.

Objective: The primary objective of the methods given here is to locate and record indications within the weld, the heat-affected zone, and the base material within approximately 1/2 thickness (T) of the weld, for flaw analysis purposes.

Responsibility: The on-site Level III examiner shall be held responsible for assuring that this procedure is followed during Phase B of the program.

General Requirements: Personnel, equipment, and calibration standards shall be in accordance with TPS-75-609.

Test Samples: Analysis is to be conducted on the samples of the complete piping and fragments examined using Procedure EPRI-1, Ultrasonic Examination Procedure.

Basic Calibration Block: All final calibration of ultrasonic systems shall be on the calibration block supplied by the program monitor. This block contains a 3/32-in. side-drilled hole in both the longitudinal and circumferential directions as well as a 3%T square bottom notch on both the ID and OD.

Equipment: The commercial pulse-echo type equipment (Krautkramer-Branson 303B) supplied by the monitor shall be used, along with the transducer, wedge, cable, and couplant (glycerin) as per his instructions. Familiarity with and linearity checks of the equipment should be completed prior to analysis of any

Page Number _____

## RECORD OF ULTRASONIC EXAMINATION

Step _____ Date _____ Recorder _____

Start Time _____ Completion Time _____

| Reflector Weld ID Sequential No. (A-1, A-2, etc.) | Initial Detected Amplitude, % of Screen | Approximate Location | | Preliminary Interpretation and/or Comments (if any) | Final Interpretation (crack or geometry) |
|---|---|---|---|---|---|
| | | From Weld Centerline, in. | Around Pipe, in. | | |
| | | | | | |

EPRI-TPS-75-609-B

test pipe. Linearity should be checked using the two SDHs according to supplement 5 of Appendix III, "Ultrasonic Examination Method for Classes 1 and 2 Piping Systems Made From Ferritic Steels." The transducers are nominally 0.25-in. focused, 2.25 MHz, 45° shear in steel. Verify the instrument's vertical linearity by setting a test reflector's signal height at the reference settings listed in the amplitude control linearity table in the "Record of Ultrasonic Calibration." Then change the instrument's sensitivity by ± 6 and ± 12 db in accordance with the table and record the pulse height in the appropriate column. The preexamination readings are to be placed to the left of the slash mark, the postexam data to the right.

Examination Calibration: System calibration includes both horizontal and vertical instrument assignments.

- The basic calibration reflector will be the 3/32 SDH of the supplied calibration block.

- An IIW-2 ultrasonic calibration block shall be used during calibration to establish sweep length and beam angle.

Determination of Angle Beam Index: The angle beam search unit is positioned on the IIW-2 calibration block so the beam is directed toward the 4-in. radius surface. Move the search unit parallel to the sides of the calibration block until a maximum echo is obtained from the reflecting radius. The beam index point is now above the centerline of the radius. Place a mark on the side of the angle beam wedge to identify the index point.

Determination of Beam Angle: Place the angle beam search unit on the IIW-2 calibration block and obtain a peak signal amplitude from the 2-in. diameter hole. Read the refracted beam angle from the side of the calibration block using the angle which corresponds with the beam index point and record it on the Calibration Data Sheet.

Sweep Range Calibration: The IIW-2 calibration block shall be used to calibrate the ultrasonic instrument search unit combination for sweep range over the metal path to be used.

Angle Beam (45°) Sensitivity and DAC Calibration: Position the search unit on the applicable calibration standard and obtain the first point on the DAC curve using a sound path no less than 3/8 of the full skip distance. (Vee path and skip distance are considered equivalent terms.) Adjust the peak signal amplitude to 75% of the full screen height and mark its position and amplitude on the display screen. Without changing the gain level, obtain the peak signal amplitude for the remaining metal paths of the sound beam. Determine the 2/8 node response (off scale) to determine shape of curve, and also include 10/8 and 14/8 positions. Mark their position and amplitudes on the display screen. (Signal responses for metal paths less than 3/8 of the full skip distance may be extrapolated by extending the DAC curve.) Join the points with a smooth line, the length of which shall cover the examination range. This DAC line represents the primary reference level (1X sensitivity) for angle beam examination. Also record amplitude and sweep position of 3% ID and OD notches. Record and plot all this calibration data on the Calibration Data Sheet.

- Time of Calibration: Prior to and following each examination of a set of test pipes. No single period of examination shall exceed four hours. Calibrations should be run when operators change. Amplitude calibration

upon completion of each examination or series of examinations shall be within ± 20% (± 2 db) of the original DAC. Sweep Calibration shall be within ± 5% of full scale. Loss of calibration voids the previous examination(s) since last successful calibration, and all affected data must be retaken.

- Calibration Documentation: Each initial calibration shall be recorded on Form EPRI-TPS-75-609-A. This includes all initial and final DAC data points and instrument settings.

Analysis Sensitivity Level: Indications shall be recorded at the primary instrument level (IX).

Angle Beam Examination of Weld: Welds shall be analyzed with a 0.25-in. focused search unit.

Scanning for Reflectors Oriented Parallel to the Weld: The search unit shall be placed on the contact surface with the beam aimed about 90 degrees to the weld and manipulated laterally and longitudinally so that the ultrasonic beam passes through all of the weld metal and 2 in. minimum of base material. In addition, the search unit shall be angulated from 0° (perpendicular to the weld) through 45° during the scan. See Figure B-1. This examination shall be performed from both sides of the weld where component geometry permits.

Scanning for Reflectors Oriented Transverse to the Weld: On prepared or sufficiently smooth surfaces, the angle beam shall be aimed parallel to the longitudinal centerline of weld with the search unit contacting the weld surface. The search unit shall be moved along the weld so that the ultrasonic beam(s) passes through all of the weld metal and 1/2T on both sides of the weld where practical. Scanning shall be done in two directions 180 degrees to each other. In addition, the search unit shall be angulated from 0° (parallel to the weld) through 45° (aimed at the weld) on both sides of the weld for parallel scanning. See Figure B-1.

- Maximum scan rate is 6 in./sec.

Analysis: Using the information from the examination, EPRI-1, each recorded area of concern must be resolved using this procedure. The examiner may use any form, analysis method, or data plot to resolve indications (material turned in to EPRI), but the final result must be plotted on EPRI data form 75-609-C (1,2,3, or 4), "Analysis of Ultrasonic Examination" (see example of plot). Indications should be identified as follows:

1. Crack

    a. Percent of UT screen height
    b. Estimated length
    c. Estimated location
    d. Estimated depth, percent through wall
    e. Estimated type of flaw

2. Geometry (normally not plotted unless final decision is made after plot)

    a. Counterbore
    b. Drop-through
    c. Any other

EPRI-3: ANALYSIS OF CALIBRATION BLOCKS

This phase of the program will examine the variability in response from various field calibration standards. Perform this evaluation in the following steps:

1. Calibrate on 10-in. Standard Axial

   Using your organization's present calibration procedure and standard, set up your ultrasonic instrument at DAC sensitivity for inspection scans in the axial direction of (reflector in circumferential direction) 10-in. pipe. Use a 45° search unit only.

2. Record Data

   Record the time and amplitude information on the data sheet supplied (EPRI-3-A) and all instrument settings. Also plot the data on the grid of data sheet EPRI-3-B.

3. IIW Correlation

   Using the IIW block, record and plot the peaked response of the 1/16-in. SDH and the 1/8-in. SDH from the near side of the block. If you have to add or reduce gain, note this on the data sheet.

4. Scan of Standards

   At the initial DAC sensitivity, record the response from the various reflectors (SDH, Notch, etc.) of the supplied test blocks as they are scanned in the axial direction (reflectors in circumferential direction). All responses should be peaked in the same manner as you did when calibrating on your own standard. Record as many nodal or "V" path positions as you can see on the screen. Put in or take out db to get as many points as possible on the screen. Record and plot all data on the supplied sheets.

5. Data Plot

   Plot all data on the grid plot sheet, EPRI-3-B. If any data points fall above the maximum amplitude value on the grid plot, indicate at the top of the chart the metal path distance, the percent of screen, and the amount of db above the maximum db of the data sheet. You will be able to plot data on the grid up to 6 db above 100% UT screen amplitude (see the example). Likewise, if data are taken at db settings below your initial DAC sensitivity, indicate the metal path on the grid, percent of screen, and the amount of db needed to read the amplitude on the screen. In all cases, record all the data on the data sheets before attempting to plot.

6. 10-in. Pipe Circumferential

   Repeat all of the above steps for calibrations and scans in the circumferential direction of 10-in. pipe. If you don't change calibration for this scan, note this on the data sheet. Plot all data on another grid plot sheet, EPRI-3-B.

7. 4-in. Axial

   Repeat the calibration and scans for 4-in. pipe for inspections in the axial direction. Record and plot all data on separate sheets.

Page ____ of ____

Inspection Group _____ Search Unit _____ Pipe Size _____

*Direction of Calibration:* Axial _____ Circumferential _____ Time: Start of Scan _____ End _____

| Standard | Side-Drilled Hole | | | | | ____ % Notch | | | | | ____ % Notch | | | | |
|---|---|---|---|---|---|---|---|---|---|---|---|---|---|---|---|
| | Symbol for Plot | Node or V | % Screen | ± db From DAC | Metal Path | ID or OD | Node or V | % Screen | ± db From DAC | Metal Path | ID or OD | Node or V | % Screen | ± db From DAC | Metal Path |
| | | | | | | | | | | | | | | | |
| | | | | | | | | | | | | | | | |
| | | | | | | | | | | | | | | | |
| | | | | | | | | | | | | | | | |
| | | | | | | | | | | | | | | | |
| | | | | | | | | | | | | | | | |
| | | | | | | | | | | | | | | | |

Instrument Settings

Matl Cal _____

Range _____

Delay _____

Reject _____

Gain _____

Damping _____

Frequency _____

RP Rate _____

Filter _____

Data Sheet EPRI-3-A

## EPRI STANDARDS EVALUATION

Pipe _____ in. _____ Direction of Beam: Axial _____ Circum _____

Test Group _____

Transducer: 1. _____ 2. Flat ¼ _____ 3. Focused ¼ _____

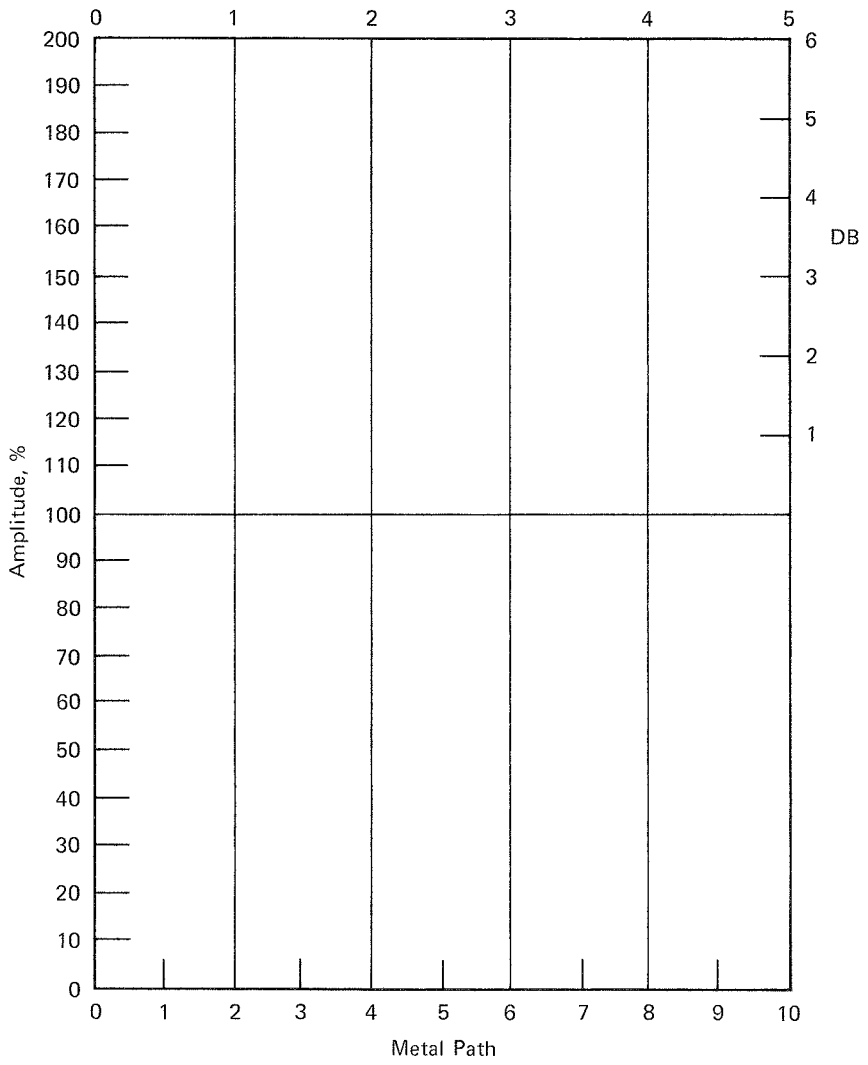


| dB | %DAC |
|---|---|
| 0 | 100 |
| 1 | 112 |
| 2 | 125 |
| 3 | 141 |
| 4 | 159 |
| 5 | 178 |
| 6 | 200 |
| 7 | 224 |
| 8 | 251 |
| 9 | 282 |
| 10 | 316 |
| 11 | 355 |
| 12 | 400 |
| 13 | 447 |
| 14 | 501 |
| 15 | 562 |
| 16 | 631 |
| 17 | 708 |
| 18 | 794 |
| 19 | 891 |
| 20 | 1000 |

Form EPRI-3-B

8. 4-in. Circumferential

Repeat the calibration and scans for 4-in. pipe in the circumferential direction. Record and plot on separate sheets.

9. 1/4-in. Flat Search Unit

Repeat the 4-in. and 10-in. evaluations using the 1/4-in. flat search unit and EPRI-1 calibration procedures.

10. 1/4-in. Focused Search Unit

Repeat the 4-in. and 10-in. evaluations using the 1/4-in. focused search unit and EPRI-2 calibration procedure.

APPENDIX C

# STATISTICAL ANALYSIS OF TEST RESULTS, COMPLETE SAMPLES

Anthony R. Olsen, Battelle, Northwest Laboratories

Appendix C

STATISTICAL ANALYSIS OF TEST RESULTS,

COMPLETE SAMPLES

This appendix describes the statistical analysis of the test results on the complete pipe samples for both Phase A and Phase B. The analysis uses the results presented in Table 6-2 of the EPRI report, "A Study of In-Service Ultrasonic Inspection Practice for BWR Piping Welds," June 1977. The purpose of this analysis is (1) to compare the test teams, (2) to compare phases A and B, and (3) to estimate the proportion of correct decisions made by each test team and across the test teams. The general approach used is to classify each pipe sample analysis according to its agreement with that sample's evaluation. A test team's analysis of a sample can be classified as a correct, incorrect, or no decision. "No decision" refers to the situation in which a crack was apparently detected in the team's original data but was not definitely called a crack in the final analysis.

A summary of the data is presented in Table C-1. Across the test teams, correct decisions were made 67 and 66% of the time for phases A and B, respectively. When viewed at this level, there is no difference between the two phases of the study. When the samples for which a crack was detected but not called ("no decision" on Table C-1) are classified as being called flawed (correct decision), the percent of correct decisions then appears as given in Table C-2. Note that all no decisions occurred on flawed samples. The ability of the test teams to make a correct decision by these criteria is indicated by the increase to 81 and 76%, respectively. Assuming a binomial distribution for the number of correct decisions, both these figures are significantly ($\alpha<0.05$) greater than 50%. This implies that the test teams are doing better than guessing.

The estimated proportion of correct decisions for each test team is also given in tables C-1 and C-2. Visually, the data indicate that the test teams perform very similarly. Teams B, D, and E appear to be conservative in not calling some cracks detected; that is, they show a larger percentage of no decisions. This holds for both Phase A and Phase B. Detailed comparison on the test teams, however, will be done separately for the flawed and unflawed sample results.

Table C-3 gives a detailed summary of the results by test team, test phase, and flaw presence or absence. To determine whether the test teams perform similarly, a 5 x 2 contingency table analysis was conducted. As an example of this analysis we shall describe the procedure for the Phase A results for unflawed samples. The relevant data extracted from Table C-3 are:

Table C-1

PERCENTAGE OF CORRECT, INCORRECT, AND NO DECISION FOR PIPE SAMPLES CLASSIFIED BY PHASE AND TEST TEAM

| Decision | Test Team | | | | | |
|---|---|---|---|---|---|---|
| | A | B | C | D | E | All |
| Phase A | | | | | | |
| Correct | 69 | 81 | 69 | 53 | 63 | 67 |
| Incorrect | 25 | 6 | 25 | 33 | 6 | 19 |
| No Decision* | 6 | 13 | 6 | 14 | 31 | 14 |
| Phase B | | | | | | |
| Correct | 75 | 81 | 69 | 40 | 63 | 66 |
| Incorrect | 25 | 6 | 25 | 47 | 19 | 24 |
| No Decision* | 0 | 13 | 6 | 13 | 19 | 10 |

*Samples with crack detected, but not called.

Table C-2

PERCENTAGE OF CORRECT DECISIONS FOR PIPE SAMPLES CLASSIFIED BY PHASE AND TEST TEAM*

| | Test Team | | | | | |
|---|---|---|---|---|---|---|
| | A | B | C | D | E | All |
| Phase A | 75 | 94 | 75 | 67 | 94 | 81 |
| Phase B | 75 | 94 | 75 | 53 | 82 | 76 |

*Samples with crack detected but not called are classified as correctly analyzed. All samples not called were flawed samples.

Table C-3

SAMPLE DECISIONS CLASSIFIED BY TEST TEAM,
TEST PHASE, AND FLAW PRESENCE

| Test Team | Actual Pipe Condition | Number of Decisions | | | | | |
|---|---|---|---|---|---|---|---|
| | | Phase A | | | Phase B | | |
| | | Correct | Incorrect | No Decision | Correct | Incorrect | No Decision |
| A | Flawed | 6 | 0 | 1 | 6 | 1 | 0 |
| | Unflawed | 5 | 4 | 0 | 6 | 3 | 0 |
| | Total | 11 | 4 | 1 | 12 | 4 | 0 |
| B | Flawed | 5 | 0 | 2 | 5 | 0 | 2 |
| | Unflawed | 8 | 1 | 0 | 8 | 1 | 0 |
| | Total | 13 | 1 | 2 | 13 | 1 | 2 |
| C | Flawed | 3 | 3 | 1 | 5 | 1 | 1 |
| | Unflawed | 8 | 1 | 0 | 6 | 3 | 0 |
| | Total | 11 | 4 | 1 | 11 | 4 | 1 |
| D | Flawed | 3 | 1 | 2 | 2 | 2 | 2 |
| | Unflawed | 5 | 4 | 0 | 4 | 5 | 0 |
| | Total | 8 | 5 | 2 | 6 | 7 | 2 |
| E | Flawed | 1 | 1 | 5 | 2 | 2 | 3 |
| | Unflawed | 9 | 0 | 0 | 8 | 1 | 0 |
| | Total | 10 | 1 | 5 | 10 | 3 | 3 |
| All | Flawed | 18 | 5 | 11 | 20 | 6 | 8 |
| | Unflawed | 35 | 10 | 0 | 32 | 13 | 0 |
| | Total | 53 | 15 | 11 | 52 | 19 | 8 |

| | A | B | C | D | E |
|---|---|---|---|---|---|
| Correct | 5 | 8 | 8 | 5 | 9 |
| Incorrect | 4 | 1 | 1 | 4 | 0 |

The calculated chi-square value for independence is 9.00 with 4 degrees of freedom. The probability of exceeding this value is 0.06. The interpretation of this test is that the number of correct (incorrect) decisions is dependent on the test team for the unflawed samples using Phase A procedures. This dependence is at an indicated significance level of 0.06. (Teams A and D each called four unflawed samples flawed, but they only agreed on two of the samples.)

Analysis for the flawed samples is complicated by the presence of samples in which a crack signal was detected but a crack was not called. When those samples are classified as being called flawed (a correct decision), there is no dependence among the test teams for the number of correct decisions ($\chi^2(4) = 6.86$, $p = 0.14$). When they are considered as called unflawed (incorrect decisions), there is a dependence ($\chi^2(4) = 8.48$, $p = 0.07$). Test team E tends not to call the sample flawed when a crack is detected. Under Phase A, an estimate of the percent of correct decisions for flawed samples across all teams is 85%. This assumes that no decision samples are called flawed. When those samples are called not flawed, the percent of correct decisions drops to 53%.

A comparison of the test teams in Phase B, when the EPRI procedure was used, leads to similar conclusions. No statistically significant dependence among the teams for correct decisions was indicated for either flawed or unflawed samples. However, the same general pattern appears as in Phase A. The percentage of correct decisions for flawed samples across teams is 82% for Phase B. This assumes that the no decision samples are called flawed. When those samples are called not flawed, only 59% correct decisions are made.

In summary, the comparison of the test teams indicates that they do not operate the same when analyzing the samples. For unflawed samples, test teams A and D make more incorrect decisions than the other teams. They call more pipes defective which are not. For flawed samples, the teams differ in the number of times they do not call a sample defective when a crack signal is detected. Team E in particular and teams B and D are conservative in stating that a sample is flawed. The teams perform similarly when the no decision samples are changed to flaw detected.

A detailed comparison of the test teams' performances during phases A and B may be drawn by pairing the analyses. For each pipe sample the decisions made by a test team under phases A and B are compared. The decisions are either the same or different. Whether the decisions agree with the sample being flawed or unflawed is not considered. The question here is whether the test team reaches the same conclusion about the sample irrespective of the test procedure. This information is summarized in tables C-4, C-5, and C-6.

For unflawed samples, Phase A and Phase B decisions are the same 76% of the time averaged across the teams. This is significantly different from 50%, which would be expected if the teams were guessing. Note that in this comparison, the anomaly associated with sample 19BL affects the outcome only if the result for the two phases differed. For the flawed samples the overall percentage is not as high as

Table C-4

COMPARISON OF PHASES A AND B DECISIONS ON
EACH PIPE SAMPLE BY TEST TEAM

| Test Team | Flawed | | | Unflawed | | |
|---|---|---|---|---|---|---|
| | Number of Decisions | | Percent Same Decisions | Number of Decisions | | Percent Same Decisions |
| | Same | Different | | Same | Different | |
| A | 6 | 1 | 86 | 6 | 3 | 67 |
| B | 3 | 4 | 43 | 7 | 2 | 78 |
| C | 5 | 2 | 71 | 7 | 2 | 78 |
| D | 3 | 3 | 50 | 6 | 3 | 67 |
| E | 5 | 2 | 71 | 8 | 1 | 89 |
| All | 22 | 12 | 65 | 34 | 11 | 76 |

Table C-5

COMPARISON OF PHASES A AND B DECISIONS ON EACH SAMPLE BY TEST TEAM *

| Test Team | Flawed | | | Unflawed | | |
|---|---|---|---|---|---|---|
| | Number of Decisions | | Percent Same Decisions | Number of Decisions | | Percent Same Decisions |
| | Same | Different | | Same | Different | |
| A | 6 | 1 | 86 | 6 | 3 | 67 |
| B | 7 | 0 | 100 | 7 | 2 | 78 |
| C | 5 | 2 | 71 | 7 | 2 | 78 |
| D | 5 | 1 | 83 | 6 | 3 | 67 |
| E | 6 | 1 | 86 | 8 | 1 | 89 |
| All | 29 | 5 | 85 | 34 | 11 | 76 |

*Detected but not called decisions are classified as flaws called.

Table C-6

COMPARISON OF PHASES A AND B DECISIONS ON EACH PIPE SAMPLE BY TEST TEAM *

| Test Team | Flawed | | | Unflawed | | |
|---|---|---|---|---|---|---|
| | Number of Decisions | | Percent Same Decisions | Number of Decisions | | Percent Same Decisions |
| | Same | Different | | Same | Different | |
| A | 7 | 0 | 100 | 6 | 3 | 67 |
| B | 3 | 4 | 43 | 7 | 2 | 78 |
| C | 5 | 2 | 71 | 7 | 2 | 78 |
| D | 3 | 3 | 50 | 6 | 3 | 67 |
| E | 5 | 2 | 71 | 8 | 1 | 89 |
| All | 23 | 11 | 68 | 34 | 11 | 76 |

*Detected but not called decisions are classified as samples called unflawed.

Table C-7

PERCENT FOR ALL TEAMS BY SAMPLE TYPE

| | Flawed | | Unflawed | | Total | |
|---|---|---|---|---|---|---|
| | Phase A | Phase B | Phase A | Phase B | Phase A | Phase B |
| Correct | 53 | 59 | 78 | 71 | 67 | 66 |
| Incorrect | 15 | 18 | 22 | 29 | 19 | 24 |
| No Decision | 32 | 23 | 0 | 0 | 14 | 10 |

the unflawed samples unless the no decisions are classed as flaws detected and called. In that case, the agreement is 85%.

The teams all behave the same in comparison of the two test procedures. Both procedures result in the same percentage of correct decisions. There is a general pattern of agreement between the procedures, but this is not universal. Moreover, the agreement is the same for both flawed and unflawed samples (see Table C-7).

APPENDIX D

# TEST SAMPLE CHARACTERIZATION

Dr. Matthew J. Golis and Stephen D. Brown

Battelle, Columbus Laboratories

Appendix D

# TEST SAMPLE CHARACTERIZATION

## INTRODUCTION

This appendix discusses the NDE and destructive characterization of several samples of BWR piping used in this NDE methodology evaluation. The pipe samples represent typical 10-in. and 4-in. Schedule 80 pipes found in core spray and bypass lines, respectively. They came from operating reactor environments and thus were affected by the presence of radiation and fouling mechanisms such as internal scale. They were production samples representing both shop- and field-fabricated welds. This effort was an extension of the previous work done by BCL in conjunction with the establishment, conducting, monitoring, and recording of the overall round robin study.

The presence of intergranular stress corrosion cracks (IGSCCs) and associated defective conditions was initially assessed in the as-received condition by General Electric Company personnel in San Jose, California. The samples were then partially covered to eliminate NDE examiner access to ID surfaces, and the round robin study was conducted as described in the body of this report. Most of the round robin test samples were later sent to Battelle, Columbus Laboratories for additional NDE and metallurgical characterization.

Thus the purpose of this BCL effort has been to review the initial descriptions of the test samples and to characterize particular samples of interest more completely. Specific interest in selected samples was predicated largely on the findings of the round robin participants. Thus the areas of most concern were those in which initial GE NDE data and the findings of the ultrasonic examiners did not appear to agree. Metallographic interpretations and detailed ultrasonic and electric resistance gauge (ERG) measurements were made of such areas. Visual inspection was done using white light photography as well as support from fluorescent penetrant observations.

Table D-1 summarizes the evaluations performed in support of the overall study. To minimize the amount of material used to comment on our findings, only overall photographs and conditions which showed anomalous conditions are included in this appendix. Table D-1 shows the basic test sample identification, pipe diameter, GE preliminary flaw description, BCL examinations performed, and BCL final evaluations. Since full sections of pipe were often not available, the pipes were further identified as consisting of a full section (360°), a half section (180°), or a relatively small sample (typically 36°). The pipe samples were marked with a zero point on the OD of the pipe as well as with an arrow designating the direction of increasing location numbers spaced at 1-in. intervals. Each pipe consisted of a

Table D-1

TEST SAMPLE LISTING AND TESTS PERFORMED

| Sample Identification | Pipe Diam. (in.) | Pipe Segment (deg.) | Preliminary Flaw Description | Standard[a] | | | | BCL Examinations[b] | | | | | | Final BCL Evaluation |
|---|---|---|---|---|---|---|---|---|---|---|---|---|---|---|
| | | | | 1 | 2 | 3 | 4 | VI | DPT | RT | ERG | UT | Met. | |
| 19AL | 10 | 180 | SCC, radial, through wall | * | | | - | X | X | o | X | | | Cracked (through wall) |
| 1028A | 10 | 36 | SCC, circular, across sample | * | | | | X | X | o | X | | | Cracked (0.5 in.) |
| 1021 | 10 | 360 | SCC, circular, 8 in. long | - | * | * | - | X | X | o | | | X | Pipe material defect (lap ~0.025 in.) |
| 10K17L | 10 | 360 | SCC, circular, small spots | - | * | * | - | X | X | o | X | o | X | Single porosity |
| 1028B | 10 | 36 | SCC, at angle; edge crack | * | | | | Not received | | | | | | |
| 1024A | 10 | 180 | SCC, circular, radial and angular, spotty | * | | | * | X | X | o | X | X | X | Cracked (0.5 in. max.) |
| 10K18 | 10 | 360 | Lack of fusion; possible SCC | * | * | * | - | X | X | o | o | X | X | Lack of fusion |
| 10K17 | 10 | 360 | None | - | - | - | - | X | o | o | | o | | Acceptable weld |
| 1020A | 10 | 360 | None | - | - | - | - | X | o | o | | | X | Overlap of weld root |
| 1024B | 10 | 180 | None | - | | | - | Not received | | | | | | |
| 1028C | 10 | 36 | None | - | | | | X | o | o | | | | Acceptable weld |
| 1028D | 10 | 36 | | - | | | | Not received | | | | | | |
| 1019A | 10 | 360 | None | - | - | - | - | X | o | o | | | | Acceptable weld |
| 19BL | 10 | 180 | None | - | | | - | X | o | o | | X | o | Acceptable weld |
| B2A | 4 | 360 | SCC, small spots | - | * | - | - | Not received | | | | | | |
| A9A | 4 | 360 | None | - | - | - | - | | | | | | | Not evaluated |

[a] * - Quadrant identified as anomalous by GE
- - Quadrant identified as good weld by GE

[b] VI: Visual inspection
DPT: Dye penetrant testing
RT: Radiographic testing
ERG: Electric resistance gauging
Met.: Metallography
o: Tests performed but not included in data set
X: Record of test included in this data set

one-quarter segment (36°), a two-quarter segment (180°), or a full four-quarter segment (360°). If GE found an anomalous condition in a given quadrant, this was designated by an asterisk in the proper location in the "Standard" column of Table D-1.

The BCL examinations included visual, fluorescent penetrant, X-ray, ultrasonic, and ERG as they applied to each sample. Where results warranted, metallographic specimens were taken and analyzed. Table D-1 shows which samples were subjected to this entire coverage as well as those which received only a partial surveillance. Some of the samples used in the round robin were not shipped to BCL. These are designated as "Not Received" in the table. The two sections of 4-in. pipe sent to BCL were not characterized because of the greater interest in the 10-in. samples.

The choice of tests to be performed was based on results gained from previous examinations. All pipe sections which were evaluated were photographed, both for general recognition purposes and for characterization of surface and ID contour conditions. All samples were subjected to careful liquid penetrant examinations as well as radiographic examination. In instances in which stress corrosion cracking was suspected, the X-ray techniques were optimized at each specific location. Ultrasonic examinations were performed on samples which exhibited unique characteristic to the round robin teams. This was usually a region with some penetrant indications but with no significant length to designate it as a stress corrosion crack (sample 10K17L) or a region with strong ultrasonic indications but with no penetrant indications at all (sample 19BL). The only stress corrosion crack which was characterized to any extent by ultrasonics was that found in sample 1024A.

The results of this characterization study have shown that the exact identification of cracked regions within pipes prior to descaling and partial sectioning may be difficult. The radiographs taken have been of the highest quality, yet the presence of known stress corrosion cracks was difficult to discern except in the obvious cases of samples 19AL, 1028A, and 1024A (large crack). The ultrasonic reflectivity from relatively small lack-of-fusion conditions and pipe material defects (∿0.020 in.) were on the same order as those found from IGSCC reflectors representing more than one-half of the wall thickness (∿0.500 in.). ERG results taken from known stress corrosion cracks suggest that these readings can be low by as much as 60 to 75%.

## BWR PIPE CHARACTERIZATION PROCEDURES

The descaling, NDE, and metallography procedures are outlined in the following paragraphs. They are included here to give a general understanding of the steps taken in the processing of the test samples and to convey the philosophy and priorities used in developing the data shown in the following pages. At the outset of this characterization, no consideration was given to totally characterizing all of the round robin samples until additional information regarding their "real" conditions could be assessed. Thus no attempt was made to obtain SEM data from samples which were obviously evaluated as cases of lack of fusion or base metal pipe defects. Locational data are generally considered to be within $\pm$ 0.2 in. when indicated on drawings and photographs.

## Pipe Descaling and Decontamination

Prior to the detailed BCL nondestructive and selected destructive evaluation of the BWR sample pipes, decontamination and descaling were performed. This was done both for health and safety reasons and to provide a better surface condition for more accurate and reliable fluorescent penetrant results. The descaling procedure was as follows:

1. Soak 1 hour in a solution containing 100 g/liter NaOH and 30 g/liter $KMnO_4$ at a temperature just below boiling.

2. Rinse in water.

3. Soak 1 hour in a solution containing 100 g/liter $(NH_4)_2HC_6H_5O_7$ (ammonium citrate) at a temperature just below boiling.

4. Scrub and rinse.

5. Repeat procedure if necessary.

The descaling was generally repeated until the level of radioactivity at the pipe surface was below 50 mr gamma and 200 mr beta. All full (360°) sections of pipe were cut in half following descaling at locations which allowed edge views of areas in question.

## Visual Inspection/Documentation (VI)

OD and ID surfaces of each specimen were visually scanned, with particular emphasis on the condition of the weld root and weld crown and the exact location of the weld. A reference grid was then placed on the ID and OD surfaces, similar to that used during the EPRI round robin inspections. Color photographs of all pipe ID surfaces, and in some cases the OD surfaces, were then taken for documentation purposes.

## Fluorescent Penetrant Testing (DPT)

Standard fluorescent postemulsifiable penetrant inspection procedures were used for all specimens. A Magnaflux high-sensitivity (22B) fluorescent penetrant with a soak time of 5 minutes was used as the probing medium. The general procedure was to clean the pipe, apply penetrant, soak, apply emulsifier, and clean and dry the specimen before applying the developer. The specimen was then viewed under an ultraviolet light for indications. When suspected false penetrant indications were identified, the area in question was recleaned and developer reapplied to confirm the legitimacy of the indication by observing the penetrant bleed-out. All legitimate penetrant indications were photographed in color under a black light.

## Radiographic Testing (RT)

General radiographs were taken for all pipe specimens with the X-ray source on the OD side of the pipe and the film on the pipe ID side for minimum unsharpness. Source voltage varied from 180 to 200 kV at 8 mA with a source-to-object distance

of 36 in. Exposure time ranged from 3 to 5 minutes. Type M film was used, with lead screens and manual processing at standard times and temperature.

For specimens containing known cracks (1024A, 19AL, and 1028A), the radiography was optimized by appropriate location of the specimen relative to the source direction. Even in this case, it was difficult to obtain or see angled crack details in specimen 1024A.

## Electric Resistance Gauging (ERG)

The depths of known cracks were assessed using a Uresco electric resistance gauge. Several gauge calibration techniques were investigated, including (1) using the calibration notch provided by Uresco, (2) using the Uresco calibration notch and then rezeroing on the BWR pipe of interest, and (3) fabricating a notch in BWR pipe material. Calibration curves for the cases mentioned are shown in Figure D-1. Figure D-1 shows that little difference exists between the latter two calibration techniques; hence the URESCO notch was used for initial gauge calibration, followed by rezeroing on the BWR pipe being examined.

## Ultrasonic Testing (UT)

Only those specimens identified as containing suspect or questionable UT indications during the EPRI round robin inspections, or samples which contained unique crack orientations (such as 1024A) were to be characterized ultrasonically. The BWR samples and the locations characterized are shown in Table D-1.

Characterization was achieved using a Matec 6600 series main frame with a model 755 plug-in, an Aerotech 0.25-in. diameter 2.25 MHz shear wave with a 45° beam angle. A Tektronix 7704 oscilloscope incorporating a dual beam sweep resulted in the simultaneous display of the video and RF signals. Initial ultrasonic characterization sensitivity was established in accordance with ASME Code Section XI requirements using the EPRI 10-in. diameter pipe containing an 1/8-in. diameter side-drilled hole (SDH). A typical distance-amplitude-correction (DAC) curve is shown in Figure D-2. The bottom trace shows the video signal response used in actual construction of the DAC curve, which is shown as an approximate exponentially decaying envelope superimposed on the scope face plate. The top trace shows the RF waveform for the video trace. This is the minimum sensitivity at which all the ultrasonic characterization was performed. Depending on the nature of the discontinuity being characterized, the actual RF and/or video scope sensitivities were increased for ease in visual identification of the scope traces.

Beam spread characteristics of the 45° shear wave, 0.25-in. diameter 2.25 MHz transducer were determined by locating the 2/8 Vee and 6/8 Vee positions and incrementing the transducer at 1/16-in. intervals toward and away from the particular Vee position. Again, the EPRI 10-in. pipe calibration block was used. The results of the beam spread test are shown in Figure D-3.

A comparison of the 1/8-in. and SDH DAC curve with the response of a 5%T notch is shown in Figure D-4. Again, the transducer was incremented at $\pm$ 1/16-in. increments about the 4/8 Vee notch/transducer position. As shown in Figure D-4, a lower effective sensitivity results when the notch is used for calibration purposes.

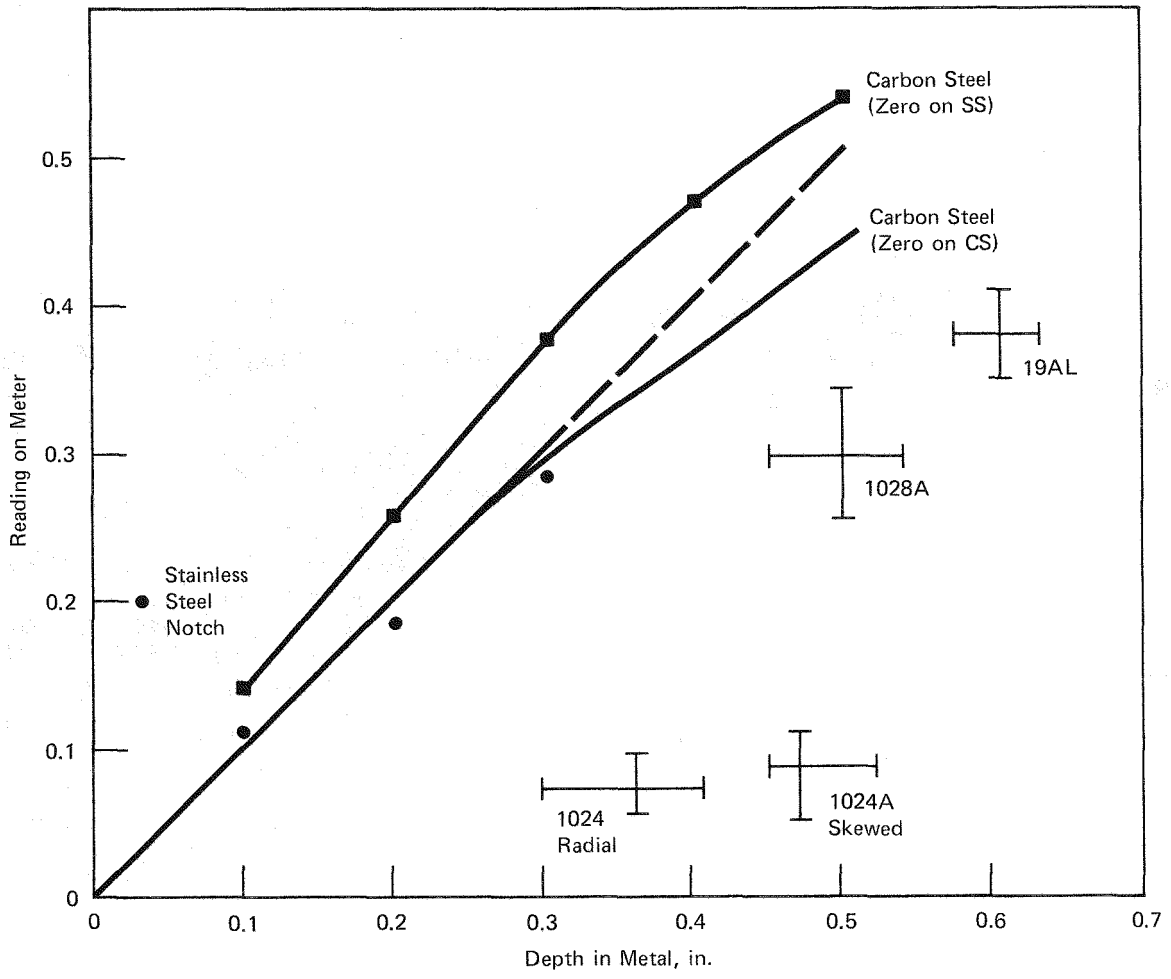


Figure D-1 ERG Calibration and IGSCC Correlation

# ASME CODE
# CALIBRATIONAL (DAC) CURVES
# (EPRI BLOCK)

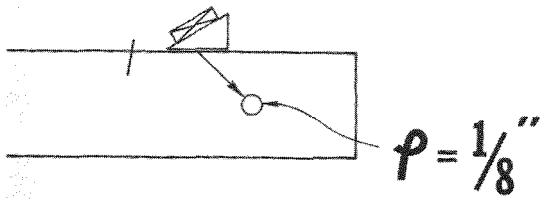


2/8 Vee PATH

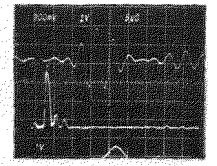

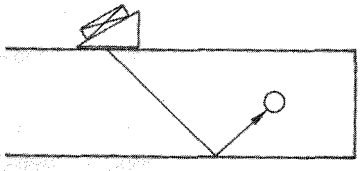

6/8 Vee PATH

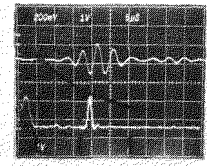

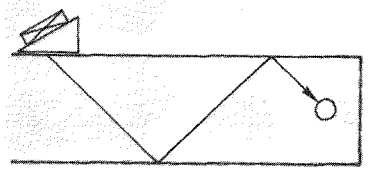

10/8 Vee PATH

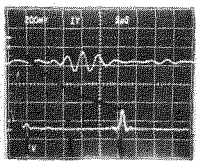

Figure D-2 ASME Code Calibration Curves

# 0.25″ DIAMETER TRANSDUCER AT 2.25 MHZ

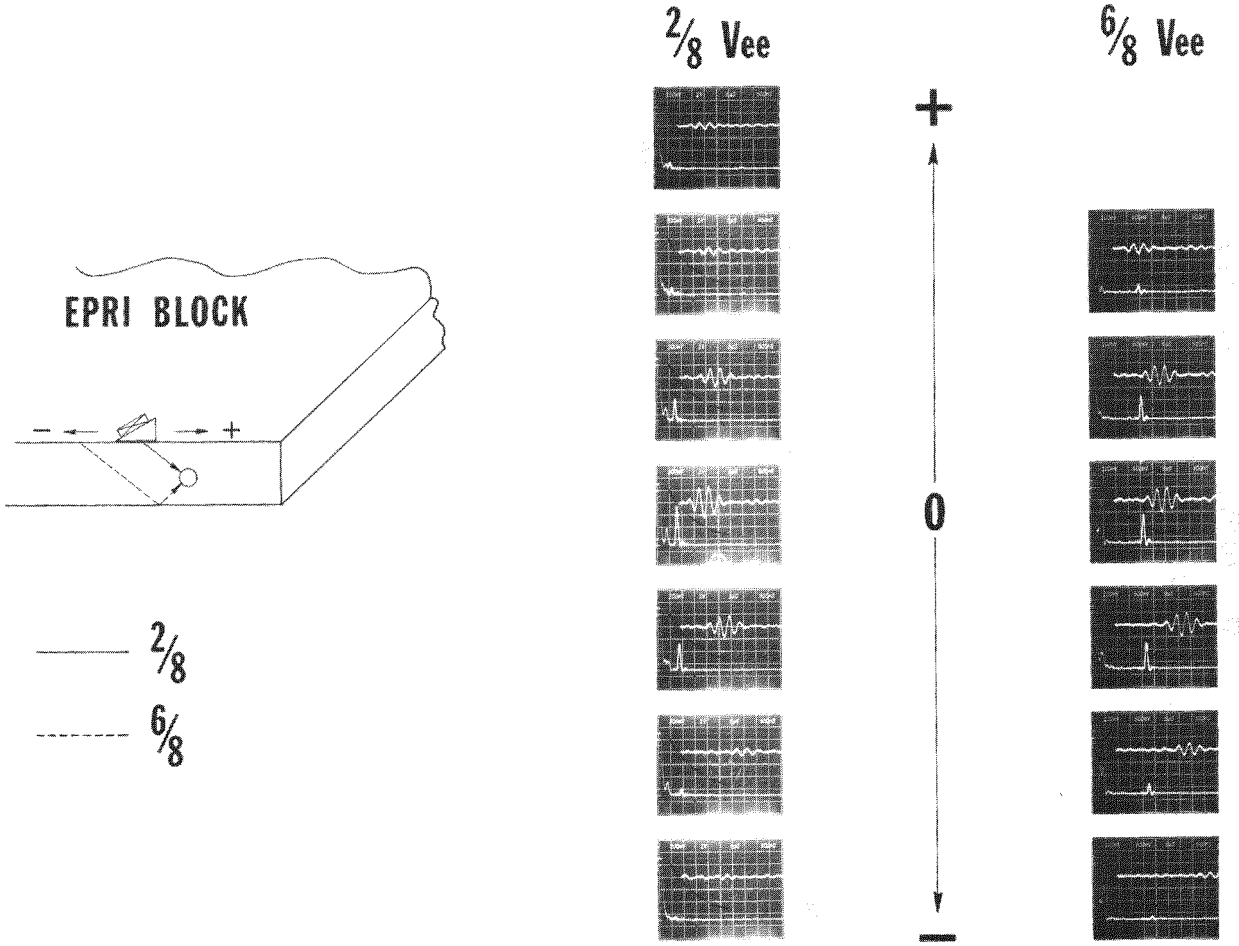


Figure D-3 UT Response From SDH

# 5% NOTCH — 1/8″ SDH DAC COMPARISON
# 0.25″ DIAMETER TRANSDUCER AT 2.25 MHZ

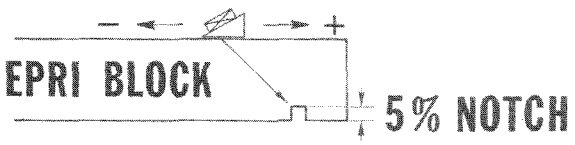


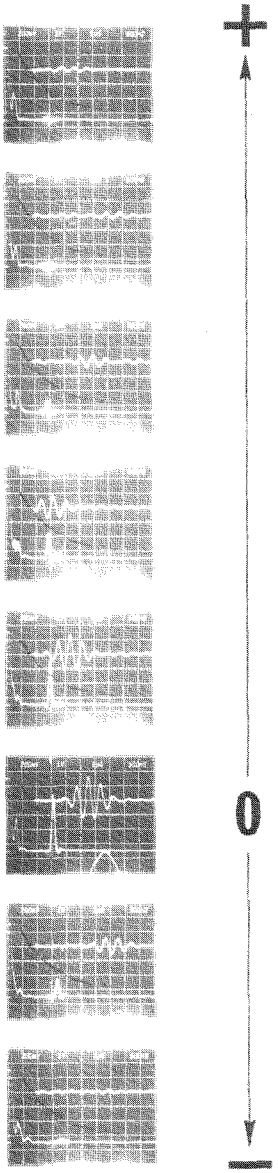


Figure D-4 UT Response From 5% Notch

Detailed probe positions for particular discontinuities being characterized are described in the findings for each pipe section. The general probing method is shown in Figure D-5. Scanning was initiated in two directions: parallel and perpendicular to the maximum ultrasonic response. In general this was clockwise and counterclockwise in a circumferential direction, and toward or away from the weld along the pipe longitudinal axis.

Metallography

Each specimen was examined under 15X to 20X magnification to assess the general condition of the pipe surface in the vicinity of reported cracks. These areas were saw cut and polished using generally approved metallographic techniques. The prepared samples were etched* by several techniques in order to determine whether these cracks were of the same nature as those observed during recent studies of such cracking at BCL. In particular, conditions such as degree of cold working, sensitization of structure, intergranular cracking, grain size, hardness, and location of the cracks with respect to the heat-affected zone were of interest. Photomicrographs and photomacrographs were taken showing crack morphology and structure when outstanding samples were available. Sample 1024A was broken open to obtain a sketch of the crack cross section and deepest penetration. SEM examinations were made of this same sample.

DESCRIPTION OF NDE AND DESTRUCTIVE TEST FINDINGS

The significant results of the overall BCL characterization of the BWR pipe samples are given here. All of the data for each pipe are summarized for continuity on a form sheet similar to that used during the EPRI round robin inspections. The white arrows on the penetrant pictures designate locations at which cuts were made for metallurgical evaluation.

19AL

19AL represents a shop-welded specimen in which the weld crown and root were both machined so that very smooth weld surfaces exist. 19AL contains a through-wall crack with the crack axis rotated approximately 10 degrees relative to the longitudinal axis of the pipe. The crack is offset below the weld approximately 2 in. A summary of crack ID and OD dimensions and ERG depth readings is shown in Figure D-6. Figure D-7. is a white light photograph of 19AL showing its ID surface conditions. A detailed ID penetrant view is shown in Figure D-8; Figure D-9 shows a close-up view of the through-wall crack from the OD side. This sample was not characterized further because of the obvious nature of the defect.

1028A

1028A is a small pipe section specimen containing a rather gross stress corrosion crack partly through the wall. Crack location and ERG depth measurements are shown in Figure D-10. A white light ID photograph is shown in Figure D-11. The weld root was in good condition, whereas the weld crown was rough and not amenable

*In most cases, 10% oxalic acid was used (electrolytically).

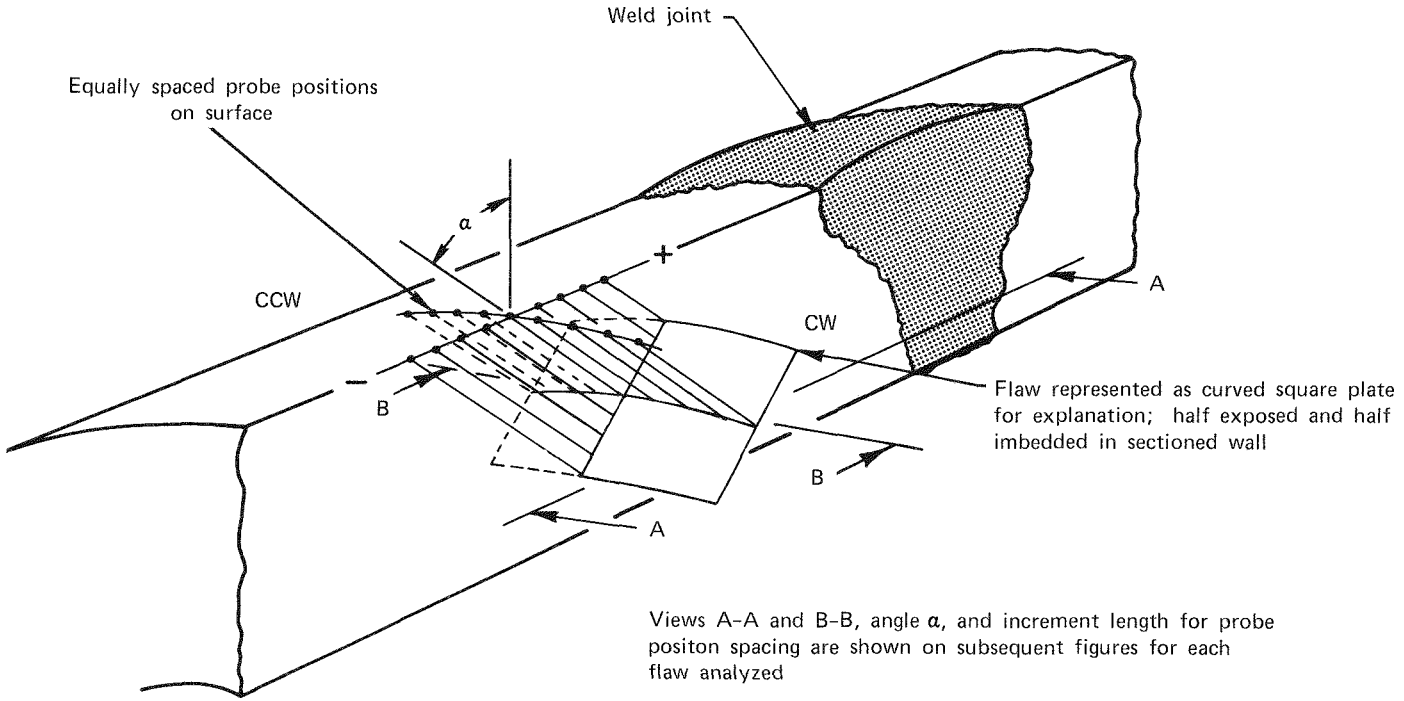


Views A-A and B-B, angle α, and increment length for probe positon spacing are shown on subsequent figures for each flaw analyzed

Center of pattern represents location of maximum ultrasonic indication

+ and − indicate longitudinal direction, + = toward weld

CW and CCW indicate clockwise and counterclockwise circumferential direction

Figure D-5 UT Probing Method

**ANALYSIS OF ULTRASONIC EXAMINATION**

Organization BCL Program Step _____ Date _____ Operator _____

Recorder _____ Observer _____ Procedure _____ Equipment _____

Transducer I.D. _____ Weld Identification 19AL Start Time _____ End Time _____

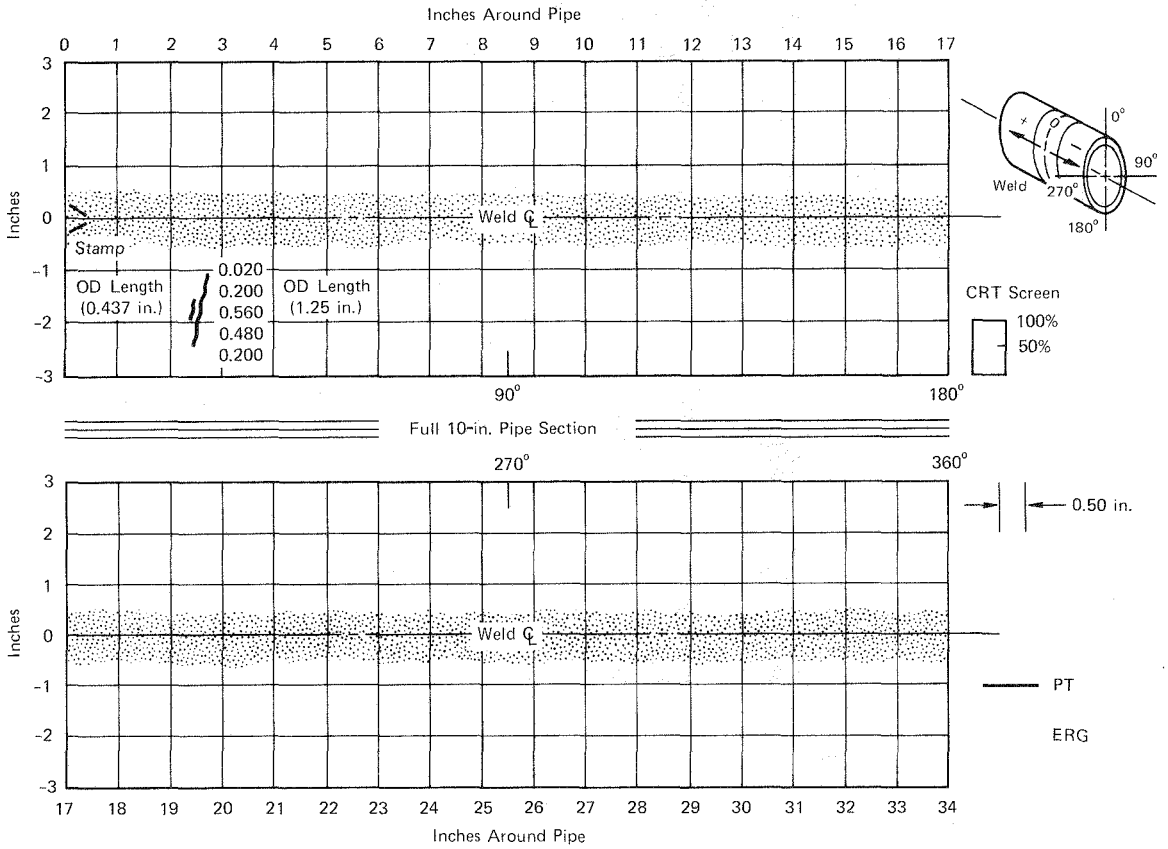


Figure D-6 ERG Readings, Sample 19AL

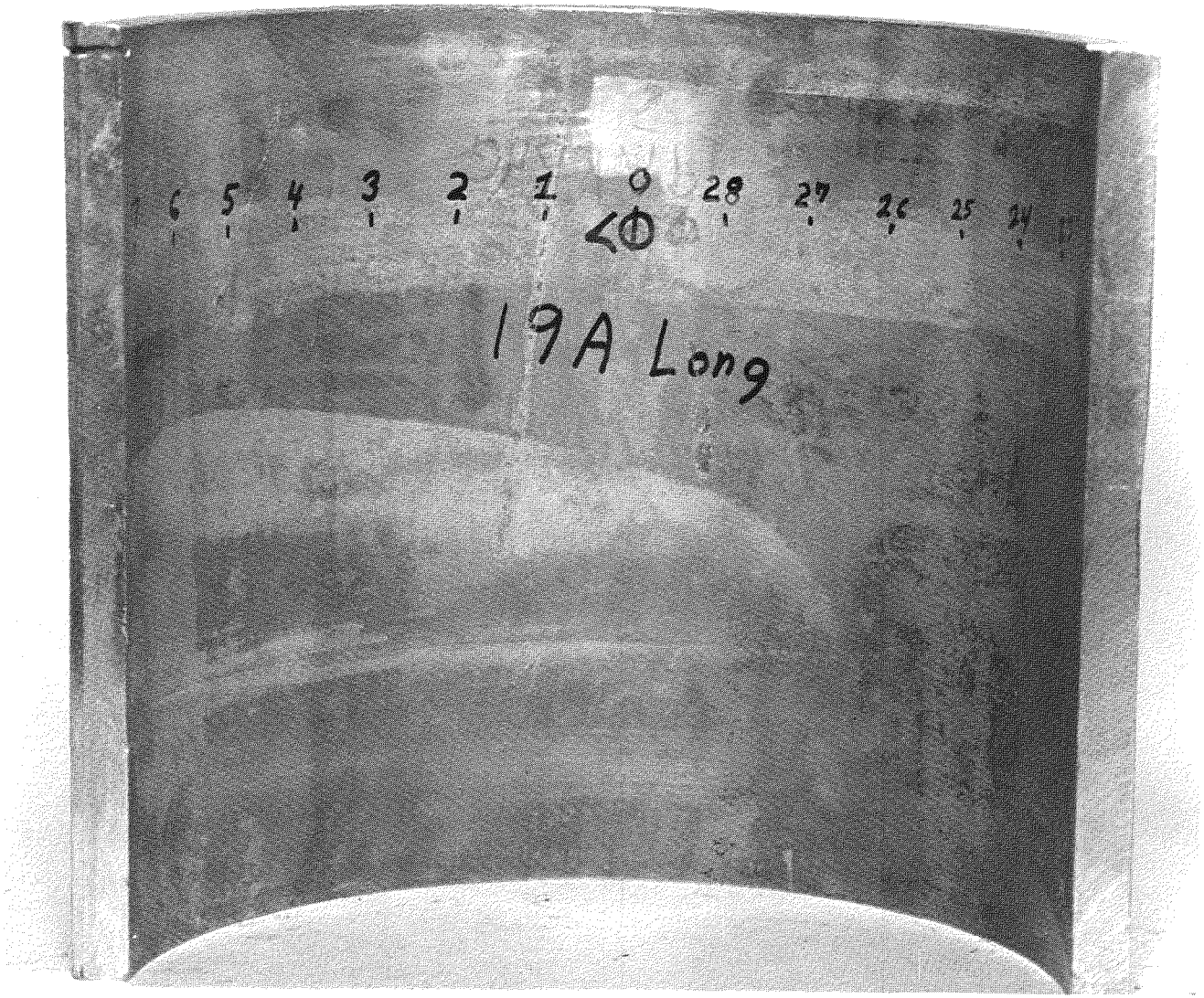


Figure D-7 Inside Surface, 19AL

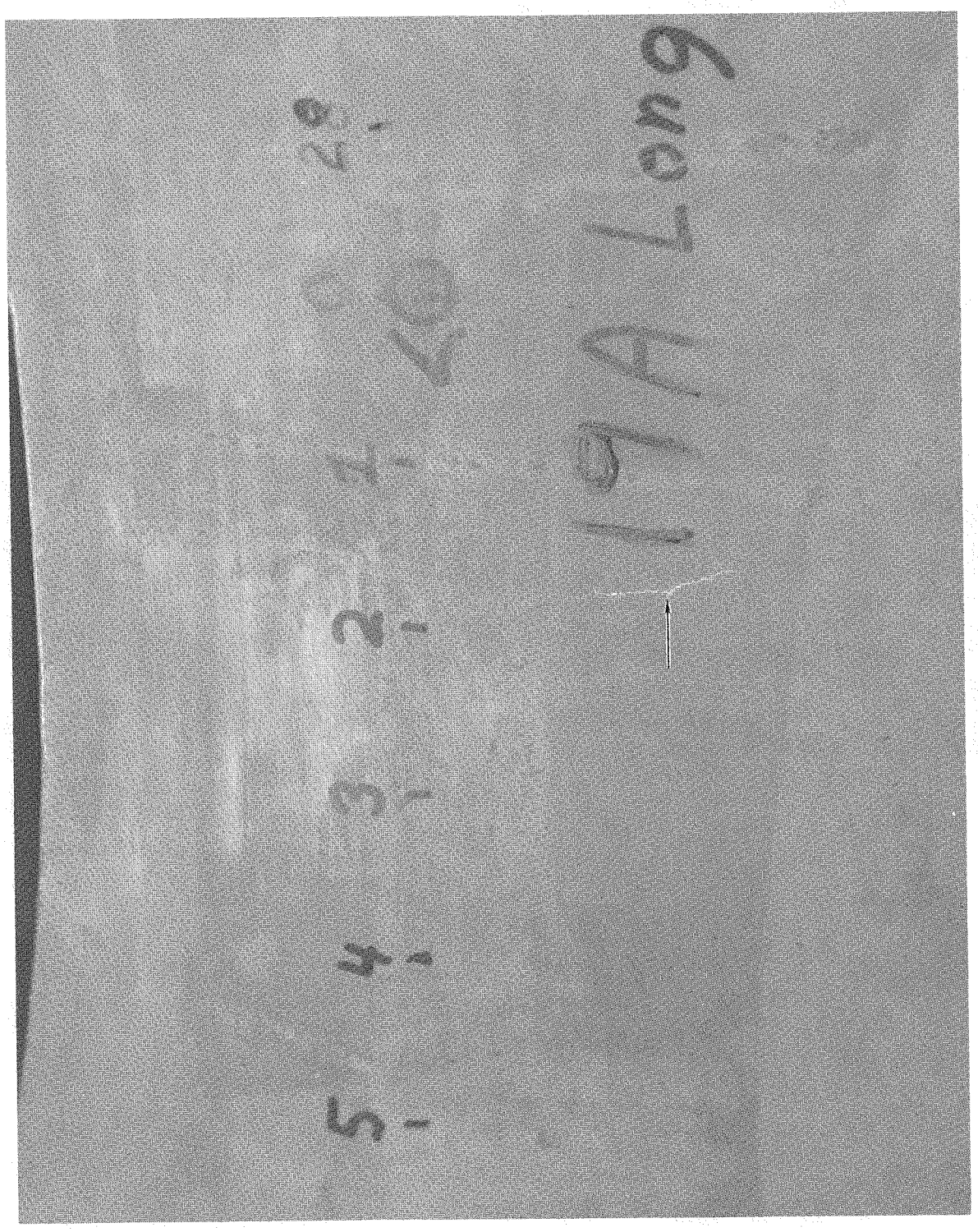


Figure D-8 IGSCC in 19AL, Inside Surface

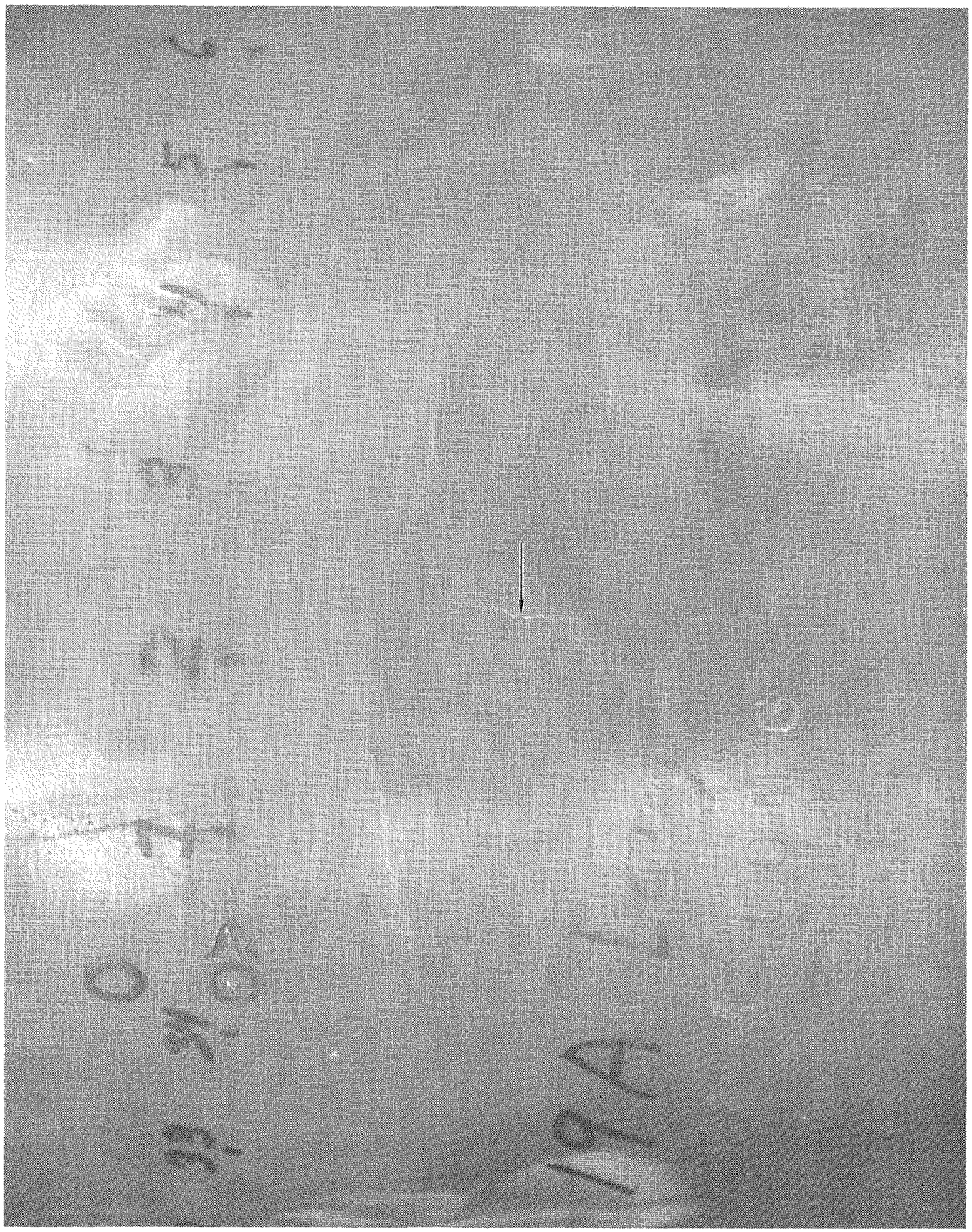

Figure D-9 IGSCC in 19AL, Outside Surface

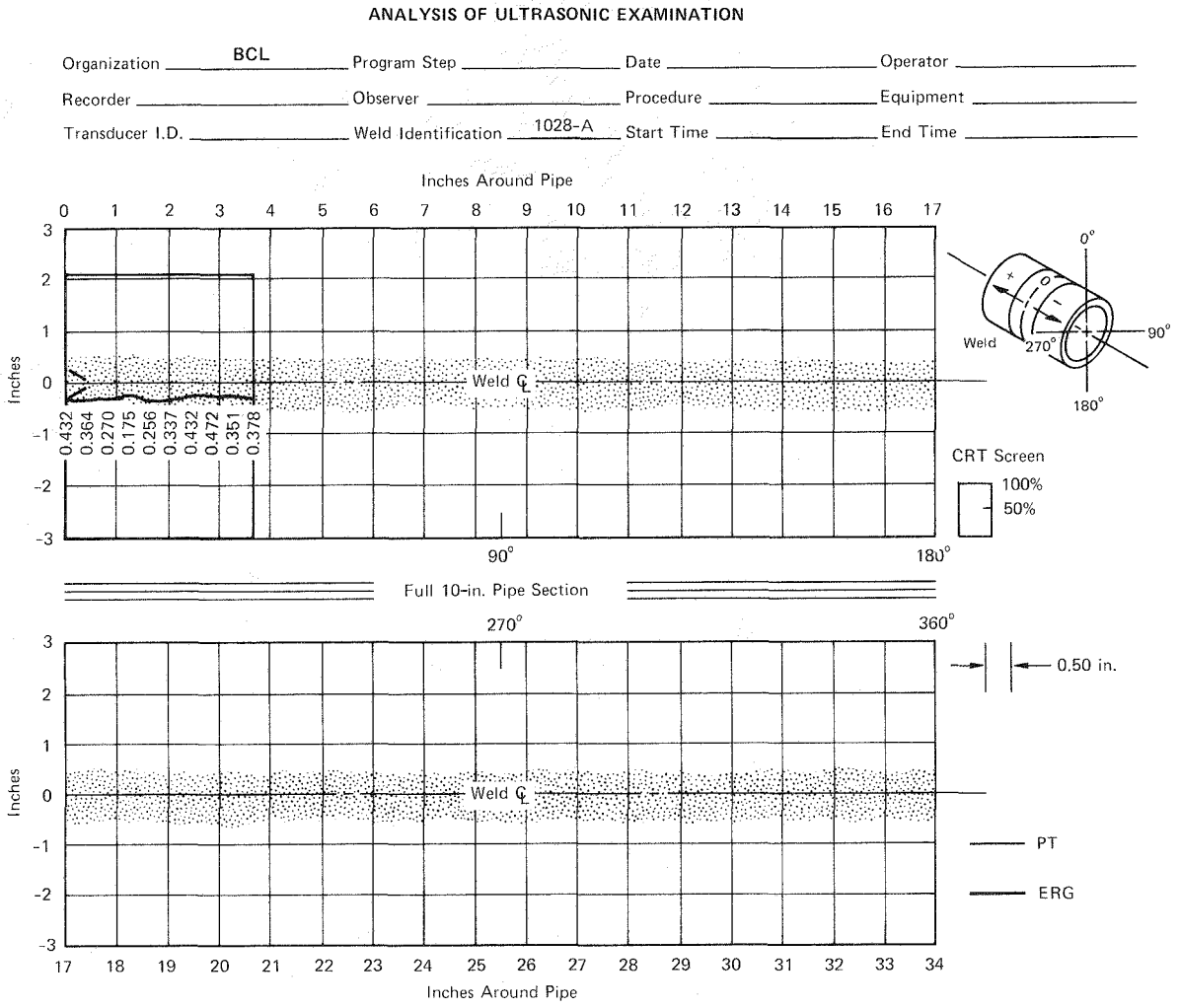


Figure D-10 ERG Readings, Sample 1028A

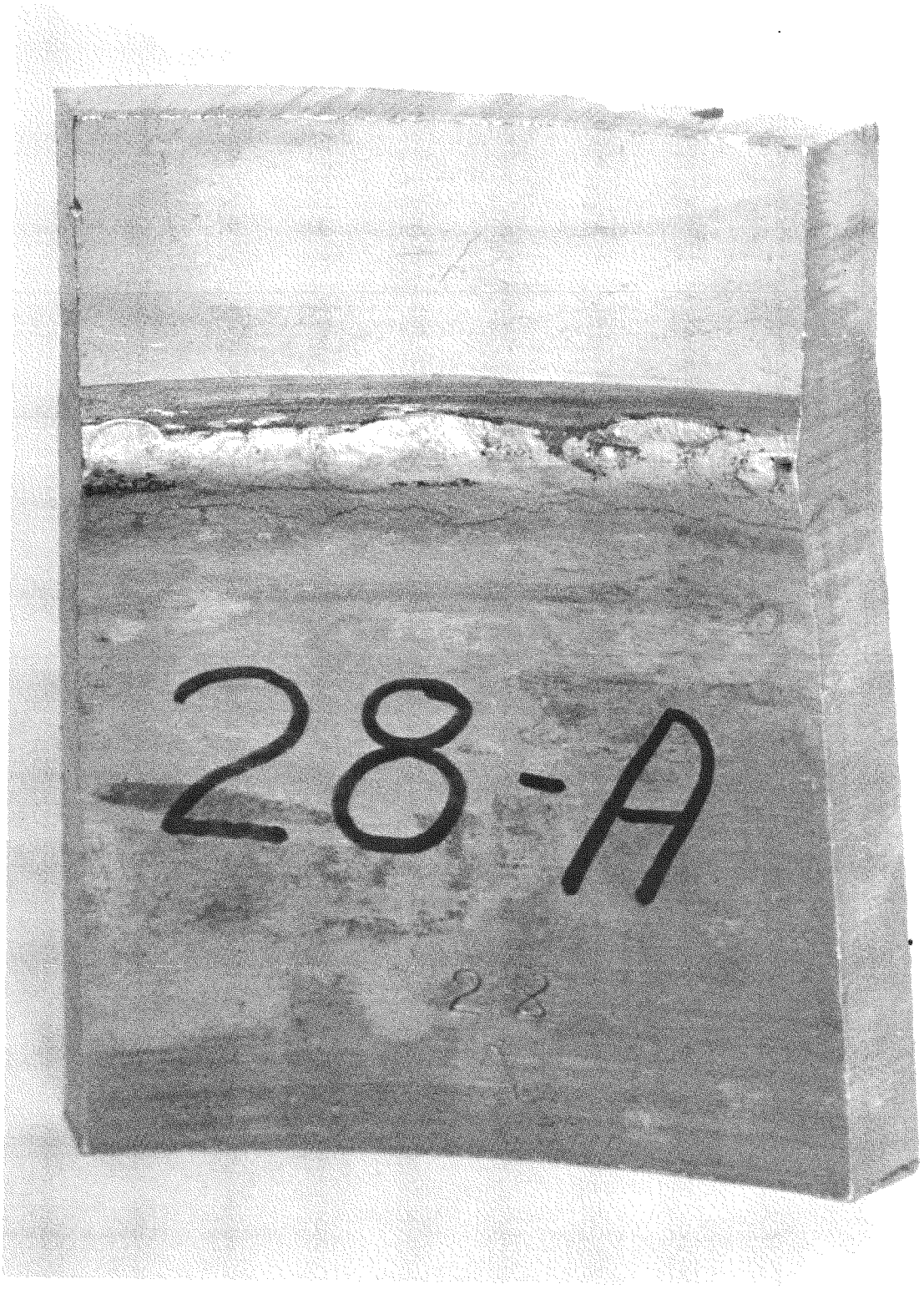


Figure D-11 Inside Surface, 1028A

to ultrasonic scanning. Fluorescent penetrant photographs showing the length and depth of the crack are shown in figures D-12 and D-13. This sample was not characterized any further.

1021

Specimen 1021 was interesting in that it was initially judged to contain a stress corrosion crack approximately 8-in. long as in Figure D-14. A white light photograph showing the condition of the pipe ID and the thickness mismatch between surfaces is shown in Figure D-15. The weld crown has been ground fairly smooth. The root area has been ground uniformly around the ID circumference of the pipe. An ID penetrant view is shown in Figure D-16. The close-up photograph shows the existence of a linear indication between ID locations 17 in. and 14 in.

1021 was sectioned transverse to the weld at an ID location of 14.2 in. for metallographic analysis of the suspect penetrant indications. A micrograph of this area at 125X is shown in Figure D-17. Figure D-17 shows a base metal material defect (a lap) which extends to a depth of approximately 22.4 mils. The weld metal fusion zone is clearly in evidence in Figure D-17, with the lap being entirely in the pipe material protruding or opening to the pipe ID surface.

10K17L

10K17L was identified for detailed ultrasonic characterization as a consequence of the EPRI round robin inspections (Figure D-18). A general white light photograph is shown in Figure D-19. A ground-out area between 14 in. and 17 in. may be readily identified in the photographs.

The original round robin penetrant characterization of the specimen had identified two spotlike indications within the ground-out area, with a faint linear penetrant indication between the two spots possibly being a stress corrosion crack. Additional penetrant characterization of this area is shown in Figure D-20. In this figure the lack of a linear penetrant indication linking the two spots is apparent. The penetrant indication at 15.5 in. ID has the appearance of a hard spot, whereas the indication at about 14.75 in. ID exhibits extensive bleed-out and appears to be porosity within the weld metal which has been opened as a result of the local grinding operation.

Macrographs of the two spots are shown in Figure D-21: view (a) shows the pore, whereas view (b) illustrates the hard spot. The pore was sectioned metallographically; the resultant macrograph (100X) is shown in Figure D-22. The depth of the pore below the ID surface is approximately 0.013 in.

Ultrasonic characterization of the area of 10K17L between 16 in. and 17 in. OD was performed, with a sample result shown in Figure D-23.

1024A

1024A contains a number of cracks, some of which had not been reported previously. The location and orientation of all cracks identified by penetrant testing are summarized in Figure D-24. A general white light ID view of 1024A is shown in Figure D-25. An ID penetrant view in Figure D-26 shows the longitudinal indication

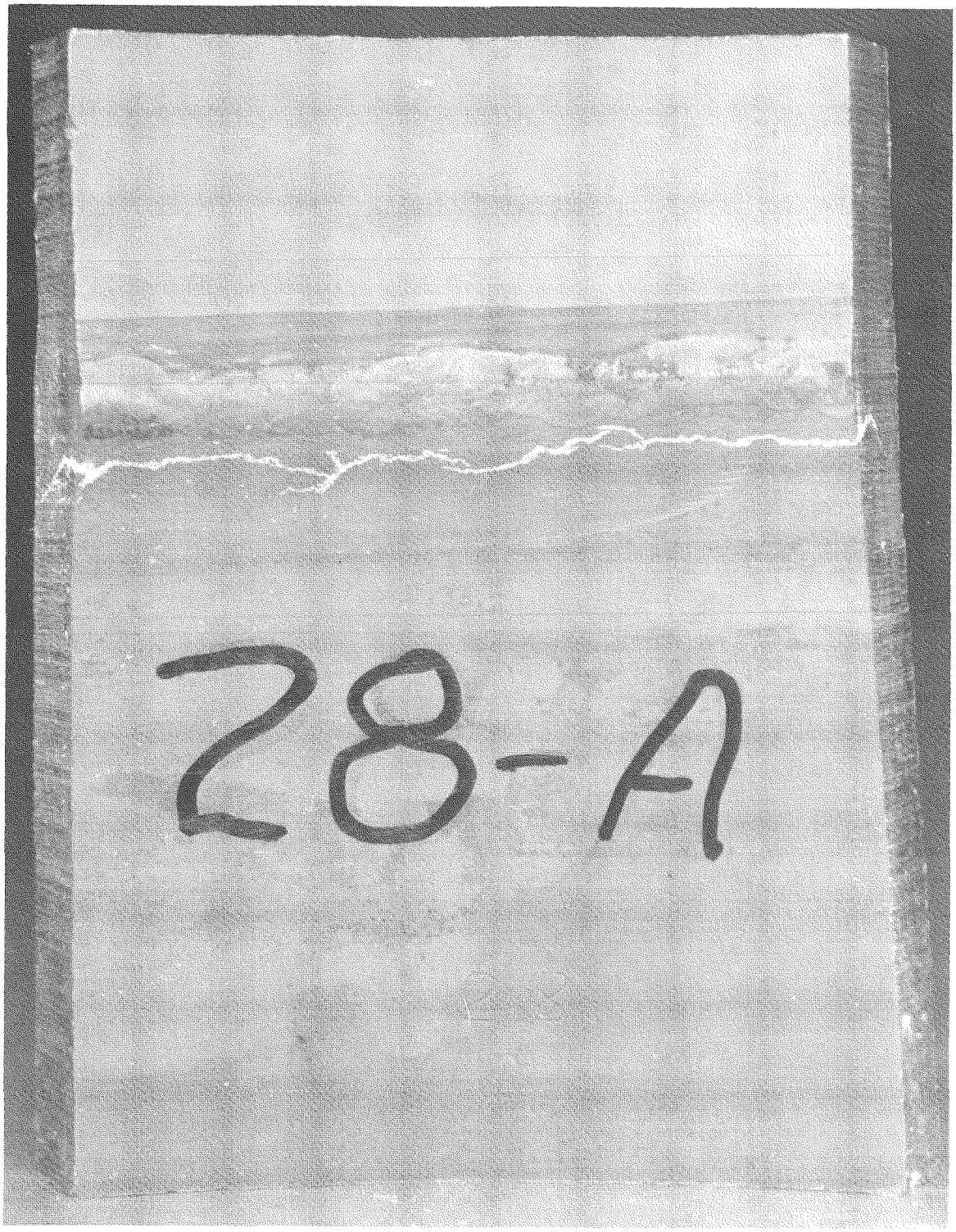


Figure D-12 IGSCC in 1028A, Inside Surface

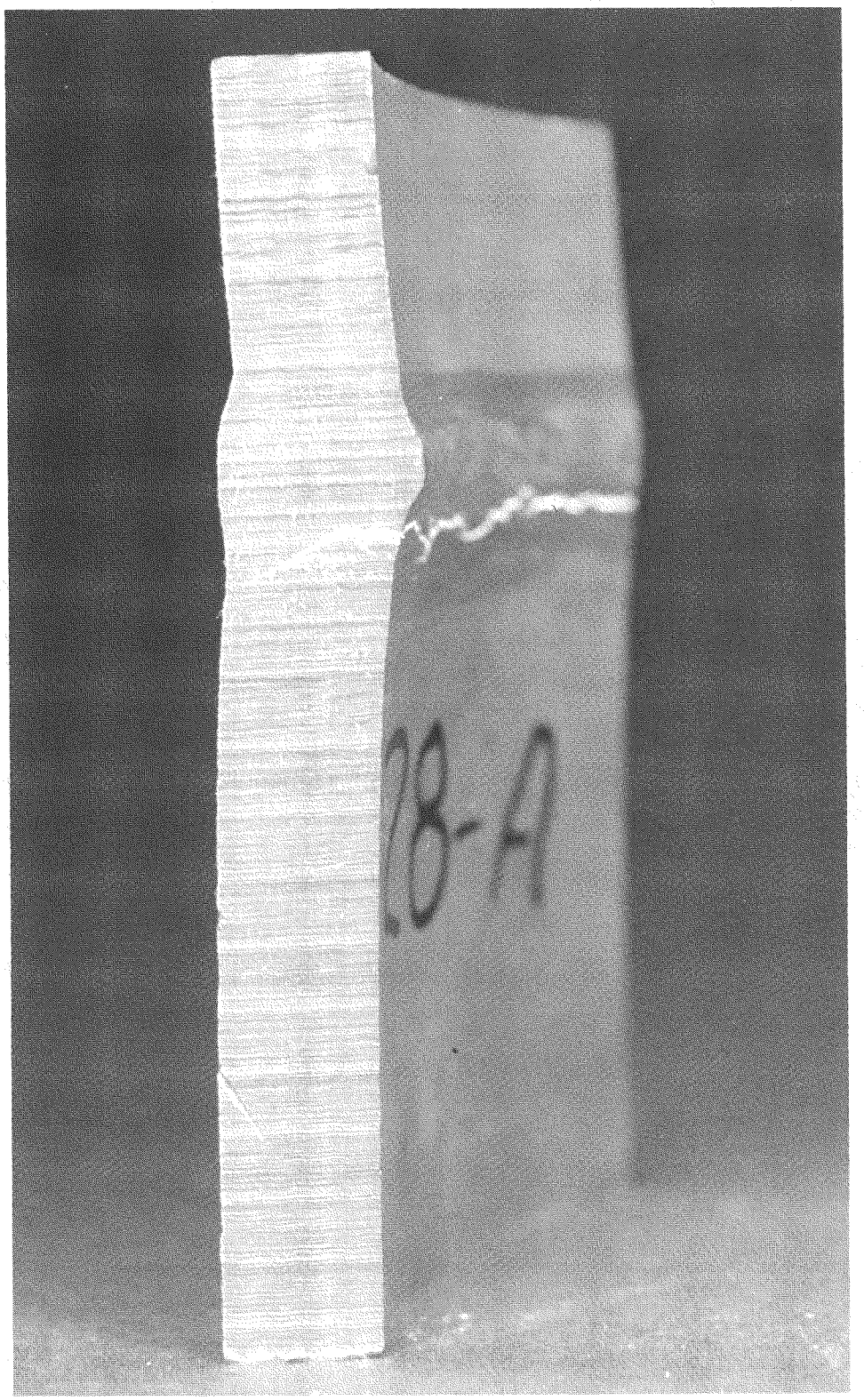


Figure D-13 IGSCC in 1028A, Cross Section

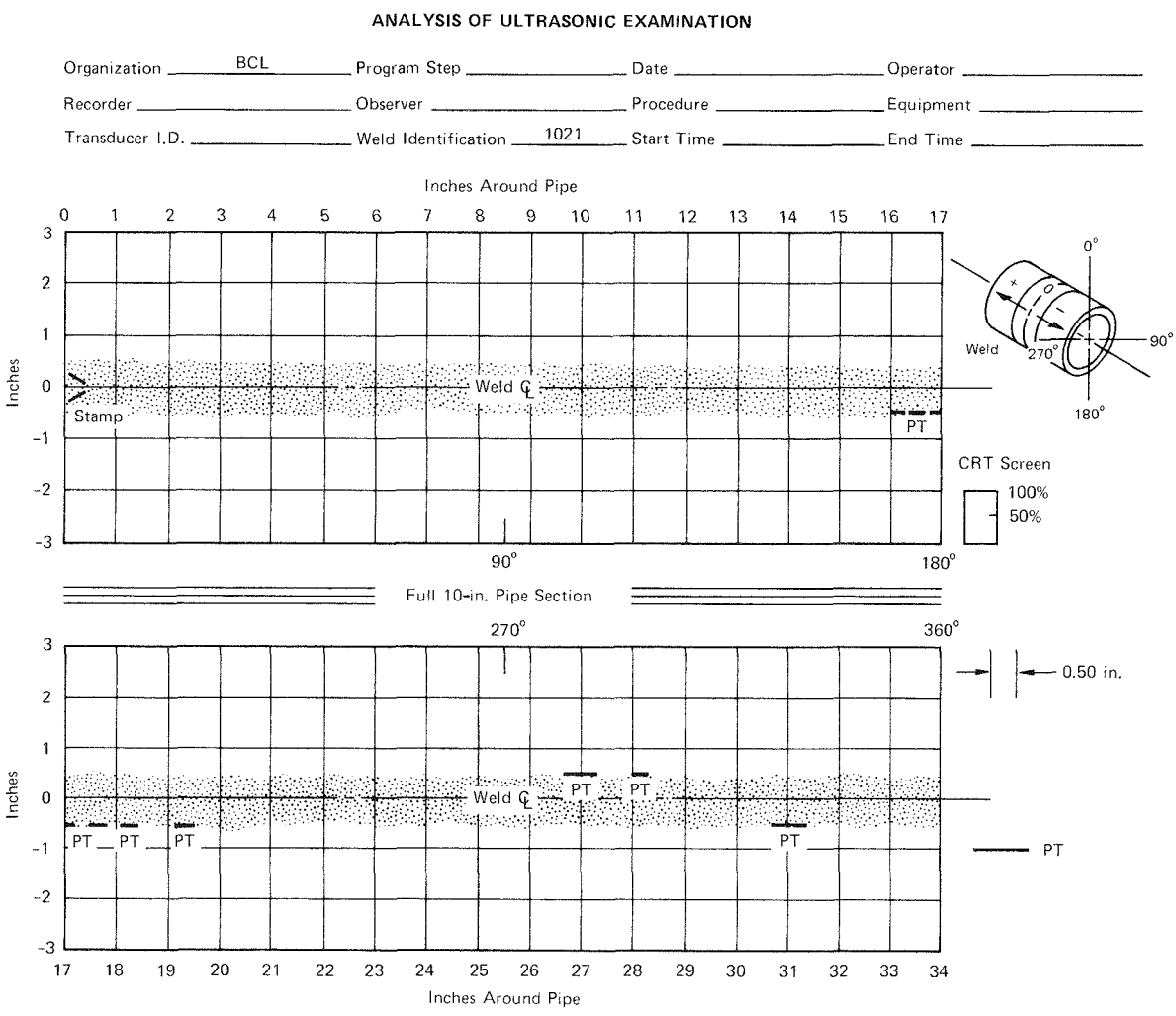


Figure D-14 DPT Data for 1021

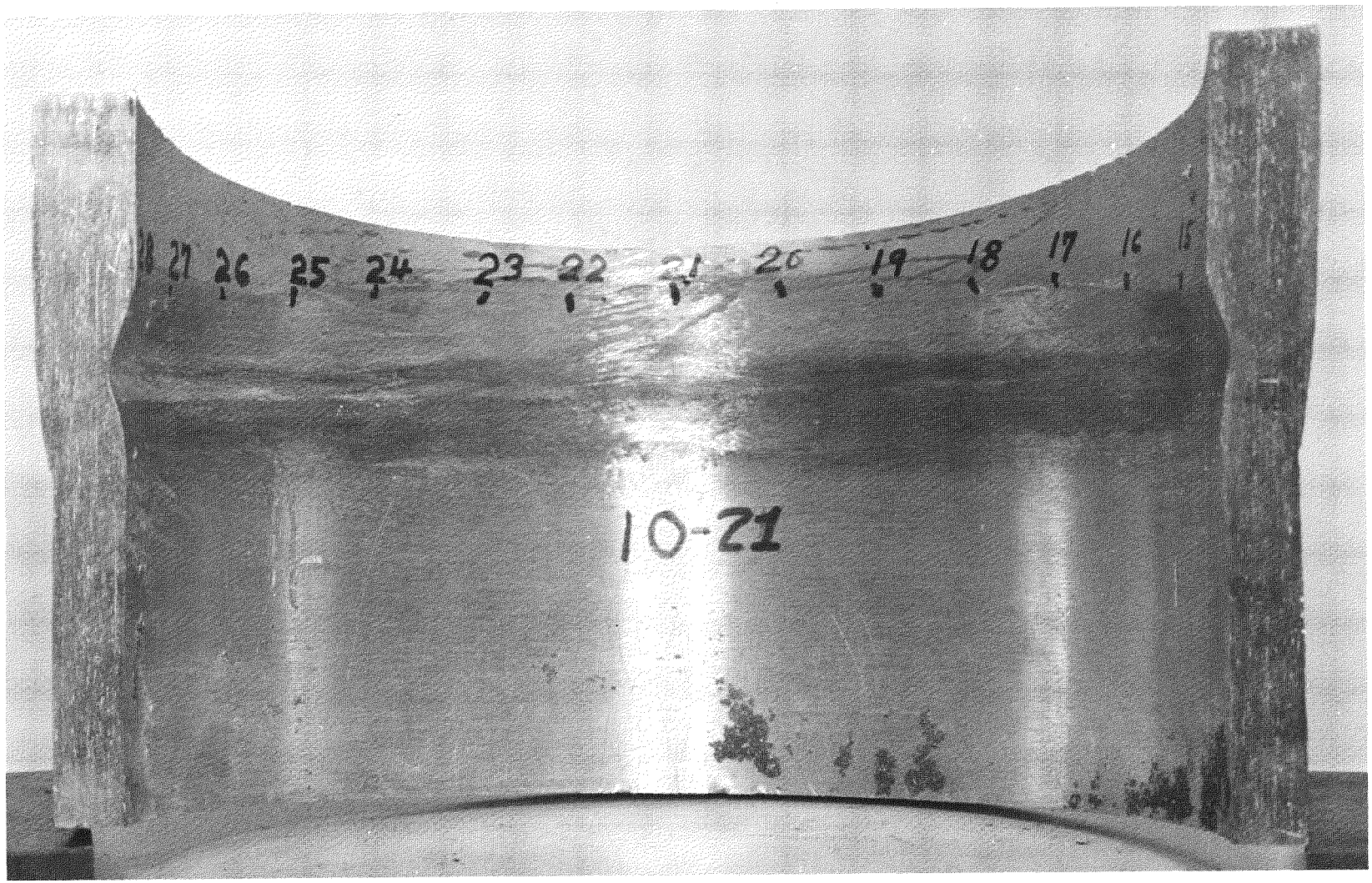


Figure D-15 Specimen 1021, Inside Surface

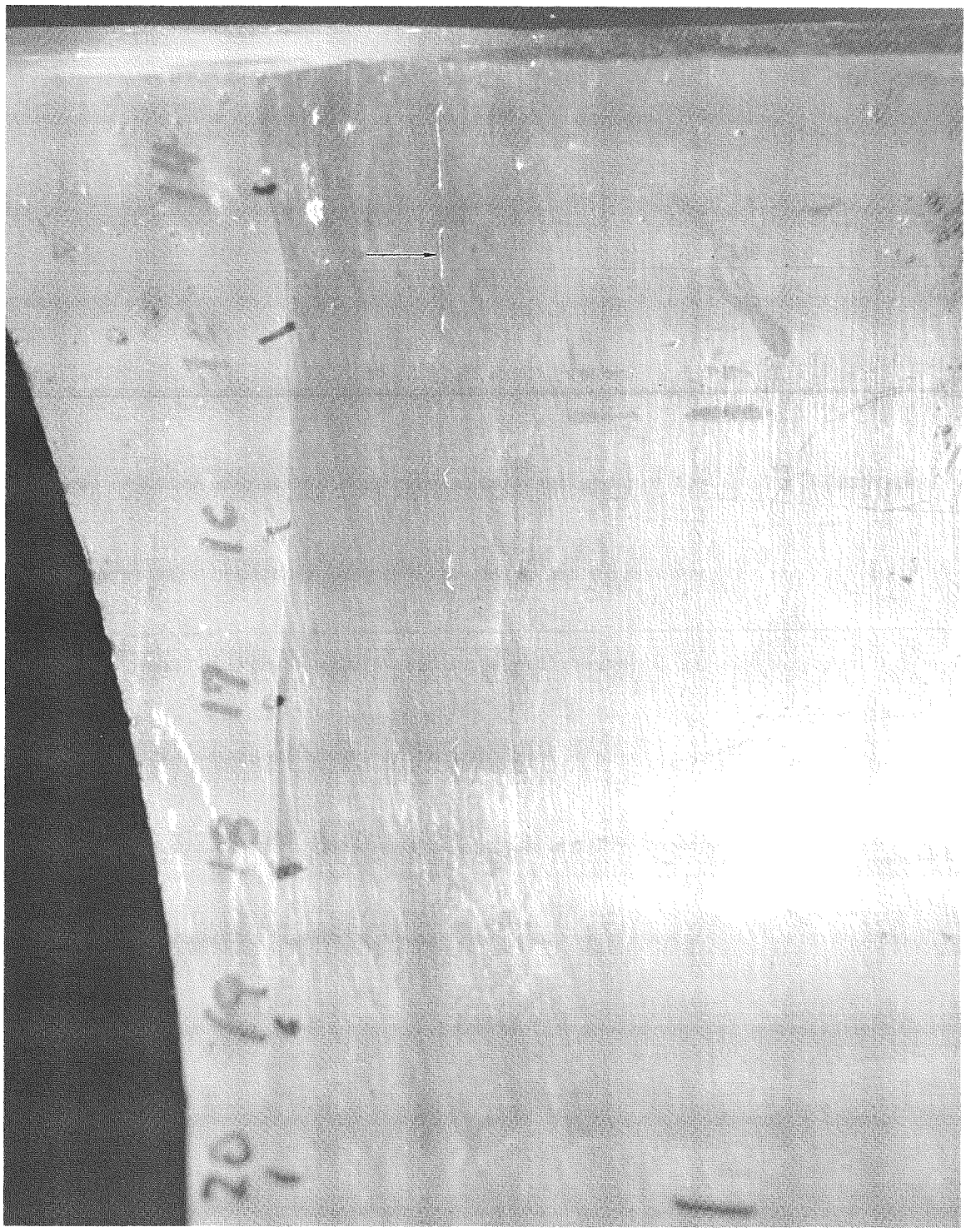

Figure D-16 Lap Defect in 1021

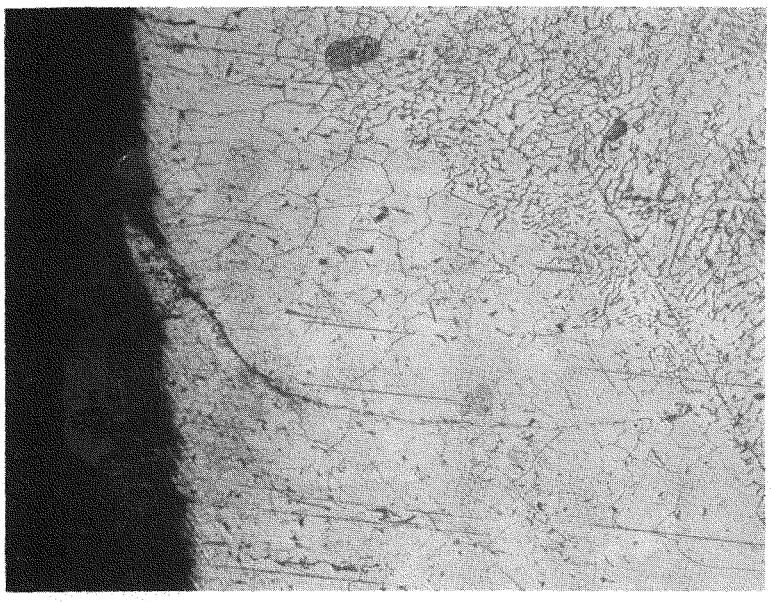

Figure D-17 Lap Defect in 1021, x125

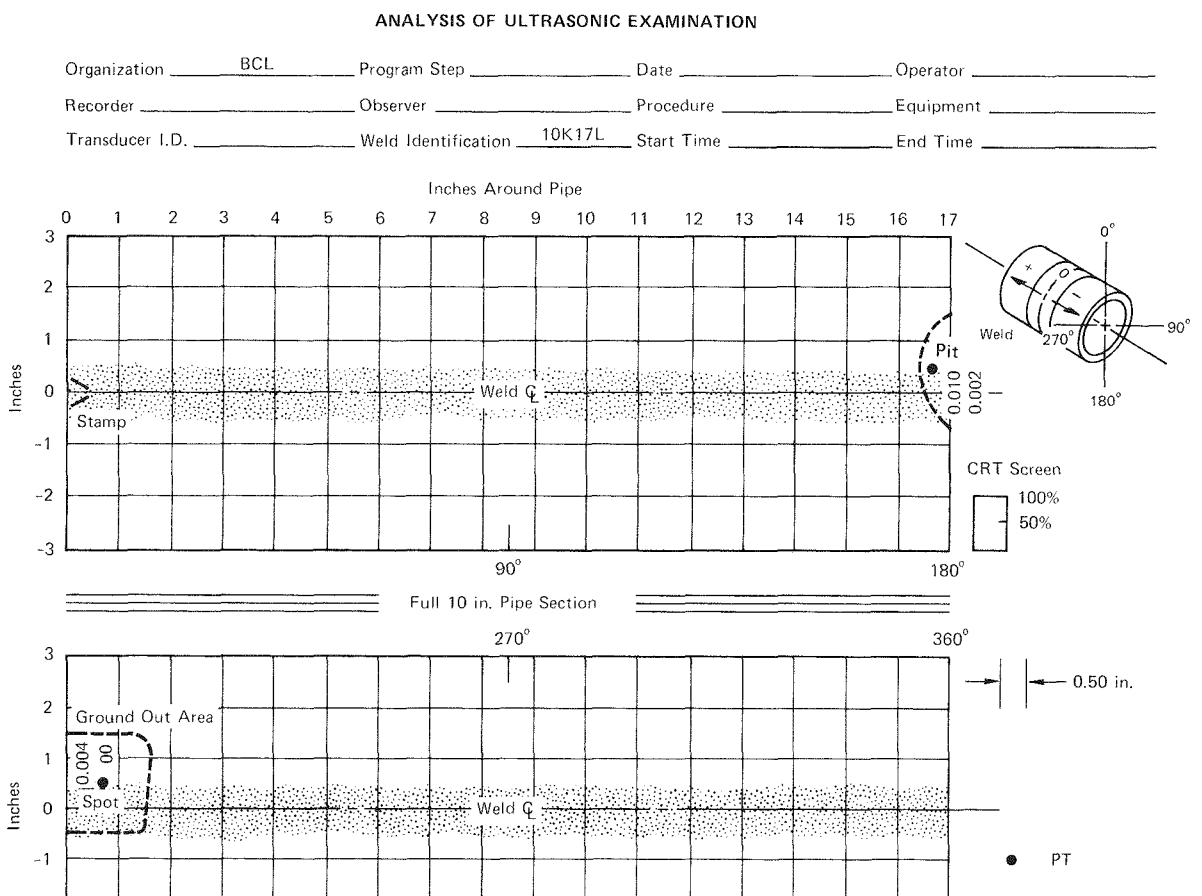


Figure D-18 ERG and DPT Data for 10K17L

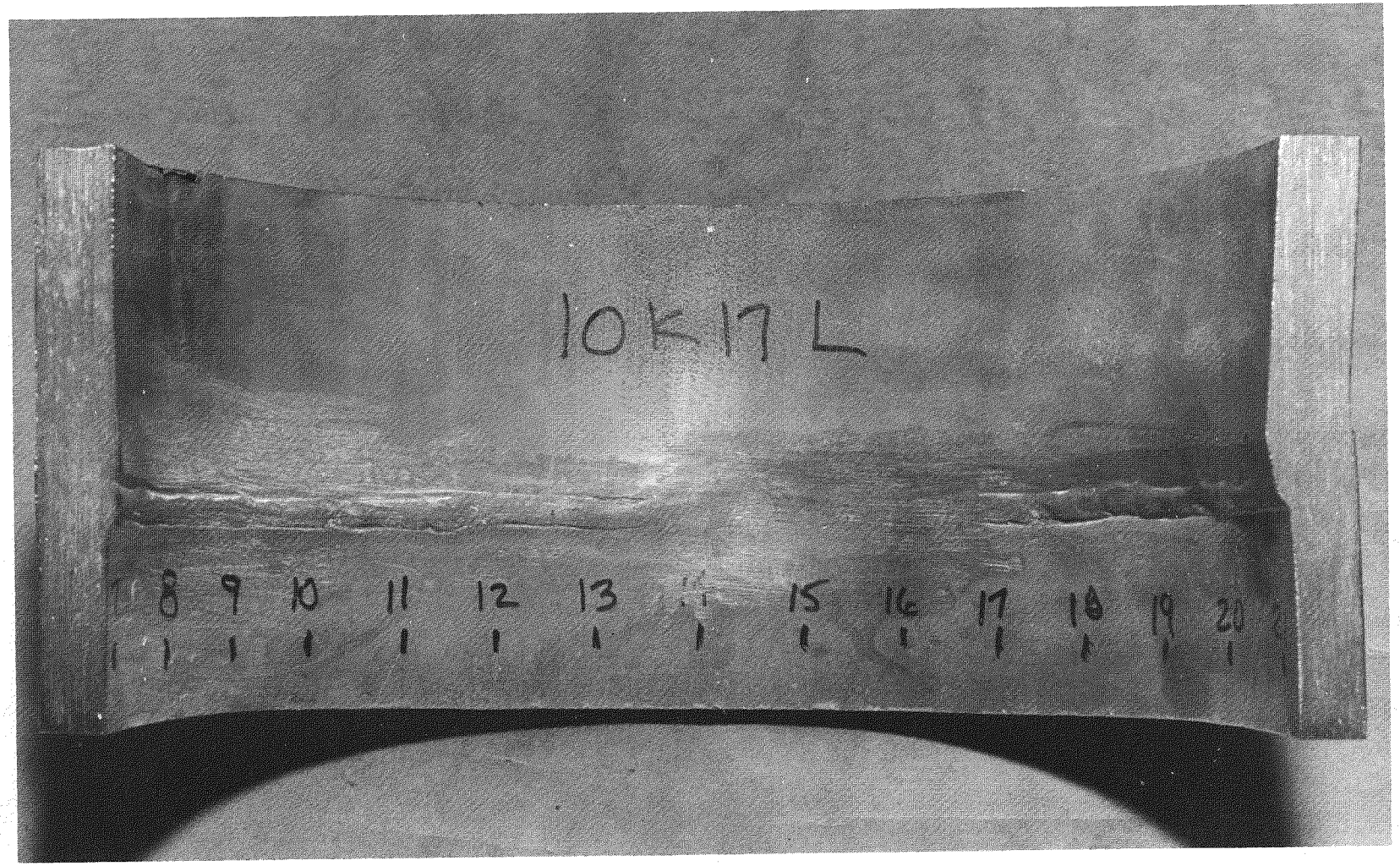


Figure D-19 Inside Surface of 10K17L

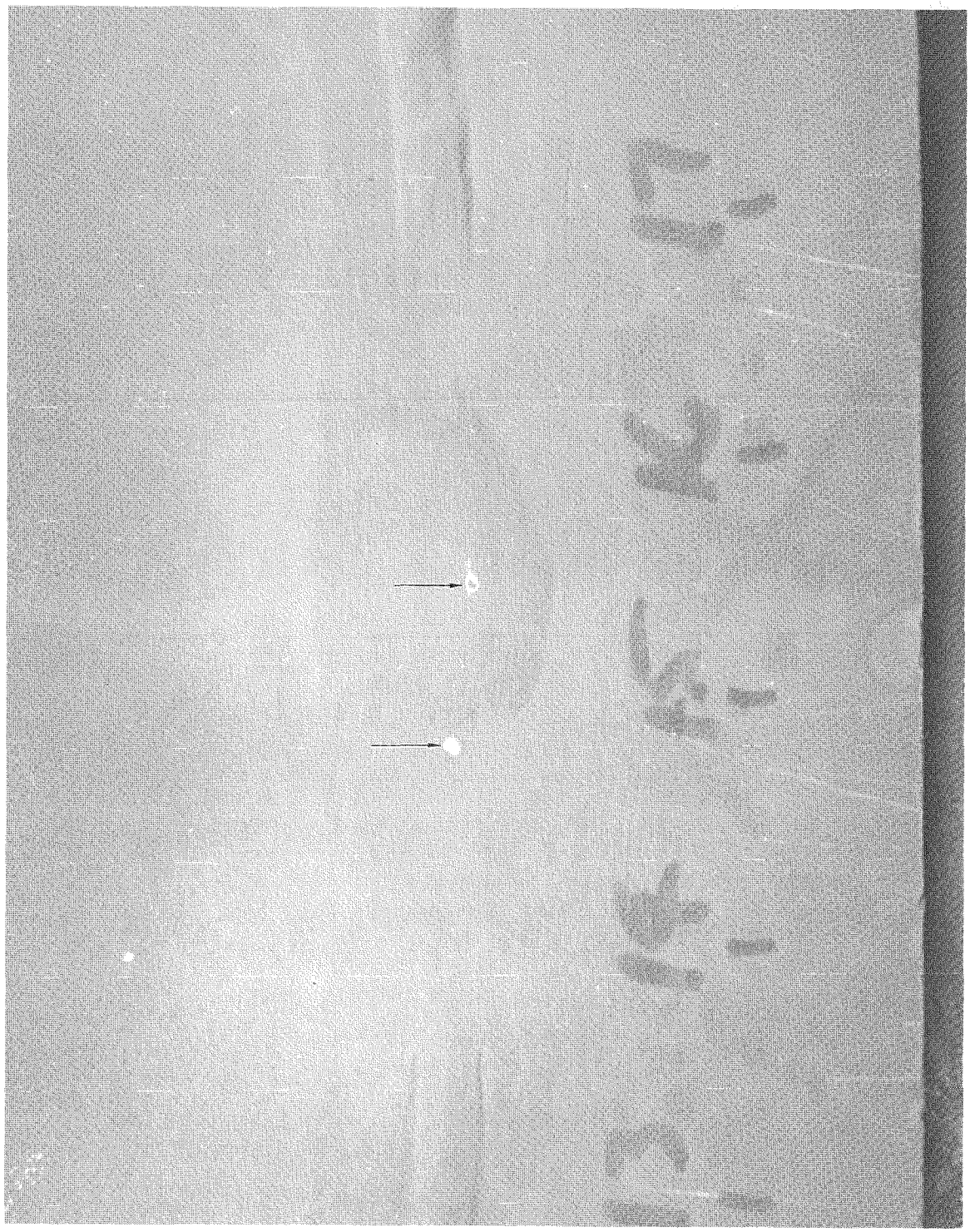

Figure D-20 DPT Indications, 10K17L

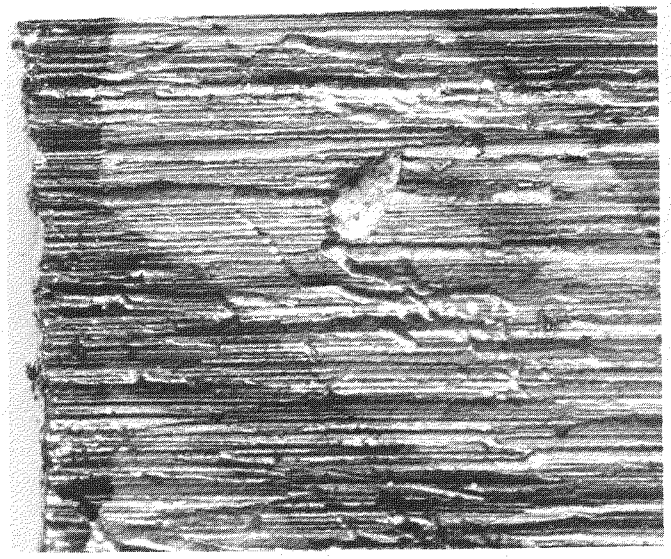

(a) 10K17L PIT AT 14.75 IN. ID, 15X

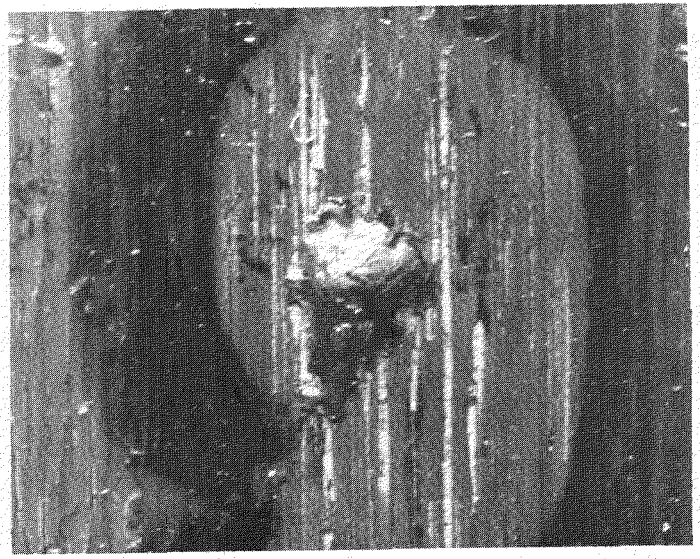

(b) 10K17L SPOT AT 15.5 IN. ID, 15X

Figure D-21 Macrographs of Indications in 10K17L

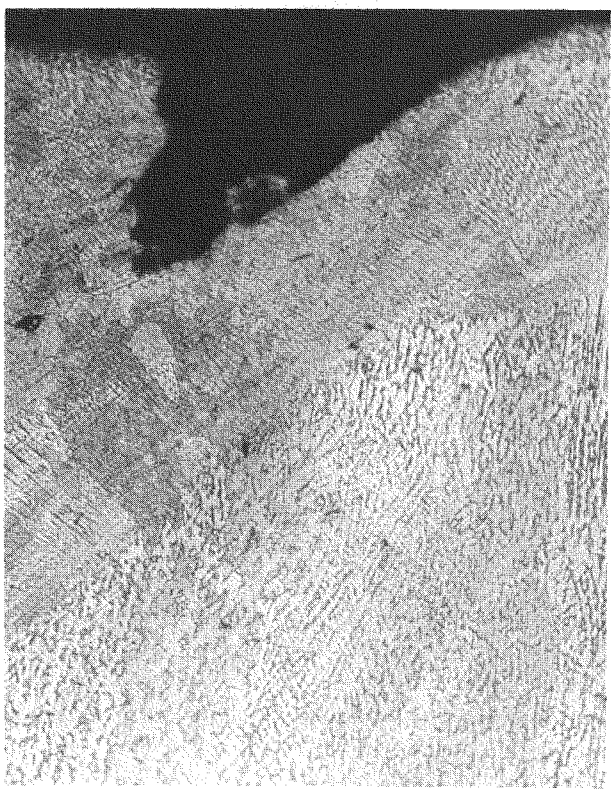

Figure D-22 Macrograph of Section Through Pore at 14.75 in. ID in 10K17L, 100x

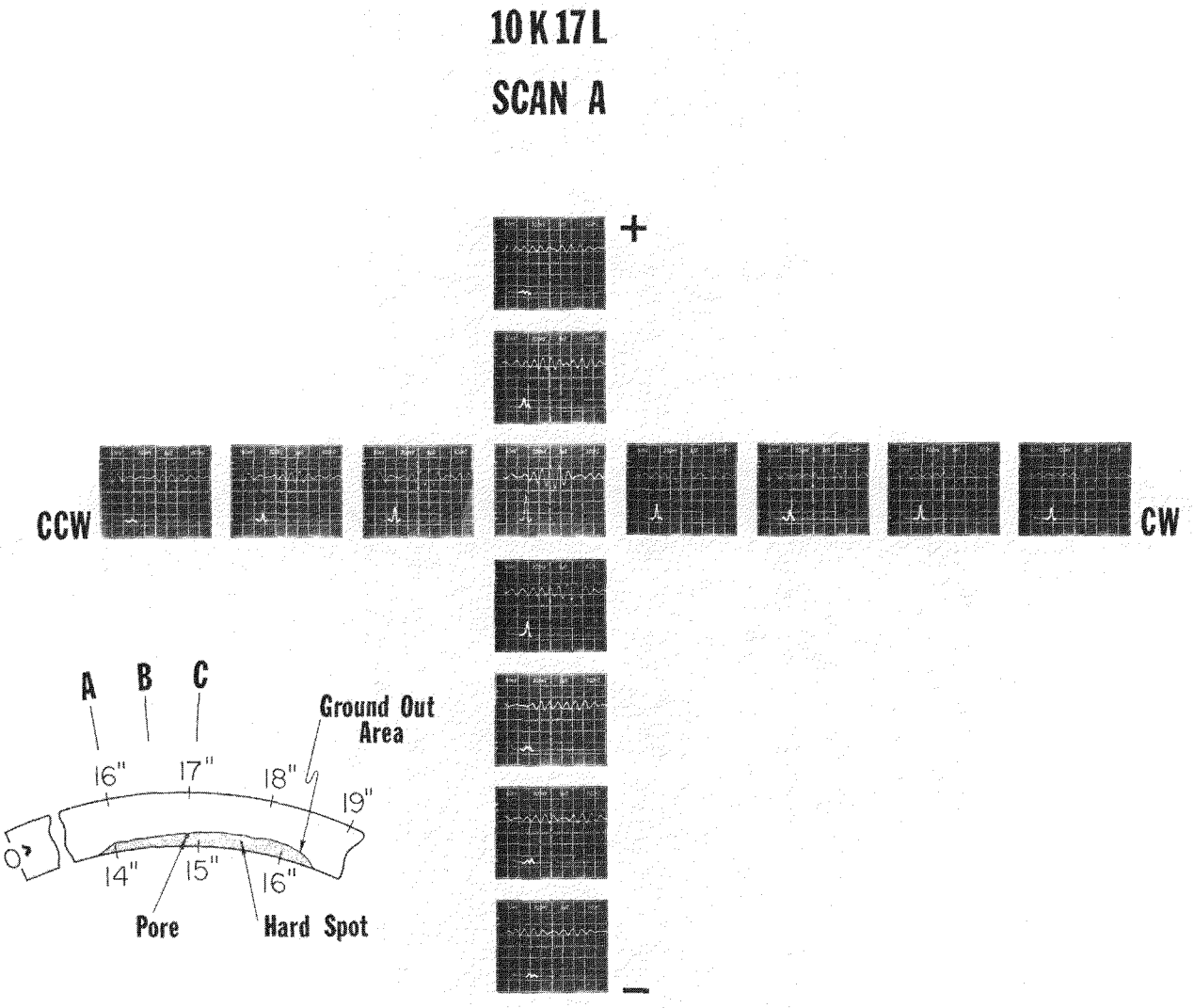


Figure D-23 UT Characterization of 10K17L

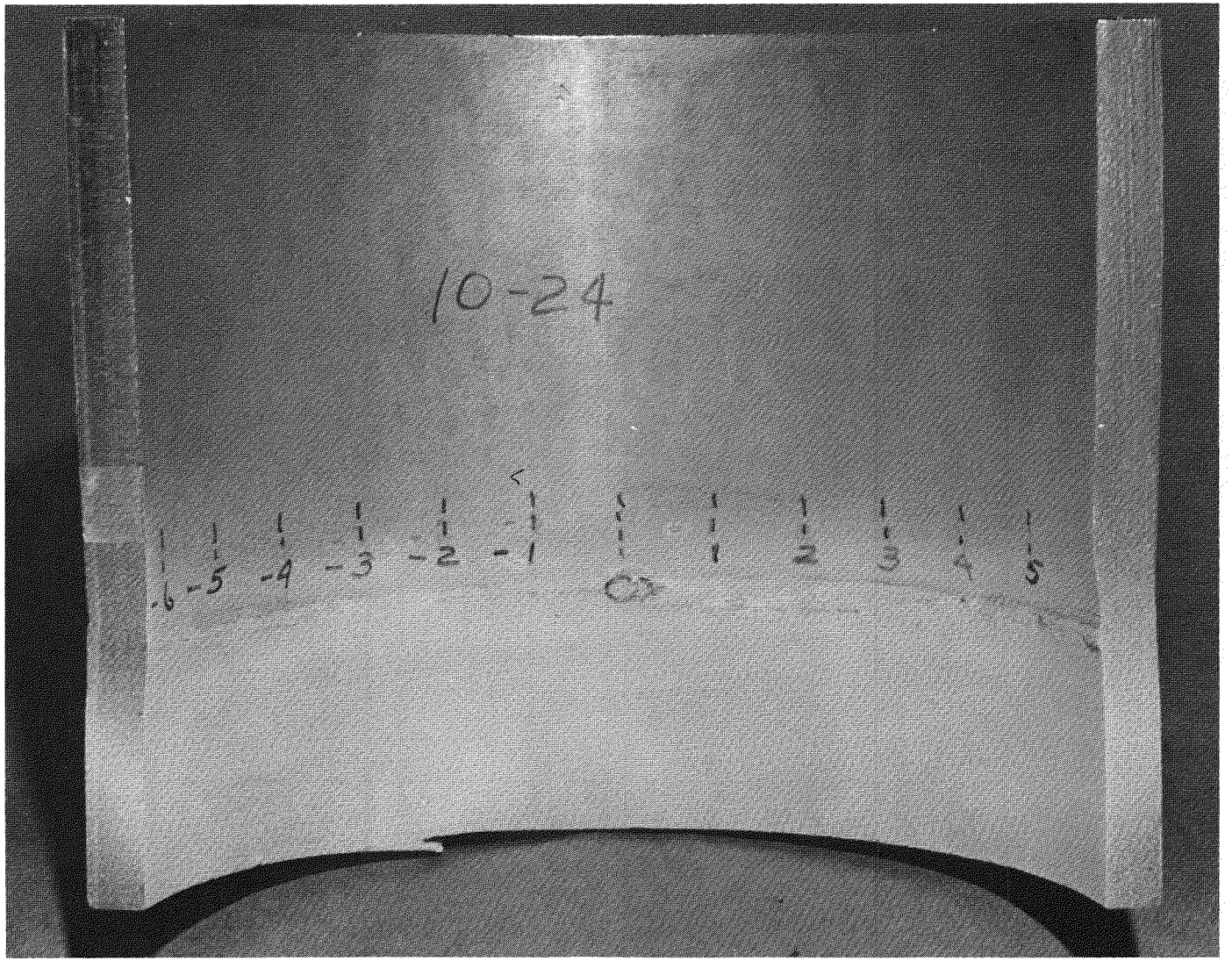


Figure D-25 Inside Surface of 1024A

**ANALYSIS OF ULTRASONIC EXAMINATION**

Organization BCL Program Step _____ Date _____ Operator _____

Recorder _____ Observer _____ Procedure _____ Equipment _____

Transducer I.D. _____ Weld Identification 1024A Start Time _____ End Time _____

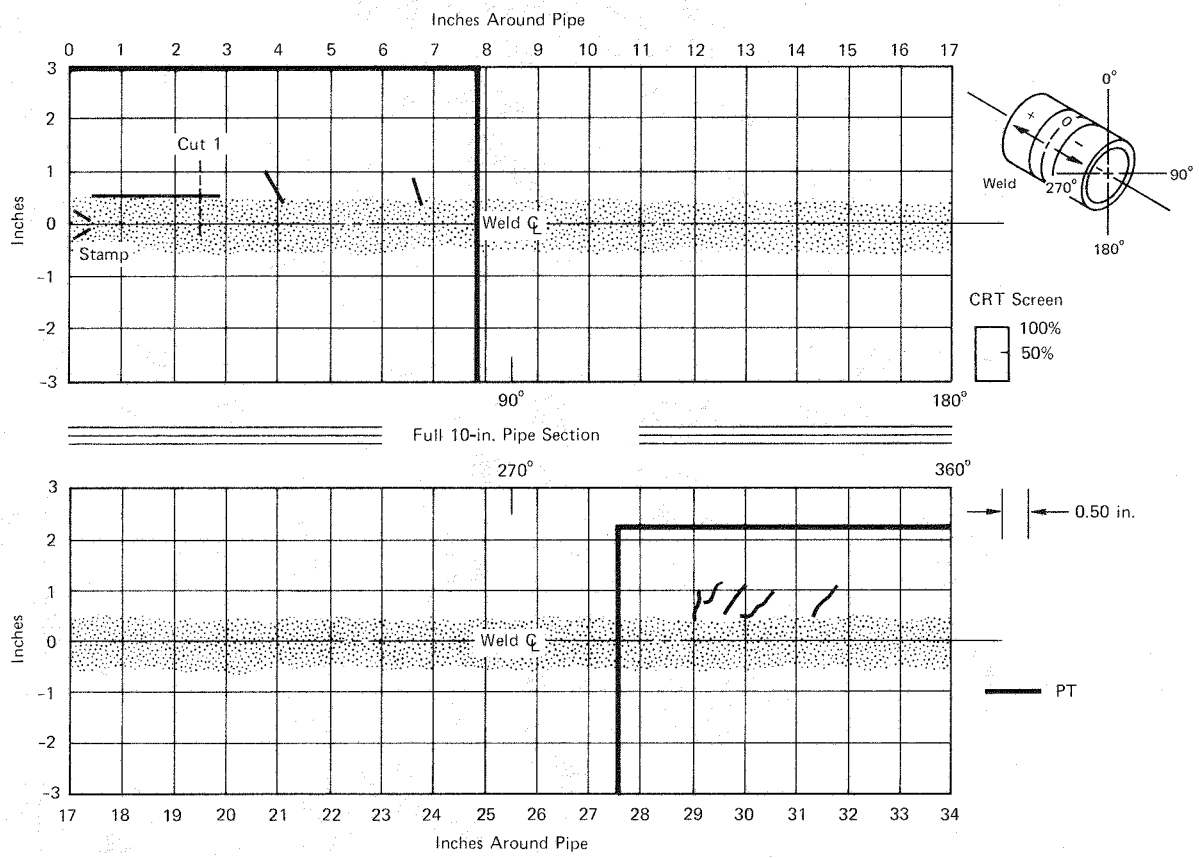


Figure D-24 DPT Results, 1024

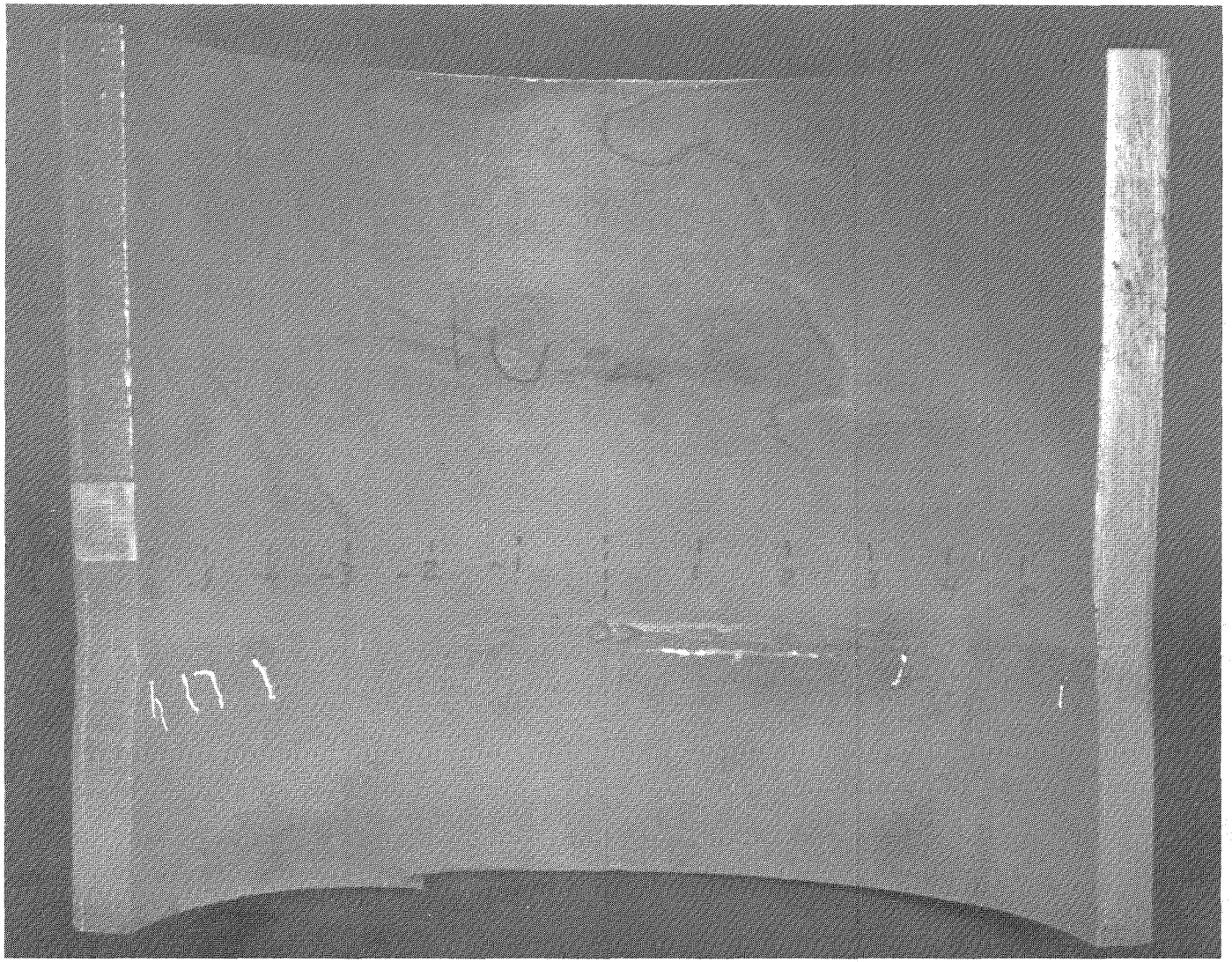

Figure D-26 DPT Indications, 1024A

at +5.5 in. and the circumferential indication at +3 in. not reported previously. Close-up penetrant photographs are shown in figures D-27 and D-28.

The ERG data are rather extensive; for this reason, they are not shown on the Figure D-24 summary sheet but are presented in figures D-29 and D-30.

The ultrasonic response of representative cracks in 1024A is now considered. Two stress corrosion cracks were chosen for detailed ultrasonic signal characterization. These were the large circumferential crack between +0.25 in. and +2.75 in. ID CW and the relatively isolated angled crack at -4 in. ID.

Ultrasonic scans in directions parallel and perpendicular to the weld for the circumferential crack are shown in figures D-31 and D-32. The transverse scanning ultrasonic signal responses, identified as the vertical columns a, b, c, and d, correspond to the locations a, b, c, and d shown on the adjacent view of the pipe cross section. The series of scope traces identified as $c_1$ through $c_9$ were obtained by scanning parallel to the weld; they again correspond to positions $c_1$ through $c_9$ shown on the adjacent sketch of the pipe. The ultrasonic scanning sensitivity was 6 db higher than that used to obtain the initial 1/8-in. SDH DAC curves.

The cross-hatched areas of figures D-31 and D-32 correspond to sections of the pipe which were removed for further metallographic characterization. The dotted areas of the curved pipe cross sections correspond to regions in which penetrant indications were obtained. The lines which bound the dotted regions correspond to the raw ERG data readings; they are drawn to scale.

The broken crack surface shown in Figure D-32 was obtained by breaking the circumferential crack between the approximate OD locations 1.1 in. and 1.8 in. The crack photograph clearly shows the sugarlike texture of the region of intergranular attack. It is important to note that the crack photo is misleading in that the crack appears to run 90% through the wall. However, the entire thickness of the pipe wall is not shown; in reality the crack runs through approximately 65% of the wall. This crack runs circumferentially and is offset from the weld root by approximately 0.1 in. Scanning electron microscope (SEM) photographs of the area of the crack surface identified by an arrow in Figure D-32 are shown in Figure D-33. In Figure D-33, one can identify the region of attack (sugarlike texture) and regions of intergranular weakening from the existence of stress corrosion crack dendrites. Unattacked material exhibits a smoother texture than that shown by the attacked regions. View (b) is an enlargement of view (a) in essentially the same area.

Another view of the circumferential crack sectioned transversely at approximately 1.9 in. OD is shown in Figure D-34. This figure clearly shows the general region of intergranular attack and depleted grain boundaries.

The single angled crack at 31 in. to 32 in. OD (or -4 in. ID on the penetrant photographs) was also characterized ultrasonically. The results of the characterization are shown in Figure D-35. The scanning sensitivity in this case was five times that of the DAC sensitivty. The crack was scanned at 1/16-in. increments in directions parallel and transverse to the crack major axis. This crack is typical of the angled cracks: even though the crack's location and orientation were known from the penetrant, it was somewhat difficult to locate ultrasonically. A circumferential metallographic section through the crack is shown in Figure D-36. The measured depth of the crack is approximately 83% through the wall. This is truly outstanding when one considers the difficulty in trying to isolate these cracks ultrasonically and radiographically.

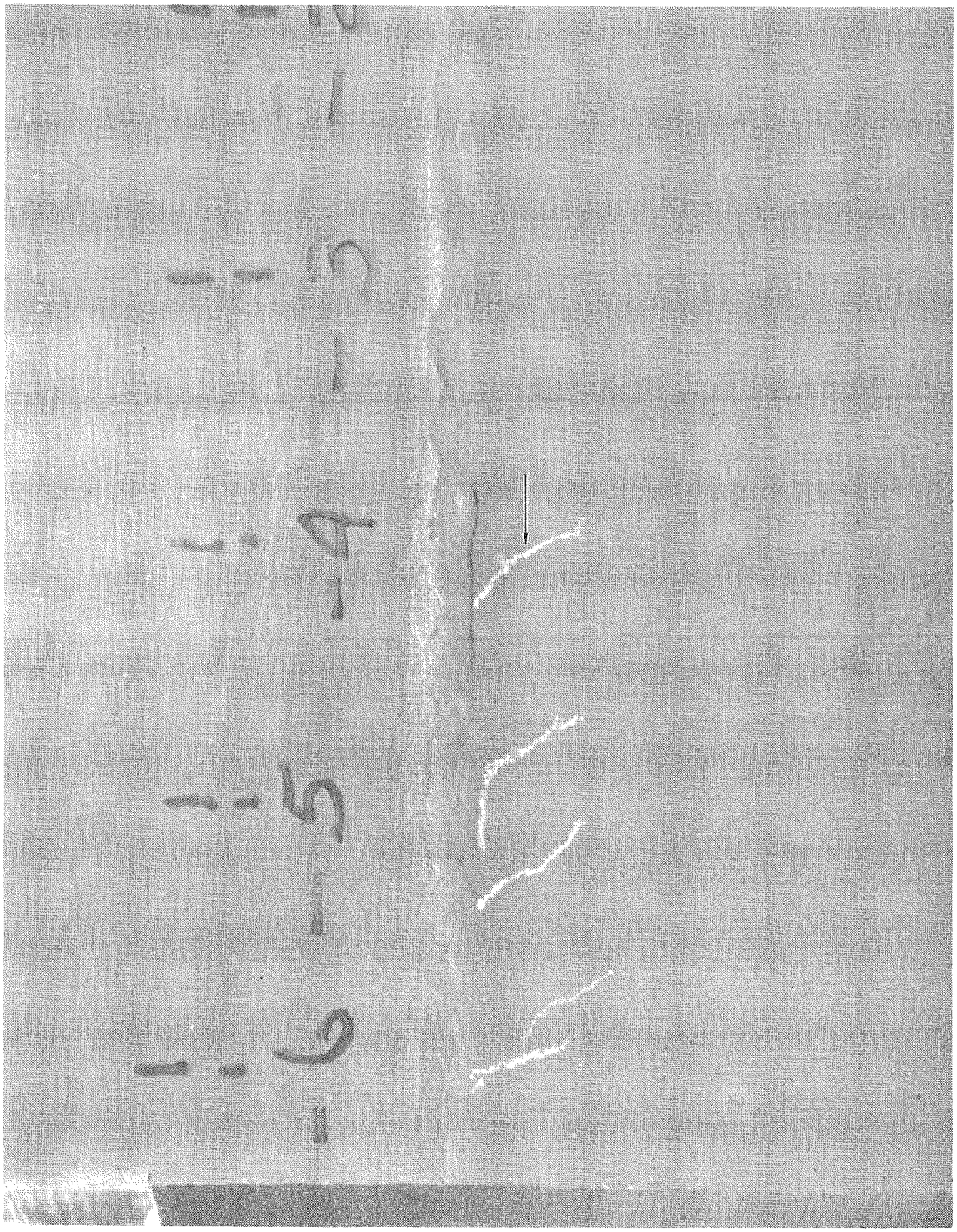

Figure D-27 Skewed DPT Indications, 1024A

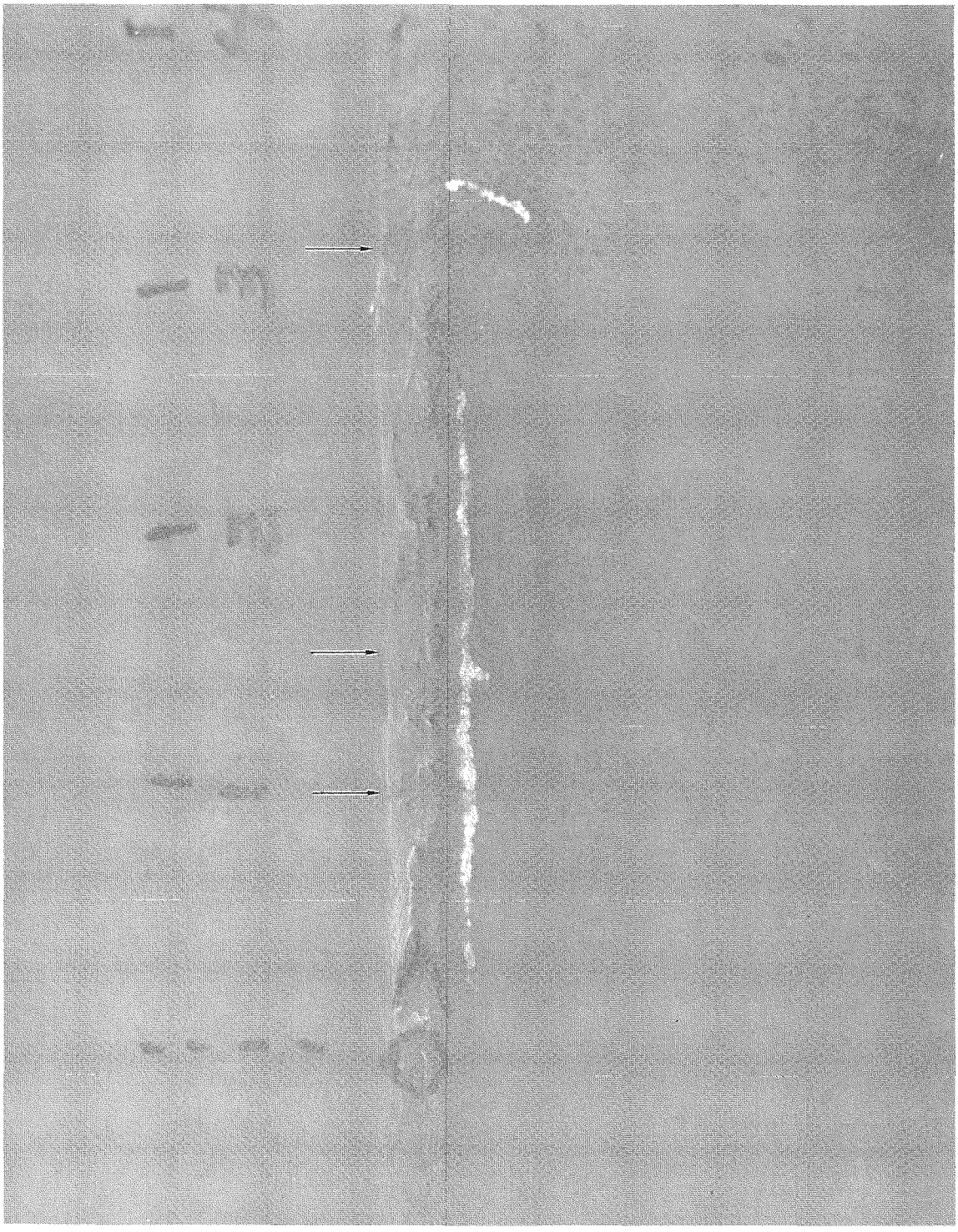

Figure D-28 Radial DPT Indications, 1024A

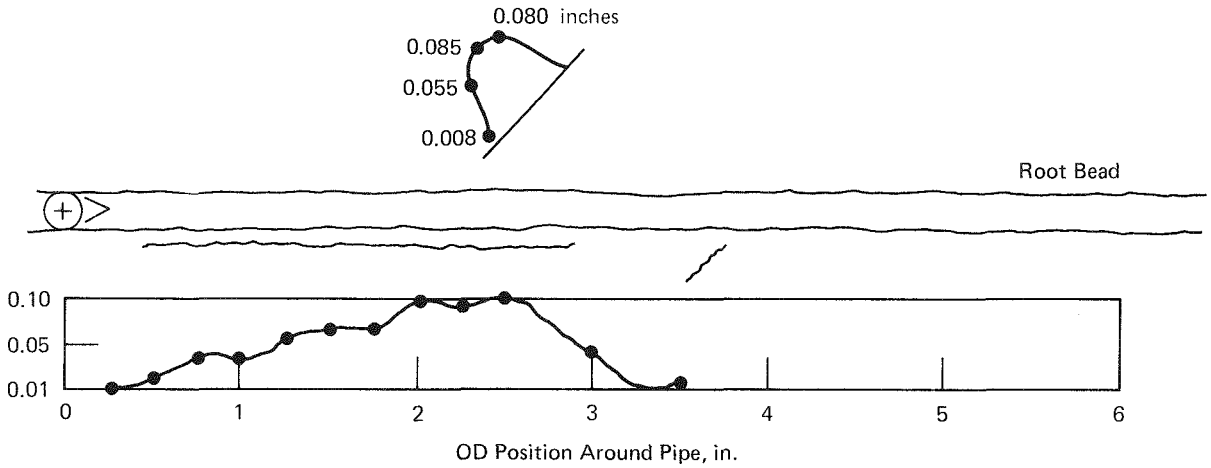


Figure D-29 ERG Data Plots for Cracks in 1024A

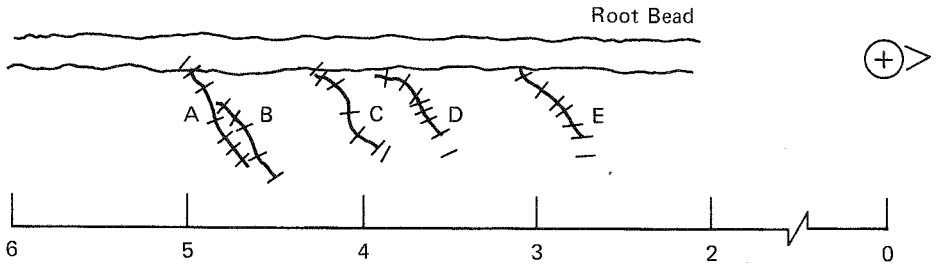


ERG Depth Readings (Top to Bottom)

| A | B | C | D | E |
|---|---|---|---|---|
| 0.010 | 0.070 | 0.000 | 0.020 | 0.020 |
| 0.100 | 0.100 | 0.030 | 0.074 | 0.052 |
| 0.160 | 0.080 | 0.080 | 0.080 | 0.110 |
| 0.130 | 0.030 | 0.090 | 0.080 | 0.080 |
| 0.060 | 0.005 | 0.095 | 0.090 | 0.090 |
| 0.020 | | 0.050 | 0.075 | 0.060 |
| 0.010 | | 0.020 | 0.003 | 0.002 |
| | | | 0.000 | |

Figure D-30 ERG Depth Readings for 1024A Angled Cracks

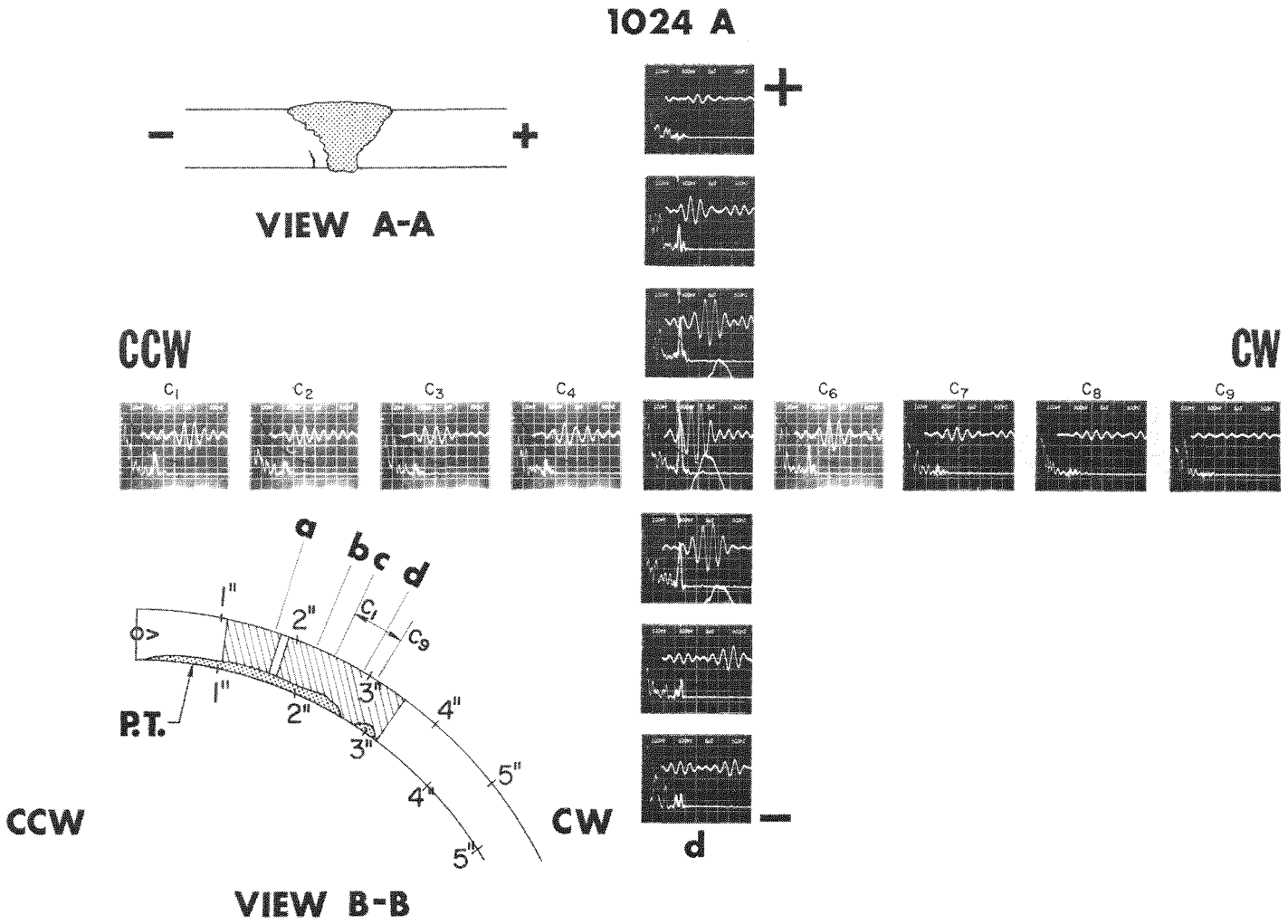


Figure D-31 UT Characterization of 1024A

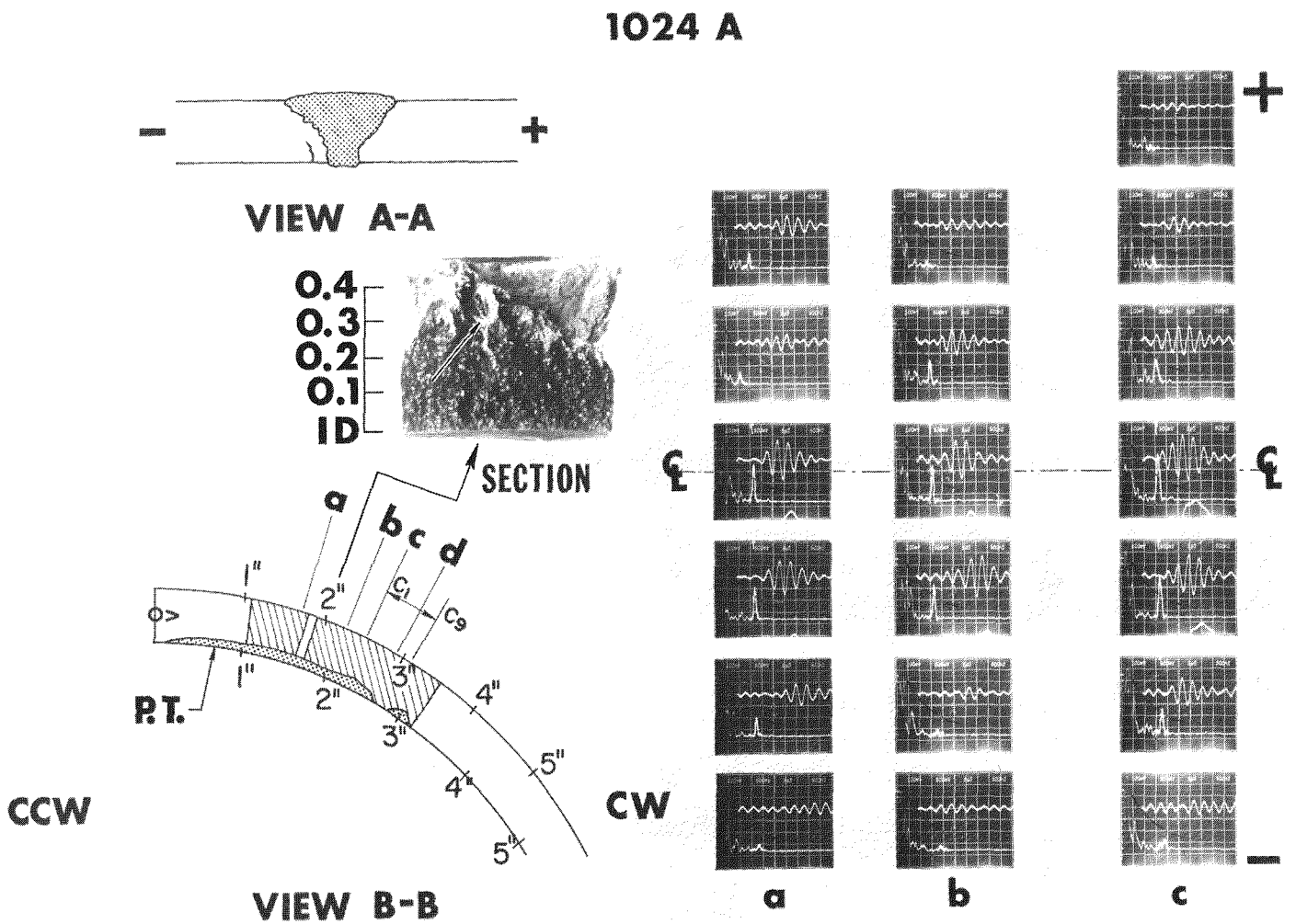


Figure D-32 UT and Metallographic Characterization of 1024A

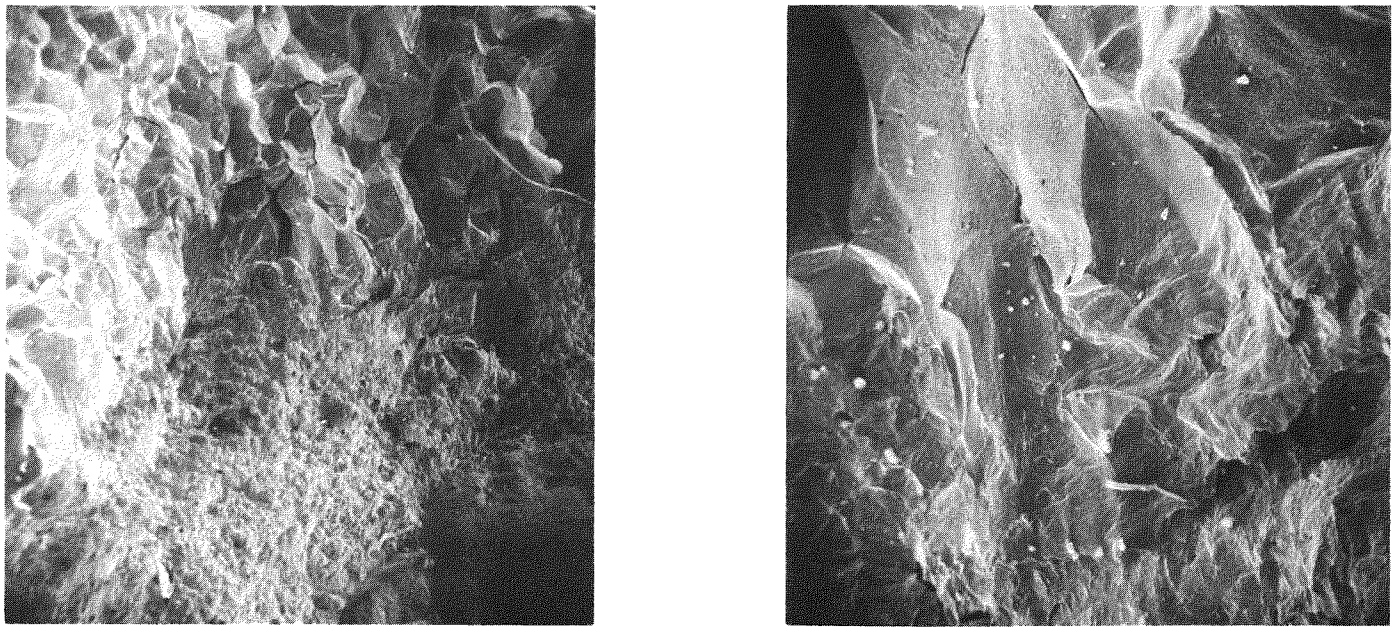

(a) 20x (b) 100x

Figure D-33 SEM Characterization of IGSCC, 1024A

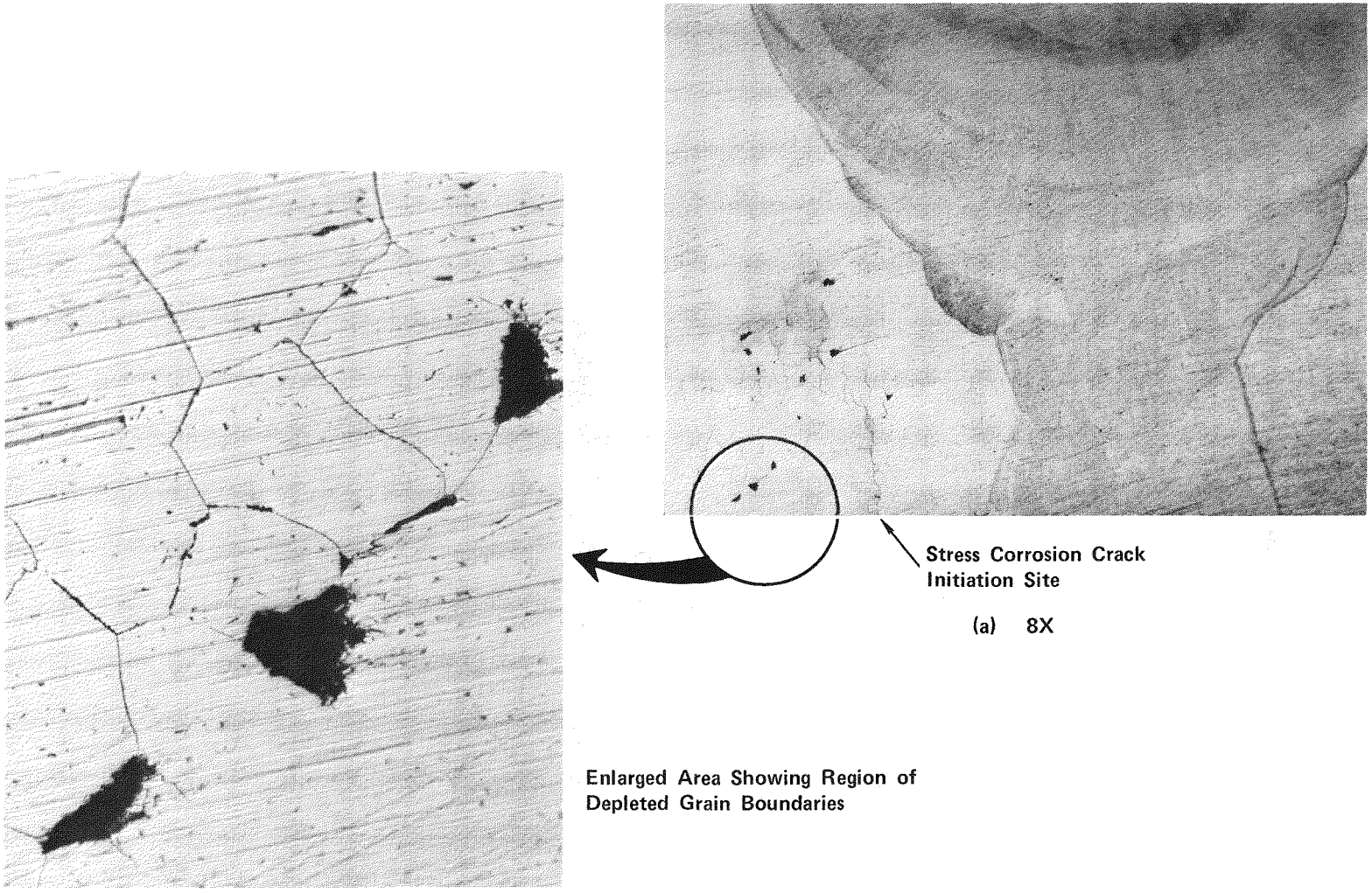


Figure D-34 Sectioned View of IGSCC at 1.9 in., 1024A

# 1024 A

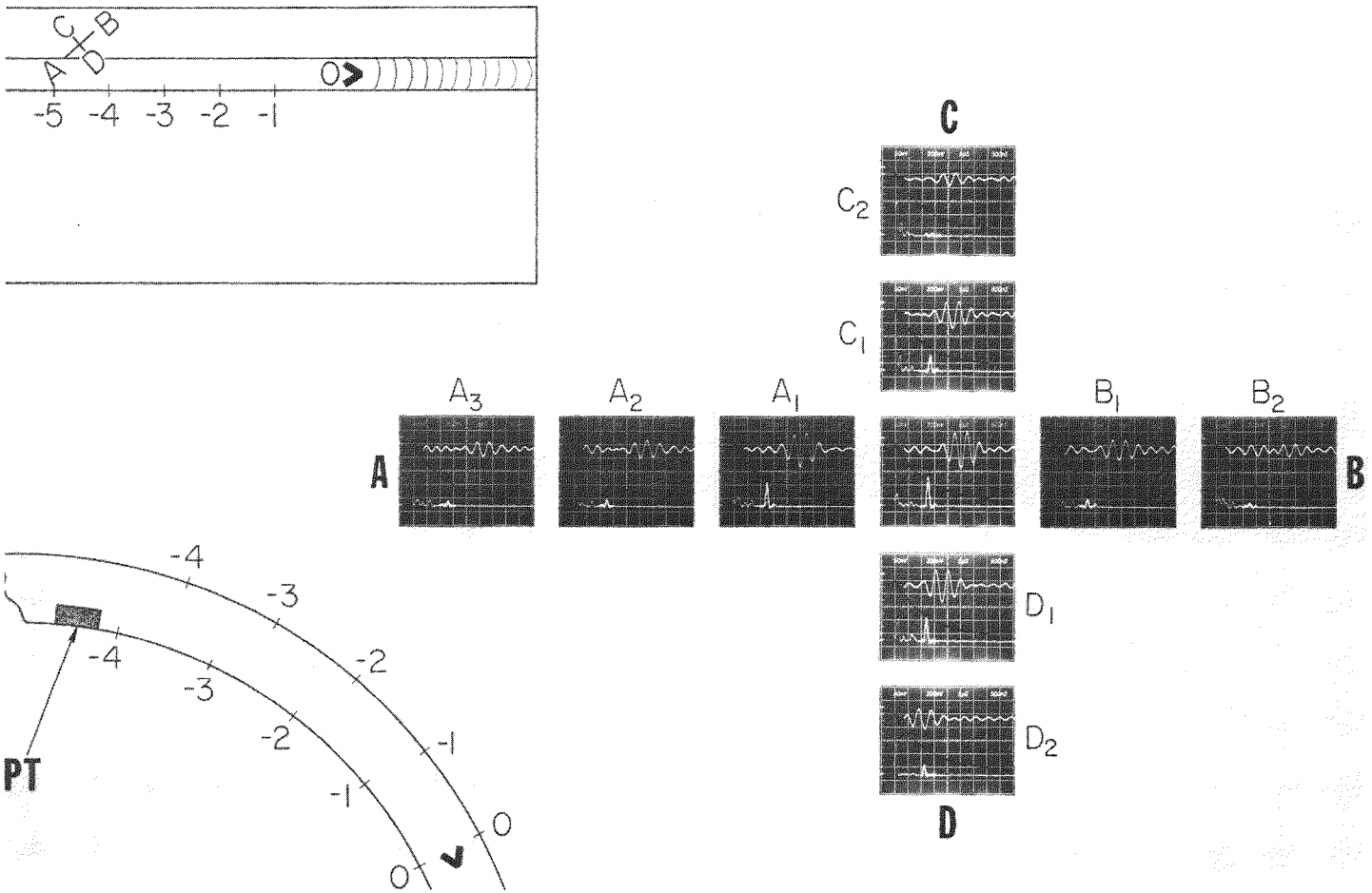


Figure D-35 UT Characterization of Angled Crack, 1024A

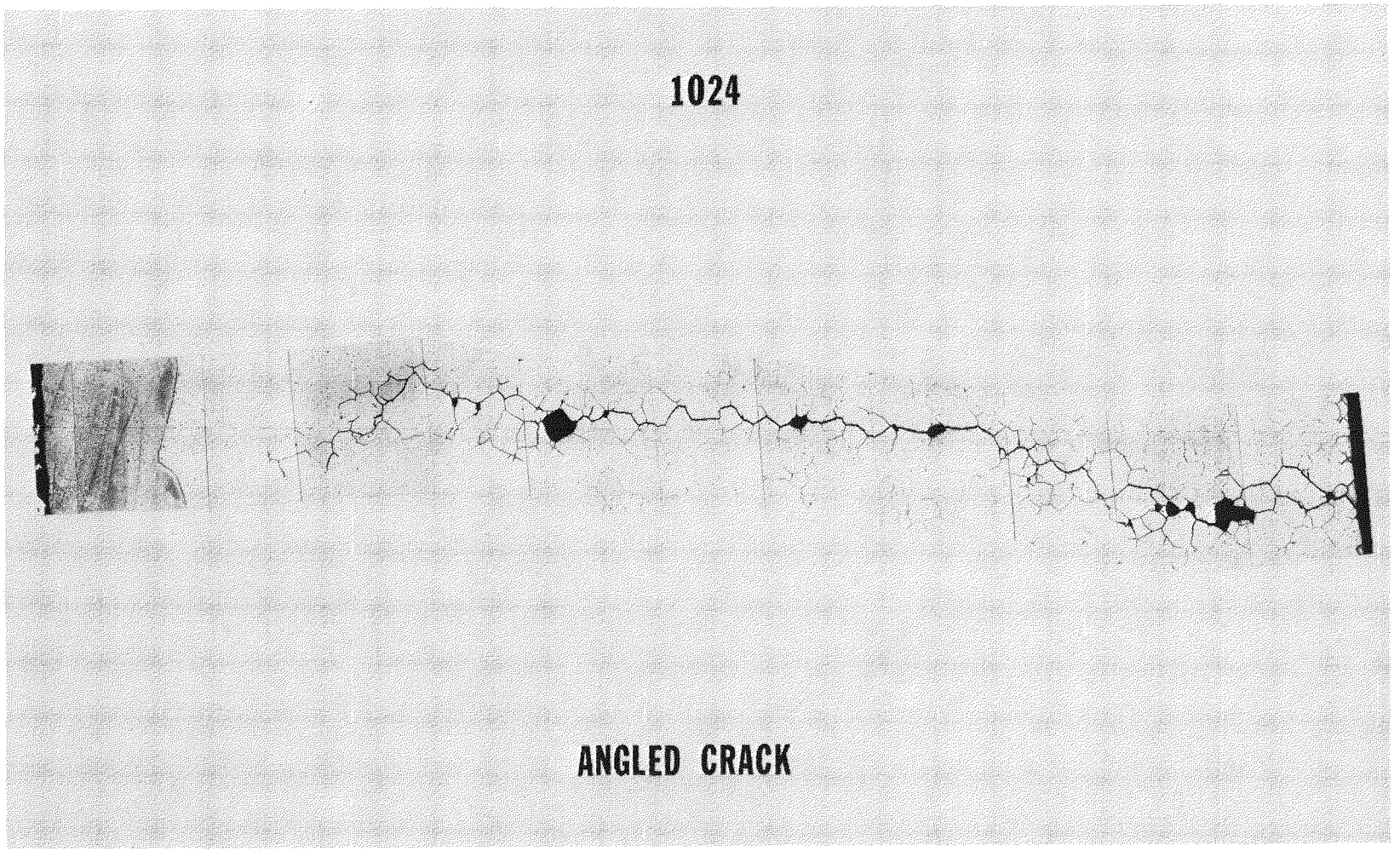


Figure D-36 Metallographic Section Through Angled Crack, 1024A

10K18

10K18 is another interesting specimen (Figure D-37). A general view of the pipe ID is shown in Figure D-38. Penetrant testing of the specimen was quite revealing; a photograph of the most prominent indications is also shown in Figure D-39. This pipe half was penetrant tested at the end which cuts through the linear indication, with the result shown in Figure D-40, where a faint linear indication can be seen at the root of the weld. This same area was metallographically examined; the resultant micrographs are shown in Figure D-41. The upper photograph clearly shows the weld metal/base metal area with lack of fusion between the two regions. An enlargement of this same area is shown in the lower photograph. It shows that the LOF has been partially filled with an oxide material. This LOF measures approximately 0.022 inches in depth.

An additional region of interest as a result of the EPRI round robin was the area at approximately 28 in. OD. This area was characterized ultrasonically, with the results shown in Figure D-42. The origin of the scan pattern was 28 in. OD, with scanning done at 1/16-in. increments parallel and transverse to the weld. The ultrasonic scanning sensitivity shown in Figure D-42 is at the DAC sensitivity. This figure also shows the extent of a penetrant indication obtained in this area, as well as micrographs of a section made through the pipe at 27.1 in. OD. Enlargements of these photomicrographs also show an apparent oxide coating partially filling the LOF.

19BL

19BL is an infamous specimen in that it was the source of several rather strong ultrasonic indications, yet neither penetrant nor radiography shows the presence of any material discontinuities. The specimen represents a shop-fabricated weld with the overall surfaces in excellent condition for field ultrasonic testing. A general ID view of the pipe is shown in Figure D-43. Previous ultrasonic characterization had identified some "geometrical" reflectors, but based on the condition of the weld (ground), the basis for this conclusion is ill founded.

Two of the round robin areas of interest--5 in. OD and 30-3/4 in. OD--were characterized ultrasonically in some detail. Figure D-44 presents the ultrasonic scope traces for the area at 5 in. OD, whereas Figure D-45 presents the results for the region at 30-3/4 in. OD. Scanning was done at the normal DAC sensitivity, and the reflectors were rather easy to locate. An analysis of the ultrasonic echo dynamics indicates that both discontinuities tend to lie in a horizontal plane. The region at 30-3/4 in. OD was carefully sectioned, with no discontinuity whatsoever being identified. In viewing the macrograph of the sectioned area there is evidence of rather extensive "buttering." Thus, the most probable nature of the unidentified discontinuity is a LOF existing in a horizontal plane as a result of the multipass weld procedure.

Remaining Specimens

No discontinuities were identified in the remaining 10-in. diameter specimens using visual, fluorescent penetrant, and radiographic techniques. Thus no additional ultrasonic characterization was performed. The remaining specimens, 1028C, 1019A, 10K16, 10K17, and 1020A, were all field welds. The surface condition of

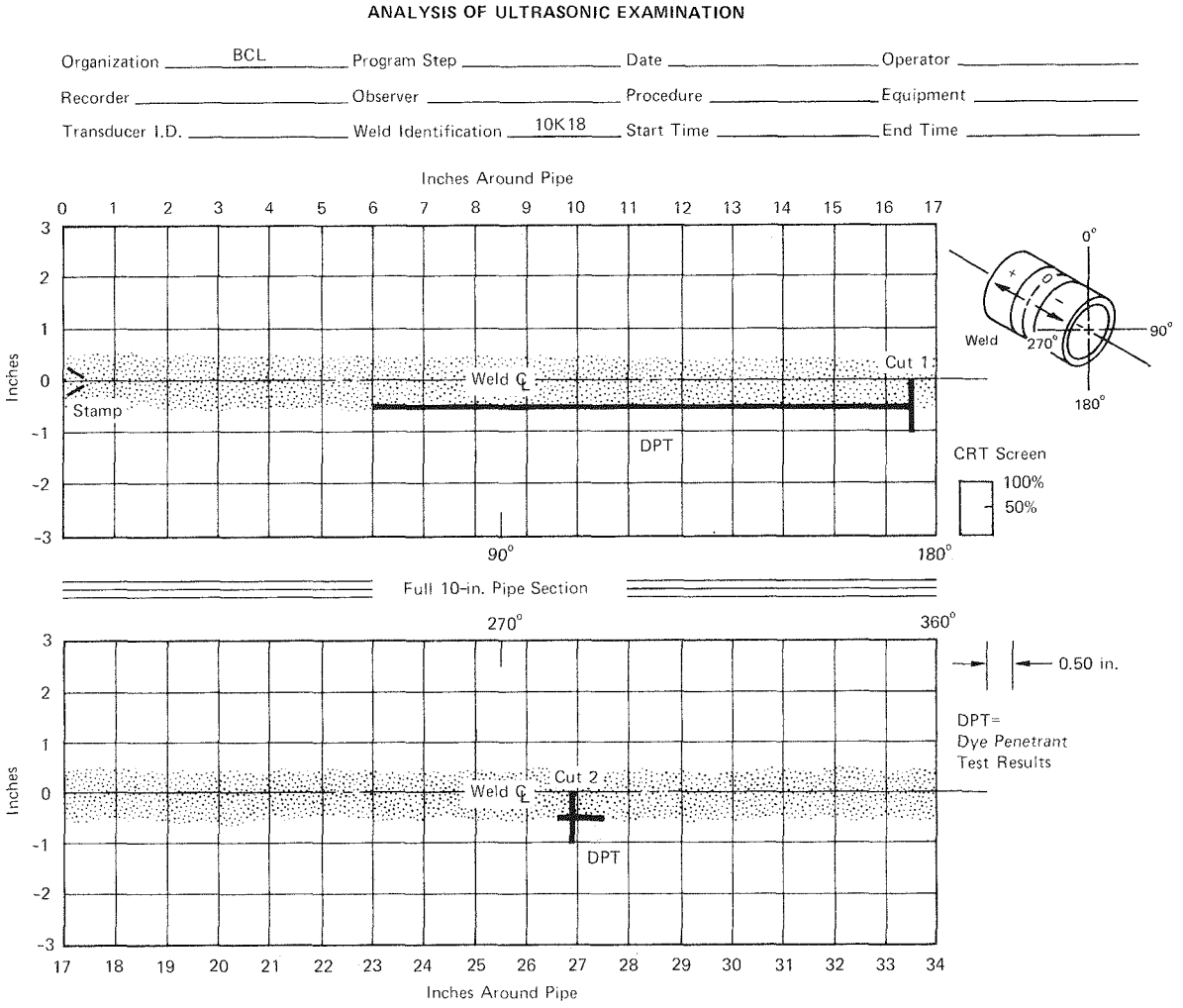


Figure D-37 DPT Characterization of Sample 10K18

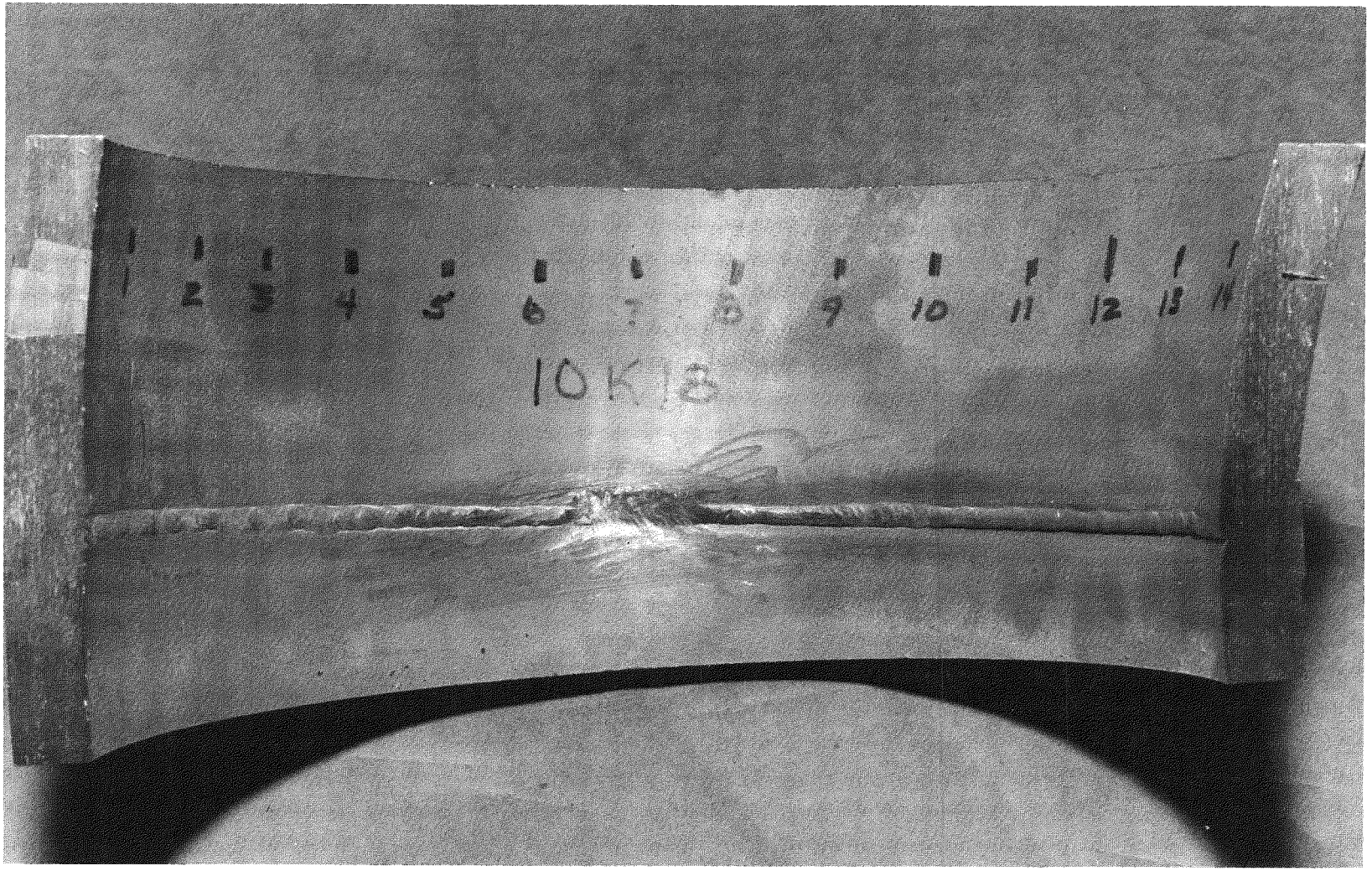


Figure D-38 Inside Surface, 10K18

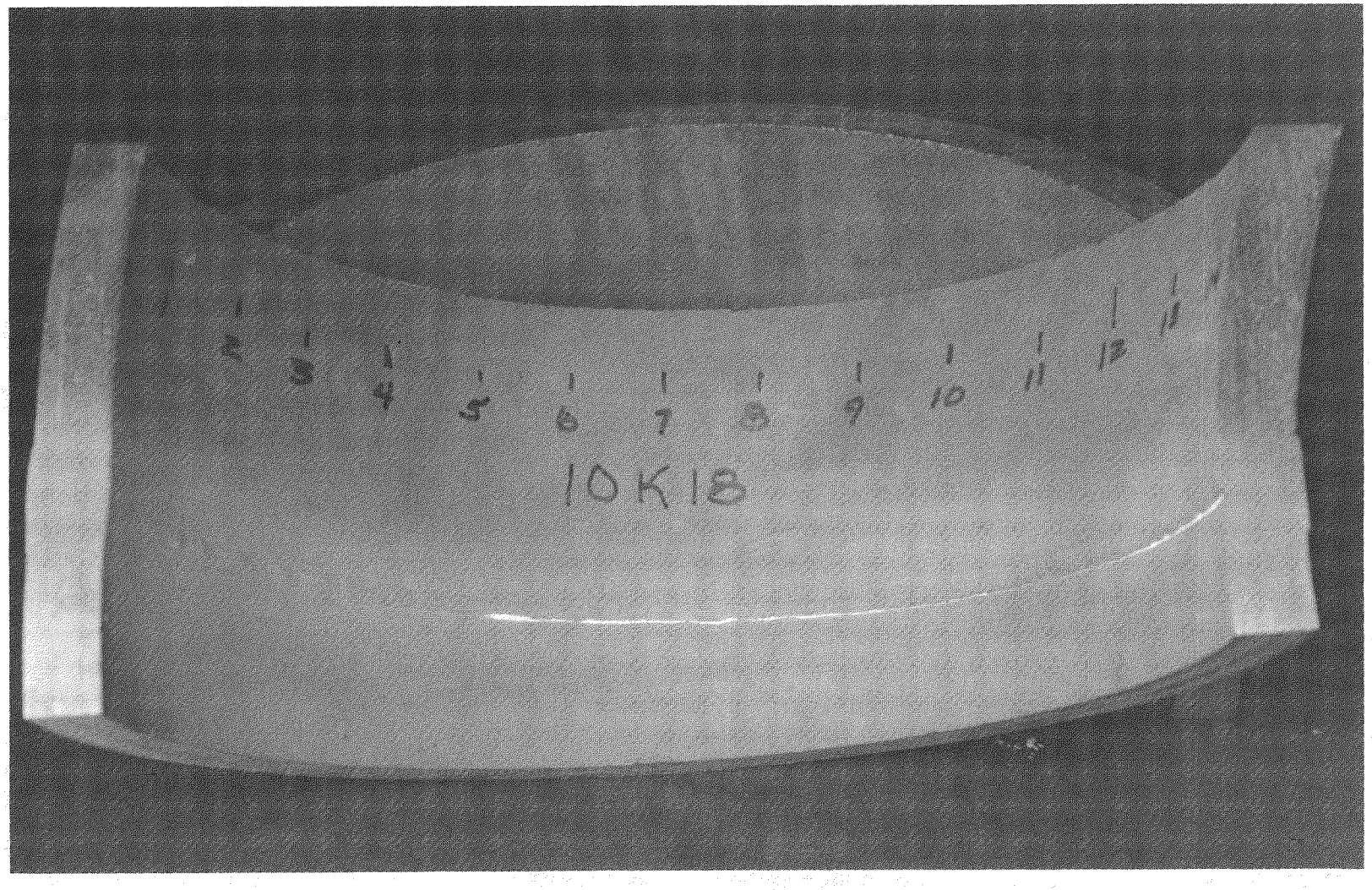


Figure D-39 DPT Results, 10K18

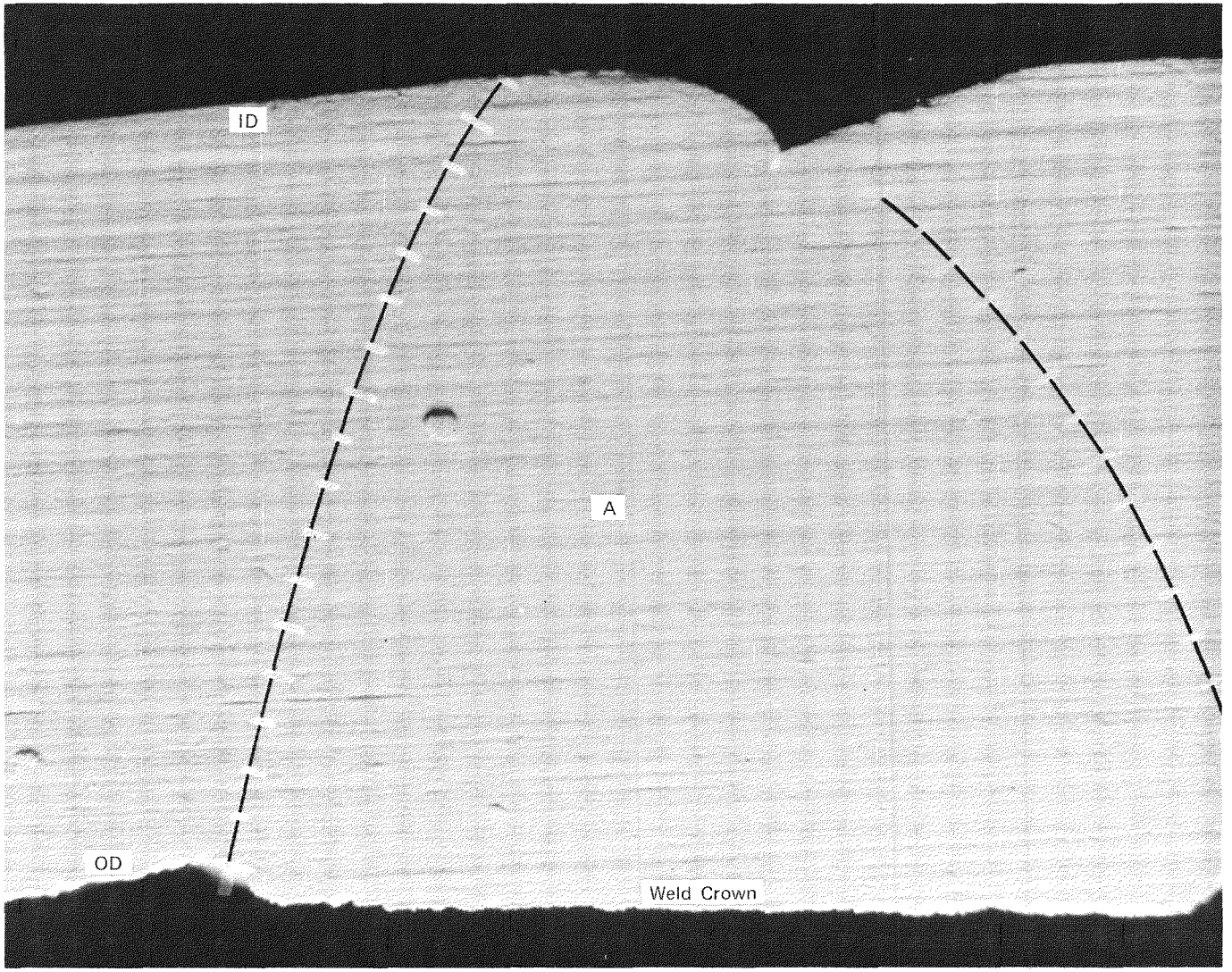


Figure D-40 DPT Results from Cross Section of 10K18

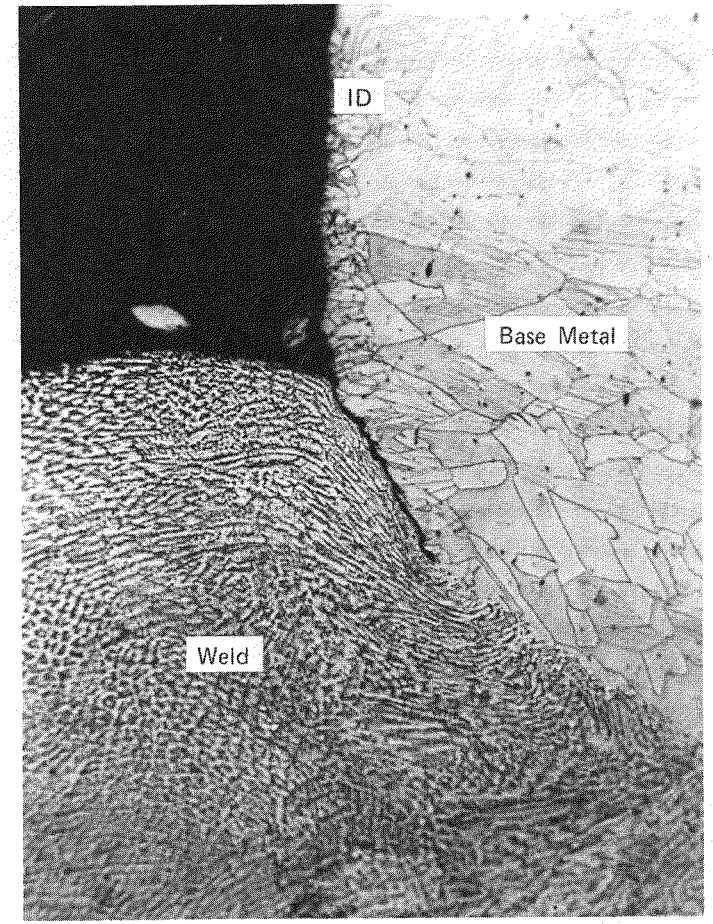


(a) 50X

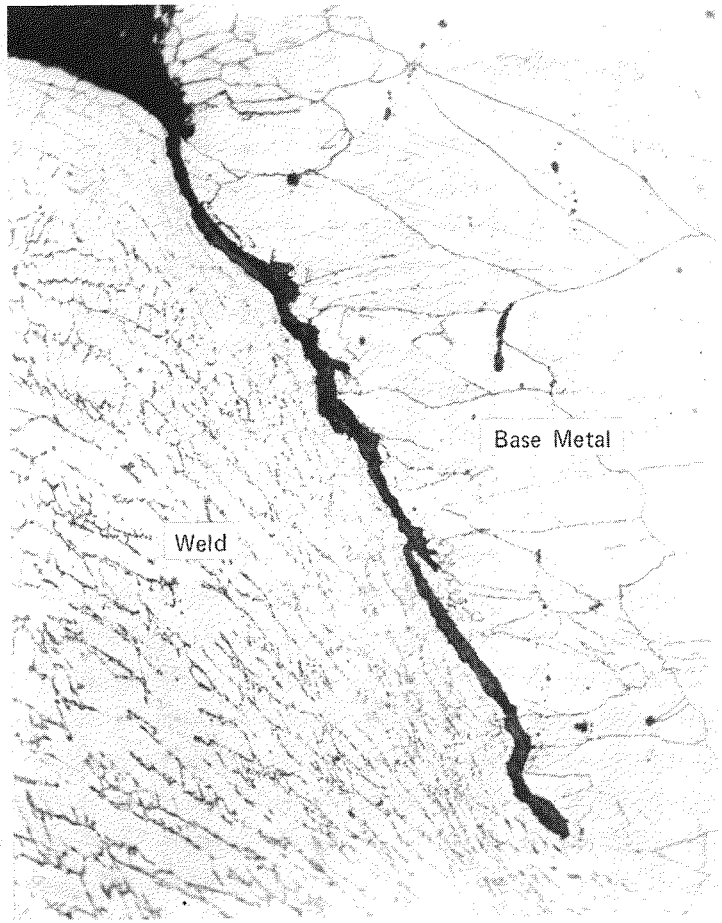


(b) 200X

Figure D-41 Micrographs of Section Through 10K18 at 15.5 in. ID, Showing Lack of Fusion

# 10K18

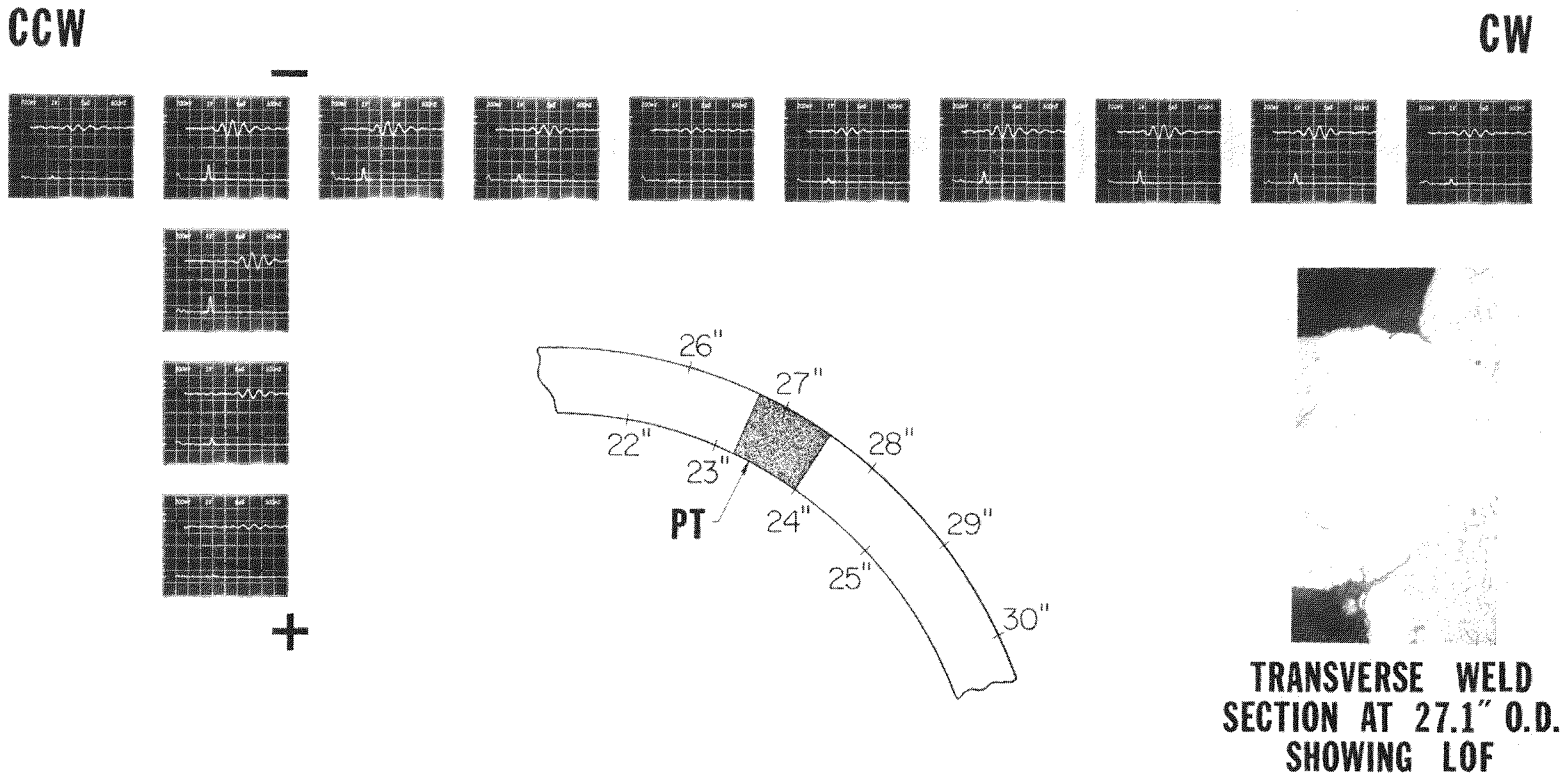


Figure D-42 Ultrasonic Characterization of 10K18


Figure D-43 Inside Surface of 19BL

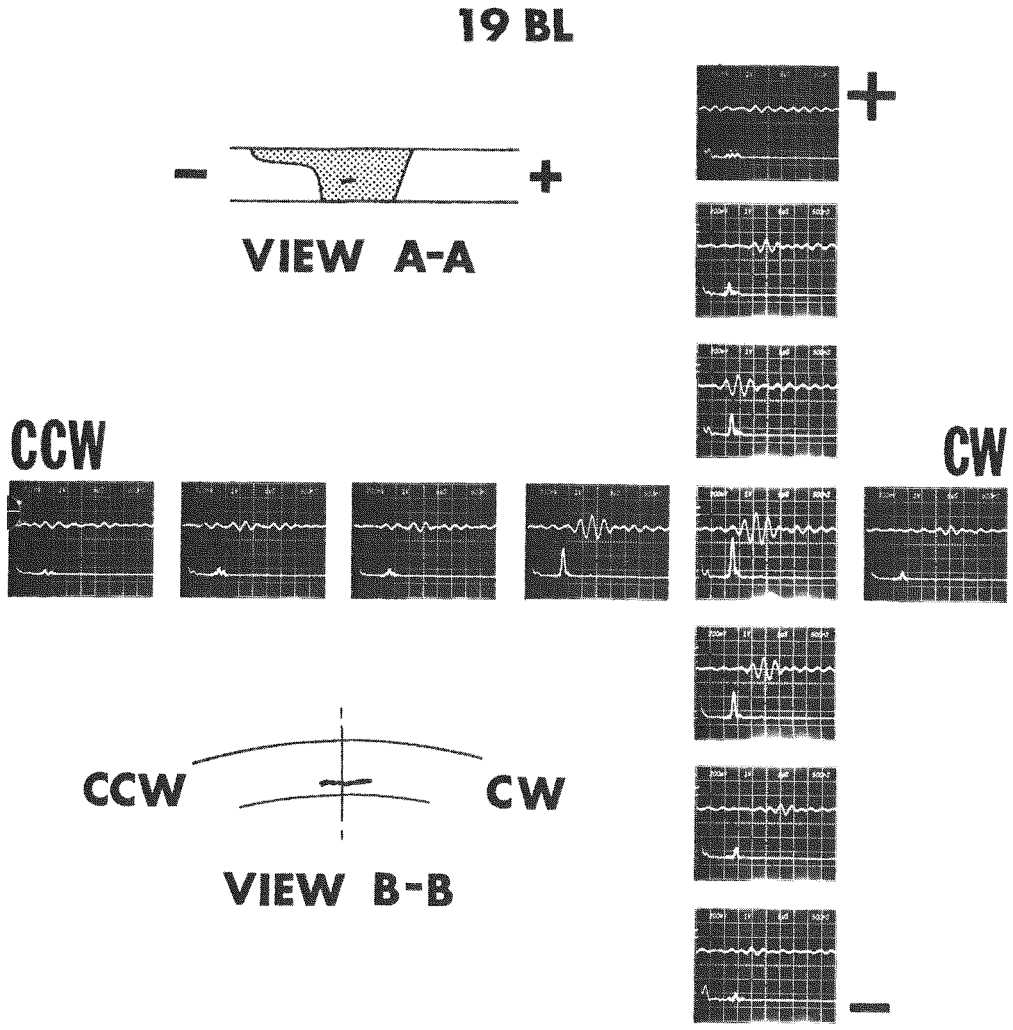


Figure D-44 UT Characterization of 19BL at 5 in. OD Location

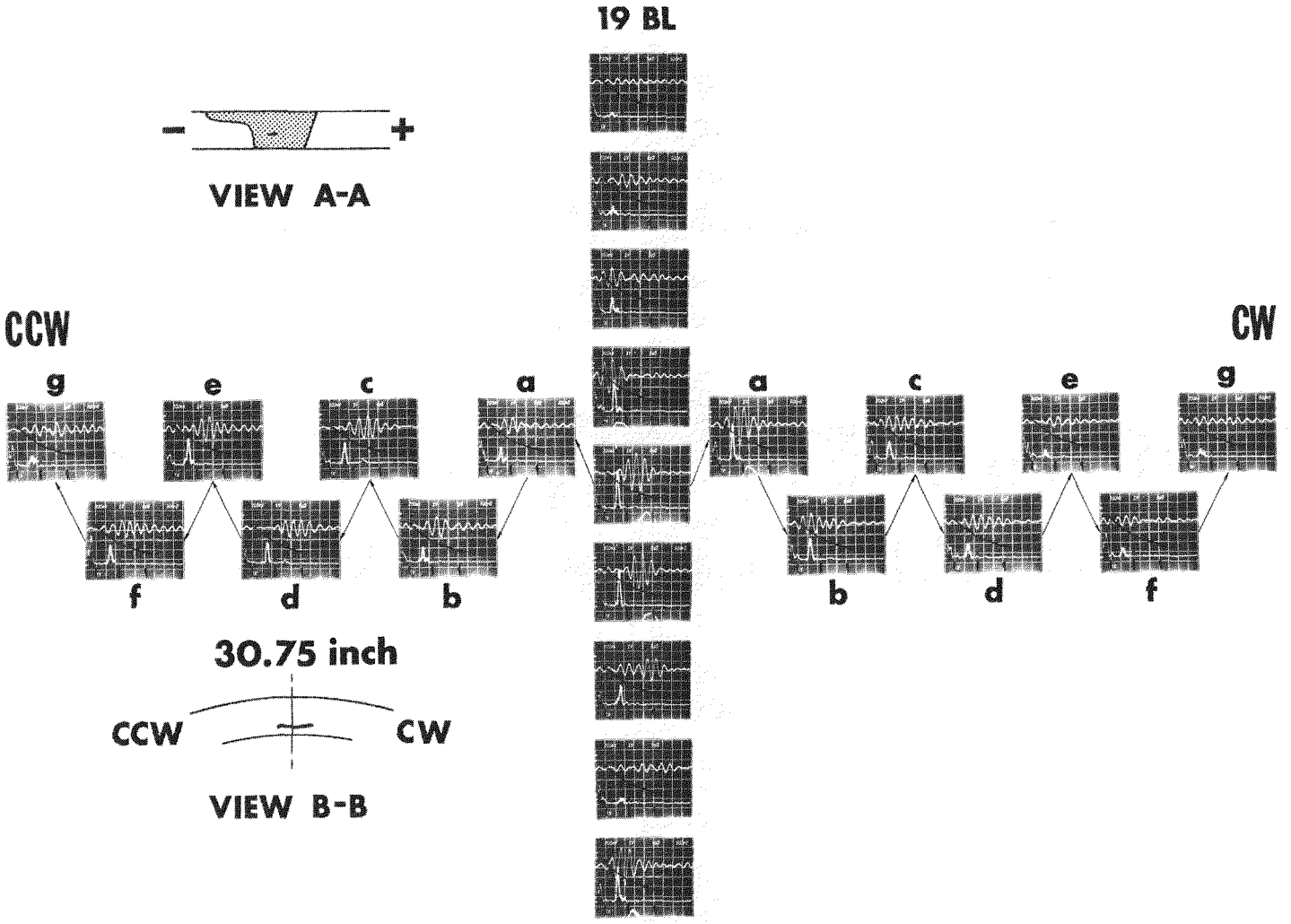


Figure D-45 UT Characterization of Specimen 19BL at OD Location of 30-3/4 in.

the specimens was in general fair, although in some instances excessive internal scale made fluorescent penetrant testing difficult. Figure D-46 shows the ID surface of 1020A, with an excessive scaling condition.

GENERAL OBSERVATIONS

Visual examination of the pipe samples shows very little evidence of a counterbore region. There were, however, many samples which exhibited a mismatch condition in the joined pipe sections. This condition would tend to compound the ultrasonic inspection of the weld joint areas by introducing a natural corner or edge reflector.

The penetrant testing was considered to be the most reliable indicator of a surface-connected discontinuity. After descaling of the pipes, the penetrant test was performed with relative ease. In some instances, however, specimens contained a scale condition on the ID surface in the vicinity of the weld which made the application of the emulsifier and subsequent cleanup somewhat tedious.

ERG data are difficult to use in accurately estimating the depth of stress corrosion cracks for several reasons. For short cracks (those less than approximately 0.5 in.), leakage currents will in general exist. These lower the effective resistivity of the material, resulting in an underestimation of the true crack depth. Also, the general nature of the stress corrosion crack introduces an additional underestimation. The somewhat diffuse or intergranular nature of the crack allows for additional current leakage.

The low sensitivity of radiography to stress corrosion cracks was demonstrated quite dramatically in this series of specimens. The jagged nature of the cracks and their intimate proximity between highly intertwined surfaces leaves only very small net density differences for X-ray techniques to detect. Although test samples were rotated in an attempt to maximize net radiation differences through the test parts, the location and extent of the cracks were difficult to assess confidently. This was especially true with the angled cracks in 1024A. The cracks in 19AL and 1028A were easily seen, as was the long crack in 1024A. Lack of fusion in test parts could also be seen in cases in which it progressed for more than an inch or so.

Ultrasonics showed the same low sensitivity to the angled cracks in 1024A as radiography. The reason for this, however, is quite different. The compound curvature of the pipe tends to degrade the effective coupling between the flat transducer and curved pipe. Thus rotation of the transducer degrades its sensitivity even to reflectors which are oriented in an ideal direction. The sensitivity to small reflectors (such as the cases of lack of fusion) was surprisingly high. The ultrasonic signals received from an 1/8-in. SHD, most of the large crack in 1024A, the lack of fusion in 10K18, and the unfound reflector in 19BL all had the same amplitude to within + 20%. Yet the amplitude from the angled crack in 1024A was only one-fifth as high as the others. Based solely on the results derived from 1024A and 10K18, this suggests that the response from a coherent reflector such as a lack of fusion may be 25 times greater than that obtained from an IGSCC. This is not surprising, due to the vastly different nature of the respective reflectors. The lack of fusion is localized to a single plane which serves to reflect the ultrasound in a coherent, nondistorted manner. The IGSCC, on the other hand, tends to scatter the reflected signal in a random

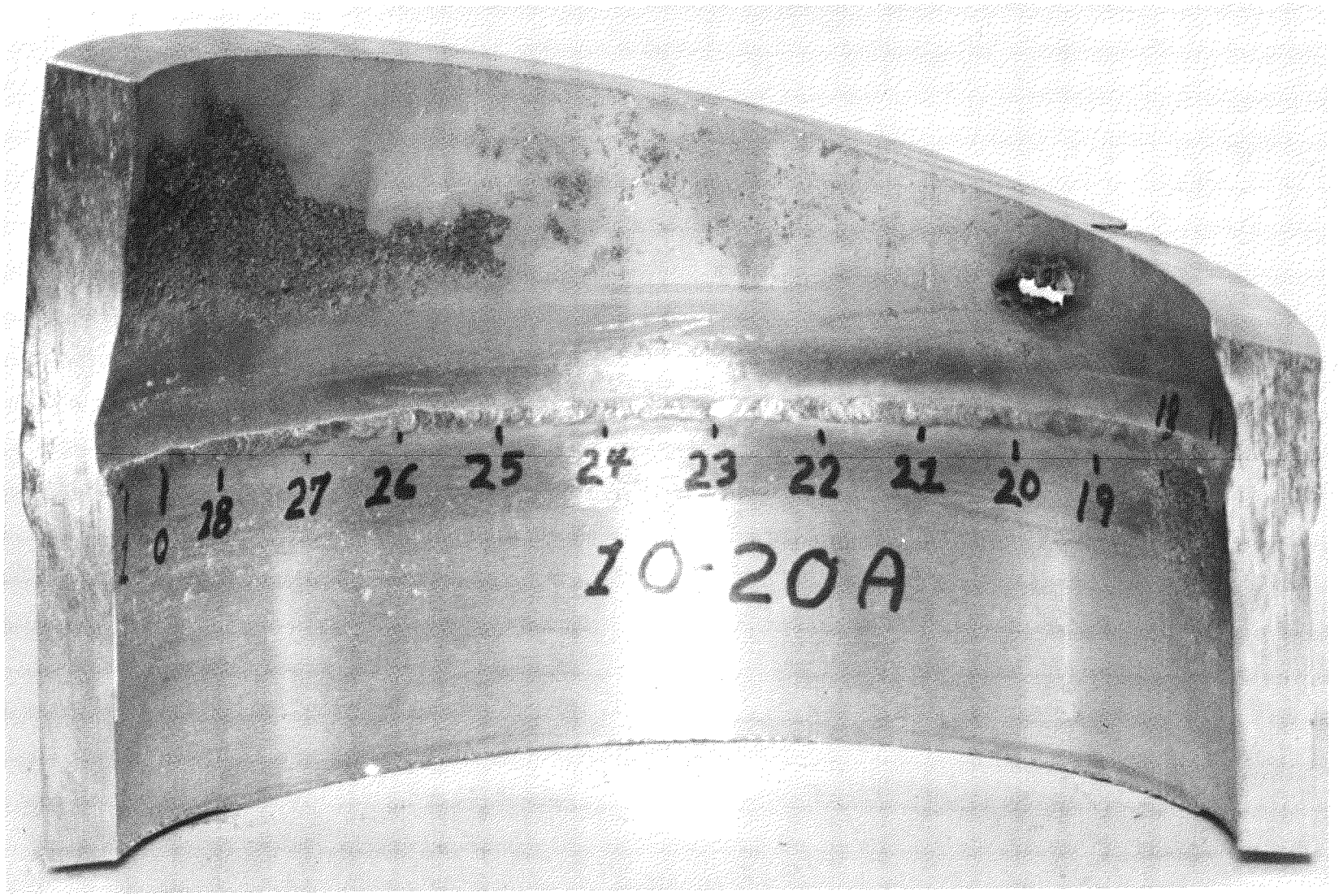


Figure D-46 Inside Surface of 1020A

manner because of its many-faceted morphology. In the case of 1024A, the evidence suggests that we are not looking at a single crack surface, but rather trying to gain a reflection from a spongelike region which does not yield coherent reflections.

It is evident from the experiences derived during this overall specimen characterization that the reliable detection of an IGSCC in its early stages of development will have to be done using highly specialized techniques which stretch the current capabilities of NDE technology.